



# Universidad de Navarra

Departamento de Química Orgánica y Farmacéutica  
Facultad de Farmacia y Nutrición

**Design, synthesis and biological evaluation of  
new organoseleno compounds as cytotoxic and  
leishmanicidal agents**

**Pablo Garnica Calvo**





# Universidad de Navarra

Departamento de Química Orgánica y Farmacéutica  
Facultad de Farmacia y Nutrición

**Design, synthesis and biological evaluation of new  
organoseleno compounds as cytotoxic and leishmanicidal  
agents**

Memoria presentada por D. Pablo Garnica Calvo para aspirar al grado de Doctor por la Universidad de Navarra.

El presente trabajo ha sido realizado bajo nuestra dirección en el Departamento de Química Orgánica y Farmacéutica y autorizamos su presentación ante el Tribunal que lo ha de juzgar.

Pamplona, 01 de junio de 2018

Dra. Carmen Sanmartín Grijalba

Dr. Juan Antonio Palop Cubillo





*What is a scientist after all? It is a curious man looking through a keyhole, the keyhole of nature, trying to know what's going on.*

(Jacques Yves Cousteau)



## AGRADECIMIENTOS/ACKNOWLEDGEMENTS

La presente memoria es en gran medida de todos aquellos que han compartido conmigo esta experiencia. Una experiencia que ha estado llena de luces pero que en momentos también ha constado de sombras. Es por ello que quiero comenzar por darles las gracias a todos y cada uno de ellos, sin vosotros no estaría donde estoy hoy ni sería quien soy a día de hoy.

Considero esta como una etapa más de mi formación, la Universidad de Navarra ha formado una parte muy importante de la misma desde la licenciatura, pasando por el master hasta el presente doctorado. Agradecer a las Facultades de Ciencias y Farmacia y Nutrición toda la formación recibida, no sólo académica sino integral. A la Asociación de Amigos de la Universidad de Navarra y a la fundación social “la Caixa” por el apoyo que ha hecho posible esta tesis.

A mis directores de tesis, la Dra. Carmen Sanmartin y el Dr. Juan Antonio Palop por haberme abierto las puertas de este maravilloso mundo de la química orgánica que sigo descubriendo día a día desde hace casi 8 años. Gracias por vuestros consejos y vuestra experiencia, gracias por guiarme en todo este proceso de descubrimiento de la química médica.

A las doctoras Elena Lizarraga y Elena Gonzalez-Peñas por las oportunidades que me han brindado de conocer las técnicas analíticas y la oportunidad de “destripar” algún que otro equipo. Al Dr Daniel Plano por su consejo y orientación dentro del mundo del selenio, gracias por alumbrar el camino con tus experiencias en el campo de la evaluación de los compuestos organoseleneados. A todos los profesores del Departamento de Química Orgánica y Farmacéutica por compartir conmigo y enriquecer esta experiencia.

Al Dr. Ignacio Encío por haber complementado mi formación con su extenso conocimiento del ámbito biológico. Muchas gracias por la confianza depositada en mi y por tener siempre abiertas las puertas del laboratorio y del despacho para la realización de experimentos e interpretación de resultados.

Al Dr. Antonio Jimenez Ruiz y su grupo por haber hecho posible la realización de los ensayos *in vitro* en *L. infantum*.

I would like to thank Dr. Thomas G Back for accepting me in his group, thank you for a pure chemistry experience and for all the lessons on chemistry. Thank you for the opportunity to work with your amazing research group, great people and great scientists.

A Carmen Elizalde, Iulen, Gorka y Rosa por su sabiduría, porque al fin y al cabo son garantía de buen hacer y de solvencia en las situaciones desconocidas para muchos. He aprendido mucho de vosotros y me habéis mostrado los entresijos del funcionamiento del laboratorio desde el principio.

A Ronces por todos los consejos prácticos del mundo de la evaluación de compuestos como antitumorales. Por tu siempre presente sonrisa, gracias a ti ahora soy un poquito más biólogo. A todos los compañeros de laboratorio que han pasado por el laboratorio, habéis dado verdadero sentido a la palabra equipo a lo largo de esta

tesis. A todas las caspaseras con las que he compartido laboratorio a lo largo de estos años, todo lo que sé sobre química práctica os lo debo a vosotras, entré para ver que era esto de la química orgánica y aquí sigo gracias a vuestro ejemplo. A mis queridos pestuncios, vosotros sabéis que sin vuestro apoyo incondicional esta tesis no hubiese sido posible y desde luego hubiese sido mucho más aburrida sin vuestra compañía.

Thank's to the chem engineers, mountain lovers and burger-eaters that took me to discover Canada from the first day I arrived as if we had been friends forever. Thank you for all those camping trips, sky trips and hikes in the beautiful Rokies.

A mi cuadrilla que ha sido un gran apoyo durante todo este tiempo, especialmente en los momentos que más lo necesitaba. A los masterianos que con su cariño empujaron al pequeño de la clase a este proyecto. A todos los que habéis hecho de este viaje un viaje inolvidable y habéis compartido conmigo todos estos momentos vividos.

A mis padres Gonzalo y Consuelo, gracias por vuestro apoyo incondicional con todos mis proyectos, esto no hubiese sido posible sin vosotros. Gracias por educarme, en el más amplio sentido de la palabra, gracias por todos los sacrificios que esto os ha supuesto. Gracias por vuestro ejemplo, siempre seréis un punto de referencia para mí.

A mi mujer María, por apoyarme todos y cada uno de los días de esta tesis, por hacerme sonreír cuando lo único que me salía era llorar. Gracias por todo el apoyo incluso cuando suponía anteponer mis proyectos a los tuyos. Gracias por quererme y confiar en mí siempre.

## ABBREVIATIONS GLOSSARY

### A

---

**AECC:** Spanish Cancer Association (Asociación Española Contra el Cáncer)

**ATP:** Adenosine triphosphate

### B

---

**Bak:** Bcl-2 antagonist killer

**Bax:** Bcl-2 associated X protein

**Bcl-2:** B-cell lymphoma 2

**Bid:** BH3 interacting-domain death agonist

### C

---

**CAT:** Chloramphenicol acetyltransferase

**CDK:** Cyclin-dependent kinases

**c-IAP:** Cellular inhibitor of apoptosis

**CKI:** Cyclin-dependent kinase inhibitor

**CL:** Cutaneous Leishmaniasis

**Cys:** Cysteine

### D

---

**DNA:** Deoxyribonucleic acid

**DIOs:** Iodothyronine deiodinases

**DISC:** Death-inducing signaling complex

**DPDS:** Diphenyldiselenide

### E

---

**EGF:** Epidermal growth factor

**EGFR:** Epidermal Growth Factor Receptor

### F

---

**FDA:** Food and drug Administration

*G*

---

**GI<sub>50</sub>**: 50% growth inhibition

**GPx**: Glutathione peroxidase

*H*

---

**H<sub>2</sub>Se**: Hydrogen selenide

**HIV**: Human Immunodeficiency virus

*I*

---

**IC<sub>50</sub>**: Inhibitory concentration 50%

**IAP**: Inhibitors of apoptosis

**IARC**: International Agency for Research on Cancer

**INE**: National Institute of Statistics (Instituto Nacional de Estadística)

**i.v.**: Intravenous

*L*

---

**LC<sub>50</sub>**: Median lethal concentration

*M*

---

**Mcl-1**: Myeloid cell leukemia 1

**MCL**: Mucocutaneous Leishmaniasis

**MMP**: Matrix metalloproteinase

**MPT**: mitochondrial permeability transition

**MSA**: Methylseleninic acid

**mTOR**: Mechanistic target of rapamycin

*N*

---

**NCCD**: Nomenclature Committee on Cell Death

**NIH**: National Institute of Health

**NPC**: Nutritional Prevention of Cancer

**NADPH**: Nicotinamide adenine dinucleotide phosphate

*P*

---

**PKDL**: Post kala-azar dermal leishmaniasis

**PBSe**: Se, Se'-1,4-fenilenobis(1,2-etanodiilo)bisisoselenourea

**p-XSC**: 1,4-phenylenebis(methylene)selenocyanate

## R

---

**RCD:** Regulated cell death

**REDECAN:** Spanish cancer registration net (Red Española de Registros de Cancer)

**RHG:** Root and hypocotyl gravitropism

**RNA:** Ribonucleic acid

**ROS:** Reactive oxygen species

## S

---

**SAHA:** suberoylanilide hydroxamic acid

**Se:** Selenium

**SeCys:** Selenocysteine

**SELECT:** Selenium and Vitamin E Cancer Prevention

**SeMet:** Selenomethionine

**SEOM:** Spanish society of medicinal oncology (Sociedad Española de Oncología Médica)

**SelP:** Selenoprotein P

**SI:** Selectivity index

**SPS2:** Selenophosphate synthetase 2

## T

---

**TNF:** tumor necrosis factor

**TryR:** Trypanothione reductase

**TRxR:** Thioredoxin reductase

## U

---

**UV:** Ultraviolet

## V

---

**VEGF:** Vascular Endothelial Growth Factor

**VL:** Visceral leishmaniasis

## W

---

**WHO:** World Health Organization

## Z

---

**Z-VAD-FMK:** N-benzyloxycarbonyl-Val-Ala-Asp-fluoromethylketone





## INDEX

INTRODUCTION.....	1
1. Cancer.....	3
1.1. Cancer epidemiology.....	4
1.2. Etiology of cancer.....	6
1.3. Cancer treatment.....	7
1.4. Biological mechanisms associated to cancer.....	11
2. Selenium.....	17
2.1. Selenium metabolism.....	17
2.2. Selenium and human health.....	18
2.3. Selenium and cancer.....	20
3. Leishmaniasis.....	23
3.1. Epidemiology.....	24
3.2. Treatments.....	25
3.3. Leishmaniasis and cancer.....	27
3.4. Leishmaniasis and selenium.....	27
4. Bibliography.....	28
BACKGROUND.....	33
1. Organoselenium compounds as antitumoral agents.....	35
1.1. Diselenide derivatives.....	36
1.2. Selenocyanate derivatives.....	36
1.3. Selenourea moiety.....	37
2. Selenium compounds as leishmanicidal agents.....	38
3. Research group experience.....	38
4. Bibliography.....	39
HYPOTHESIS AND OBJECTIVES.....	43
RESULTS.....	47
PAPER 1.....	49
PAPER 2.....	75
PAPER 3.....	117
PAPER 4.....	129
PAPER 5.....	161
DISCUSSION.....	179
Bibliography.....	184
CONCLUSIONS.....	185
APENDIX 1: SYNTHESIZED COMPOUNDS.....	189



## SUMMARY

A series of thirty-three novel selenium-containing compounds with potential antitumoral and/or leishmanicidal activity have been synthesized and evaluated in this work. Numerous preclinical studies have proven the strong dependency between chemical form of Se and its biological activity. Taking into account the experience of our research group in this field, we selected two leader compounds bis(4-aminophenyl)diselenide and 4-aminophenylselenocyanate to design second generation derivatives. The structural modifications performed on these core structures had the aim of improving their activity and selectivity.

The novel derivatives containing the functionalities diselenide and selenocyanate have been tested against a panel of several human cancer cell lines and two cell lines derived for non-malignant tissue. Once obtained their cytotoxic profiles and selectivity, derivatives were ranked to establish the hit compounds. The most promising molecules have been selected to perform further biological studies relative to cell death and cell cycle status in order to elucidate their mechanism of action. Moreover, the development of new methodologies that enable the possibility to study the glutathione peroxidase mimetic ability of new derivatives has been explored.

The leishmanicidal activity of the synthesized Se-containing compounds was analyzed against *Leishmania Infantum* axenic amastigotes. In order to assess selectivity cytotoxicity against THP-1 cells was tested. According to potency and selectivity six derivatives were selected to further study the mechanism of action by which they cause their effect. Also, we decided to explore the ability of these compounds to inhibit Trypanothione Reductase, enzyme that plays a crucial role in the survival of the parasite.

In addition, their stability under formulation conditions such as temperature, acid or alkaline conditions have been evaluated. The objective was to predict the non-desired transitions or degradation processes that may occur along the pharmaceutical manufacturing processing.



## **INTRODUCTION**

---



## 1. CANCER

The term cancer makes reference to a vast group of diseases characterized by an uncontrolled cell growth and spread to nearby tissues. This tissue alteration leads to an increase in volume known as tumor. Tumoral cells can detach and migrate through the blood stream and lymphatic system to distant tissues. This phenomenon enables tumor formation in remote areas away from the main tumor. This process is known as metastasis and is the main cause of death in cancer disease (1,2).

The tumorigenesis is a gradual process in which a series of genetic alterations are accumulated leading to a progressive transformation of normal cells into malign cells. During this process, the cells acquire some characteristics that enable their survival, proliferation and dissemination; those hallmarks are described in **Figure 1** and encompass (3):

- Six hallmark capabilities: evading growth suppression, sustaining proliferative signaling, cell death resistance, replicative immortality, angiogenesis induction and activation of invasion processes.
- Two emerging hallmarks such as avoidance of immune destruction, and reprogramming of energetic metabolism to survive the continuous growth and proliferation
- Two enabling characteristics, genome instability and thus mutability endow and inflammation by innate immune cells.

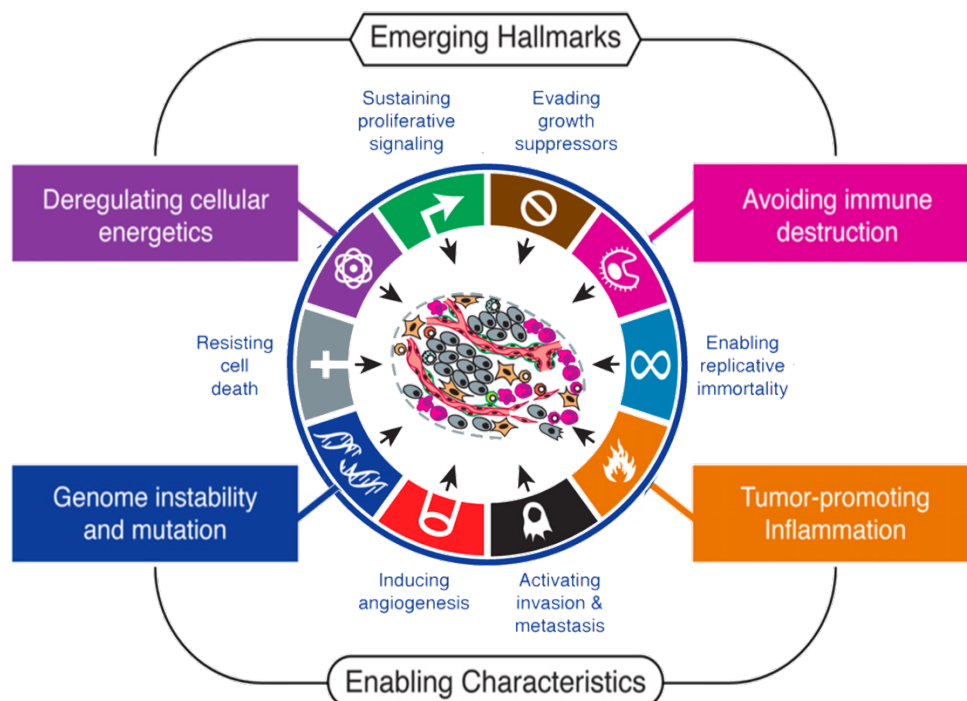


**Figure 1.** Hallmarks of cancer. Image adapted from Hanahan, *D. Cell*, 2011 (3).

## 1.1. Cancer epidemiology

According to the World Health Organization (WHO), cancer is one of the leading causes of death worldwide. In the high-income countries cancer represents the second leading cause of death, only exceeded by cardiovascular diseases. This tendency is now affecting low-middle-income countries where 50% of deaths are associated to this group of diseases (4,5). According to the last published statistics from the International Agency for Research on Cancer (IARC), the GLOBOCAN 2012, 14.1 million new cases were diagnosed and 8.2 million deaths were due to this disease in 2012. The estimations predict that the number of new cases will reach the 20 million mark by 2025. This increment is mainly due to population aging and birth rates, specially, in low-income countries. Moreover, lifestyle habits such as smoking, excess of body weight, physical inactivity, and change in reproductive patterns, are proven risk factors for cancer development. The burden of cancer will continue to shift to less developed countries now accounting for 57% of cases and 65% of cancer deaths worldwide (6,7).

Lung cancer is the most frequent at a worldwide level both in incidence and fatality. Breast cancer is ranked second in terms of incidence but the fifth most deadly cancer due to its good prognosis. Other common cancer cases are in order of frequency, colon and rectal, prostate and liver (**Figure 2**) (6).

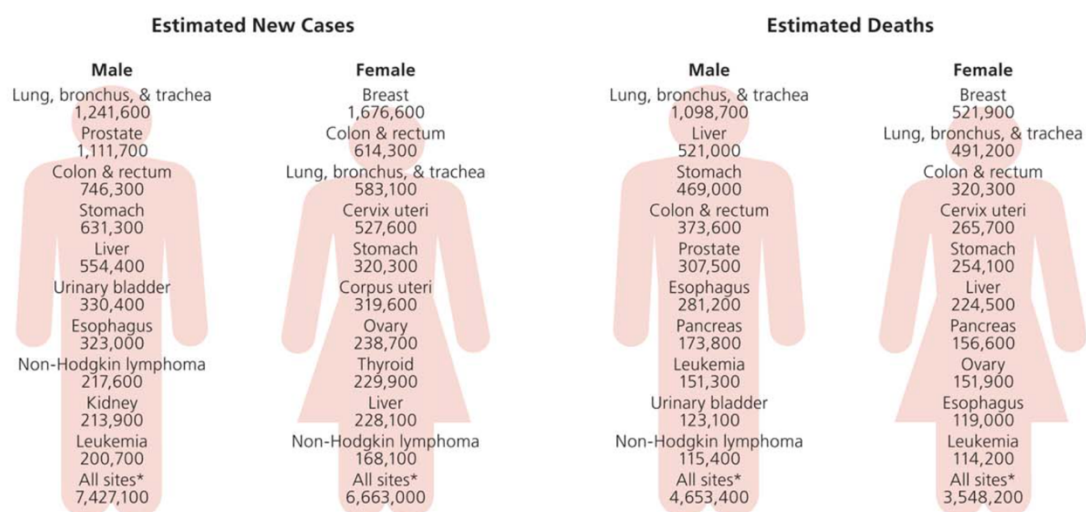


**Figure 2.** Estimated new cancer cases and deaths worldwide by sex (6).

Regarding geographical distribution most cases and deaths occurred in Eastern Asia due to its vast population. Northern America ranks second and third in terms of number of new cases and deaths respectively. Nearly a quarter of the new cases (3.44 million) and one fifth of the deaths (1.75 million) occurred in the four European regions, despite the fact that their population only represent 10% of the global population (8). These results are illustrated in **Figure 3**, statistics vary when types of cancer considered individually responding to risk factor distribution as well as diagnose availability and sociopolitical factors.



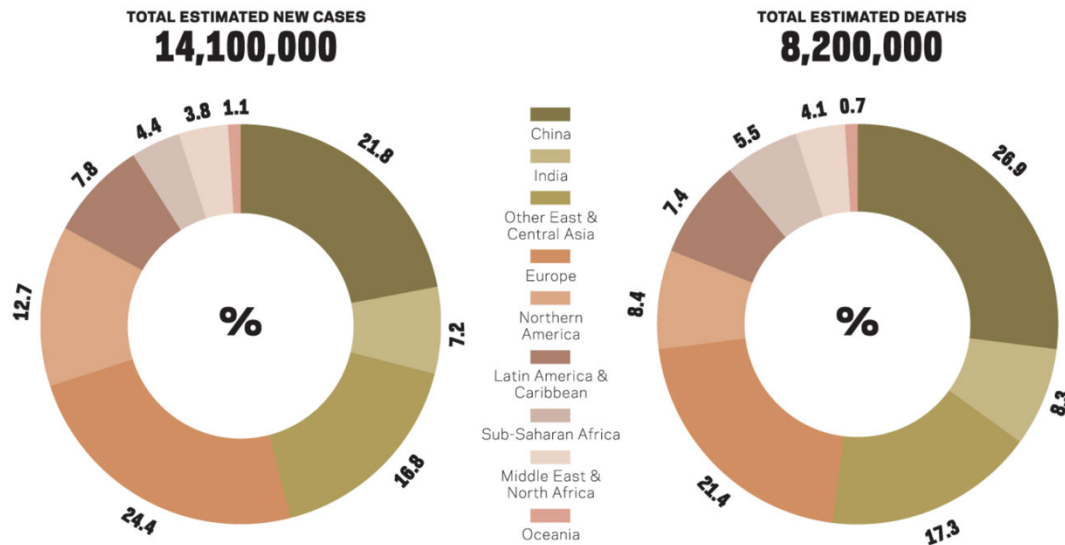


**Figure 3.** Estimated global 2012 numbers of new cases and deaths for all malignant cancers (excluding non-melanoma skin cancer) (9)

### 1.1.1. Cancer in Spain

In Spain, the number of new cases reported in 2015 was of almost 250,000 patients according to data provided by Red Española de Registros de Cancer (REDECAN). Analyzing these data, colon and rectal cancer were the most frequently diagnosed cancers followed by prostate, lung and breast cancers. In the last twenty years the number of new cases has experienced a steady increase due to early detection and ageing of the Spanish population (10).

The national institute of statistics recently revealed that tumors constitute one of the main hospitalization causes, right after circulatory and respiratory system-related diseases. If we draw our attention to mortality rates reflected in the data provided by REDECAN, more than one of every four deaths was due to cancer in the year 2015 (10). When mortality rates are separated by types of cancer as in **Figure 4**, we can establish that 20% of cancer-caused deaths were due to lung cancer followed by colon, rectum and anus cancers out of a total of 107,244 in 2013.

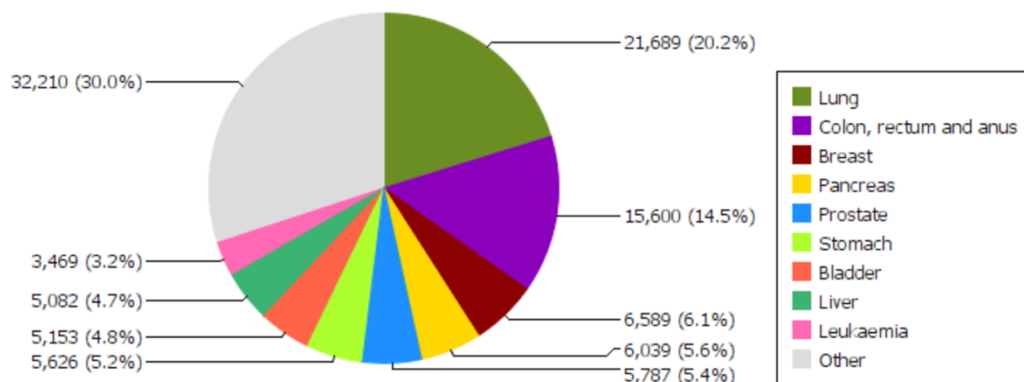


**Figure 4.** Number of cancer deaths in Spain in 2013 for both sexes and all ages, data provided by IARC database.

## 1.2. Etiology of cancer

The development of cancer is a process mediated by gradual changes that enable the progression from a precancerous lesion to a malign tumor. Those changes are encouraged by genetics and exposure to carcinogenic agents that can be of physical, chemical or biological nature (11). Ageing of global population is another crucial factor as it is associated with the accumulation of risk factors and a notable loss in cell repairing mechanisms.

The risk factors are diverse, some of them are known and preventable. Cancer can be caused by innate biology but is more often caused by external agents, the major cancer risks are (9):

- Tobacco: smoking is related to at least sixteen types of cancer and is responsible for roughly 70% of lung cancer. A substantial portion of cancer deaths are caused by tobacco consumption, 700,000 in low and middle-income countries.
- Infection: 2 million new cancer cases annually are due to infectious agents. Besides, it is much higher in less developed areas (22.9%) versus more developed regions (7.4%). The main cancer-related infectious agents are *Helicobacter pylori*, human papillomavirus and hepatitis B and C viruses.
- Physical inactivity and dietary factors: excess of body weight is a common factor in a large number of endometrial, esophageal, kidney and breast cancer cases. Physical activity on its own is associated with reduced risk of certain cancers.
- Ultraviolet radiation: major risk factor for melanoma, accounting for 55,000 deaths yearly worldwide. Sun is the main source of ultraviolet radiation. However, the use of tanning devices multiplies radiation potency by 10 to 15 folds and is widely used by young population.
- Reproductive factors: female breast and endometrial cancer are directly related with estrogen levels in the body. Combined oral contraceptives and menopausal estrogen-progestogen therapy are carcinogenic.
- Environmental pollutants and occupational exposures: radon and arsenic have proven influence on cancer probability and are common in USA and China respectively. In certain industries, the duration of the exposures to certain IARC-classified group I carcinogens are alarming. This last case scenario is especially relevant in low-middle-income countries where regulations and enforcement in this area is less strict.

Based on sufficient epidemiological studies, carcinogenic agents such as individual chemicals, biological and physical agents, as well as personal habits and occupational exposures are classified by the IARC in the next groups:

- Group 1: carcinogenic to humans
- Group 2A: probably carcinogenic to humans
- Group 2B: possibly carcinogenic to humans
- Group 3: not classifiable as to their carcinogenicity to humans
- Group 4: probably not carcinogenic to humans

### **1.3. Cancer treatment**

The ultimate objective of a cancer treatment is the complete elimination of any traces of tumoral cells and when this is not possible the reduction of the tumor size and the palliation of the symptoms. The recent technological and scientific innovations have provided a better knowledge on formation, development and spreading of cancer. This understanding has led to both an improvement of treatments and a reduction of secondary effects. The main treatments available currently are surgery, radiotherapy, chemotherapy, immunotherapy and targeted therapies.

#### **1.3.1. Surgery**

Surgery was the first treatment available. At first its aim was to remove the primary tumor and the nearby regions. Nowadays, the applications of surgery are numerous including cancer prevention such as benign tumor extraction and diagnostics through biopsy. Depending on its objective, cancer surgery can be classified in diagnostic, cancer staging, curative, palliative, prophylactic and supportive surgery. A combination of several of them may be needed to achieve the ultimate objective of cancer treatment (12).

#### **1.3.2. Radiation therapy**

Radiotherapy uses high-energy particles or waves to destroy or damage cancer cells, such as x-rays, gamma rays, electron beams, or protons. Consequently, we are talking about a local treatment; nearby cells can also be affected but in a localized area. The main uses for this type of treatment is curing or shrinking early stage cancers, stopping cancer from recurring somewhere else or treating symptoms in advanced cancers (12).

#### **1.3.3. Immunotherapy**

Sometimes called biologic therapy or biotherapy, immunotherapy uses part of the person's immune system to fight cancer. It can be achieved by stimulation of the immune system or by the administration of immune system components such as immune-system proteins. The different types of immunotherapies used in cancer treatment include: monoclonal antibodies, immune checkpoint inhibitors, cancer vaccines and non-specific immunotherapies (1).

#### **1.3.4. Targeted therapy**

Technically considered as chemotherapy, these drugs target certain parts of cancer cells that separate them aside from normal cells. These therapies block specific signaling pathways and proteins associated with tumor progression and growth that are altered in cancer cells but not in normal cells. Other approach commonly used by targeted therapies is the guided release of chemotherapics by the conjugation with monoclonal antibodies or peptic ligands that bind to malign cells. The adverse effects are minimized if compared to classic chemotherapy (13). Some examples of targeted therapies are (14):

- Tyrosine kinase inhibitors such as Imatinib and lapatinib (**Figure 5**).

- Inhibitors of epidermal growth factor receptor: erlotinib and gefitinib.
- Angiogenesis inhibitors: sorafenib and sunitinib (**Figure 5**).
- BRAF<sup>V600E</sup> inhibitor: vemurafenib (**Figure 5**).

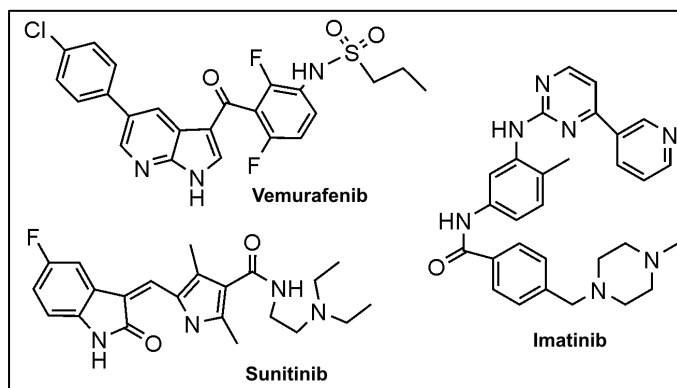


**Figure 5.** Some representative examples of targeted therapies chemical structures.

### 1.3.5. Chemotherapy

Chemotherapy refers to the use of drugs to treat cancer. It is considered a systemic therapy, so it can also treat metastasis (12). This systemic characteristic has the disadvantage that it also affects normal cells causing limitations in terms of treatment and causing non-desired effects such as vomiting, renal insufficiency, anemia, hepatic injuries, necrosis (15). Resistances to antitumor drugs may appear from the beginning of the treatment or can be developed by adaptation processes of the tumoral cells. Those are the two main reasons why the development of new selective and safe antitumor chemotherapies are necessary.

A number of chemotherapeutic drug families are available both with preventive and cytotoxic activities. The main families will be described further on in depth.

#### *Alkylating agents*

Alkylating agents are drugs capable of establishing covalent bonds between their alkyl groups and nucleophilic molecules present in DNA and proteins. As a result of this bonding cell cycle is affected, specially in phase S. There are serious adverse effects on bone marrow that limit the maximal dose administered. Examples of the main structures for alkylating agents are summarized in **Figure 6** (16).

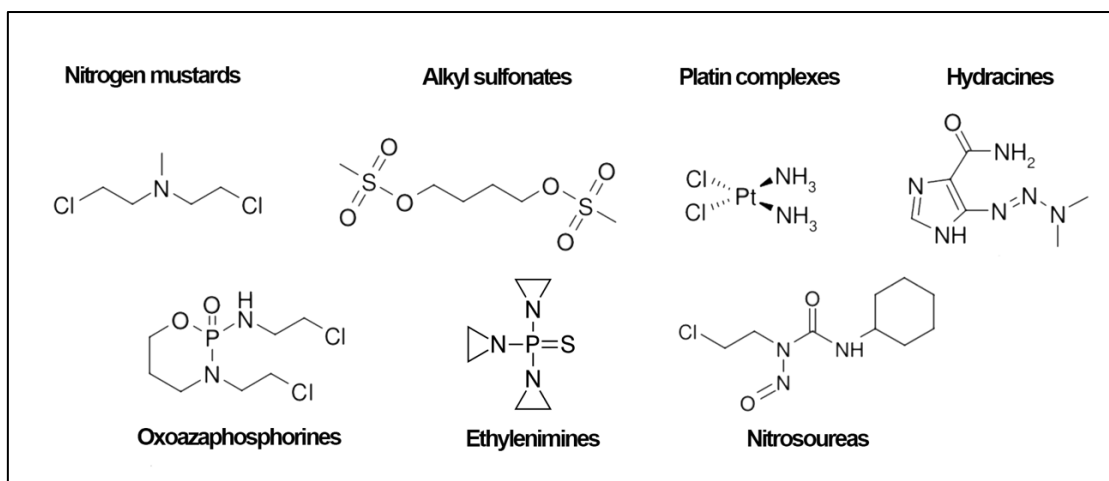


**Figure 6.** Structure examples of main alkylating agents.

### Antimetabolites

Antimetabolites are structural analogs of metabolites implicated in cell growth pathways. When the cancer cells incorporate antimetabolites, they become unable to divide due to incorporation to this DNA or RNA or enzyme inhibition. Antimetabolites are cell-cycle specific, they attack cells at very specific phases in the cycle, mainly S phase. Antimetabolites are classified relative to the substances with which they interfere.

- Pyrimidine antagonist: 5-Fluorouracil (**Figure 7**), Fluorouridine, Cytarabine, Capecitabine, and Gemcitabine.
- Folic acid antagonist: Methotrexate (**Figure 7**).
- Purine antagonist: 6-Mercaptopurine (**Figure 7**) and 6-Thioguanine.
- Adenosine deaminase inhibitor: Cladribine, Fludarabine, Nelarabine and Pentostatin (**Figure 7**).

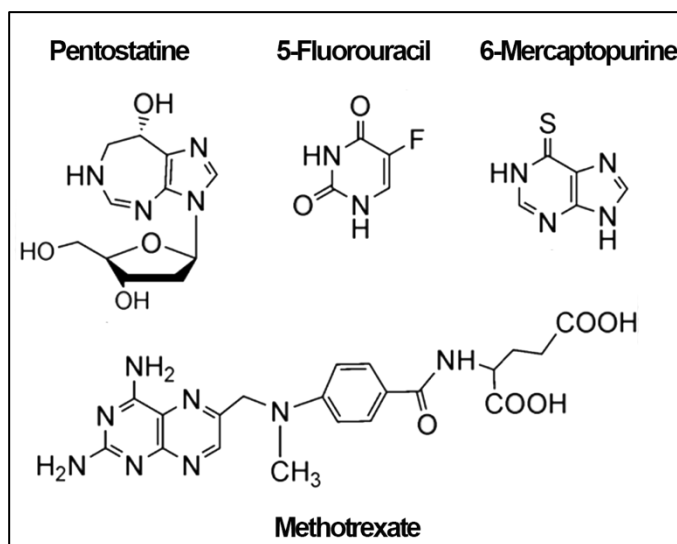


**Figure 7.** Structure of some antimetabolite representative drugs.

### Topoisomerase inhibitors

Topoisomerases are enzymes that participate in the overwinding or underwinding of DNA during replication and transcription. The inhibition of any of the two topoisomerases (I or II) induces programmed cell death (17). They can be classified in:

- Topoisomerase I inhibitors: Irinotecan, topotecan, camptothecin (**Figure 8**).
- Topoisomerase II inhibitors: Amsacrine, etoposide, etoposide phosphate, teniposide (**Figure 8**).

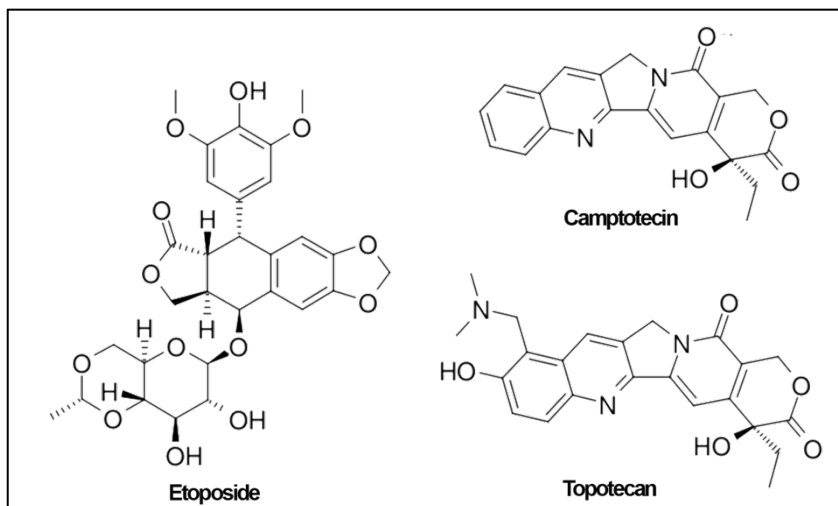


**Figure 8.** Representative structures of topoisomerase inhibitors.

### *Antimitotic drugs*

Classical antimitotic drugs were designed as tubulin binders that either stabilize (taxanes) or de-stabilize (vinka-alkaloids) microtubule dynamics. This therapy targets mitotic cells as their microtubule turnover is exacerbated. Major side effects are hematological alterations and neutropenia as microtubule are essential for many basal cell functions (18). New antimitotic drugs are now designed to target mitotic kinases and kinesins. Some antimitotic drug examples are illustrated in **Figure 9**.

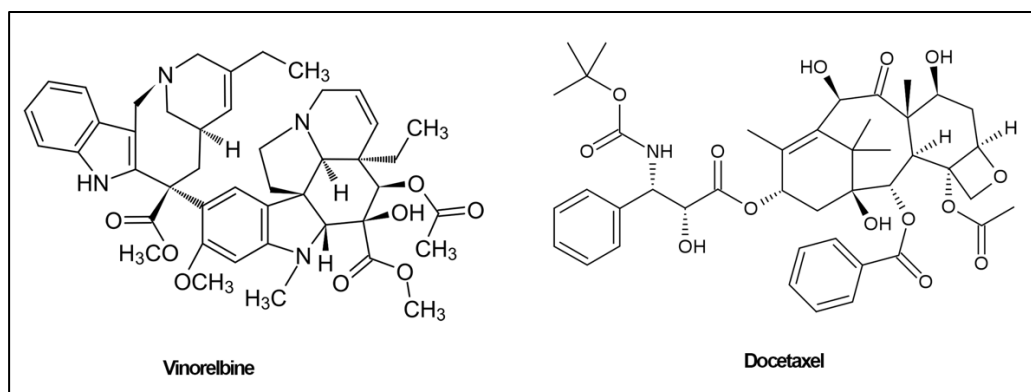


**Figure 9.** Structure of some antimitotic drugs.

### *Antibiotics*

Antibiotics used in chemotherapy act in many diverse ways: some are potent intercalating agents (doxorubicin) (**Figure 10**) whereas other are DNA damagers (bleomycines) (**Figure 10**) or topoisomerases inhibitors (mitoxantrone).

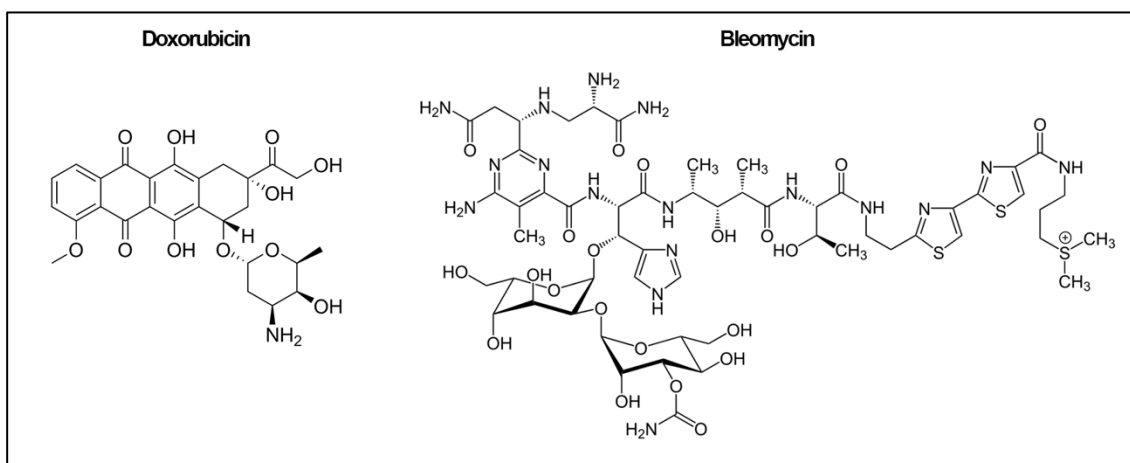


**Figure 10.** Examples of antitumor cancer antibiotics.

#### 1.4. Biological mechanisms associated to cancer

As previously mentioned, carcinogenesis is a complex and gradual process, understanding of the involved mechanisms is essential to develop new anticancer drugs. Since the structures described in this work alter cell cycle basal status and cause cell death by apoptosis and autophagy, those concepts will be explained in depth in the subsequent sections.

##### 1.4.1. Cell cycle

Cell division is a sequential process highly regulated by which the cell duplicates its genetic material and divides to yield two separate cells. Cycle is formed by four phases: mitosis (M phase), a phase during which DNA replication takes place (S phase) and two gap phases ( $G_1$  and  $G_2$ ). In those two last phases cell prepares itself for the synthesis of DNA ( $G_1$  phase) and for mitosis ( $G_2$ ). Resting cell population ( $G_0$ ) accounts for the major part of the non-growing, non-proliferating cells in the human body (**Figure 11**) (19).

The amount of DNA present in a cell can be used as an indicator of its population cell cycle status. The DNA content is  $2n$  in phases  $G_1$ , duplicates to  $4n$  in phase S and remains constant in phases  $G_2$  and M and reverts to its original value of  $2n$  after cell division.

Several checkpoints regulate that cell cycle progression is correct and follows the established requirements. Key proteins in this activity are cyclin-dependent kinases (CDK) and cyclins. Interaction between them is necessary for cell cycle progression. For example, D type cyclins bind to CDK4 and to CDK6, these complexes are crucial for  $G_1$  entry. CDK1-cyclin A complex regulates S/ $G_2$  transition and CDK1-cyclin B controls  $G_2$  progression to M phase (**Figure 11**).

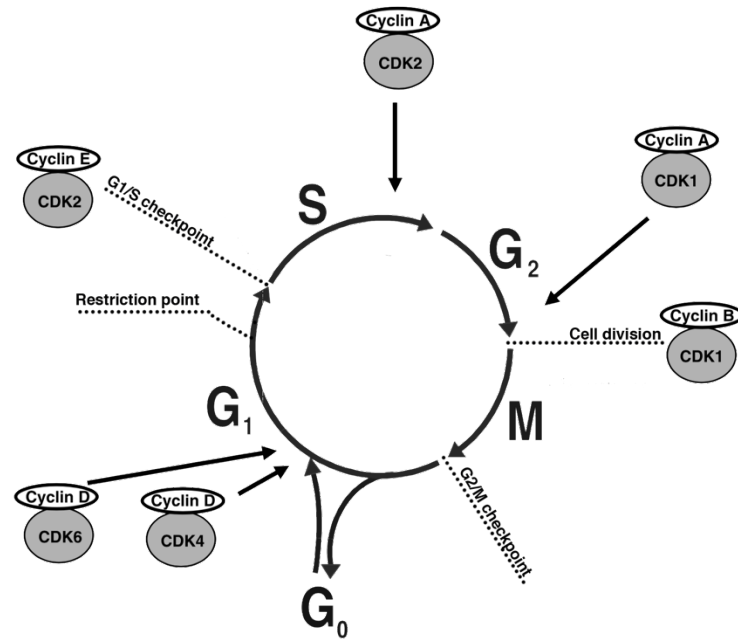


**Figure 11.** Cell cycle phases and regulatory activity of CDK/cyclin complexes (19).

Cycle checkpoints function to ensure that incomplete or damaged chromosomes are not replicated and passed on to daughter cells. They ensure that all the events of a particular phase have occurred correctly before entering the next. Those checkpoints are (**Figure 11**):

- Restriction point: located in late G<sub>1</sub> phase is a point of no return, cell is committed to the rest of the cell cycle even in the absence of growth factors.
- DNA damage checkpoints: located before cells enter S phase and before M phase. They lead to cell cycle arrest in order to repair DNA before continuing to next phase.
- The “spindle checkpoint”: located on the mitotic spindle and stops the cycle in metaphase when improper alignment of chromosomes is detected.

#### 1.4.2. Cell death

The Nomenclature Committee on Cell Death (NCCD) established two criteria in order to identify a dead cell, irreversible plasma membrane permeability or complete cellular fragmentation (20). The latest classification proposed by this committee depicted in **Figure 12** focuses on molecular mechanisms of the cell death process (21). A description of those cell death subroutines that have been identified for derivatives designed by our research group in the past have been included in this work.



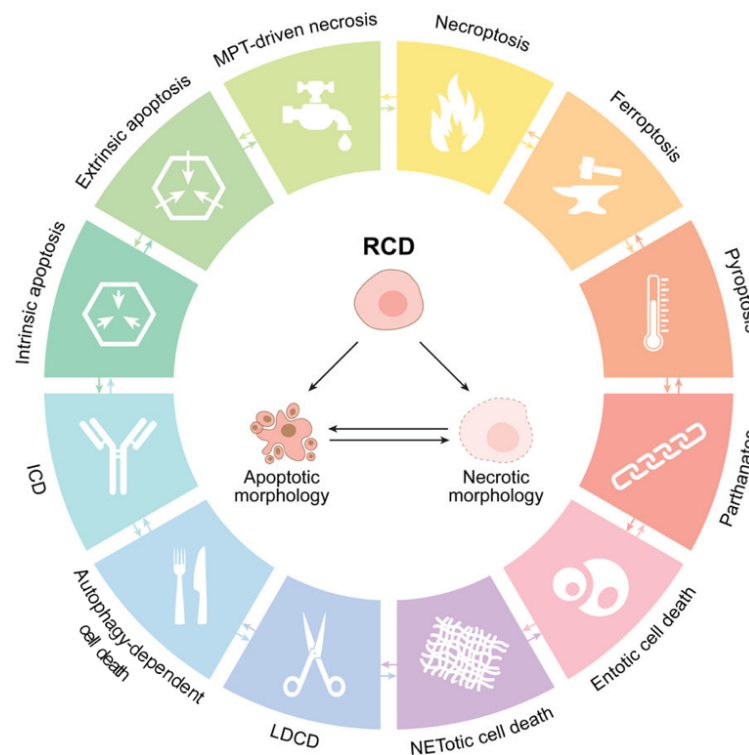


**Figure 12.** Classification of cell death subroutines (21)

### *Intrinsic and extrinsic apoptosis*

Apoptotic cells can morphologically be marked by the rounding-up of the cell, reduction of cellular volume, condensation of chromatin, karyorrhexis, retraction of pseudopods, little ultrastructural modifications and finally engulfment by phagocytes (22). During carcinogenesis cells develop molecular mechanisms that enable them to avoid apoptosis and following this strategy create resistances to drug targeting this pathway (23).

This route can be triggered both intrinsically, or extrinsically. The two subroutines are illustrated in **Figure 13** and described further below:

- Intrinsic pathway: is initiated by a wide variety of intracellular stress signals/conditions which lead to the activation of the pro-apoptotic Bcl-2 family members Bax and Bak. The result is mitochondrial outer membrane permeabilization, mitochondrial dysfunction and release of pro-apoptotic factors, such as cytochrome c, and Endo G into the cytosol (24). This leads to the formation of apoptosomes by caspase-9 activation.
- Extrinsic pathway: due to extracellular death signals that act via specific transmembrane receptors. This pathway starts with the binding of a tumor necrosis factor (TNF) to its receptor, leading to the formation of a death-inducing signaling complex (DISC) by the activation of caspase-8 (25). This pathway is also linked with the activation of the intrinsic pathway by the activation of Bid caused by caspase-8 (26).

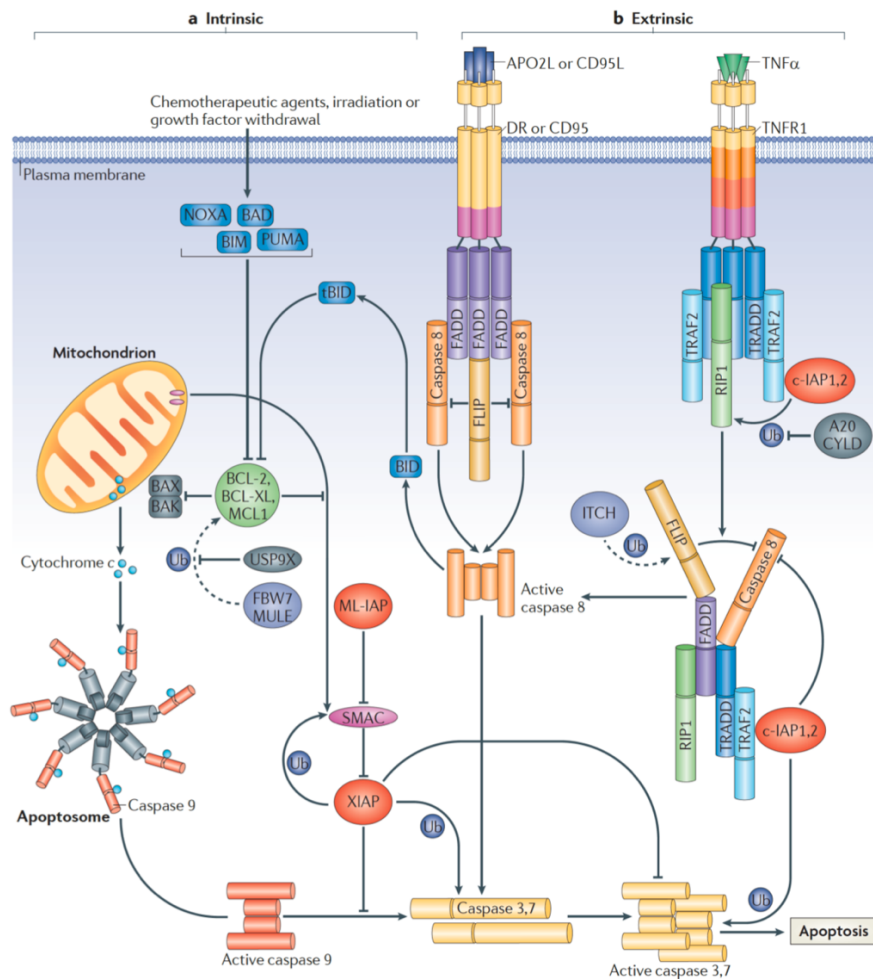


**Figure 13.** Apoptosis pathways: intrinsic and extrinsic (27).

As mentioned, both pathways include the activation of a class of cysteine proteases called caspases. They can be divided in initiator caspases (caspase -2, -8, -9 and -10) and effector (caspases -3, -6 and -7). Effector caspases are responsible for most of the substrate proteolysis seen during apoptosis (28). The role of inhibition apoptosis proteins (IAPs) is crucial for cancer development as they inhibit caspases. Deletion of RHG genes blocks apoptosis, and their ectopic expression is sufficient for the killing of many different cell types, although many other pro-apoptotic factors are implicated and gives us an idea of the complexity of apoptosis regulation.

#### *Autophagy-dependent cell death*

Autophagy is a catabolic degradation process in which cellular material is engulfed by double-membrane autophagosomes and degraded in lysosomes. (22,29). Autophagy was first described as a survival mechanism to maintain cellular homeostasis and to respond to environmental stresses (nutrient depletion or pathogen attack), but may also function as a programmed cell death pathway. Several subtypes of autophagy have been described, microautophagy, chaperone-mediated autophagy, but macroautophagy is the most extensively studied (30).

There are five stages of autophagy categorized as initiation, elongation, membrane closure, maturation and degradation of cytoplasmic cargo. Autophagy can be initiated by inhibition of mTOR, causing the release of the ULK complex that then phosphorylates Beclin1 and BCL2.

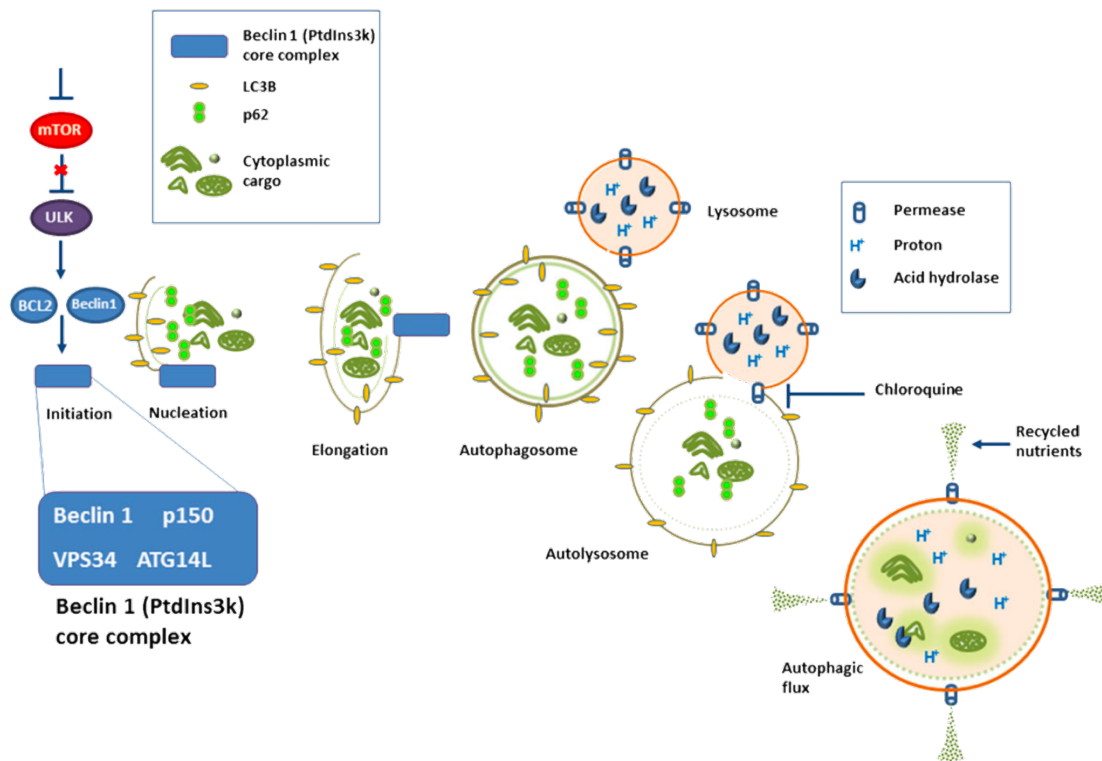


**Figure 14.** Autophagy phases and activation pathways (31).

Nucleation of the phagophore starts with the inclusion of LC3B. The phagophore elongates around cytoplasmic cargo and then closes into a mature autophagosome. Fusion with lysosome leads to autolysosome formation. The last step is the degradation of components by acid hydrolases (31).

Due to its crucial role in carcinogenesis, autophagy has emerged as a therapeutic target for cancer drug design. Moreover, autophagy is necessary for tumor progression as cancer cells require a high rate of nutrients and this accelerated metabolism needs autophagosomes to maintain homeostasis (32).

#### *MPT-driven necrosis*

Mitochondrial permeability transition (MPT) is the sudden permeabilization of mitochondria membranes leading to their osmotic breakdown (21). Morphologically characterized by a gain in cell volume, swelling of organelles, plasma membrane rupture and subsequent loss of intracellular contents. Specific perturbations of the intracellular microenvironment cause the initiation of this process. For some time this cell death was considered accidental but recent evidence suggests that it is regulated by catabolic mechanism and signal transduction pathways (22).

*Entotic cell death*

This cell death subroutine is characterized by the engulfment of one cell by a nearby live cell, with the subsequent death of the engulfed cell within the phagosome. Mechanistically entosis is initiated by the formation of epithelial adherent junctions that lead to cell engulfment. Once inside the host cell, the inner cell is in the majority of cases killed by lysosomal degradation and the maturation of entotic vacuole (33).

## 2. SELENIUM

Selenium (Se) was discovered by the Swedish chemist doctor Jöns Jakob Berzelius in 1817. Selenium is present in the WHO list of essential trace elements for human life but for many years it was considered poisonous. Actually there is a fine line between beneficial effects concentration and concentrations at which selenium is toxic (34,35).

The National Institute of Health of the United States of America (NIH) recommended intake is 55-70 µg/day with a tolerable upper intake level of 400 µg. Seafoods and organ meats are the richest food sources of selenium. Other sources include muscle meats, cereals and other grains, and dairy products (36,37). When dairy intake is geographically studied an uneven distribution can be observed. Countries like USA, Venezuela, Canada and Japan are over the 100 µg/day mark. Intake in china covers a wide range, from Se intake deficiency to an excessive consumption. If we draw the focus to Europe we can observe some deficit in the eastern area (35). In Spain 50% of the population has been estimated to have suboptimal values of Se in blood (38).

### 2.1. Selenium metabolism

The chemical form in which Se is ingested has a crucial effect on the resulting biological activities. Selenium metabolism is complex and diverse therefore the followed metabolic pathway and final metabolites entwine disease treatment and prevention efficacy. All pathways have the aim of generating selenoproteins and excretion through methylation. They intersect at the common metabolite H<sub>2</sub>Se or hydrogen selenide ion at physiological pH. Metabolic pathways have been classified downstream of the putative selenide ion where pathways are common to all the selenium dietary compounds. Upstream pathways of the selenide intermediate have unique pathways for each compound.

Selenomethionine (SeMet) can be transformed into its selenocysteine (SeCys) form through tans-sulfuration, then dietary and metabolized SeCys can be metabolized by β-lyase to H<sub>2</sub>Se. Storing of SeMet into proteins in place of methionine or of SeCys in place of Cys can be released upon degradation of proteins and selenoproteins. Selenocysteine conjugates can be metabolized to selenols by γ-lyase pathway. Selenolates and diselenides are redox active and can potentially generate selenols. Moreover, selenolates undergo redox-cyclin with thiols present in the cell (39). **Figure 14** exemplifies the major metabolic pathways of selenium-containing compounds. The use of Se to synthesize proteins needs the formation of selenophosphate and a Se donor, usually formed using ATP and H<sub>2</sub>Se as starting materials (40).

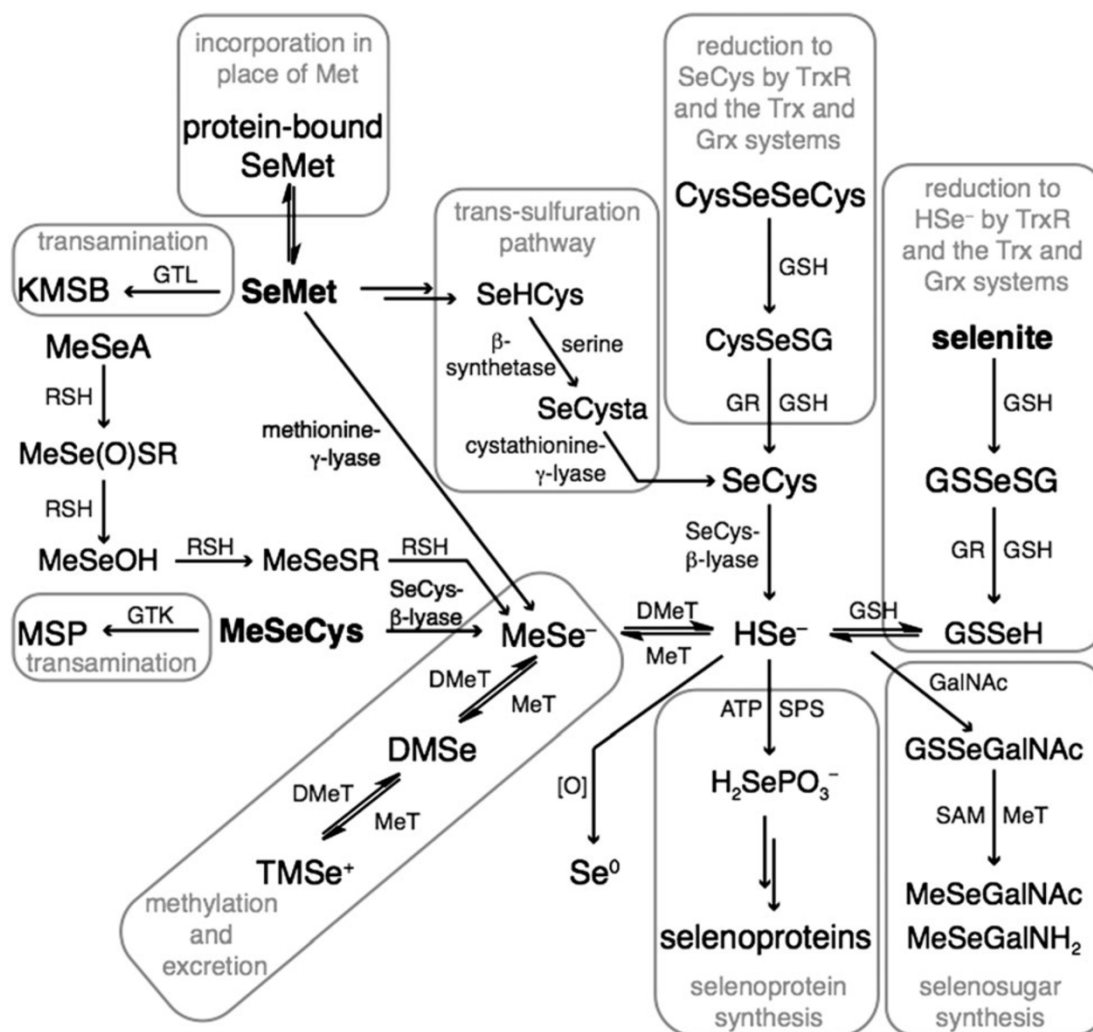


**Figure 15.** Metabolic pathways of dietary selenium compounds (41).

The elimination of Se excess can be done through Se-sugars in urine or in the form of dimethylselenide and trimethylselenide (42). The equilibrium between  $\text{H}_2\text{Se}$  and methylselenol is regulated by methyl-transferases and demethylases (43).

## 2.2. Selenium and human health

It is via selenoproteins that Se mainly has its effect (44). Twenty-five selenoproteins have been identified so far in the human proteome, most of them participate in antioxidant defense and redox state regulation. Glutathione peroxidases (GPxs) and thioredoxin reductases (TrxRs) form the most studied families. Other more specific enzymes have also an essential role, iodothyronine deiodinases (DIOs), involved in the thyroid hormones metabolism pathways and selenophosphate synthetases 2 (SPS2) necessary for selenoprotein synthesis (40). The classification of those selenoproteins by function is showed in **Figure 16**.

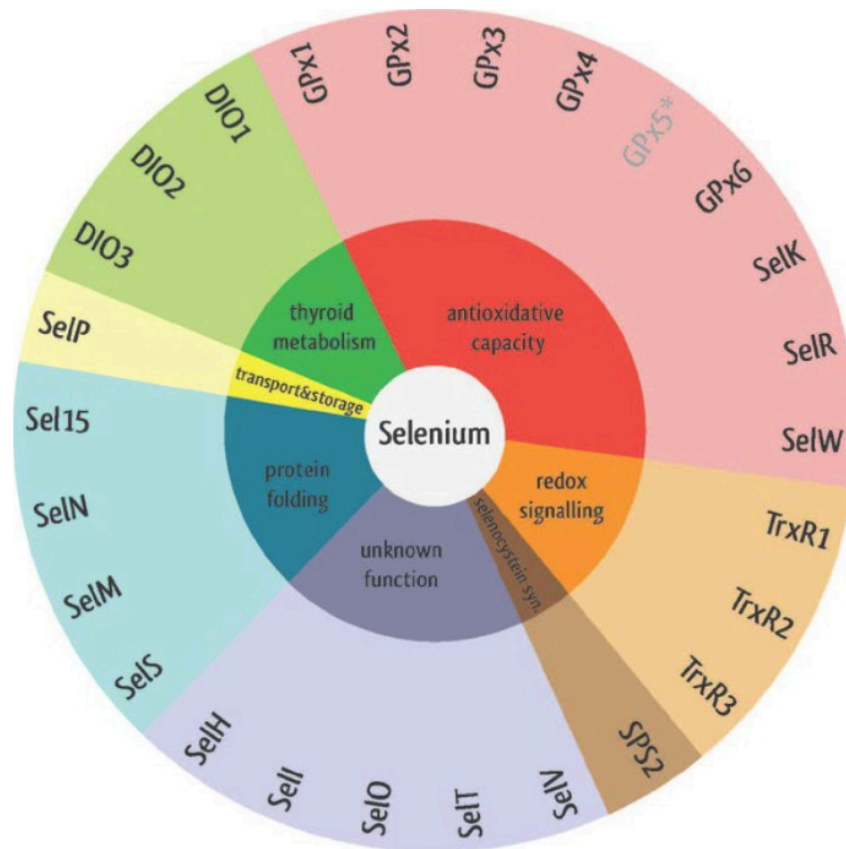


**Figure 16.** Selenoprotein classification according to putative function (45).

Health consequences are derived of both too low and to high concentrations as it is implicated in many physiological processes (46). In **Figure 17** some of the biological effects of Se depending on plasmatic concentration are showed. At high doses selenium metabolites have a pro-oxidant activity promoting growth inhibition and cytotoxic activity. Nutritional doses are related to maximization of selenoprotein activities. Under the recommended diary intake range, the risk of suffering from Keshan disease (endemic heart disease) (47), Kaschin-Beck disease (degenerative osteoarthropathy) (48) and endemic cretinism (49) increase. High concentrations of dietary Se leads to selenosis, a condition that is observed when Se levels reach toxic concentrations (46).

Deficit in Se levels has proven repercussion on human health in the next systems:

- Brain: Selenoprotein P (SelP) has a neuroprotective role promoting neuron survival and preventing apoptosis. Abnormal levels of Se were found in patients with impaired cognitive functions and neurological disorders (50).
- Immune system: T cells are sensitive to oxidative stress, consequently, selenoprotein activity is crucial for their correct performance. A relationship has been described between Se plasma levels and mortality rates of viral infection (51).
- Fertility: Se is necessary for a correct sperm motility in men. In female the risk of miscarriage and pre-eclampsia requires an optimal selenoprotein expression status (52).

- Diabetes: some studies prove that nonstandard levels of Se are related to the risk of type 2 diabetes (35).
- Mood: Selenium deficiency has also been related with depression, anxiety, hostility and mental confusion appearance in psychological patterns (53).
- Thyroid function and autoimmune thyroid disease: The thyroid gland has the highest selenium concentration of all tissues. Iodothyronine deiodinases selenium dependent enzymes produce active thyroid hormone (50).
- Other affections: Se deficiency has also been reported to cause cardiac and skeletal muscle disorders (54).

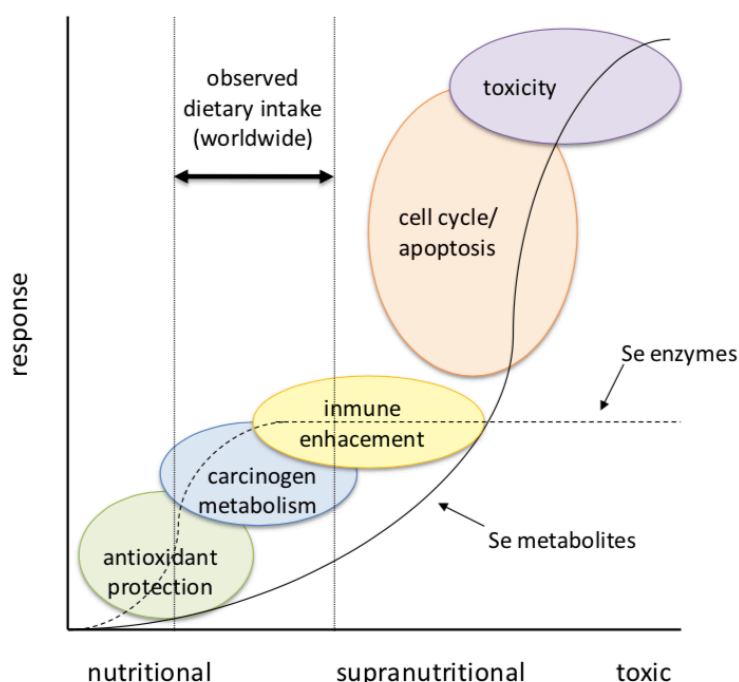


Figure 17. Dose-response curve exhibited by Se compounds (55)

### 2.3. Selenium and cancer

Numerous preclinical and epidemiological studies have described a clear role of Se in tumor prevention. First evidence of this activity was detected as an observation of soil Se levels effects on cancer risk in those areas (56). Several clinical trials have evaluated the influence of selenium supplementation on cancer risk. For example, the nutritional prevention of cancer (NPC) trial demonstrated that the supplementation with 200 µg of Se in the form of selenized yeast reduced significantly the incidence of several cancers alongside with a decrease in mortality (46). These promising results encouraged the proposal of the Selenium and Vitamin E Cancer Trial (SELECT) that studied the effect of SeMet and Vitamin E on prostate cancer risk. The study was prematurely ended due to the lack of results. This disparity could be explained by significant differences in formulation, dose and study design. The selenized yeast used in the NPC study contained various selenium-containing derivatives other than SeMet.



Also, the  $<106 \mu\text{g/L}$  dose range was barely considered for the SELECT study, dose range that had exhibited risk reduction on the previous studies.

With those results in mind we can conclude that Se anticancer activity is both dose, form and cancer type dependent. The concentrations at which Se causes these effects is supranutritional, therefore, metabolites such as  $\text{H}_2\text{Se}$  and methyselenol might be implicated. Mechanisms by which Se causes its chemopreventive effect include carcinogen metabolism modulation, stimulation of DNA repair, regulation of cell cycle, cell growth inhibition, inhibition of angiogenesis and modulation of inflammatory and immune response among others (42,46). The main mechanisms are described further below:

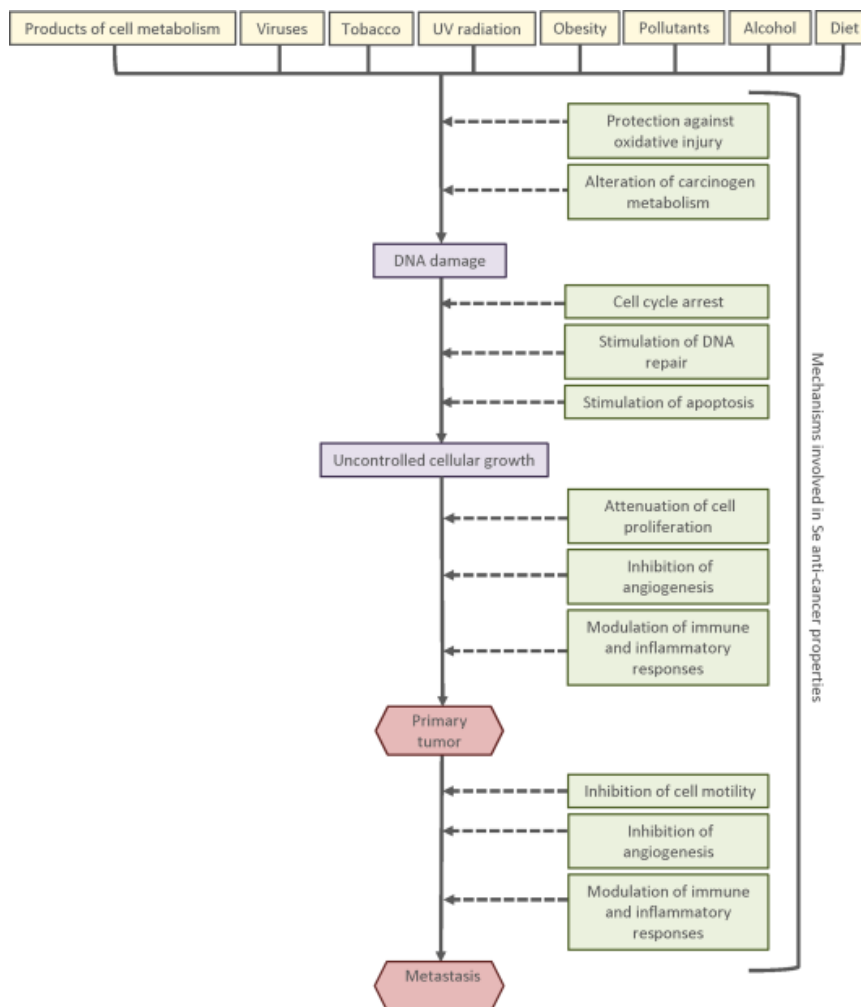


**Figure 18.** Mechanisms involved in Se anticancer activity (46).

### *Oxidative stress*

Carcinogenesis start-up and progression is limited by the antioxidant properties of selenoproteins. SeMet is capable of suppressing the negative effects caused by oxidative damage of hydrogen peroxide by increasing GPx activity (57).

*Angiogenesis inhibition and metastasis*

Selenols and selenites can inhibit the expression and secretion of vascular endothelial growth factor (VEGF) and of matrix metalloproteinase-2 (MMP-2) (58). In C57BL/6 murine model metastasis was inhibited by selenite by cell cycle arrest and apoptosis induction (59,60)

*DNA repair*

SeMet induces a DNA repair response and protects normal human fibroblasts from DNA damage. Tumor suppressor gene p53 is modulated by selenium containing compounds by redox modifications (61).

*Apoptosis and cell cycle arrest*

The mechanisms by which selenium containing molecules induce apoptosis are various, from caspase activation to p53 phosphorylation and reactive oxygen species (ROS). For example, sodium selenite produces S/G<sub>2</sub>M arrest with apoptosis not dependent from caspases (62). On the other hand, methylselenol precursor compounds cause G1 arrest and caspase dependent apoptosis (63).

### 3. LEISHMANIASIS

Leishmaniasis are a group of diseases caused by >20 species of flagellated protozoa that belong to the genus *Leishmania*. Those protozoan parasites spread by the bite of phlebotomies sandflies (64). Leishmaniasis is categorized by the WHO as a neglected tropical disease since it affects mainly low-middle-income countries un regions with tropical climate.

There are three main forms of the disease, depending on the species of the infectious parasite, the host genotype, the vector and of social and environmental factors. Those forms range from asymptomatic diseases to affection to vital organs. Most common classification of the diseases are:

- Visceral leishmaniasis (VL) or kala-azar: most serious and is almost always fatal if untreated. Mainly characterized by spleen and liver enlargement, irregular bouts of fever, weight loss and anemia. In some classifications, it also includes the post kala-azar dermal leishmaniasis (PKDL), a syndrome that represents one of the major parasite reservoir.
- Cutaneous leishmaniasis (CL): most common form of the disease. CL is characterized by the development of an ulcerative skin lesion. Although the clinical features of CL can vary because of different causative species, a classical lesion starts as a papule or nodule at the site of parasite inoculation and slowly expand. The effects are ulcers on exposed parts of the body, leaving life-long scars and serious disability. One of the main social repercussions of VL is margination due to physical appearance (65).
- Mucocutaneous leishmaniasis (MCL): derived from CL due to the spreading ability to mucosal tissue in the mouth and upper respiratory tract by lymphatic or haematogenous dissemination. This disease is typically resistant to treatment and patients usually die due to secondary infections or malnutrition.

*Leishmania* organisms have a life cycle characterized by two stages: the flagellated mobile promastigotes located in the midgut of the sandfly vector and the amastigote form within macrophages of the vertebrate host (66). Biological cycle summarized in **Figure 19** starts by the inoculation of the promastigote form by the infected female sandflies into the skin. Parasites are phagocytosed by macrophages of the vertebrate host where they survive inside the phagolysosomes. Transformation takes place in 12-24 h time into amastigotes that rapidly grow inside the phagolysosome. When these infected macrophages are acquired by the sandfly while taking a blood meal they develop to dividing procyclic promastigotes. Though metacyclogenesis those noninfective promastigotes acquire virulence in the form of metacyclic nondividing form.

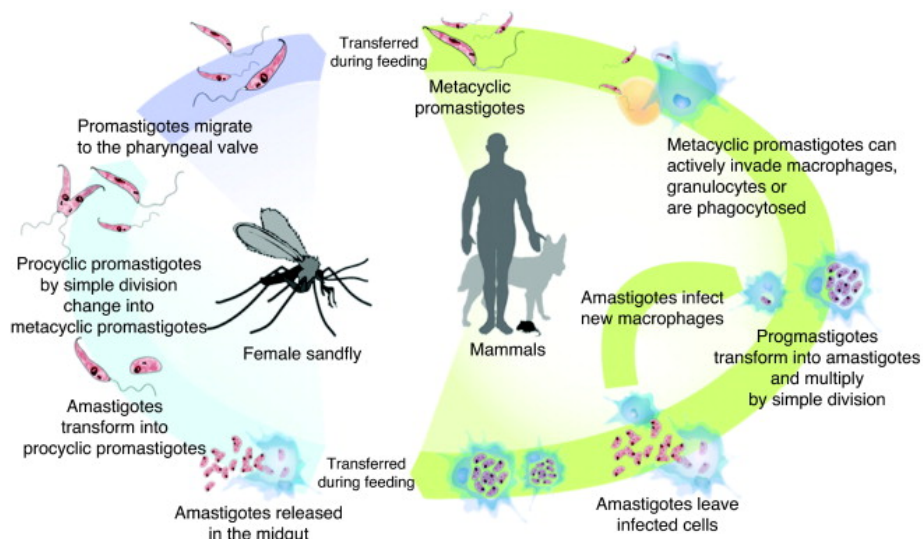


Figure 19. *Leishmania* spp. life cycle (67).

### 3.1. Epidemiology

Leishmaniasis affects some of the poorest populations of the globe due to its association to malnutrition, immune system weakness and lack of resources. In 2015 87 countries were considered by WHO as endemic for CL and 75 for VL (68). Geographical distribution is shown in **Figure 20** were endemic countries for CL are shown in **Figure 19a** and for VL in **Figure 19b**.

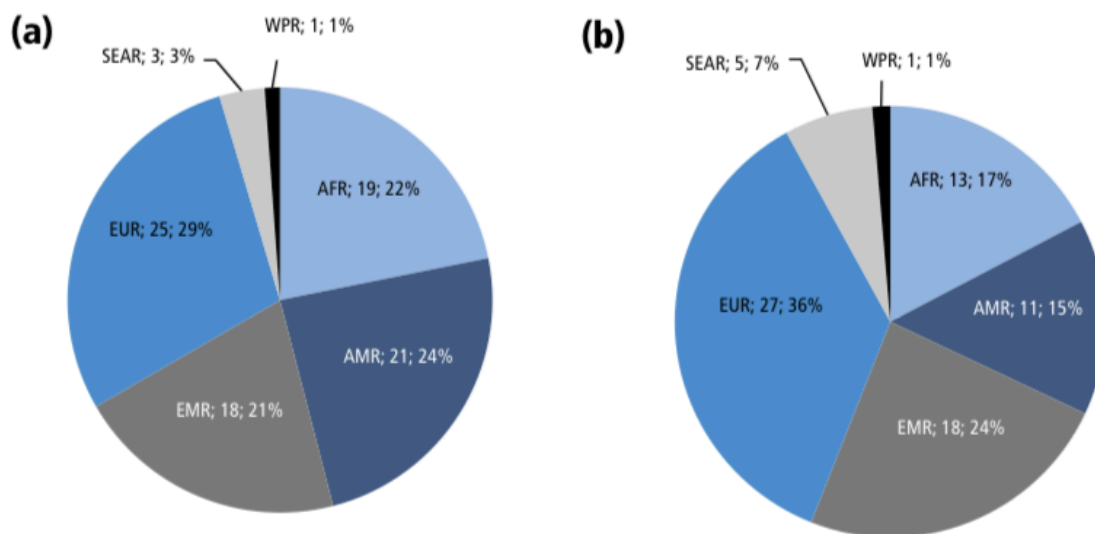
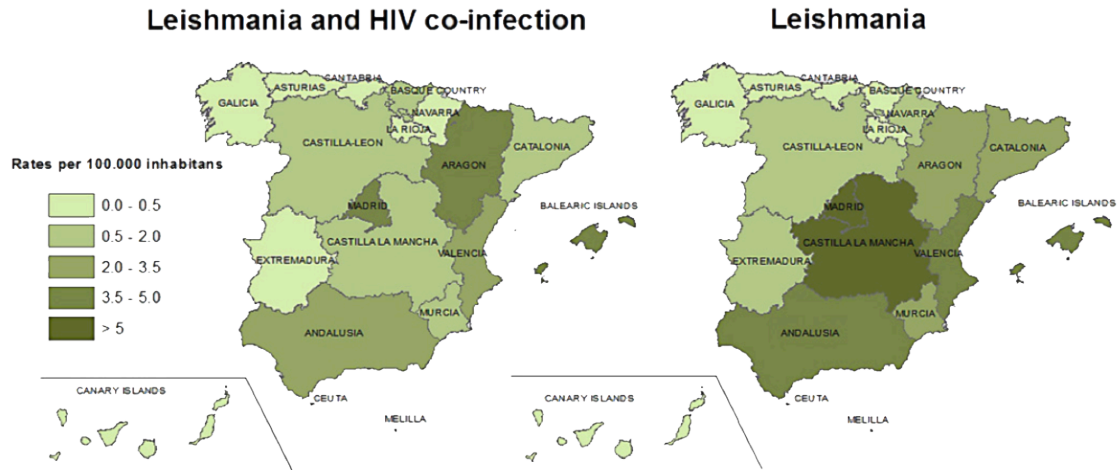


Figure 20. Number of endemic countries for leishmaniasis. WHO regions: AFR: African Region, AMR: Region of the Americas, EMR: Eastern Mediterranean Region, EUR: European Region, SEAR: South East Asia Region, WPR: Western Pacific Region (68).

Annually 1.3 million new cases are diagnosed worldwide. The estimated number of deaths range from 20,000 to 50,000 annually. The collection of data is difficult since in only 34% of endemic countries its report is compulsory. Its expansion has been exponential in the past two decades. Coinfection with *Leishmania* and HIV increases VL susceptibility, this factor was reported by 35 of the endemic countries in 2015 (69).

In Spain leishmaniasis is endemic in most of its territory **Figure 21**, the main species is *Leishmania infantum* and the detected vectors are *Phlebotomus perniciosus* and *P. ariasi*. The main reservoir host in our country is the dog. A change in the clinical pattern has been observed with other co-morbidities associated such as type 2 diabetes or subjects receiving therapy for autoimmune diseases (70).



**Figure 21.** Rates of hospitalizations in Spanish territory with leishmaniasis as first diagnosis.

### 3.2. Treatments

Drugs used currently for the treatment of leishmaniasis encompass important disadvantages such as toxicity, high economical costs and low adherence to treatment. *Leishmania* has the ability to develop resistance which makes the development of new molecules that are long-term reliable, safe and of easy administration compulsory. The most used drugs for leishmaniasis treatment are:

#### *Pentavalent urea stibamine derivatives*

Most common treatments for CL and VL in many endemic countries. Their mechanism of action is dual, molecular process effect in the parasite as well as macrophage parasitocidal activity. Two main formulations are available: meglumine antimoniate (Glucantime ®) and sodium stibogluconate (Pentostam ®) (**Figure 22**). Due to their accumulation in tissue they cause cardiotoxicity, pancreatitis and acute nephrotoxicity. Resistances are common, efficacy ranges to 35% to 95% depending on the geographical area studied (71,72).

#### *Amphotericin B*

It is a polyene antifungal antibiotic agent (**Figure 22**) which selectively inhibits the membrane synthesis of the parasite and causes pores in the membrane, leading to parasite death. Nephrotoxicity and heat instability even with the newest formulations limit the use even though pharmacokinetic properties have been enhanced (71,73).

#### *Pentamidine*

Drug (**Figure 22**) that interferes with macromolecule synthesis (DNA, RNA, phospholipids and proteins) (74). Its high toxicity and resistant strains limit its use (71).

*Alkylphosphocholine analogues*

Miltefosine (**Figure 22**) was used at first because of its antineoplastic activity. As disadvantages, it is teratogenic and treatment lasts 28 days which limits patient compliance. Edelfosine has anti-inflammatory properties which palliates one of the main cause for the symptomatology.

*Paromomycin*

Aminoglycoside antibiotic (**Figure 22**) that has proven antileishmanial activity since 1960s, its action mechanism targets *Leishmania*'s ribosome inhibiting protein synthesis. Severe nephrotoxicity, ototoxicity and hepatotoxicity are the main shortcomings for this treatment (71,74).

*Sitamaquine*

Its molecular targets are still unknown but recent *in vitro* parasite evaluation confirmed the antileishmanial properties of sitamaquine dihydrochloride (**Figure 22**) against a range of *Leishmania* species responsible for either CL or VL (75).

*TryR inhibitors*

TryR is an essential enzyme for parasite survival and infective properties, it regulates the redox balance as parasites lack glutathione peroxidase/reductase system. The blockage of this enzyme leads to parasite death (76). An example of these derivatives is trans-dehydrocrotonin (**Figure 22**).

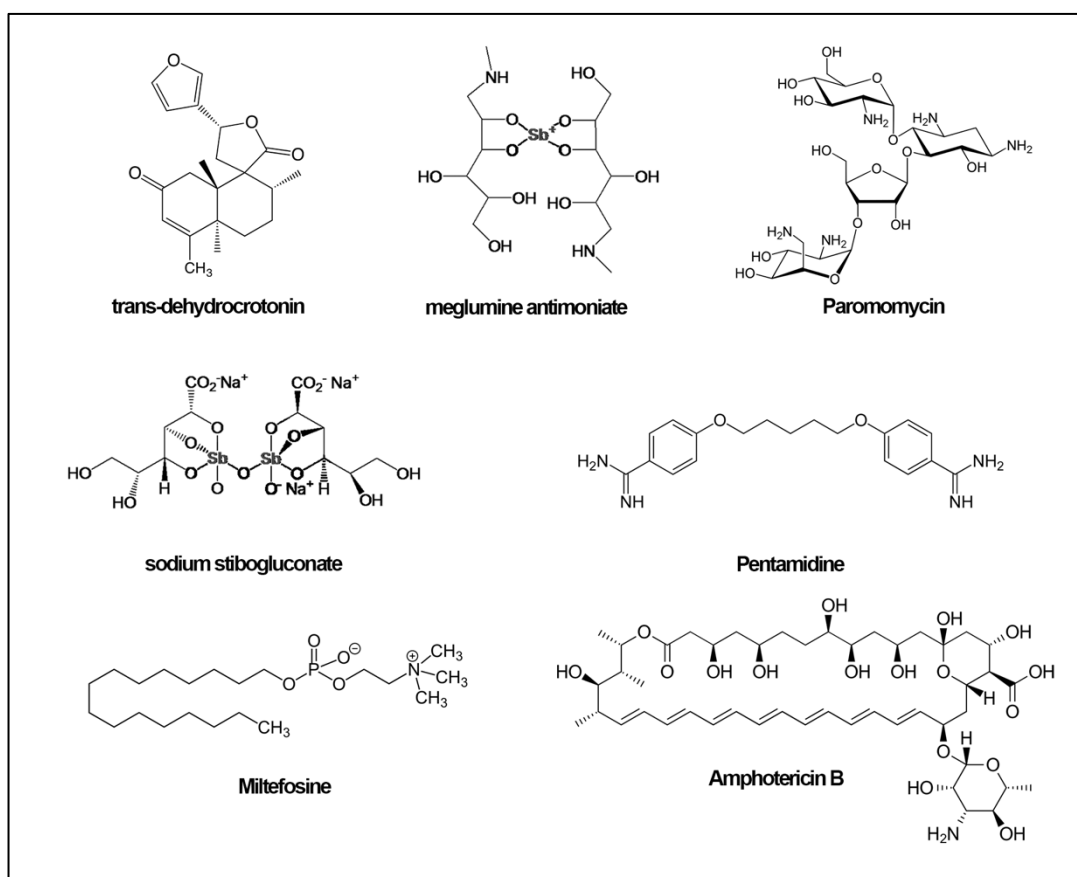


**Figure 21.** Chemical structures of some of the leishmanicidal drugs.

### 3.3. Leishmaniasis and cancer

Cancer and leishmaniasis may seem very apart in terms of biological similarities but they share some common biochemical pathways and enzymes. Both diseases are apoptosis resistant and have unlimited proliferation ability, can avoid immune response and can migrate from a primary area to other body areas (77,78).

Some antitumor drugs have proven leishmanicidal activity, miltefosine was one of the first described dual agents (79). Receptor blockage of tyrosine kinases crucial in tumor development modulation also improves immune response against *Leishmania* parasite (80) some drug examples are unitinib, sorafenib and lapatinib (81).

New synthesis structures with this dual activity are numerous: dihydroartemisinin and dihydroartemisinin acetal dimers (82), seco-cyclopropylpyrido[e]indolone analog (83), 2-phenoxy-1,4-naphthoquinones (84)...

Mechanistically this duality may be explained by CDK inhibition present in both diseases, common metabolic pathways, immune response activation, apoptosis induction and growth inhibition (78).

### 3.4. Leishmaniasis and selenium

Various studies have proven the important role of Se in macrophage functions, Se supplementation in *in vitro* studies enhances phagocytosis and superoxide production besides cytokine liberation. Immune system modulation has also been proven for Se, low levels of Se are related with a loss in neutrophil destruction potential. Those effects are caused by GPx inhibition leading to a ROS accumulation (85).

As a consequence, Se levels influencing immune response relates to trypanosomiasis parasitemia and anemia reduction. The oxidative stress due to GPx inhibition is caused by an accumulation of hydrogen peroxide and has been found in VL patients with low Se blood levels (86).

The *Leishmania* genome codes for three selenoproteins, homologs of mammalian SelK, SelT and SelTryp, a multidomain selenoprotein. SelTryp has no homologs in human host and therefore is Kinetoplastida-specific turning this selenoprotein into a very interesting drug target. Its function is still not clear but seems to be redox-balance related. Therefore, parasites depend on Se and that this trace element has a vital role in their survival (87).

#### 4. BIBLIOGRAPHY

1. What is cancer? cancer.gov2015 [Available from: <https://www.cancer.gov/about-cancer/understanding/what-is-cancer>].
2. Fact sheet n° 297: [www.who.org](http://www.who.org); 2013.
3. Hanahan D, Weinberg RA. Hallmarks of cancer: The next generation. *Cell*. **2011**;144(5):646-674.
4. Farmer P, Frenk J, Knaul FM, Shulman LN, Alleyne G, Armstrong L, et al. Expansion of cancer care and control in countries of low and middle income: A call to action. *Lancet*. **2010**;376(9747):1186-1193.
5. Bray F, Jemal A, Grey N, Ferlay J, Forman D. Global cancer transitions according to the human development index (2008-2030): A population-based study. *Lancet Oncol*. **2012**;13(8):790-801.
6. Torre LA, Bray F, Siegel RL, Ferlay J, Lortet-Tieulent J, Jemal A. Global cancer statistics, 2012. *CA Cancer J Clin*. **2015**;65(2):87-108.
7. Torre LA, Siegel RL, Ward EM, Jemal A. Global cancer incidence and mortality rates and trends--an update. *Cancer Epidemiol Biomarkers Prev*. **2016**;25(1):16-27.
8. Ferlay J, Soerjomataram I, Dikshit R, Eser S, Mathers C, Rebelo M, et al. Cancer incidence and mortality worldwide: Sources, methods and major patterns in globocan 2012. *Int J Cancer*. **2015**;136(5):E359-386.
9. Jemal A. The cancer atlas. Second edition. ed. Atlanta, Georgia: American Cancer Society/Health Promotion; 2015.
10. (SEOM) SEOM. Las cifras del cancer en españa 2017 2017
11. Vineis P, Wild CP. Global cancer patterns: Causes and prevention. *Lancet*. **2014**;383(9916):549-557.
12. Treatment types [www.cancer.org](http://www.cancer.org): American Cancer Society; 2017 [Available from: <https://www.cancer.org/treatment/treatments-and-side-effects/treatment-types.html>].
13. Perez-Herrero E, Fernandez-Medarde A. Advanced targeted therapies in cancer: Drug nanocarriers, the future of chemotherapy. *Eur J Pharm Biopharm*. **2015**;93:52-79.
14. Afghahi A, Sledge GW, Jr. Targeted therapy for cancer in the genomic era. *Cancer J*. **2015**;21(4):294-298.
15. Airley R. Cancer chemotherapy. Chichester, UK ; Hoboken, NJ: Wiley-Blackwell; 2009. x, 341 p., 348 p. of plates p.
16. Puyo S, Montaudon D, Pourquier P. From old alkylating agents to new minor groove binders. *Crit Rev Oncol Hematol*. **2014**;89(1):43-61.
17. Aristil P. Manual.De.Farmacologia.Basica.Y.Clinica: McGrawHil; 2010. 338 p.
18. Domenech E, Malumbres M. Mitosis-targeting therapies: A troubleshooting guide. *Curr Opin Pharmacol*. **2013**;13(4):519-528.
19. Vermeulen K, Van Bockstaele DR, Berneman ZN. The cell cycle: A review of regulation, deregulation and therapeutic targets in cancer. *Cell Prolif*. **2003**;36(3):131-149.



20. Kroemer G, El-Deiry WS, Golstein P, Peter ME, Vaux D, Vandenabeele P, et al. Classification of cell death: Recommendations of the nomenclature committee on cell death. *Cell Death Differ.* **2005**;12 Suppl 2:1463-1467.
21. Galluzzi L, Vitale I, Aaronson SA, Abrams JM, Adam D, Agostinis P, et al. Molecular mechanisms of cell death: Recommendations of the nomenclature committee on cell death 2018. *Cell Death Differ.* **2018**;25(3):486-541.
22. Kroemer G, Galluzzi L, Vandenabeele P, Abrams J, Alnemri ES, Baehrecke EH, et al. Classification of cell death: Recommendations of the nomenclature committee on cell death 2009. *Cell Death Differ.* **2009**;16(1):3-11.
23. de Vries EG, Gietema JA, de Jong S. Tumor necrosis factor-related apoptosis-inducing ligand pathway and its therapeutic implications. *Clin Cancer Res.* **2006**;12(8):2390-2393.
24. Fulda S, Kogel D. Cell death by autophagy: Emerging molecular mechanisms and implications for cancer therapy. *Oncogene.* **2015**;34(40):5105-5113.
25. Fuchs Y, Steller H. Live to die another way: Modes of programmed cell death and the signals emanating from dying cells. *Nat Rev Mol Cell Biol.* **2015**;16(6):329-344.
26. Vermeulen K, Van Bockstaele DR, Berneman ZN. Apoptosis: Mechanisms and relevance in cancer. *Ann Hematol.* **2005**;84(10):627-639.
27. Vucic D, Dixit VM, Wertz IE. Ubiquitylation in apoptosis: A post-translational modification at the edge of life and death. *Nat Rev Mol Cell Biol.* **2011**;12(7):439-452.
28. Li J, Yuan J. Caspases in apoptosis and beyond. *Oncogene.* **2008**;27(48):6194-6206.
29. Zhi X, Zhong Q. Autophagy in cancer. *Prime Rep.* **2015**;7:18.
30. Hofius D, Munch D, Bressendorff S, Mundy J, Petersen M. Role of autophagy in disease resistance and hypersensitive response-associated cell death. *Cell Death Differ.* **2011**;18(8):1257-1262.
31. Petibone DM, Majeed W, Casciano DA. Autophagy function and its relationship to pathology, clinical applications, drug metabolism and toxicity. *J Appl Toxicol.* **2017**;37(1):23-37.
32. White E. The role for autophagy in cancer. *J Clin Invest.* **2015**;125(1):42-46.
33. Durgan J, Florey O. Cancer cell cannibalism: Multiple triggers emerge for entosis. *Biochim Biophys Acta.* **2018**;1865(6):831-841.
34. Kieliszek M, Blazejak S. Selenium: Significance, and outlook for supplementation. *Nutrition.* **2013**;29(5):713-718.
35. Rayman MP. Food-chain selenium and human health: Emphasis on intake. *Br J Nutr.* **2008**;100(2):254-268.
36. NIH. Selenium. Dietary supplement fact sheet nih.gov: NIH; 2016 [Available from: <https://ods.od.nih.gov/factsheets/Selenium-HealthProfessional/>].
37. Rayman MP, Combs GF, Jr., Waters DJ. Selenium and vitamin e supplementation for cancer prevention. *JAMA.* **2009**;301(18):1876; author reply 1877.
38. Lopez-Bellido Garrido FJ, Lopez Bellido L. Selenium and health; reference values and current status of spanish population. *Nutr Hosp.* **2013**;28(5):1396-1406.
39. Weekley CM, Aitken JB, Finney L, Vogt S, Witting PK, Harris HH. Selenium metabolism in cancer cells: The combined application of xas and xfm techniques to

- the problem of selenium speciation in biological systems. *Nutrients*. **2013**;5(5):1734-1756.
40. Roman M, Jitaru P, Barbante C. Selenium biochemistry and its role for human health. *Metallomics*. **2014**;6(1):25-54.
  41. Weekley CM, Harris HH. Which form is that? The importance of selenium speciation and metabolism in the prevention and treatment of disease. *Chem Soc Rev*. **2013**;42(23):8870-8894.
  42. Fernandes AP, Gandin V. Selenium compounds as therapeutic agents in cancer. *Biochim Biophys Acta*. **2015**;1850(8):1642-1660.
  43. Brozmanova J, Manikova D, Vlckova V, Chovanec M. Selenium: A double-edged sword for defense and offence in cancer. *Arch Toxicol*. **2010**;84(12):919-938.
  44. Kipp AP, Strohm D, Brigelius-Flohe R, Schomburg L, Bechthold A, Leschik-Bonnet E, et al. Revised reference values for selenium intake. *J Trace Elem Med Biol*. **2015**;32:195-199.
  45. Benstoem C, Goetzenich A, Kraemer S, Borosch S, Manzanares W, Hardy G, et al. Selenium and its supplementation in cardiovascular disease--what do we know? *Nutrients*. **2015**;7(5):3094-3118.
  46. Wrobel JK, Power R, Toborek M. Biological activity of selenium: Revisited. *IUBMB Life*. **2016**;68(2):97-105.
  47. Chen J. An original discovery: Selenium deficiency and keshan disease (an endemic heart disease). *Asia Pac J Clin Nutr*. **2012**;21(3):320-326.
  48. Jirong Y, Huiyun P, Zhongzhe Y, Birong D, Weimin L, Ming Y, et al. Sodium selenite for treatment of kashin-beck disease in children: A systematic review of randomised controlled trials. *Osteoarthritis Cartilage*. **2012**;20(7):605-613.
  49. Dumont JE, Corvilain B, Contempre B. The biochemistry of endemic cretinism: Roles of iodine and selenium deficiency and goitrogens. *Mol Cell Endocrinol*. **1994**;100(1-2):163-166.
  50. Rayman MP. Selenium and human health. *Lancet*. **2012**;379(9822):1256-1268.
  51. Hoffmann FW, Hashimoto AC, Shafer LA, Dow S, Berry MJ, Hoffmann PR. Dietary selenium modulates activation and differentiation of cd4+ t cells in mice through a mechanism involving cellular free thiols. *J Nutr*. **2010**;140(6):1155-1161.
  52. Rayman MP, Infante HG, Sargent M. Food-chain selenium and human health: Spotlight on speciation. *Br J Nutr*. **2008**;100(2):238-253.
  53. Benton D. Selenium intake, mood and other aspects of psychological functioning. *Nutr Neurosci*. **2002**;5(6):363-374.
  54. Flores-Mateo G, Navas-Acien A, Pastor-Barruso R, Guallar E. Selenium and coronary heart disease: A meta-analysis. *Am J Clin Nutr*. **2006**;84(4):762-773.
  55. Combs GF, Jr., Gray WP. Chemopreventive agents: Selenium. *Pharmacol Ther*. **1998**;79(3):179-192.
  56. Nicastro HL, Dunn BK. Selenium and prostate cancer prevention: Insights from the selenium and vitamin e cancer prevention trial (select). *Nutrients*. **2013**;5(4):1122-1148.
  57. Hatfield DL, Tsuji PA, Carlson BA, Gladyshev VN. Selenium and selenocysteine: Roles in cancer, health, and development. *Trends Biochem Sci*. **2014**;39(3):112-120.

58. Jiang C, Ganther H, Lu J. Monomethyl selenium-specific inhibition of mmp-2 and vegf expression: Implications for angiogenic switch regulation. *Mol Carcinog.* **2000**;29(4):236-250.
59. Chen YC, Prabhu KS, Das A, Mastro AM. Dietary selenium supplementation modifies breast tumor growth and metastasis. *Int J Cancer.* **2013**;133(9):2054-2064.
60. Song H, Hur I, Park HJ, Nam J, Park GB, Kong KH, et al. Selenium inhibits metastasis of murine melanoma cells through the induction of cell cycle arrest and cell death. *Immune Netw.* **2009**;9(6):236-242.
61. Seo YR, Kelley MR, Smith ML. Selenomethionine regulation of p53 by a ref1-dependent redox mechanism. *Proc Natl Acad Sci U S A.* **2002**;99(22):14548-14553.
62. Li GX, Hu H, Jiang C, Schuster T, Lu J. Differential involvement of reactive oxygen species in apoptosis induced by two classes of selenium compounds in human prostate cancer cells. *Int J Cancer.* **2007**;120(9):2034-2043.
63. Zeng H, Wu M, Botnen JH. Methylselenol, a selenium metabolite, induces cell cycle arrest in g1 phase and apoptosis via the extracellular-regulated kinase 1/2 pathway and other cancer signaling genes. *J Nutr.* **2009**;139(9):1613-1618.
64. WHO. Leishmaniasis 2017 [Available from: <http://www.who.int/leishmaniasis/disease/en/>].
65. Bhandari V, Kulshrestha A, Deep DK, Stark O, Prajapati VK, Ramesh V, et al. Drug susceptibility in leishmania isolates following miltefosine treatment in cases of visceral leishmaniasis and post kala-azar dermal leishmaniasis. *PLoS Negl Trop Dis.* **2012**;6(5):e1657.
66. Van Assche T, Deschacht M, da Luz RA, Maes L, Cos P. Leishmania-macrophage interactions: Insights into the redox biology. *Free Radic Biol Med.* **2011**;51(2):337-351.
67. Harhay MO, Olliaro PL, Costa DL, Costa CH. Urban parasitology: Visceral leishmaniasis in brazil. *Trends Parasitol.* **2011**;27(9):403-409.
68. WHO. Weekly epidemiological record. Weekly [Internet]. 2017; (38):[557-572 pp.].
69. WHO. Investing to overcome the global impact of neglected tropical diseases. Third who report on neglected tropical diseases. **2015**.
70. Herrador Z, Gherasim A, Jimenez BC, Granados M, San Martin JV, Aparicio P. Epidemiological changes in leishmaniasis in spain according to hospitalization-based records, 1997-2011: Raising awareness towards leishmaniasis in non-hiv patients. *PLoS Negl Trop Dis.* **2015**;9(3):e0003594.
71. de Menezes JP, Guedes CE, Petersen AL, Fraga DB, Veras PS. Advances in development of new treatment for leishmaniasis. *Biomed Res Int.* **2015**;2015:815023.
72. Pace D. Leishmaniasis. *J Infect.* **2014**;69 Suppl 1:S10-18.
73. Chattopadhyay A, Jafurulla M. A novel mechanism for an old drug: Amphotericin b in the treatment of visceral leishmaniasis. *Biochem Biophys Res Commun.* **2011**;416(1-2):7-12.
74. McGwire BS, Satoskar AR. Leishmaniasis: Clinical syndromes and treatment. *QJM.* **2014**;107(1):7-14.
75. Kobets T, Grekov I, Lipoldova M. Leishmaniasis: Prevention, parasite detection and treatment. *Curr Med Chem.* **2012**;19(10):1443-1474.

76. Walton JG, Jones DC, Fau - Kiuru P, Kiuru P Fau - Durie AJ, Durie AJ Fau - Westwood NJ, Westwood NJ Fau - Fairlamb AH, Fairlamb AH. Synthesis and evaluation of indatraline-based inhibitors for trypanothione reductase. (1860-7187 (Electronic)).
77. Fuertes MA, Nguewa PA, Castilla J, Alonso C, Perez JM. Anticancer compounds as leishmanicidal drugs: Challenges in chemotherapy and future perspectives. *Curr Med Chem.* **2008**;15(5):433-439.
78. Dorosti Z, Yousefi M, Sharafi SM, Darani HY. Mutual action of anticancer and antiparasitic drugs: Are there any shared targets? *Future Oncol.* **2014**;10(15):2529-2539.
79. Eibl H, Unger C. Hexadecylphosphocholine: A new and selective antitumor drug. *Cancer Treat Rev.* **1990**;17(2-3):233-242.
80. Dalton JE, Maroof A, Owens BM, Narang P, Johnson K, Brown N, et al. Inhibition of receptor tyrosine kinases restores immunocompetence and improves immune-dependent chemotherapy against experimental leishmaniasis in mice. *J Clin Invest.* **2010**;120(4):1204-1216.
81. Sanderson L, Yardley V, Croft SL. Activity of anti-cancer protein kinase inhibitors against leishmania spp. *J Antimicrob Chemother.* **2014**;69(7):1888-1891.
82. Galal AM, Gul W, Slade D, Ross SA, Feng S, Hollingshead MG, et al. Synthesis and evaluation of dihydroartemisinin and dihydroartemisinin acetal dimers showing anticancer and antiprotozoal activity. *Bioorg Med Chem.* **2009**;17(2):741-751.
83. Chavda S, Babu B, Yanow SK, Jardim A, Spithill TW, Kiakos K, et al. A novel achiral seco-cyclopropylpyrido[e]indolone (cpyi) analog of cc-1065 and the duocarmycins: Synthesis, DNA interactions, in vivo anticancer and anti-parasitic evaluation. *Bioorg Med Chem.* **2010**;18(14):5016-5024.
84. Prati F, Bergamini C, Molina MT, Falchi F, Cavalli A, Kaiser M, et al. 2-phenoxy-1,4-naphthoquinones: From a multitarget antitrypanosomal to a potential antitumor profile. *J Med Chem.* **2015**;58(16):6422-6434.
85. da Silva MT, Silva-Jardim I, Thiemann OH. Biological implications of selenium and its role in trypanosomiasis treatment. *Curr Med Chem.* **2014**;21(15):1772-1780.
86. Farzin L, Moassesi ME. A comparison of serum selenium, zinc and copper level in visceral and cutaneous leishmaniasis. *J Res Med Sci.* **2014**;19(4):355-357.
87. Lobanov AV, Gromer S, Salinas G, Gladyshev VN. Selenium metabolism in trypanosoma: Characterization of selenoproteomes and identification of a kinetoplast-specific selenoprotein. *Nucleic Acids Res.* **2006**;34(14):4012-4024.

**BACKGROUND**

---



## 1. ORGANOSELENIUM COMPOUNDS AS ANTITUMORAL AGENTS

Promising results have been described for cancer treatment in *in vitro* and *in vivo* studies (88). As previously described chemical form plays an important part in anticancer activity and a huge variety of selenium-containing chemical entities have been explored (42).

Some organoselenium compounds such as sodium selenite or ebselen are under phase I clinical studies (89). 2-phenyl-1,2-benzoisoselenazol-3(2*H*)-one (ebselen) (**Figure 22**) anti-inflammatory and antioxidant activities have been widely described. They are attributed to its capacity to inhibit glutathione peroxidase, reducing the ROS accumulation (90). Its antioxidant properties have proven protective effects on cardiovascular system (91), liver (92), kidney (93) and neurological system (94). Cytotoxicity for various tumor cell lines have been described in the past (95,96) and even though mechanism is still unclear data shows that apoptosis may play an important role in this compound's action (97).

In general terms inorganic Se compounds have genotoxic properties while organic structures containing Se are present better toleration to medical use (98). This fact leads to another strategy followed for drug design which is the inclusion of Se on organic structures with proven antitumor activity. This approach can be exemplified by isatin (*1H*-indole-2,3-dione) derivatives (**Figure 22**), Se introduction in the structure enhanced cytotoxic activity against breast, colon, lung and melanoma cell lines (99). Similar results were found for suberoylanilide hydroxamic acid (SAHA) derivatives (**Figure 22**) SelSA-1 and SelSA-2 in lung cancer cell lines (100).

Incorporation of Se to nonsteroidal anti-inflammatories such as acetylsalicylic acid (**Figure 22**) results in antitumor activities much more potent than those exhibited by the original compounds (101).

Taking into account the research group experience and the results found in the bibliography three main Se-containing moieties were selected to design and synthesize the molecules presented in this work.

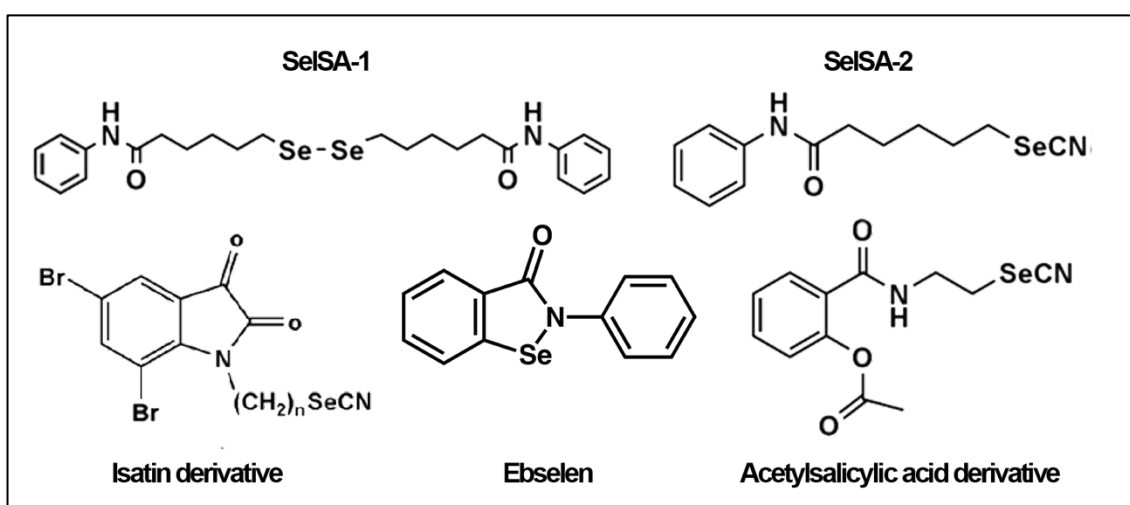


**Figure 22.** Se-containing structures with antitumoral activity derived from known cytotoxic fragments.

### 1.1. Diselenide derivatives

Diselenide compounds are characterized by their potent antioxidant properties protecting cells against oxidative damage. This activity has been attributed to the Se-Se bond mimicking disulphur bond present in GPxs and therefore protecting cells against ROS accumulation (102,103).

One of the most studied compounds containing this moiety is diphenyl diselenide (DPDS) (**Figure 23**). Among the protective DNA damage properties associated to this structure the following have been described: protection against tamoxifen (104) and of peroxynitrite-mediated cytotoxicity (105). DPDS has also enzyme modulation properties such as GPx, TrxR and CAT (106,107). DPDS is a substrate for TrxR which has proven neuroprotective effects on *in vivo* studies (108). Furthermore, DPDS has proven ability to promote apoptosis in human colon adenocarcinoma cell line HT-29 (109).

Other diselenide derivatives have exhibited mimetic GPx properties and reduced apoptosis such as 3'3-dipropionic acid (110,111) (**Figure 23**).

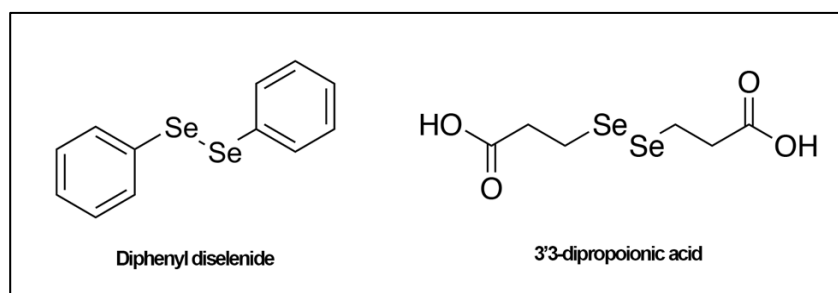


**Figure 23.** Structure of antitumoral diselenides.

### 1.2. Selenocyanate derivatives

Selenocyanates have proven chemopreventive and antitumoral activities. An example of this properties can be found for p-XCS (**Figure 24**), which has proven to reduce tumor incidence in colon, breast, lung, liver and intestine in murine models (112). This structure inhibits cell viability on prostate cancer (113), lung (114) and colon cancer by the modification of apoptosis regulatory pathways. *In vivo* studies have proven that this structure inhibits angiogenesis process in *in vivo* models (112).

Another selenocyanate derivative, diphenylmethyl selenocyanate (**Figure 24**) has a chemopreventive effect on skin tumors and phase II detoxifying enzymes (GST, catalase and SOD) activation as well as peroxidation inhibition in liver and skin (115). It also reduces toxicity caused by cisplatin and increments efficacy in murine models (116).



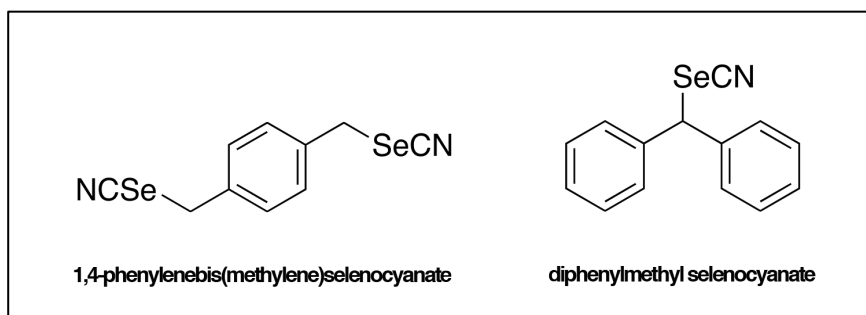


**Figure 24.** Structure of antitumoral selenocyanate.

### 1.3. Selenourea moiety

The urea vast bibliography data that reports this moiety as an interesting hydrogen-bond donor. Diarylureas have the ability to inhibit various kinases, for example sorafenib, an FDA approved drug for kidney tumor treatment that interferes with tyrosine kinase signaling (117). 1,3-disubstituted urea have proven antitumor properties (118), along with benzoyl ureas (119) and pyrazlyureas (120).

With the aim of enhancing the therapeutic potential of the urea group S has been included in this moiety to form thioureas that have the ability to interact with enzymes implicated in tumor progression pathways: topoisomerase, protein tyrosine kinase, somatostatin, sirtuins, and carbonic anhydrase (121).

The introduction of the Se homologs was also purposed in the form of selenourea moieties with the previous promising results in mind. Antioxidant and antiproliferative properties for selenourea derivatives has already been confirmed in some studies (122-124) (**Figure 25**).

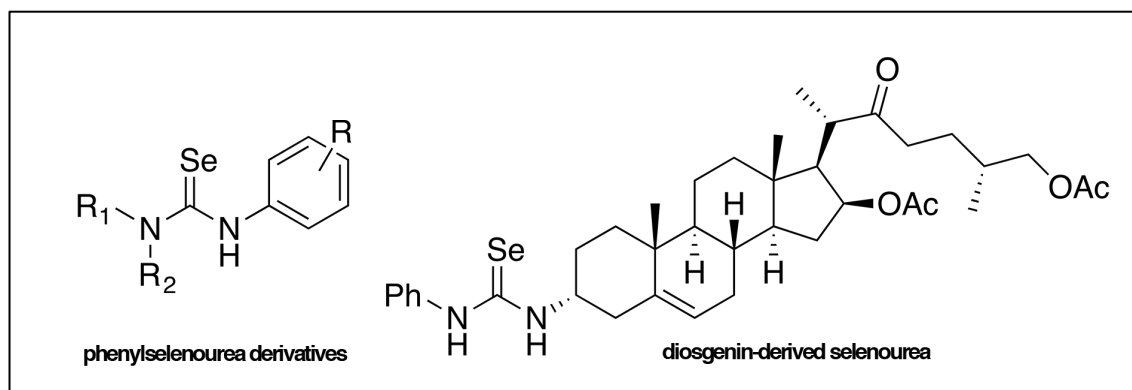


**Figure 25.** Structures for antiproliferative selenourea derivatives

## 2. SELENIUM COMPOUNDS AS LEISHMANICIDAL AGENTS

The use of organoselenium-containing compounds for the treatment of Leishmaniasis is a relatively new strategy and the background bibliography is not quite of the magnitude of the one reported for the antitumoural activity.

*In vitro* and *in vivo* effectiveness of selenium nanoparticles against *Leishmania major* have been used to treat localized lesions typical of CL (125). In a study referring *Leishmania tropica* in the promastigote and amastigote stages, promising inhibition rates were found. Moreover, infection rate of macrophages with promastigotes was mitigated when they were pre-treated with Se nanoparticles (126).

## 3. RESEARCH GROUP EXPERIENCE

Over the past decade the research group from the Organic and Pharmaceutical Organic Chemistry Department of the University of Navarra has focused efforts on the development of Se-containing molecules with anticancer and leishmanicidal activity with very promising results.

Some diphenyl diselenide derivatives have shown promising results in the anticancer area with autophagy induction in lung cancer cells (127) and broad spectrum antiproliferative activity was found for several cancer cell lines (128,129). Selenocyanate derived compounds have also exhibited interesting antitumor properties (128-130). Recently our group has published a comparative of thiourea derivatives against selenourea homologs where we confirmed that selenium-containing derivatives were much more potent (131) and as a result this moiety is included in the design of the studied derivatives of this work.

On the other hand, Se-containing molecules have also exhibited leishmanicidal activity, among those structures selenocyanate and diselenide moieties (132,133), selenosulphonamides (134) and imidocarbamates and methy-imidocarbamates (135,136).

Selenocyanates and diselenides are common in both diseases as the most promising structures and the objective of this work comes around those two structures alongside with selenourea group.

#### 4. BIBLIOGRAPHY

42. Fernandes AP, Gandin V. Selenium compounds as therapeutic agents in cancer. *Biochim Biophys Acta*. **2015**;1850(8):1642-1660.
88. Chen YC, Prabhu KS, Mastro AM. Is selenium a potential treatment for cancer metastasis? *Nutrients*. **2013**;5(4):1149-1168.
89. Brodin O, Eksborg S, Wallenberg M, Asker-Hagelberg C, Larsen EH, Mohlkert D, et al. Pharmacokinetics and toxicity of sodium selenite in the treatment of patients with carcinoma in a phase i clinical trial: The secar study. *Nutrients*. **2015**;7(6):4978-4994.
90. Muller A, Cadenas E, Graf P, Sies H. A novel biologically active seleno-organic compound--i. Glutathione peroxidase-like activity in vitro and antioxidant capacity of pz 51 (ebselen). *Biochem Pharmacol*. **1984**;33(20):3235-3239.
91. Chew P, Yuen DY, Stefanovic N, Pete J, Coughlan MT, Jandeleit-Dahm KA, et al. Antiatherosclerotic and renoprotective effects of ebselen in the diabetic apolipoprotein e/gpx1-double knockout mouse. *Diabetes*. **2010**;59(12):3198-3207.
92. Basarslan F, Yilmaz N, Davarci I, Akin M, Ozgur M, Yilmaz C, et al. Effects of ebselen on radiocontrast media-induced hepatotoxicity in rats. *Toxicol Ind Health*. **2013**;29(8):746-752.
93. Kizilgun M, Poyrazoglu Y, Oztas Y, Yaman H, Cakir E, Cayci T, et al. Beneficial effects of n-acetylcysteine and ebselen on renal ischemia/reperfusion injury. *Ren Fail*. **2011**;33(5):512-517.
94. Yin Z, Lee E, Ni M, Jiang H, Milatovic D, Rongzhu L, et al. Methylmercury-induced alterations in astrocyte functions are attenuated by ebselen. *Neurotoxicology*. **2011**;32(3):291-299.
95. Shi H, Liu S, Miyake M, Liu KJ. Ebselen induced c6 glioma cell death in oxygen and glucose deprivation. *Chem Res Toxicol*. **2006**;19(5):655-660.
96. Yang CF, Shen HM, Ong CN. Ebselen induces apoptosis in hepg(2) cells through rapid depletion of intracellular thiols. *Arch Biochem Biophys*. **2000**;374(2):142-152.
97. Zhang L, Zhou L, Du J, Li M, Qian C, Cheng Y, et al. Induction of apoptosis in human multiple myeloma cell lines by ebselen via enhancing the endogenous reactive oxygen species production. *Biomed Res Int*. **2014**;2014:696107.
98. Sanmartin C, Plano D, Sharma AK, Palop JA. Selenium compounds, apoptosis and other types of cell death: An overview for cancer therapy. *Int J Mol Sci*. **2012**;13(8):9649-9672.
99. Krishnegowda G, Prakasha Gowda AS, Tagaram HR, Carroll KF, Irby RB, Sharma AK, et al. Synthesis and biological evaluation of a novel class of isatin analogs as dual inhibitors of tubulin polymerization and akt pathway. *Bioorg Med Chem*. **2011**;19(20):6006-6014.
100. Karelia N, Desai D, Hengst JA, Amin S, Rudrabhatla SV, Yun J. Selenium-containing analogs of saha induce cytotoxicity in lung cancer cells. *Bioorg Med Chem Lett*. **2010**;20(22):6816-6819.
101. Plano D, Karelia DN, Pandey MK, Spallholz JE, Amin S, Sharma AK. Design, synthesis, and biological evaluation of novel selenium (se-nsaid) molecules as anticancer agents. *J Med Chem*. **2016**;59(5):1946-1959.

102. Orian L, Toppo S. Organochalcogen peroxidase mimetics as potential drugs: A long story of a promise still unfulfilled. *Free Radic Biol Med.* **2014**;66:65-74.
103. Stefanello ST, Prestes AS, Ogunmoyole T, Salman SM, Schwab RS, Brender CR, et al. Evaluation of in vitro antioxidant effect of new mono and diselenides. *Toxicol In Vitro.* **2013**;27(5):1433-1439.
104. Melo MT, de Oliveira IM, Grivicich I, Guecheva TN, Saffi J, Henriques JA, et al. Diphenyl diselenide protects cultured mcf-7 cells against tamoxifen-induced oxidative DNA damage. *Biomed Pharmacother.* **2013**;67(4):329-335.
105. Fiuza B, Subelzu N, Calcerrada P, Straliozzo MR, Piacenza L, Cassina A, et al. Impact of sin-1-derived peroxynitrite flux on endothelial cell redox homeostasis and bioenergetics: Protective role of diphenyl diselenide via induction of peroxiredoxins. *Free Radic Res.* **2015**;49(2):122-132.
106. Dobrachinski F, da Silva MH, Tassi CL, de Carvalho NR, Dias GR, Golombieski RM, et al. Neuroprotective effect of diphenyl diselenide in a experimental stroke model: Maintenance of redox system in mitochondria of brain regions. *Neurotox Res.* **2014**;26(4):317-330.
107. Glaser V, Moritz B, Schmitz A, Dafre AL, Nazari EM, Rauh Muller YM, et al. Protective effects of diphenyl diselenide in a mouse model of brain toxicity. *Chem Biol Interact.* **2013**;206(1):18-26.
108. de Freitas AS, Rocha JB. Diphenyl diselenide and analogs are substrates of cerebral rat thioredoxin reductase: A pathway for their neuroprotective effects. *Neurosci Lett.* **2011**;503(1):1-5.
109. Nedel F, Campos VF, Alves D, McBride AJ, Dellagostin OA, Collares T, et al. Substituted diaryl diselenides: Cytotoxic and apoptotic effect in human colon adenocarcinoma cells. *Life Sci.* **2012**;91(9-10):345-352.
110. Kunwar A, Mishra B, Barik A, Kumbhare LB, Pandey R, Jain VK, et al. 3,3'-diselenodipropionic acid, an efficient peroxy radical scavenger and a gpx mimic, protects erythrocytes (rbc) from aaph-induced hemolysis. *Chem Res Toxicol.* **2007**;20(10):1482-1487.
111. Kunwar A, Bag PP, Chattopadhyay S, Jain VK, Priyadarsini KI. Anti-apoptotic, anti-inflammatory, and immunomodulatory activities of 3,3'-diselenodipropionic acid in mice exposed to whole body gamma-radiation. *Arch Toxicol.* **2011**;85(11):1395-1405.
112. Nogueira CW, Zeni G, Rocha JB. Organoselenium and organotellurium compounds: Toxicology and pharmacology. *Chem Rev.* **2004**;104(12):6255-6285.
113. Facompre ND, El-Bayoumy K, Sun YW, Pinto JT, Sinha R. 1,4-phenylenebis(methylene)selenocyanate, but not selenomethionine, inhibits androgen receptor and akt signaling in human prostate cancer cells. *Cancer Prev Res (Phila).* **2010**;3(8):975-984.
114. El-Bayoumy K, Das A, Narayanan B, Narayanan N, Fiala ES, Desai D, et al. Molecular targets of the chemopreventive agent 1,4-phenylenebis (methylene)-selenocyanate in human non-small cell lung cancer. *Carcinogenesis.* **2006**;27(7):1369-1376.
115. Das RK, Bhattacharya S. Anti-tumour promoting activity of diphenylmethyl selenocyanate against two-stage mouse skin carcinogenesis. *Asian Pac J Cancer Prev.* **2005**;6(2):181-188.

116. Chakraborty P, Roy SS, Bhattacharya S. Molecular mechanism behind the synergistic activity of diphenylmethyl selenocyanate and cisplatin against murine tumor model. *Anticancer Agents Med Chem.* **2015**;15(4):501-510.
117. Wilhelm SM, Adnane L, Newell P, Villanueva A, Llovet JM, Lynch M. Preclinical overview of sorafenib, a multikinase inhibitor that targets both raf and vegf and pdgf receptor tyrosine kinase signaling. *Mol Cancer Ther.* **2008**;7(10):3129-3140.
118. Li HQ, Zhu TT, Yan T, Luo Y, Zhu HL. Design, synthesis and structure-activity relationships of antiproliferative 1,3-disubstituted urea derivatives. *Eur J Med Chem.* **2009**;44(2):453-459.
119. Li HQ, Lv PC, Yan T, Zhu HL. Urea derivatives as anticancer agents. *Anticancer Agents Med Chem.* **2009**;9(4):471-480.
120. Kennedy NJ, Cellurale C, Davis RJ. A radical role for p38 mapk in tumor initiation. *Cancer Cell.* **2007**;11(2):101-103.
121. Kumar V, Chimni SS. Recent developments on thiourea based anticancer chemotherapeutics. *Anticancer Agents Med Chem.* **2015**;15(2):163-175.
122. Romero-Hernandez LL, Merino-Montiel P, Montiel-Smith S, Meza-Reyes S, Vega-Baez JL, Abasolo I, et al. Diosgenin-based thio(seleno)ureas and triazolyl glycoconjugates as hybrid drugs. Antioxidant and antiproliferative profile. *Eur J Med Chem.* **2015**;99:67-81.
123. Neganova ME, Proshin AN, Redkozubova OM, Serkov IV, Serkova TP, Dubova LG, et al. N,n'-substituted selenoureas as polyfunctional antioxidants. *Bull Exp Biol Med.* **2016**;160(3):340-342.
124. Hussain RA, Badshah A, Pezzuto JM, Ahmed N, Kondratyuk TP, Park EJ. Ferrocene incorporated selenoureas as anticancer agents. *J Photochem Photobiol B.* **2015**;148:197-208.
125. Beheshti N, Soflaei S, Shakibaie M, Yazdi MH, Ghaffarifar F, Dalimi A, et al. Efficacy of biogenic selenium nanoparticles against leishmania major: In vitro and in vivo studies. *J Trace Elem Med Biol.* **2013**;27(3):203-207.
126. Mahmoudvand H, Shakibaie M, Tavakoli R, Jahanbakhsh S, Sharifi I. In vitro study of leishmanicidal activity of biogenic selenium nanoparticles against iranian isolate of sensitive and glucantime-resistant leishmania tropica. *Iran J Parasitol.* **2014**;9(4):452-460.
127. Diaz M, Gonzalez R, Plano D, Palop JA, Sanmartin C, Encio I. A diphenyldiselenide derivative induces autophagy via jnk in htb-54 lung cancer cells. *J Cell Mol Med.* **2017**.
128. Romano B, Plano D, Encio I, Palop JA, Sanmartin C. In vitro radical scavenging and cytotoxic activities of novel hybrid selenocarbamates. *Bioorg Med Chem.* **2015**;23(8):1716-1727.
129. Plano D, Baquedano Y, Ibanez E, Jimenez I, Palop JA, Spallholz JE, et al. Antioxidant-prooxidant properties of a new organoselenium compound library. *Molecules.* **2010**;15(10):7292-7312.
130. Alcolea V, Plano D, Encio I, Palop JA, Sharma AK, Sanmartin C. Chalcogen containing heterocyclic scaffolds: New hybrids with antitumoral activity. *Eur J Med Chem.* **2016**;123:407-418.
131. Alcolea V, Plano D, Karella DN, Palop JA, Amin S, Sanmartin C, et al. Novel seleno- and thio-urea derivatives with potent in vitro activities against several cancer cell lines. *Eur J Med Chem.* **2016**;113:134-144.

132. Plano D, Baquedano Y, Moreno-Mateos D, Font M, Jimenez-Ruiz A, Palop JA, et al. Selenocyanates and diselenides: A new class of potent antileishmanial agents. *Eur J Med Chem.* **2011**;46(8):3315-3323.
133. Baquedano Y, Alcolea V, Toro MA, Gutierrez KJ, Nguewa P, Font M, et al. Novel heteroaryl selenocyanates and diselenides as potent antileishmanial agents. *Antimicrob Agents Chemother.* **2016**;60(6):3802-3812.
134. Baquedano Y, Moreno E, Espuelas S, Nguewa P, Font M, Gutierrez KJ, et al. Novel hybrid selenosulfonamides as potent antileishmanial agents. *Eur J Med Chem.* **2014**;74:116-123.
135. Fernandez-Rubio C, Campbell D, Vacas A, Ibanez E, Moreno E, Espuelas S, et al. Leishmanicidal activities of novel methylseleno-imidocarbamates. *Antimicrob Agents Chemother.* **2015**;59(9):5705-5713.
136. Moreno D, Plano D, Baquedano Y, Jimenez-Ruiz A, Palop JA, Sanmartin C. Antileishmanial activity of imidothiocarbamates and imidoselenocarbamates. *Parasitol Res.* **2011**;108(1):233-239.

## **HYPOTHESIS AND OBJECTIVES**

---





With the data obtained by the exhaustive bibliography revision and the experience from our research group the next hypothesis is established for this work.

The structural modulation of selenium-containing structures with proven anticancer and leishmanicidal activity can enhance the biological activity in terms of potency and selectivity as cytotoxic and/or leishmanicidal agents. It is of special importance that selectivity indexes against cancer cell lines increase leading to a not only potent but highly selective action. The results obtained for the evaluation of those new derivatives would enable us to evaluate the proposed relationship between the biological pathways involved in cancer and leishmaniasis treatment.

Among the wide range of Se chemistry moieties explored by our research group, bis(4-aminophenyl)diselenide and 4-aminophenylselenocyanate (**Figure 26**) were selected as they have been proven to have cytotoxic and leishmanicidal potential. The chemical space covered by the modifications proposed on the structures should enable us a better understanding of the molecular basis behind their properties.

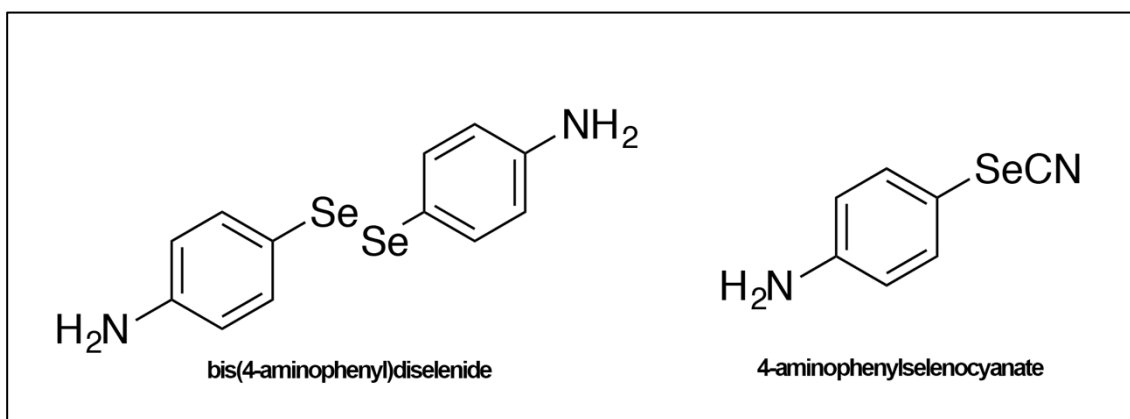


**Figure 26.** Start-up structures for this work.

Several strategies were followed, a fragment-based drug design strategy was applied for the design of bis(4-aminophenyl)diselenide derivatives. The inclusion selenourea moiety due to the antioxidant and antiproliferative properties already described in the background section and heterocycles with proven biological activity in the fields of cancer and leishmaniasis treatment. On the other hand, another series of derivatives was proposed with the aim of improving pharmacokinetic properties and to establish a comparison between diselenide and selenocyanate homologs.

The main objective of this work was to improve the potency and selectivity of the parent compounds bis(4-aminophenyl)diselenide and 4-aminophenylselenocyanate in their leishmanicidal and antitumor applications as exemplified in **Figure 27**.

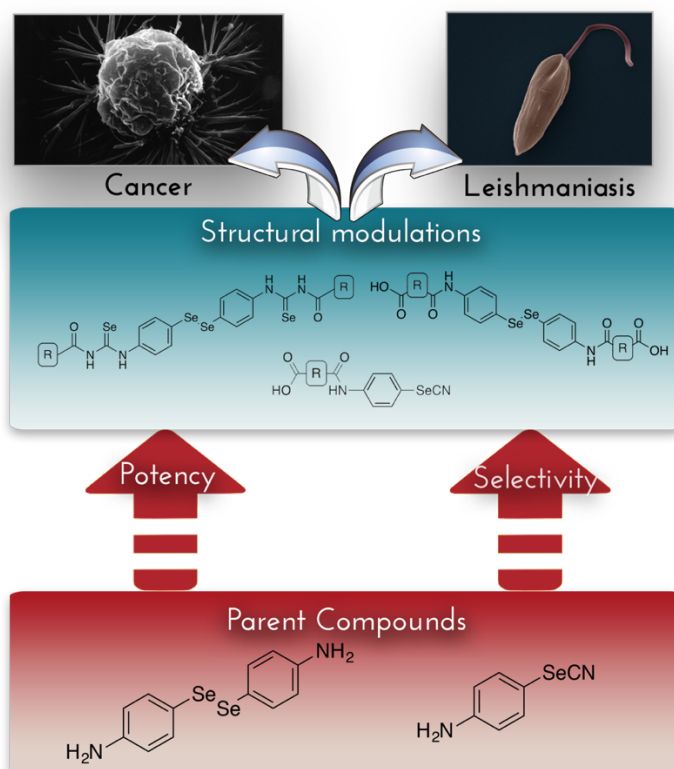


**Figure 27.** General objective graphical representation.

A series of specific objectives were programmed with the aim of demonstrating the hypothesis previously stated:

1. Design and synthesize of the new Se-containing derivatives with potential cytotoxic and leishmanicidal activities.
  - a. Elucidate unequivocally the structure of the novel derivatives and confirm required purity for biological evaluation is meet.
2. Evaluate the cytotoxic and cytostatic potential of the new structures and assess their selectivity for tumoral cells.
  - a. Compare structural modulation effects.
  - b. Compare new derivatives with parent structures.
3. Clarify the mechanism of action for the leader compounds on cancer cells.
  - a. Analyze their effect on cell cycle.
  - b. Evaluate their cell death induction potential.
  - c. Explore pathways that might be implicated.
4. Test the *in vitro* antileishmanial activity of the synthesized compounds and their selectivity.
5. Test the new derivative's ability to inhibit trypanothione reductase.
6. Asses possible drawbacks in drug development process due to stability.
7. Explore GPx mimetic determination methodologies.

## **RESULTS**

---



**PAPER 1**

---



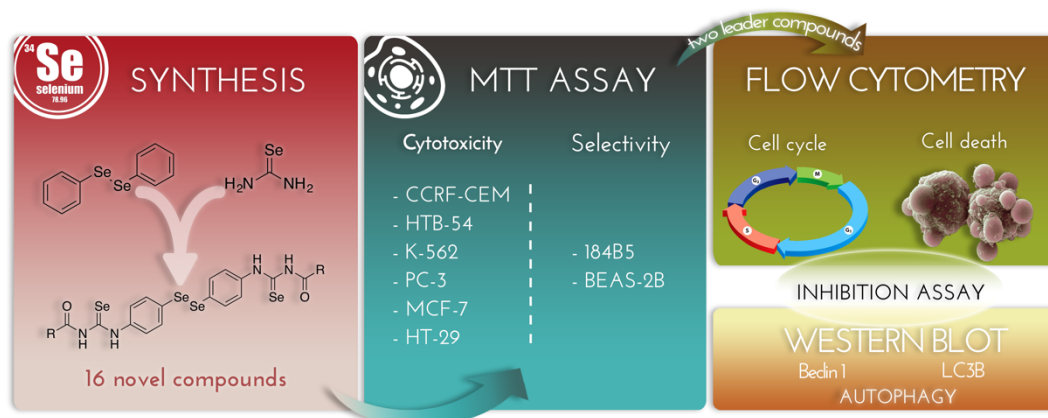
## Combined Acylselenourea–Diselenide Structures: New Potent and Selective Antitumoral Agents as Autophagy Activators

Pablo Garnica,<sup>†,‡,⊙</sup> Ignacio Encío,<sup>§</sup> Daniel Plano,<sup>†,‡</sup> Juan A. Palop,<sup>†,‡</sup> and Carmen Sanmartín<sup>\*,†,‡,⊙</sup>

<sup>†</sup>University of Navarra, Faculty of Pharmacy and Nutrition, Department of Organic and Pharmaceutical Chemistry, Irunlarrea 1, E-31008 Pamplona, Spain

<sup>‡</sup>Instituto de Investigación Sanitaria de Navarra (IdiSNA), Irunlarrea 3, E-31008 Pamplona, Spain

<sup>§</sup>Department of Health Sciences, Public University of Navarra, Avda. Barañain s/n, E-31008 Pamplona, Spain



In this paper, the synthesis of sixteen novel diselenide derivatives containing the selenourea group is described. This series of compounds has been designed following the fragment-based drug design and the endings of the symmetric proposed derivatives respond to two goals. The first one is to modulate volume and electronic factors and the second, the inclusion of antitumoral active heterocycles. Compounds were screened to determine their cytotoxic potential and selectivity against a panel of six cancer cell lines and two non-malignant derived. The two leader compounds **2** and **7** have been selected due to their high potency and staggering selectivity for breast adenocarcinoma cells. Cell cycle affection and their ability to induce cell death was evaluated to further understand their mechanism of action. The effect of pan-caspase and autophagy inhibitors on cell death cause by these compounds was also studied and this preliminary data was confirmed by protein analysis.

Enciso JM, Sánchez A, López de Ceráin A, Azqueta A. Does the duration of lysis affect the sensitivity of the in vitro alkaline comet assay? [Mutagenesis](#), 2015, 30(1):21-28.  
doi:10.1093/mutage/geu047







,

**PAPER 2**

---

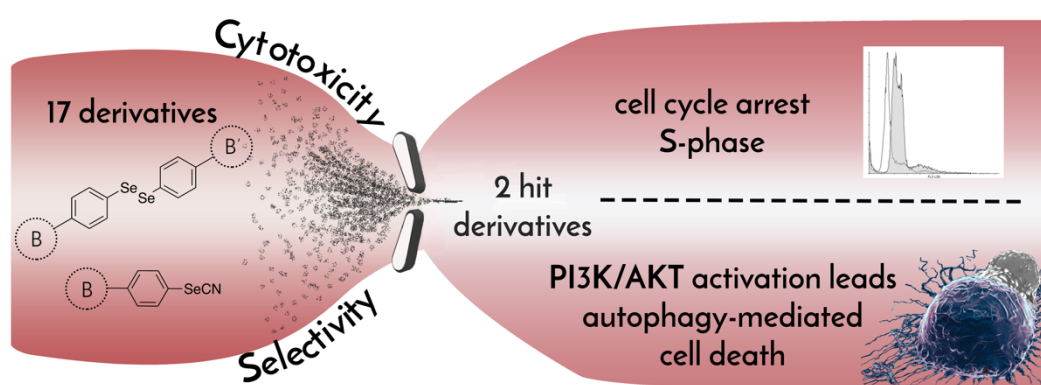


## Organoseleno cytostatic derivatives: autophagic cell death inducers that activate the PI3K/AKT pathway

Pablo Garnica <sup>1,2</sup>, Ignacio Encío <sup>3</sup>, Daniel Plano <sup>1,2</sup>, Juan A. Palop <sup>1,2</sup>, Carmen Sanmartín <sup>1,2\*</sup>

<sup>1</sup> University of Navarra, Faculty of Pharmacy and Nutrition, Department of Organic and Pharmaceutical Chemistry, Irunlarrea 1, E-31008 Pamplona, Spain. <sup>2</sup> Instituto de Investigación Sanitaria de Navarra (IdiSNA), Irunlarrea 3, E-31008 Pamplona, Spain. <sup>3</sup> Department of Health Sciences, Public University of Navarra, Avda. Barañain s/n, E-31008 Pamplona, Spain

This paper has been submitted to *ACS Medicinal Chemistry Letters*.



The synthesis of seventeen organoseleno compounds derived from two core structures which have already proven to have antitumoural activity is describe in this paper. The series of compounds include bis(4-aminophenyl)diselenide derivatives and 4-aminophenylselenocyanate and structural modifications were include to enhance physical properties such as solubility and increase selectivity for cancer cells. Compounds were first screened at two concentrations in a panel of seven cancer cell lines and two non-malignant derived. Compounds were ranked according to potency and selectivity and full dose-response curves for the selected compounds were built for all nine cell lines. Starting core structures were also included to be able to compare results. Two compounds were selected due to their high selectivity for breast adenocarcinoma cell line (**8b** and **10a**). Flow cytometry analysis of cell cycle and cell death was performed as a preliminary approach to their mechanism of action.



Garnica P, Encío I, Plano D, Palop JA, Sanmartín C. Organoseleno cytostatic derivatives: autophagic cell death inducers that activate the PI3K/AKT pathway. [ACS Med Chem Lett](#) [pre-print]

## Supplementary information

### Organoseleno cytostatic derivatives: autophagic cell death inducers that activate the PI3K/AKT pathway

Pablo Garnica <sup>1,2</sup>, Ignacio Encío <sup>3</sup>, Daniel Plano <sup>1,2</sup>, Juan A. Palop <sup>1,2</sup>, Carmen Sanmartín <sup>1,2\*</sup>

<sup>1</sup> University of Navarra, Faculty of Pharmacy and Nutrition, Department of Organic and Pharmaceutical Chemistry, Irunlarrea 1, E-31008 Pamplona, Spain. <sup>2</sup> Instituto de Investigación Sanitaria de Navarra (IdiSNA), Irunlarrea 3, E-31008 Pamplona, Spain. <sup>3</sup> Department of Health Sciences, Public University of Navarra, Avda. Barañain s/n, E-31008 Pamplona, Spain

#### Contents:

1. Chemistry of synthesized derivatives
2. NMR spectra of synthesized derivatives
  - NMR Spectra of compounds **1a-11a**
  - NMR Spectra of compounds **1b-8b**
3. Biological evaluation
  - Methodology
  - Dose response full data
  - Representative examples of cell cycle and subdiploid population analysis



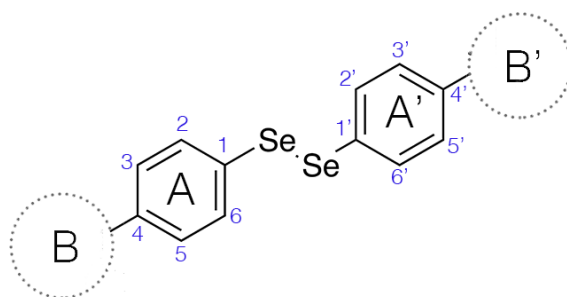
## 1. Chemistry

### 1.1. Material and methods

Proton ( $^1\text{H}$ ) carbon ( $^{13}\text{C}$ ) and selenium ( $^{77}\text{Se}$ ) NMR spectra were recorded on a Bruker 400 Ultra-shield<sup>TM</sup> spectrometer (Rheinstetten, Germany) using  $\text{DMSO-}d_6$  as solvent. IR spectra were recorded on a Thermo Nicolet FT-IR Nexus spectrophotometer using KBr pellets for solid samples. Elemental analysis was performed on a LECO CHN-900 Elemental Analyzer. Purity of all final compounds was 95% or higher. Chemicals were purchased from E. Merck (Darmstadt, Germany), Panreac Química S.A. (Montcada i Reixac, Barcelona, Spain), Sigma-Aldrich Química, S.A. (Alcobendas, Madrid, Spain) and Acros Organics (Janssen Pharmaceutica, Geel, Belgium).

#### 1.1.1. General procedure for the synthesis of compounds **1a–8a**

Bis(4-aminophenyl)diselenide (1 mmol) was dissolved in dry acetone (10 mL) and the corresponding anhydride (2.1 mmol) then added. The reaction was then stirred for a variable time of 8 h up to 24 h at room temperature. Then reaction was quenched with water, compound is filtered and purified by stirring or washing with ethyl ether.



**Scheme 1S.** General NMR assignment for compounds of series **a**

#### 1.1.1.1. (2*Z*,2'*Z*)-4,4'-[diselenodiy]bis(benzene-4,1-diylimino)]bis(4-oxobut-2-enoic acid) (**1a**)

From maleic anhydride. Conditions: 8 h at room temperature. The product was kept under stirring with water (25 mL) for 2 h, filtered and then washed with ethyl ether ( $2 \times 25$  mL). A yellow powder was obtained. Yield: 73.6 %. Mp: 186–186.5°C. IR (KBr)  $\text{cm}^{-1}$ : 3305, 3193 (N-H), 1723 (C=O carboxylic acid), 1623 (C=O, amide), 818 (Se-Se).  $^1\text{H}$  NMR (400 MHz,  $\text{DMSO-}d_6$ )  $\delta$ : 13.24–12.85 (bs, 2H, COOH), 10.54 (s, 2H, NH), 7.60 (d, 4H, A+A',  $J_{2-3}=J_{6-5}=8.8$  Hz,  $\text{H}_2+\text{H}_6$ ), 7.57 (d, 4H, A+A',  $J_{3-2}=J_{5-6}=8.8$  Hz,  $\text{H}_3+\text{H}_5$ ), 6.47 (d, 2H, B+B',  $J_{1-2}=12.0$  Hz,  $\text{H}_1$ ), 6.31 (d, 2H, B+B',  $J_{1-2}=12.0$  Hz,  $\text{H}_2$ ).  $^{13}\text{C}$  NMR (100 MHz,  $\text{DMSO-}d_6$ )  $\delta$ : 166.76 (COOH), 163.17 (C=O), 138.71 (A+A',  $\text{C}_4$ ), 132.88 (A+A',  $\text{C}_2+\text{C}_6$ ), 131.33 (B+B',  $\text{C}_1$ ), 130.23 (B+B',  $\text{C}_2$ ), 124.19 (A+A',  $\text{C}_1$ ), 120.02 (A+A',  $\text{C}_3+\text{C}_5$ ). MS [ $m/z$  (% abundance)]: 172 (100), 344 (25). Elemental analysis calculated (%) for  $\text{C}_{20}\text{H}_{16}\text{N}_2\text{O}_6\text{Se}_2 \cdot \text{HCl}$ : C: 38.63, H: 2.41, N: 6.43; found: C: 38.27, H: 2.03, N: 6.04.

#### 1.1.1.2. 2,2'-[(diselenodiy]dibenzene-4,1-diyl)dicarbamoyl]bis(benzoic acid) (**2a**)

From phthalic anhydride. Conditions: 12 h at room temperature. The product was kept under stirring with water (25 mL) for 1 h, filtered and then washed with ethyl ether ( $2 \times 25$  mL). A yellow powder was obtained. Yield: 28.3 %. Mp: 154–155°C. IR (KBr)  $\text{cm}^{-1}$ : 1708 (C=O carboxylic acid), 1657 (C=O, amide), 819 (Se-Se).  $^1\text{H}$  NMR (400 MHz,  $\text{DMSO-}d_6$ )  $\delta$ : 11.02 (s, 2H, NH), 7.85 (d, 2H, B+B',  $J_{3-4}=8.8$  Hz,  $\text{H}_3$ ), 7.72–7.66 (m, 4H, B+B',  $\text{H}_4+\text{H}_6$ ), 7.63–7.52 (m, 10H, A+A',  $\text{H}_2+\text{H}_3+\text{H}_4+\text{H}_5$ , B+B',  $\text{H}_5$ ).  $^{13}\text{C}$  NMR (100 MHz,  $\text{DMSO-}d_6$ )  $\delta$ : 171.22 (COOH), 168.50 (C=O), 140.48 (A+A',  $\text{C}_4$ ), 134.06 (A+A',  $\text{C}_2+\text{C}_6$ ), 132.02 (A+A',  $\text{C}_1$ ), 130.40 (B+B',  $\text{C}_5$ ),

130.27 (B+B', C<sub>4</sub>), 128.65 (B+B', C<sub>1</sub>), 126.48 (B+B', C<sub>2</sub>), 124.60 (A+A', C<sub>3</sub>+C<sub>5</sub>), 121.03 (B+B', C<sub>3</sub>), 120.51 (B+B', C<sub>6</sub>). <sup>77</sup>Se NMR (76 MHz, DMSO-*d*<sub>6</sub>) δ: 482.83 (Se-Se). MS [*m/z* (% abundance)]: 104 (100), 172 (93), 344 (25). Elemental analysis calculated (%) for C<sub>28</sub>H<sub>20</sub>N<sub>2</sub>O<sub>6</sub>Se<sub>2</sub> · 2HCl: C: 49.83, H: 3.14, N: 4.15; found: C: 49.74, H: 3.53, N: 4.38.

1.1.1.3. 4,4'-[diselenodiylbis(benzene-4,1-diylimino)]bis(4-oxobutanoic acid) (**3a**)

From succinic anhydride. Conditions: 24 h at room temperature. The product was kept under stirring with water (25 mL) for 2 h, filtered, then stirred with 100 mL of ethyl ether for 24 h and then filtered. A yellow powder was obtained. Yield: 75.0 %. Mp: 179–180°C. IR (KBr) cm<sup>-1</sup>: 3318 (NH), 1696 (C=O carboxylic acid), 1666 (C=O, amide), 818 (Se-Se). <sup>1</sup>H NMR (400 MHz, DMSO-*d*<sub>6</sub>) δ: 12.43–11.90 (bs, 2H, COOH), 10.11 (s, 2H, NH), 7.56 (d, 4H, A+A', J<sub>2,3</sub>=J<sub>6,5</sub>= 8.4 Hz, H<sub>2</sub>+H<sub>6</sub>), 7.51 (d, 4H, A+A', J<sub>3,2</sub>=J<sub>5,6</sub>= 8.4 Hz, H<sub>3</sub>+H<sub>5</sub>), 2.60–2.46 (m, 8H, B+B', H<sub>1</sub>+H<sub>2</sub>). <sup>13</sup>C NMR (100 MHz, DMSO-*d*<sub>6</sub>) δ: 174.21 (COOH), 170.04 (C=O), 140.03 (A+A', C<sub>4</sub>), 133.70 (A+A', C<sub>2</sub>+C<sub>6</sub>), 123.79 (A+A', C<sub>1</sub>), 120.06 (A+A', C<sub>3</sub>+C<sub>5</sub>), 31.51 (B+B', C<sub>2</sub>), 29.17 (B+B', C<sub>1</sub>). MS [*m/z* (% abundance)]: 172 (100), 344 (15), 424 (10). Elemental analysis calculated (%) for C<sub>20</sub>H<sub>20</sub>N<sub>2</sub>O<sub>6</sub>Se<sub>2</sub> · HCl: C: 41.51, H: 3.66, N: 4.84; found: C: 41.11, H: 3.79, N: 4.77.

1.1.1.4. 2,2'-[(diselenodiylbis(benzene-4,1-diylimino)]bis(2-oxoethane-2,1-diylloxy)diacetic acid (**5a**)

From diglycolic anhydride. Conditions: 24 h at room temperature. The product was kept under stirring with water (25 mL) for 2 h, filtered, then stirred with 100 mL of ethyl ether for 24 h and then filtered. A yellow powder was obtained. Yield: 69.7 %. Mp: 140–141°C. IR (KBr) cm<sup>-1</sup>: 1709 (C=O carboxylic acid), 1683 (C=O, amide), 818 (Se-Se). <sup>1</sup>H NMR (400 MHz, DMSO-*d*<sub>6</sub>) δ: 13.13–12.46 (bs, 2H, COOH), 10.09 (s, 2H, NH), 7.62 (d, 4H, A+A', J<sub>2,3</sub>=J<sub>6,5</sub>= 8.5 Hz, H<sub>2</sub>+H<sub>6</sub>), 7.55 (d, 4H, A+A', J<sub>3,2</sub>=J<sub>5,6</sub>= 8.5 Hz, H<sub>3</sub>+H<sub>5</sub>), 4.19 (s, 4H, B+B', H<sub>1</sub>), 4.17 (s, 4H, B+B', H<sub>2</sub>). <sup>13</sup>C NMR (100 MHz, DMSO-*d*<sub>6</sub>) δ: 172.68 (COOH), 168.99 (C=O), 139.56 (A+A', C<sub>4</sub>), 133.94 (A+A', C<sub>2</sub>+C<sub>6</sub>), 125.01 (A+A', C<sub>1</sub>), 121.22 (A+A', C<sub>3</sub>+C<sub>5</sub>), 71.38 (B+B', C<sub>2</sub>), 69.11 (B+B', C<sub>1</sub>). MS [*m/z* (% abundance)]: 93 (95), 172 (100). Elemental analysis calculated (%) for C<sub>20</sub>H<sub>20</sub>N<sub>2</sub>O<sub>8</sub>Se<sub>2</sub>: C: 41.83, H: 3.51, N: 4.88; found: C: 41.83, H: 3.82, N: 5.19.

1.1.1.5. 2,2'-[(diselenodiyl dibenzene-4,1-diyl)dicarbamoyl]bis(cyclohexanecarboxylic acid) (**7a**)

From *cis*-1,2-cyclohexanecarboxylic anhydride. Conditions: 24 h at room temperature. The product was kept under stirring with water (25 mL) for 2 h, filtered, then stirred with 100 mL of ethyl ether for 24 h and then filtered. A light brown powder was obtained. Yield: 97.7 %. Mp: 150–151°C. IR (KBr) cm<sup>-1</sup>: 3307 (NH), 2930 (C-H st), 1698 (C=O carboxylic acid), 1665 (C=O, amide), 820 (Se-Se). <sup>1</sup>H NMR (400 MHz, DMSO-*d*<sub>6</sub>) δ: 12.13–11.62 (bs, 2H, COOH), 9.87 (s, 2H, NH), 7.55 (d, 4H, A+A', J<sub>2,3</sub>=J<sub>6,5</sub>= 8.8 Hz, H<sub>2</sub>+H<sub>6</sub>), 7.57 (d, 4H, A+A', J<sub>3,2</sub>=J<sub>5,6</sub>= 8.8 Hz, H<sub>3</sub>+H<sub>5</sub>), 2.94 (d, 2H, B+B', J<sub>1,6e</sub>= 5.4 Hz, H<sub>1</sub>), 2.60 (m, 2H, B+B', H<sub>2</sub>), 2.09 (d, 2H, B+B', J<sub>6e,1</sub>= 5.4 Hz, H<sub>6e</sub>), 1.99 (d, 2H, B+B', J<sub>3e</sub>= 8.9 Hz, H<sub>3e</sub>), 1.71 (m, 6H, B+B', H<sub>3a</sub>+H<sub>6a</sub>+H<sub>5a</sub>), 1.35 (m, 6H, B+B', H<sub>5e</sub>+H<sub>4a</sub>+H<sub>4e</sub>). <sup>13</sup>C NMR (100 MHz, DMSO-*d*<sub>6</sub>) δ: 175.56 (COOH), 173.36 (C=O), 140.42 (A+A', C<sub>4</sub>), 133.78 (A+A', C<sub>2</sub>+C<sub>6</sub>), 123.66 (A+A', C<sub>1</sub>), 120.26 (A+A', C<sub>3</sub>+C<sub>5</sub>), 43.00 (B+B', C<sub>2</sub>), 42.44 (B+B', C<sub>1</sub>), 28.13 (B+B', C<sub>6</sub>), 25.62 (B+B', C<sub>3</sub>), 24.47 (B+B', C<sub>4</sub>), 22.78 (B+B', C<sub>5</sub>). MS [*m/z* (% abundance)]: 81 (70), 172 (100), 344 (25). Elemental analysis calculated (%) for C<sub>28</sub>H<sub>32</sub>N<sub>2</sub>O<sub>6</sub>Se<sub>2</sub>: C: 51.70, H: 4.96, N: 4.31; found: C: 52.06, H: 5.09, N: 4.71.

1.1.1.6. 3,3'-[(diselenodiyl dibenzene-4,1-diyl)dicarbamoyl]bis(7-oxabicyclo[2.2.1]hept-5-ene-2-carboxylic acid) (**8a**)

From 3,6-epoxy-1,2,3,6-tetrahydrophthalic anhydride obtained by the classic procedure described for a Diels-Alder reaction using furan and maleic anhydride as reagents to yield the Diels-Alder adduct. Conditions: 24 h at room temperature. The product was kept under stirring with water (25 mL) for 2 h, filtered, then stirred with 100 mL of ethyl ether for 24 h and then filtered. A yellow powder was obtained. Yield: 23.7%. Mp: 126–127°C IR

(KBr)  $\text{cm}^{-1}$ : 3299 (NH), 1706 (C=O carboxylic acid), 1669 (C=O, amide), 819 (Se-Se).  $^1\text{H}$  NMR (400 MHz, DMSO- $d_6$ )  $\delta$ : 9.93 (s, 2H, NH), 7.65 (d, 4H, A+A',  $J_{2,3}=J_{6,5}=9.0$  Hz,  $\text{H}_2+\text{H}_6$ ), 7.62 (d, 4H, A+A',  $J_{3,2}=J_{5,6}=9.0$  Hz,  $\text{H}_3+\text{H}_5$ ), 6.50 (s, 4H, B+B',  $\text{H}_3+\text{H}_5$ ), 5.14 (s, 2H, B+B',  $\text{H}_5$ ), 5.05 (s, 2H, B+B',  $\text{H}_2$ ), 2.82 (d, 2H, B+B',  $J_{1,6}=9.1$  Hz,  $\text{H}_1$ ), 2.71 (d, 2H, B+B',  $J_{6,1}=9.1$  Hz,  $\text{H}_6$ ).  $^{13}\text{C}$  NMR (100 MHz, DMSO- $d_6$ )  $\delta$ : 173.08 (COOH), 170.48 (C=O), 141.07 (A+A',  $\text{C}_4$ ), 137.49 (B+B',  $\text{C}_4$ ), 137.08 (B+B',  $\text{C}_5$ ), 135.29 (A+A',  $\text{C}_2+\text{C}_6$ ), 120.79 (A+A',  $\text{C}_1$ ), 116.51 (A+A',  $\text{C}_3+\text{C}_5$ ), 80.82 (B+B',  $\text{C}_6$ ), 79.61 (B+B',  $\text{C}_3$ ), 47.96 (B+B',  $\text{C}_1$ ), 47.36 (B+B',  $\text{C}_2$ ). MS [ $m/z$  (% abundance)]: 172 (100), 344 (25). Elemental analysis calculated (%) for  $\text{C}_{28}\text{H}_{24}\text{N}_2\text{O}_8\text{Se}_2 \cdot 2\text{H}_2\text{O}$ : C: 47.34, H: 3.97, N: 3.94; found: C: 47.66, H: 4.13, N: 4.23.

### 1.1.2. General procedure for the synthesis of compounds **9a–11a**

A reaction mixture containing 1.3 mmol of the corresponding carboxylic derivatives (**1a**, **2a** or **5a**) in 15 mL of acetic anhydride and 200 mg of sodium acetate was heated for 3 h under reflux, then quenched with water. The aqueous solution was extracted with  $\text{CH}_2\text{Cl}_2$ , dried with sodium sulphate anhydrous and the solvent was evaporated under vacuum.

#### 1.1.2.1. *1,1'-(diselenodiyldibenzene-4,1-diyl)bis(1H-pyrrole-2,5-dione) (9a)*

From compound **1a**. The reaction was cooled, quenched with water (50 mL) and kept under stirring for 3 h. The aqueous solution was extracted with  $\text{CH}_2\text{Cl}_2$  (2  $\times$  25 mL), dried with  $\text{Na}_2\text{SO}_4$ , filtered, and the solvent was evaporated under vacuum. The product was then washed with *n*-hexane (100 mL). A yellow solid was obtained. Yield: 57.4 %. Mp: 91.5–92.5°C. IR (KBr)  $\text{cm}^{-1}$ : 1710 (C=O), 818 (Se-Se).  $^1\text{H}$  NMR (400 MHz, DMSO- $d_6$ )  $\delta$ : 7.77 (d, 4H, A+A',  $J_{2,3}=J_{6,5}=8.6$  Hz,  $\text{H}_2+\text{H}_6$ ), 7.33 (d, 4H, A+A',  $J_{3,2}=J_{5,6}=8.6$  Hz,  $\text{H}_3+\text{H}_5$ ), 7.19 (s, 4H, B+B',  $\text{H}_1+\text{H}_2$ ).  $^{13}\text{C}$  NMR (100 MHz, DMSO- $d_6$ )  $\delta$ : 169.69 (C=O), 134.75 (A+A',  $\text{C}_4$ ), 131.37 (A+A',  $\text{C}_2+\text{C}_6$ ), 131.27 (B+B',  $\text{C}_1+\text{C}_2$ ), 129.15 (A+A',  $\text{C}_1$ ), 127.51 (A+A',  $\text{C}_3+\text{C}_5$ ). MS [ $m/z$  (% abundance)]: 57 (75), 252 (100), 311 (65). Elemental analysis calculated (%) for  $\text{C}_{20}\text{H}_{12}\text{N}_2\text{O}_4\text{Se}_2 \cdot \text{H}_2\text{O}$ : C: 46.17, H: 2.71, N: 5.38; found: C: 46.10, H: 3.03, N: 4.94.

#### 1.1.2.2. *1,1'-(diselenodiyldibenzene-4,1-diyl)bis(1H-isoindole-1,3(2H)-dione) (10a)*

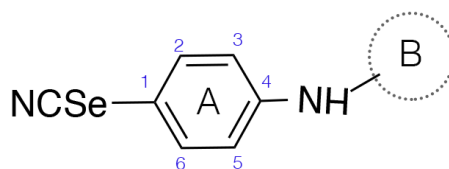
From compound **2a**. The reaction was cooled, quenched with water (50 mL) and kept under stirring for 3 h. The aqueous solution was extracted with  $\text{CH}_2\text{Cl}_2$  (2  $\times$  25 mL), dried with  $\text{Na}_2\text{SO}_4$ , filtered, and the solvent was evaporated under vacuum. The product was then washed with *n*-hexane. A yellow solid was obtained. Yield: 96%. Mp: 248–249°C. IR (KBr)  $\text{cm}^{-1}$ : 1709 (C=O), 815 (Se-Se).  $^1\text{H}$  NMR (400 MHz, DMSO- $d_6$ )  $\delta$ : 8.15–7.79 (10H, A+A',  $\text{H}_2+\text{H}_6$ , B+B',  $\text{H}_2+\text{H}_3+\text{H}_4+\text{H}_5$ ), 7.55 (d, 4H, A+A',  $J_{3,2}=J_{5,6}=8.4$  Hz,  $\text{H}_3+\text{H}_5$ ).  $^{13}\text{C}$  NMR (100 MHz, DMSO- $d_6$ )  $\delta$ : 172.73 (C=O), 140.18 (A+A',  $\text{C}_4$ ), 140.09 (B+B',  $\text{C}_1+\text{C}_6$ ), 133.49 (B+B',  $\text{C}_4+\text{C}_5$ ), 131.99 (A+A',  $\text{C}_1$ ), 131.73 (A+A',  $\text{C}_2+\text{C}_6$ ), 128.65 (B+B',  $\text{C}_2+\text{C}_5$ ), 120.26 (A+A',  $\text{C}_3+\text{C}_5$ ).  $^{77}\text{Se}$  NMR (76 MHz, DMSO- $d_6$ )  $\delta$ : 481.88 (Se-Se). MS [ $m/z$  (% abundance)]: 93 (65), 172 (100), 302 (15), 604 (5). Elemental analysis calculated (%) for  $\text{C}_{28}\text{H}_{16}\text{N}_2\text{O}_4\text{Se}_2 \cdot 2\text{H}_2\text{O}$ : C: 52.68, H: 3.16, N: 4.39; found: C: 52.82, H: 3.20, N: 4.77.

#### 1.1.2.3. *1,1'-(diselenodiyldibenzene-4,1-diyl)bis(morpholine-3,5-dione) (11a)*

From compound **5a**. The reaction was cooled and quenched with water. The reaction was cooled, quenched with water (50 mL) and kept under stirring for 3 h. The aqueous solution was extracted with  $\text{CH}_2\text{Cl}_2$  (2  $\times$  25 mL), dried with  $\text{Na}_2\text{SO}_4$ , filtered, and the solvent was evaporated under vacuum. The product was then washed with ethyl ether (3  $\times$  10 mL). A yellow solid was obtained. Yield: 75%. MP: 150–152. IR (KBr)  $\text{cm}^{-1}$ : 1708 (C=O), 819 (Se-Se).  $^1\text{H}$  NMR (400 MHz, DMSO- $d_6$ )  $\delta$ : 7.76 (d, 4H, A+A',  $J_{2,3}=J_{6,5}=7.8$  Hz,  $\text{H}_2+\text{H}_6$ ), 7.23 (d, 4H, A+A',  $J_{3,2}=J_{5,6}=7.8$  Hz,  $\text{H}_3+\text{H}_5$ ), 4.54 (s, 8H, B+B',  $\text{H}_2+\text{H}_3$ ).  $^{13}\text{C}$  NMR (100 MHz, DMSO- $d_6$ )  $\delta$ : 170.19 (C=O), 133.32 (A+A',  $\text{C}_4$ ), 131.42 (A+A',  $\text{C}_2+\text{C}_6$ ), 130.71 (A+A',  $\text{C}_1$ ), 130.30 (A+A',  $\text{C}_3+\text{C}_5$ ), 67.74 (B+B',  $\text{C}_1+\text{C}_2$ ). MS [ $m/z$  (% abundance)]: 184 (100), 271 (25), 538 (15). Elemental analysis calculated (%) for  $\text{C}_{20}\text{H}_{16}\text{N}_2\text{O}_6\text{Se}_2 \cdot \text{H}_2\text{O}$ : C: 43.18, H: 3.26, N: 5.04; found: C: 43.65, H: 3.52, N: 5.36.

1.1.3. General procedure for the synthesis of compounds **1b–8b**

4-Aminophenyl selenocyanate (2 mmol) was dissolved in dry acetone (15 mL) and the corresponding anhydride (2 mmol) then added. The reaction was then stirred for a variable time of 12 h up to 48 h at room temperature. Reaction was quenched with water, compound is then filtered and purified by stirring or washing with solvents such as *n*-hexane and ethyl ether.

**Scheme 2S.** NMR assignation rules followed for series **b**.1.1.3.1. (2*Z*)-4-oxo-4-[(4-selenocyanatophenyl)amino]but-2-enoic acid (**1b**)

From maleic anhydride. Conditions: 14 h at room temperature. The product was kept under stirring with water (25 mL) for 2 h, filtered and then washed with 25 mL of *n*-hexane and 25 mL of ethyl ether. A yellow powder was obtained. Yield: 51.8 %. Mp: 161–162°C. IR (KBr)  $\text{cm}^{-1}$ : 3299, 3196 (N-H), 2157 (CN), 1722 (C=O carboxylic acid), 1624 (C=O, amide).  $^1\text{H}$  NMR (400 MHz, DMSO- $d_6$ )  $\delta$ : 12.96 (s, 1H, COOH), 10.58 (s, 1H, NH), 7.76–7.60 (bs, 4H, A,  $\text{H}_2+\text{H}_3+\text{H}_5+\text{H}_6$ ), 6.47 (d, 2H, B,  $J_{1-2}=12.0$  Hz,  $\text{H}_1$ ), 6.33 (d, 2H, B,  $J_{2-1}=12.0$  Hz,  $\text{H}_2$ ).  $^{13}\text{C}$  NMR (100 MHz, DMSO- $d_6$ )  $\delta$ : 167.37 (COOH), 164.02 (C=O), 140.42 (A,  $\text{C}_4$ ), 135.24 (A,  $\text{C}_2+\text{C}_6$ ), 132.04 (B,  $\text{C}_1$ ), 130.75 (B,  $\text{C}_2$ ), 121.16 (A,  $\text{C}_3+\text{C}_5$ ), 117.57 (A,  $\text{C}_1$ ), 105.77 (CN).  $^{77}\text{Se}$  NMR (76 MHz, DMSO- $d_6$ )  $\delta$ : 322.45 (SeCN). MS [ $m/z$  (% abundance)]: 118 (100), 198 (25), 278 (10), 296 (7). Elemental analysis calculated (%) for  $\text{C}_{11}\text{H}_8\text{N}_2\text{O}_3\text{Se}$ : C: 44.74, H: 2.71, N: 9.49; found: C: 44.35, H: 3.08, N: 9.10.

1.1.3.2. 2-[(4-selenocyanatophenyl)carbamoyl]benzoic acid (**2b**)

From phthalic anhydride. Conditions: overnight at room temperature. The product was kept under stirring with water (25 mL) for 2 h, filtered and then washed with 25 mL of *n*-hexane and 25 mL of ethyl ether. A white powder was obtained. Yield: 89.5 %. Mp: 162–164°C. IR (KBr)  $\text{cm}^{-1}$ : 3317, 3122 (N-H), 2149 (CN), 1718 (C=O carboxylic acid), 1647 (C=O, amide).  $^1\text{H}$  NMR (400 MHz, DMSO- $d_6$ )  $\delta$ : 13.14 (s, 1H, COOH), 10.60 (s, 1H, NH), 7.92 (d, 1H, B,  $J_{3-4}=7.5$  Hz,  $\text{H}_3$ ), 7.78 (d, 2H, A,  $J_{2-3}=J_{6-5}=8.3$  Hz,  $\text{H}_2+\text{H}_6$ ), 7.73–7.64 (m, 3H, A,  $\text{H}_3+\text{H}_5$ , B,  $\text{H}_4$ ), 7.59 (m, 2H, B,  $\text{H}_5+\text{H}_6$ ).  $^{13}\text{C}$  NMR (100 MHz, DMSO- $d_6$ )  $\delta$ : 168.23 (COOH), 167.80 (C=O), 141.32 (A,  $\text{C}_4$ ), 139.03 (B,  $\text{C}_1$ ), 135.29 (A,  $\text{C}_2+\text{C}_6$ ), 132.31 (B,  $\text{C}_5$ ), 130.30 (B,  $\text{C}_2$ ), 130.09 (B,  $\text{C}_4$ ), 130.05 (B,  $\text{C}_3$ ), 128.25 (B,  $\text{C}_6$ ), 121.16 (A,  $\text{C}_1$ ), 116.99 (A,  $\text{C}_3+\text{C}_5$ ), 105.91 (CN). MS [ $m/z$  (% abundance)]: 76 (50), 104 (55), 118 (100), 198 (20). Elemental analysis calculated (%) for  $\text{C}_{15}\text{H}_{10}\text{N}_2\text{O}_3\text{Se}$ : C: 52.19, H: 2.92, N: 8.11; found: C: 52.06, H: 3.24, N: 8.06.

1.1.3.3. 4-oxo-4-[(4-selenocyanatophenyl)amino]butanoic acid (**3b**)

From succinic anhydride. Conditions: 24 h at room temperature. The product was kept under stirring with water (25 mL) for 2 h, filtered, then stirred with 100 mL of ethyl ether for 24 h and then filtered. A brown powder was obtained. Yield: 38.9 %. Mp: 154–156°C. IR (KBr)  $\text{cm}^{-1}$ : 3340 (NH), 2158 (CN), 1693 (C=O carboxylic acid), 1636 (C=O, amide).  $^1\text{H}$  NMR (400 MHz, DMSO- $d_6$ )  $\delta$ : 12.32–12.07 (bs, 1H, COOH), 10.21 (s, 1H, NH), 7.70–7.62 (bs, 4H, A,  $\text{H}_2+\text{H}_6+\text{H}_3+\text{H}_5$ ), 2.58 (d, 2H, A,  $J_{2-1}=6.0$  Hz,  $\text{H}_2$ ), 2.54 (d, 2H, A,  $J_{1-2}=6.0$  Hz,  $\text{H}_1$ ).  $^{13}\text{C}$  NMR (100 MHz, DMSO- $d_6$ )  $\delta$ : 174.27 (COOH), 171.03 (C=O), 141.06 (A,  $\text{C}_4$ ), 135.36 (A,  $\text{C}_2+\text{C}_6$ ), 120.60 (A,  $\text{C}_3+\text{C}_5$ ), 116.47 (A,  $\text{C}_1$ ), 105.90 (CN), 31.54 (B,  $\text{C}_2$ ), 29.10 (B,  $\text{C}_1$ ). MS [ $m/z$  (% abundance)]: 101 (25), 118 (100), 198 (40), 298 (28). Elemental analysis calculated (%) for  $\text{C}_{11}\text{H}_{10}\text{N}_2\text{O}_3\text{Se}_2 \cdot \text{H}_2\text{O}$ : C: 41.88, H: 3.80, N: 8.88; found: C: 41.59, H: 3.58, N: 8.69.

1.1.3.4. 3-[(4-selenocyanatophenyl)carbamoyl]pyrazine-2-carboxylic acid (**4b**)

From 2,3-pyrazinedicarboxylic anhydride. Conditions: 24 h at room temperature. The product was kept under stirring with water (25 mL) for 3 h, filtered, then stirred with 100 mL of ethyl ether for 24 h and then filtered. A yellow powder was obtained. Yield: 49.3 %. Mp: 164–165°C. IR (KBr)  $\text{cm}^{-1}$ : 3280 (NH), 2153 (CN), 1765 (C=O carboxylic acid), 1671 (C=O, amide).  $^1\text{H}$  NMR (400 MHz, DMSO- $d_6$ )  $\delta$ : 14.12–13.54 (bs, 1H, COOH), 11.03 (s, 1H, NH), 8.92 (s, 2H, B, H<sub>3</sub>+H<sub>4</sub>), 7.87 (d, 2H, A,  $J_{2-3}=J_{6-5}=8.6$  Hz, H<sub>2</sub>+H<sub>6</sub>), 7.74 (d, 2H, A,  $J_{3-2}=J_{5-6}=8.6$  Hz, H<sub>3</sub>+H<sub>5</sub>).  $^{13}\text{C}$  NMR (100 MHz, DMSO- $d_6$ )  $\delta$ : 167.05 (COOH), 163.64 (C=O), 146.99 (B, C<sub>4</sub>), 146.75 (B, C<sub>1</sub>), 146.15 (B, C<sub>3</sub>), 145.49 (B, C<sub>2</sub>), 140.49 (A, C<sub>4</sub>), 135 (A, C<sub>2</sub>+C<sub>6</sub>), 122.19 (A, C<sub>3</sub>+C<sub>5</sub>), 118 (A, C<sub>1</sub>), 106.37 (CN). MS [ $m/z$  (% abundance)]: 79 (100), 107 (95), 118 (30), 304 (75). Elemental analysis calculated (%) for C<sub>13</sub>H<sub>8</sub>N<sub>4</sub>O<sub>3</sub>Se: C: 44.97, H: 2.32, N: 16.14; found: C: 44.73, H: 2.72, N: 15.82.

1.1.3.5. {2-oxo-2-[(4-selenocyanatophenyl)amino]ethoxy}acetic acid (**5b**)

From diglycolic anhydride. Conditions: 24 h at room temperature. The product was kept under stirring with water (25 mL) for 1 h, filtered and then washed with ethyl ether (2  $\times$  25 mL). A white powder was obtained. Yield: 51.1 %. Mp: 141–142°C. IR (KBr)  $\text{cm}^{-1}$ : 3305 (NH), 2151 (CN), 1716 (C=O carboxylic acid), 1660 (C=O, amide).  $^1\text{H}$  NMR (400 MHz, DMSO- $d_6$ )  $\delta$ : 13.04–12.76 (bs, 1H, COOH), 10.10 (s, 1H, NH), 7.73 (d, 2H, A,  $J_{2-3}=J_{6-5}=8.8$  Hz, H<sub>2</sub>+H<sub>6</sub>), 7.67 (d, 2H, A,  $J_{3-2}=J_{5-6}=8.8$  Hz, H<sub>3</sub>+H<sub>5</sub>), 4.21 (s, 2H, B, H<sub>1</sub>), 4.20 (s, 2H, B, H<sub>2</sub>).  $^{13}\text{C}$  NMR (100 MHz, DMSO- $d_6$ )  $\delta$ : 172.25 (COOH), 168.78 (C=O), 140.14 (A, C<sub>4</sub>), 135.27 (A, C<sub>2</sub>+C<sub>6</sub>), 121.30 (A, C<sub>3</sub>+C<sub>5</sub>), 117.43 (A, C<sub>1</sub>), 105.92 (CN), 70.83 (B, C<sub>1</sub>), 68.51 (B, C<sub>2</sub>). MS [ $m/z$  (% abundance)]: 118 (85), 198 (40), 211 (30), 314 (100). Elemental analysis calculated (%) for C<sub>11</sub>H<sub>10</sub>N<sub>2</sub>O<sub>4</sub>Se: C: 42.19, H: 3.22, N: 8.95; found: C: 41.92, H: 3.53, N: 8.82.

1.1.3.6. 2'-[(4-selenocyanatophenyl)carbamoyl]-[1,1'-biphenyl]-2-carboxylic acid (**6b**)

From diphenic anhydride. Conditions: 48 h at room temperature. The product was kept under stirring with water (25 mL) for 3 h, filtered and then washed with ethyl ether (2  $\times$  25 mL). A white powder was obtained. Yield: 23.7 %. Mp: 146–147°C. IR (KBr)  $\text{cm}^{-1}$ : 3296 (NH), 2153 (CN), 1726 (C=O, carboxylic acid), 1631 (C=O, amide).  $^1\text{H}$  NMR (400 MHz, DMSO- $d_6$ )  $\delta$ : 13.17–12.52 (bs, 1H, COOH), 10.24 (s, 1H, NH), 7.83 (d, 1H, B,  $J_{9-10}=7.6$  Hz, H<sub>9</sub>), 7.67–7.58 (m, 3H, B, H<sub>2</sub>+H<sub>5</sub>+H<sub>12</sub>), 7.58–7.48 (m, 5H, A, H<sub>2</sub>+H<sub>3</sub>+H<sub>5</sub>+H<sub>6</sub>, B, H<sub>11</sub>), 7.41 (t, 1H, B,  $J_{4-3}=J_{4-5}=7.4$  Hz, H<sub>4</sub>), 7.24 (t, 2H, B,  $J_{3-2}=J_{3-4}=J_{10-9}=J_{10-11}=5.9$  Hz, H<sub>3</sub>+H<sub>10</sub>).  $^{13}\text{C}$  NMR (100 MHz, DMSO- $d_6$ )  $\delta$ : 169.20 (COOH), 167.55 (C=O), 141.41 (A, C<sub>4</sub>), 140.79 (B, C<sub>7</sub>), 140.76 (B, C<sub>6</sub>), 136.14 (B, C<sub>8</sub>), 135.19 (A, C<sub>2</sub>+C<sub>6</sub>), 131.67 (B, C<sub>1</sub>), 131.42 (B, C<sub>11</sub>), 131.07 (B, C<sub>4</sub>), 130.45 (B, C<sub>9</sub>), 130.11 (B, C<sub>2</sub>), 129.84 (B, C<sub>3</sub>), 127.88 (B, C<sub>10</sub>), 127.78 (B, C<sub>5</sub>), 127.55 (B, C<sub>12</sub>), 121.06 (A, C<sub>3</sub>+C<sub>5</sub>), 117.14 (A, C<sub>1</sub>), 105.89 (CN). MS [ $m/z$  (% abundance)]: 152 (70), 181 (100), 225 (30), 422 (10). Elemental analysis calculated (%) for C<sub>21</sub>H<sub>14</sub>N<sub>2</sub>O<sub>3</sub>Se  $\cdot$  2H<sub>2</sub>O: C: 55.15, H: 3.97, N: 6.13; found: C: 55.39, H: 3.59, N: 6.22.

1.1.3.7. 2-[(4-selenocyanatophenyl)carbamoyl]cyclohexanecarboxylic acid (**7b**)

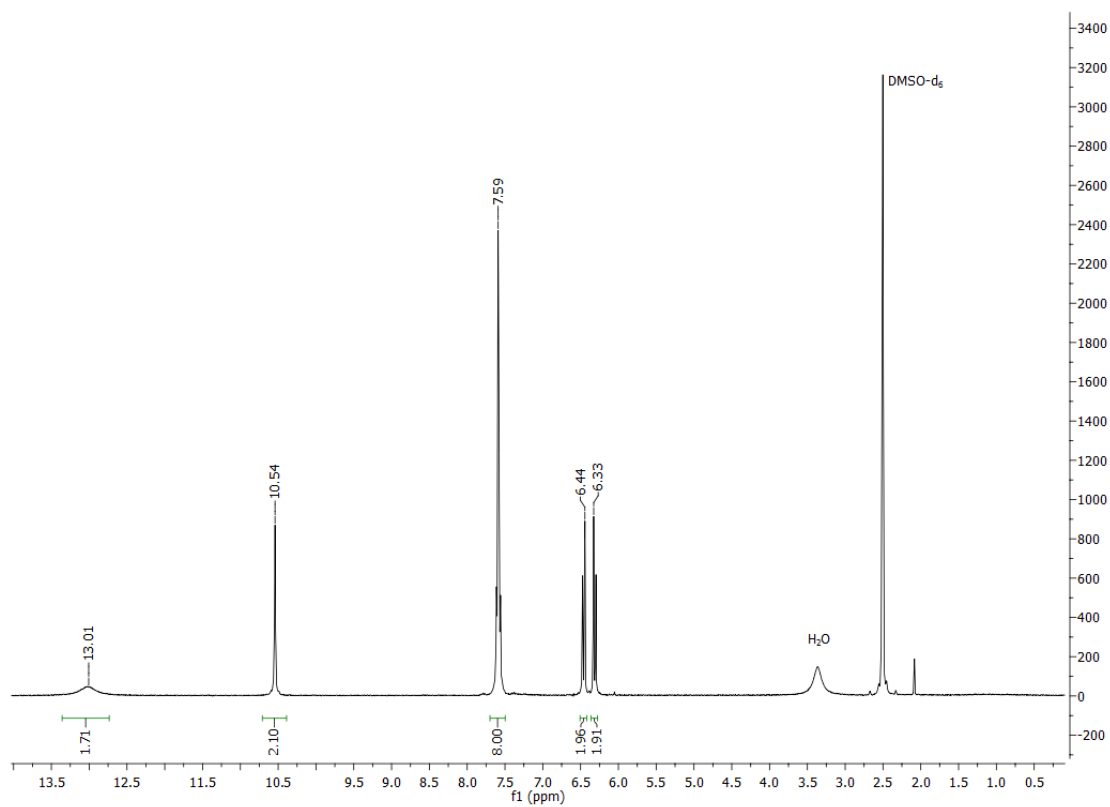
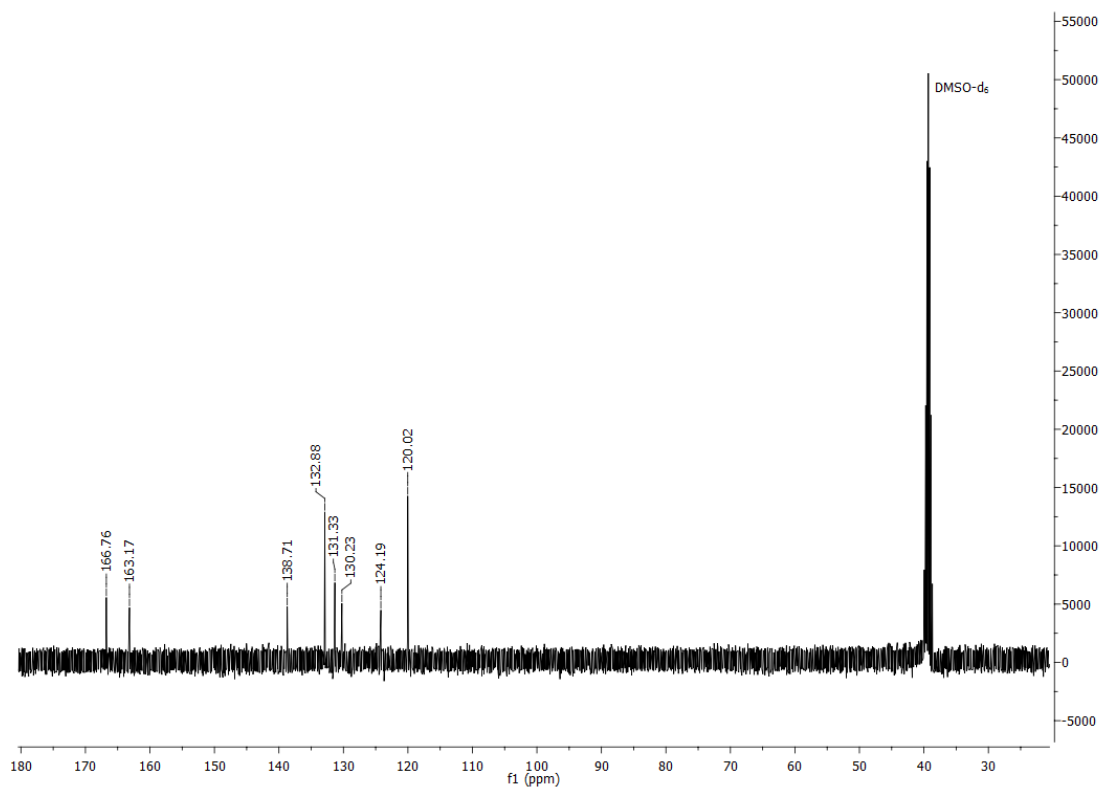
From cis-1,2-cyclohexanecarboxylic anhydride. Conditions: 24 h at room temperature. The product was kept under stirring with water (25 mL) for 2 h, filtered and then washed with ethyl ether (2  $\times$  25 mL). A white powder was obtained. Yield: 47.0 %. Mp: 150–151°C. IR (KBr)  $\text{cm}^{-1}$ : 3335 (NH), 2152 (CN), 1702 (C=O, carboxylic acid), 1677 (C=O, amide).  $^1\text{H}$  NMR (400 MHz, DMSO- $d_6$ )  $\delta$ : 12.17–11.85 (bs, 1H, COOH), 9.95 (s, 1H, NH), 7.66 (d, 4H, A,  $J_{2-3}=J_{6-5}=8.5$  Hz, H<sub>2</sub>+H<sub>6</sub>), 7.62 (d, 4H, A,  $J_{3-2}=J_{5-6}=8.5$  Hz, H<sub>3</sub>+H<sub>5</sub>), 2.94 (d, 1H, B,  $J_{1-6e}=5.4$  Hz, H<sub>1</sub>), 2.60 (m, 1H, B, H<sub>2</sub>), 2.09 (d, 1H, B,  $J_{6e-1}=5.4$  Hz, H<sub>6e</sub>), 1.99 (d, 1H, B,  $J_{3e}=8.9$  Hz, H<sub>3e</sub>), 1.71 (m, 3H, B, H<sub>3a</sub>+H<sub>6a</sub>+H<sub>5a</sub>), 1.35 (m, 3H, B, H<sub>5e</sub>+H<sub>4a</sub>+H<sub>4e</sub>).  $^{13}\text{C}$  NMR (100 MHz, DMSO- $d_6$ )  $\delta$ : 175.55 (COOH), 173.56 (C=O), 141.39 (A, C<sub>4</sub>), 135.24 (A, C<sub>2</sub>+C<sub>6</sub>), 120.76 (A, C<sub>3</sub>+C<sub>5</sub>), 116.18 (A, C<sub>1</sub>), 105.87 (CN), 43.05 (B, C<sub>2</sub>), 42.42 (B, C<sub>1</sub>), 28.06 (B, C<sub>6</sub>), 25.64 (B, C<sub>3</sub>), 24.44 (B, C<sub>5</sub>), 22.78 (B, C<sub>4</sub>). MS [ $m/z$  (% abundance)]: 67 (90), 81 (93),

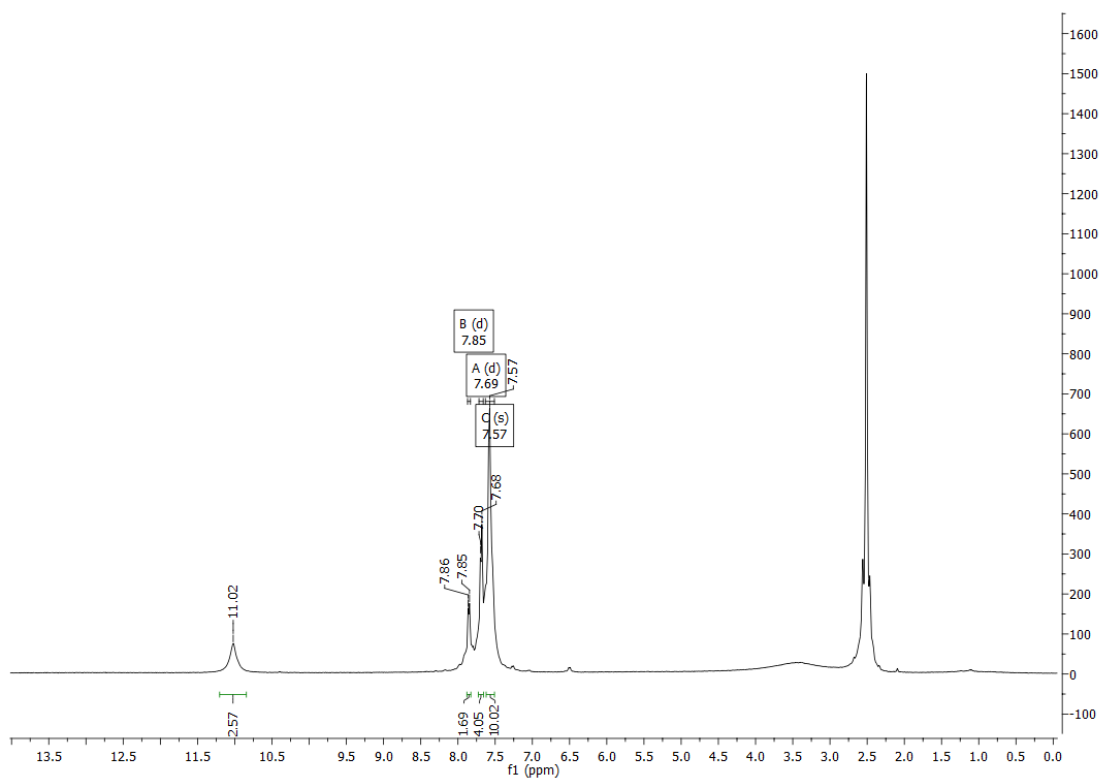
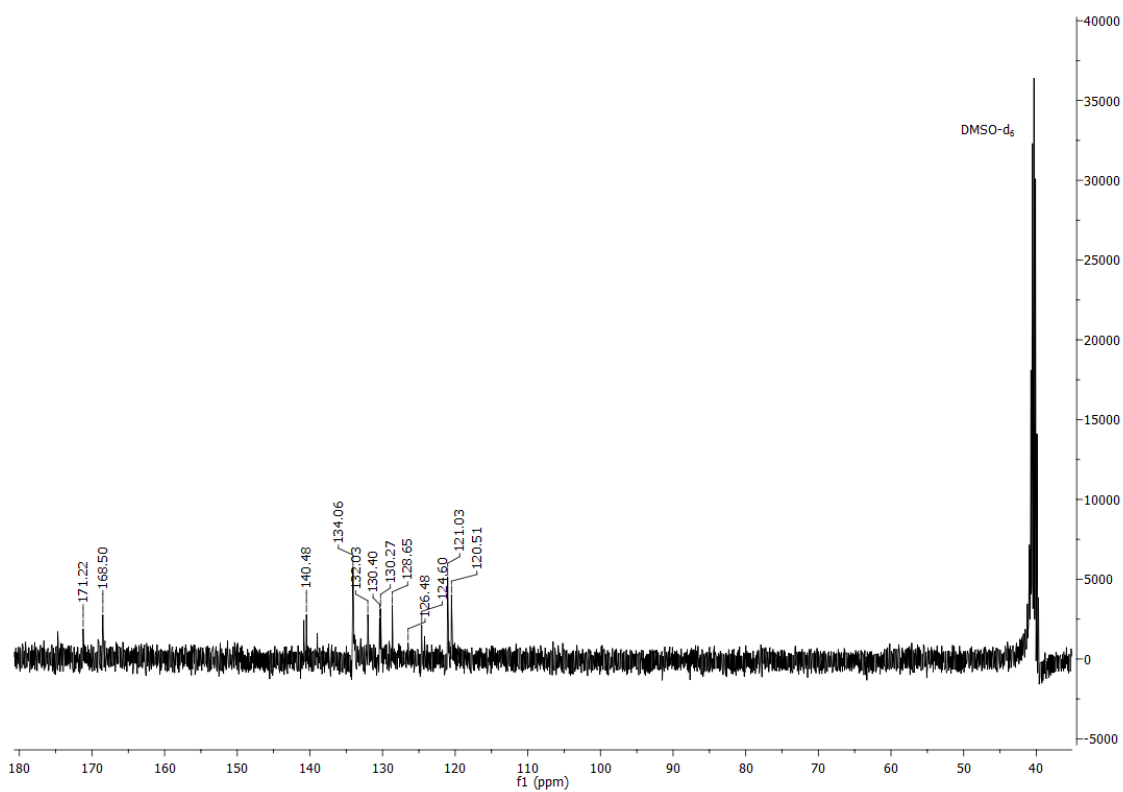
118 (100), 198 (60), 334 (100). Elemental analysis calculated (%) for  $C_{15}H_{16}N_2O_3Se \cdot H_2O$ : C: 48.79, H: 4.91, N: 7.59; found: C: 48.56, H: 4.72, N: 7.66.

1.1.3.8. 3-[(4-selenocyanatophenyl)carbamoyl]-7-oxabicyclo[2.2.1]hept-5-ene-2-carboxylic acid (**8b**)

From 3,6-epoxy-1,2,3,6-tetrahydrophthalic anhydride obtained by the classic procedure described for a Diels-Alder reaction using furan and maleic anhydride as reagents to yield the Diels-Alder adduct. Conditions: 24 h at room temperature. The product was kept under stirring with water (25 mL) for 4 h, filtered and then washed with ethyl ether ( $2 \times 25$  mL). A light-yellow powder was obtained. Yield: 20.8%. Mp: °C. 155–156°C IR (KBr)  $cm^{-1}$ : 3267 (NH), 1711 (C=O carboxylic acid), 1689 (C=O, amide).  $^1H$  NMR (400 MHz, DMSO- $d_6$ )  $\delta$ : 12.19 (s, 1H, COOH), 10.03 (s, 1H, NH), 7.65 (d, 2H, A,  $J_{2-3}=J_{6-5}=9.0$  Hz,  $H_2+H_6$ ), 7.62 (d, 2H, A,  $J_{3-2}=J_{5-6}=9.0$  Hz,  $H_3+H_5$ ), 6.50 (s, 2H, B,  $H_3+H_5$ ), 5.14 (s, 1H, B,  $H_5$ ), 5.06 (s, 1H, B,  $H_2$ ), 2.82 (d, 1H, B,  $J_{1-6}=9.1$  Hz,  $H_1$ ), 2.71 (d, 1H, B,  $J_{6-1}=9.1$  Hz,  $H_6$ ).  $^{13}C$  NMR (100 MHz, DMSO- $d_6$ )  $\delta$ : 173.08 (COOH), 170.48 (C=O), 141.07 (A,  $C_4$ ), 137.49 (B,  $C_4$ ), 137.08 (B,  $C_5$ ), 135.29 (A,  $C_2+C_6$ ), 120.79 (A,  $C_3+C_5$ ), 116.51 (A,  $C_1$ ), 105.93 (CN), 80.82 (B,  $C_6$ ), 79.61 (B,  $C_3$ ), 47.96 (B,  $C_1$ ), 47.36 (B,  $C_2$ ).  $^{77}Se$  NMR (76 MHz, DMSO- $d_6$ )  $\delta$ : 320.95 (SeCN). MS [ $m/z$  (% abundance)]: 68 (100), 118 (100), 198 (25), 278 (10). Elemental analysis calculated (%) for  $C_{15}H_{12}N_2O_4Se \cdot \frac{1}{2} H_2O$ : C: 48.35, H: 3.49, N: 7.52; found: C: 48.30, H: 3.70, N: 7.53.

## 2. NMR spectra of final products

Figure 1S. <sup>1</sup>H NMR of 1a.Figure 2S. <sup>13</sup>C NMR of 1a.

Figure 3S.  $^1\text{H}$  NMR of 2a.Figure 4S.  $^{13}\text{C}$  NMR of 2a.



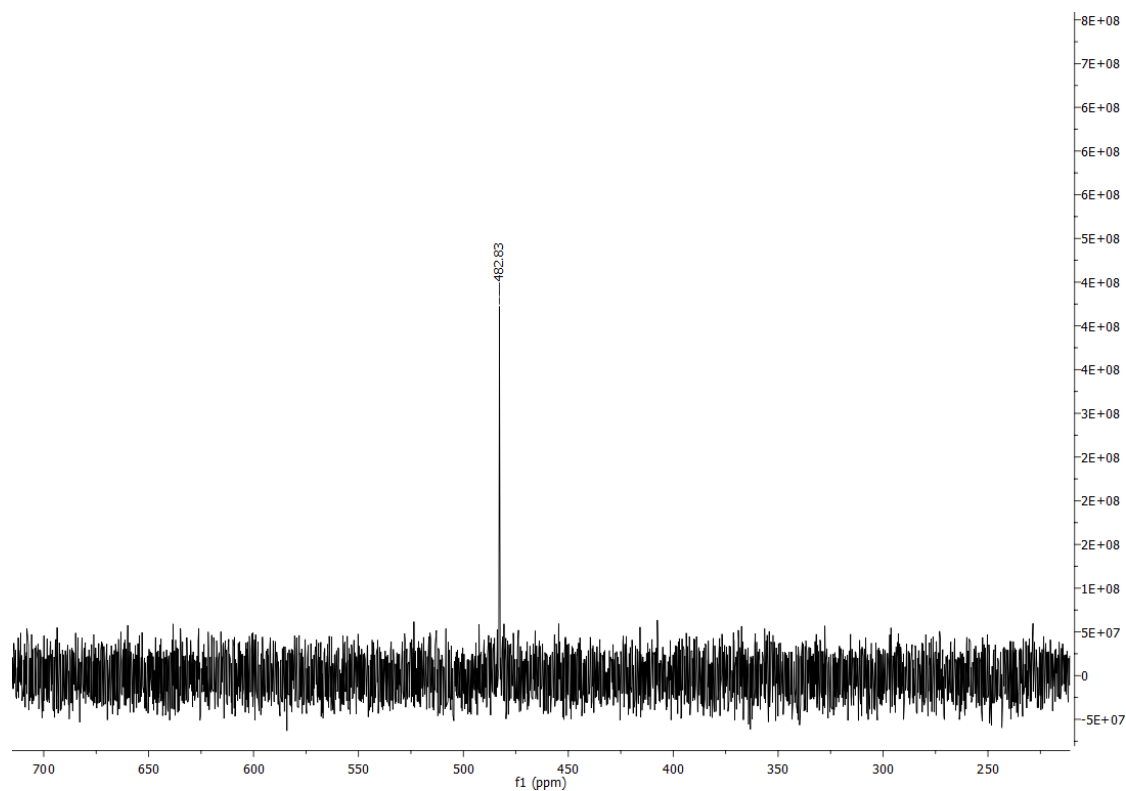


Figure 5S.  $^{77}\text{Se}$  NMR of 2a.

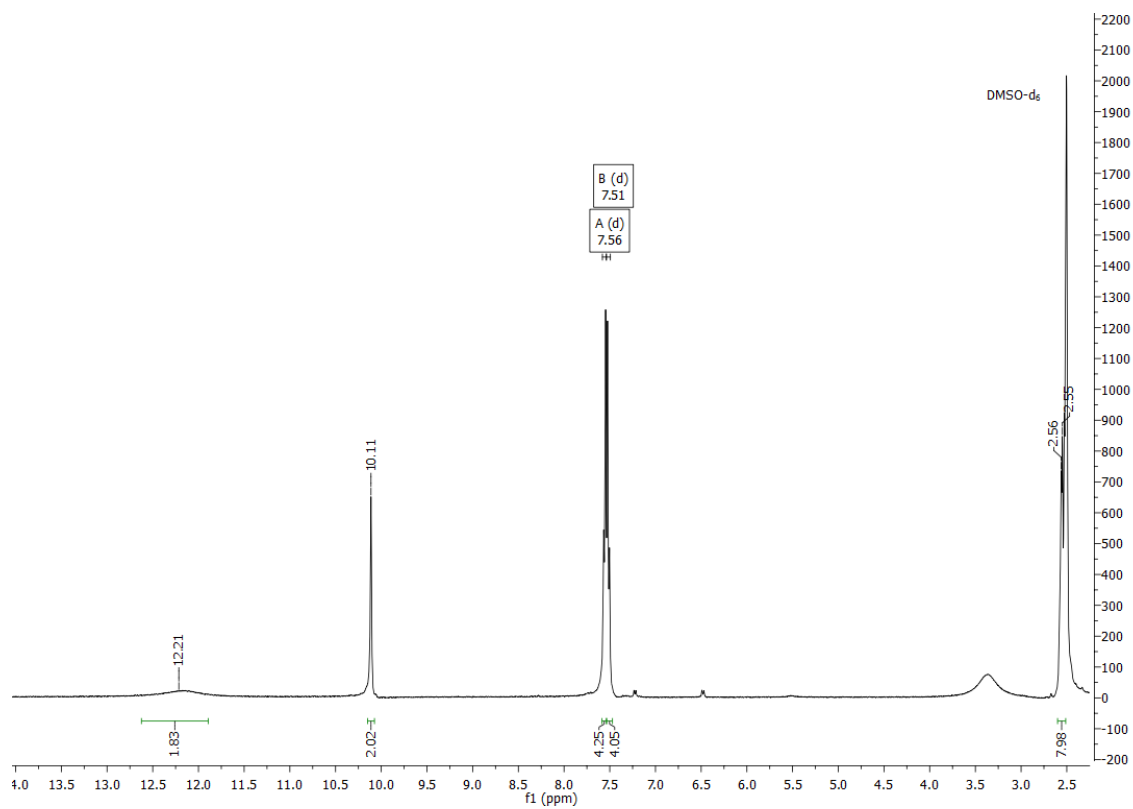
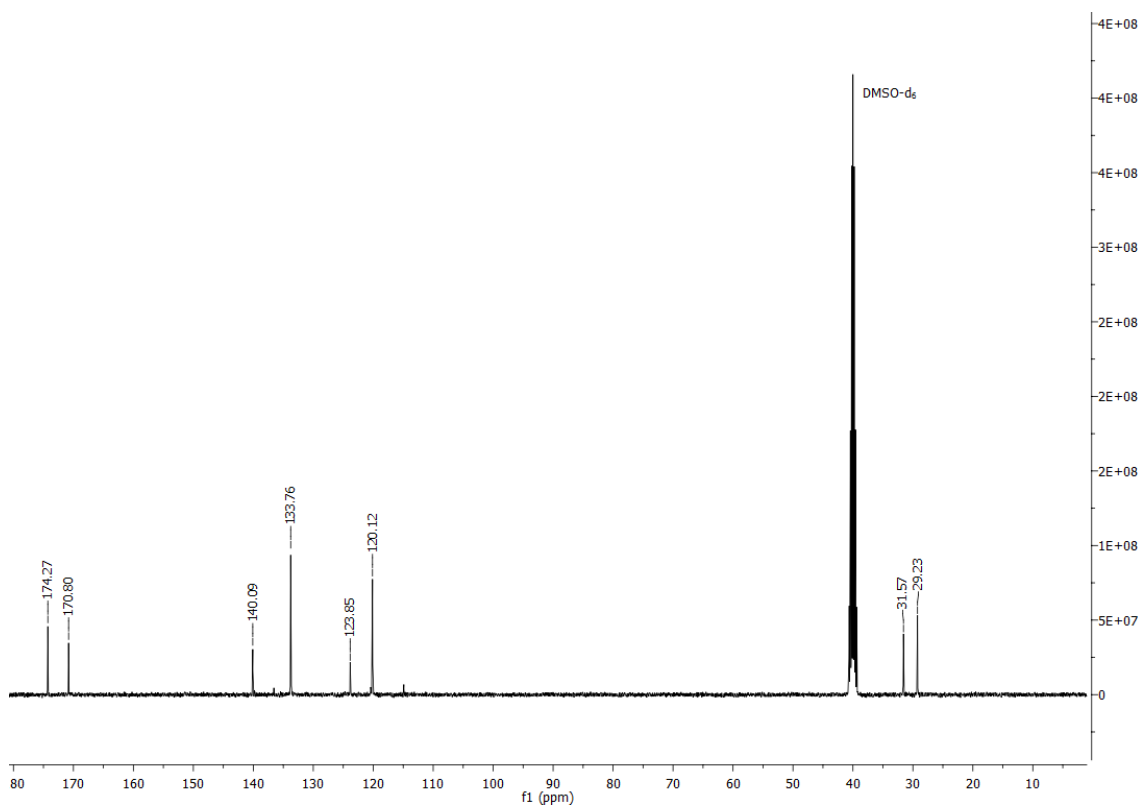
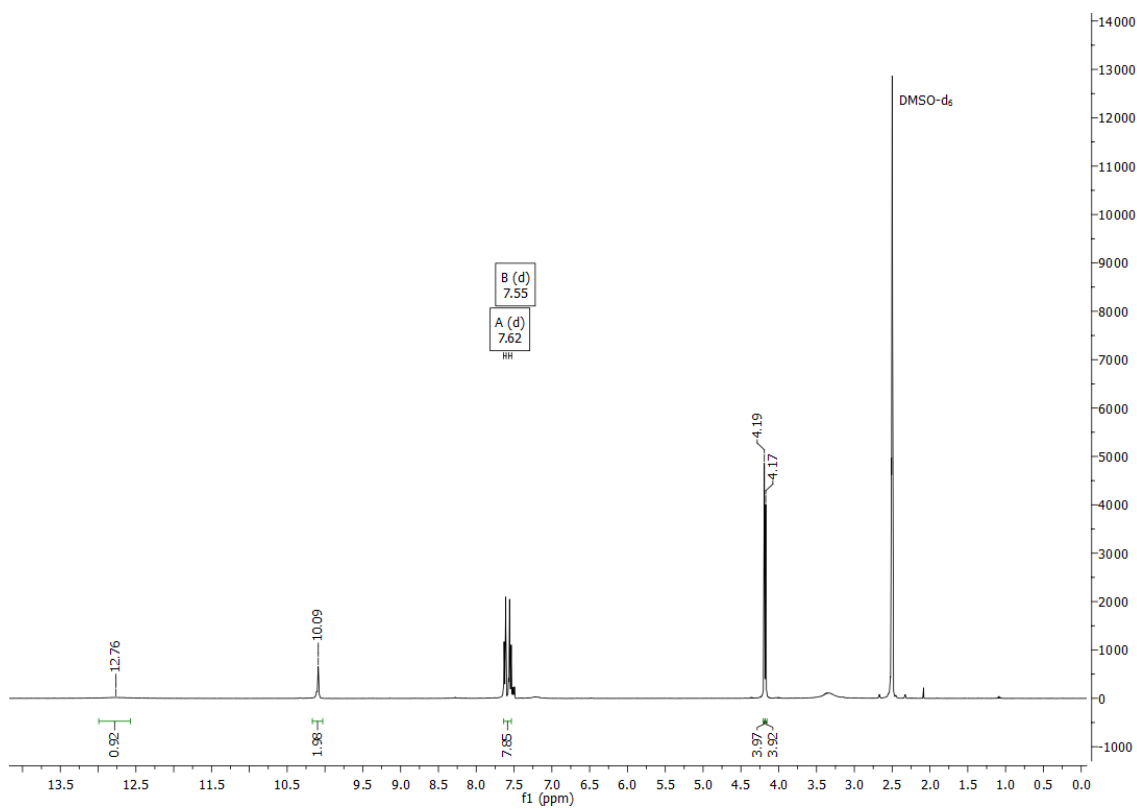


Figure 6S.  $^1\text{H}$  NMR of 3a.

Figure 7S.  $^{13}\text{C}$  NMR of 3a.Figure 8S.  $^1\text{H}$  NMR of 5a.

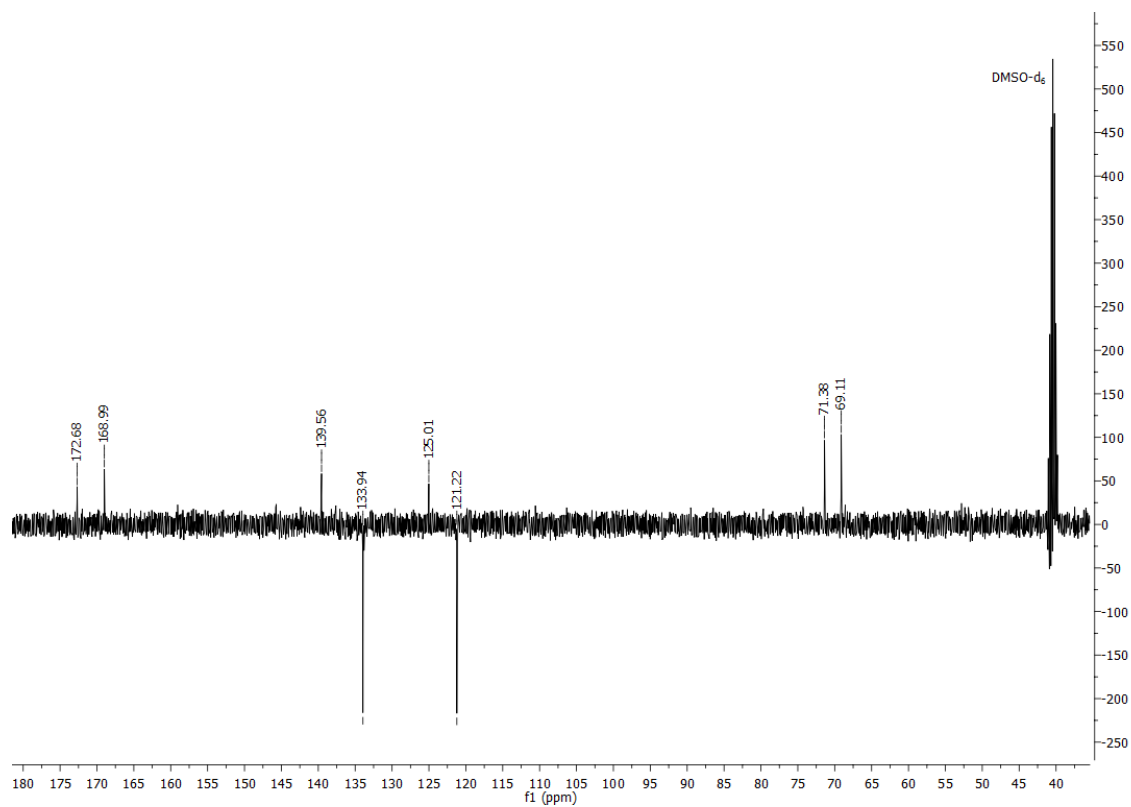


Figure 9S. <sup>13</sup>C APT NMR of 5a.

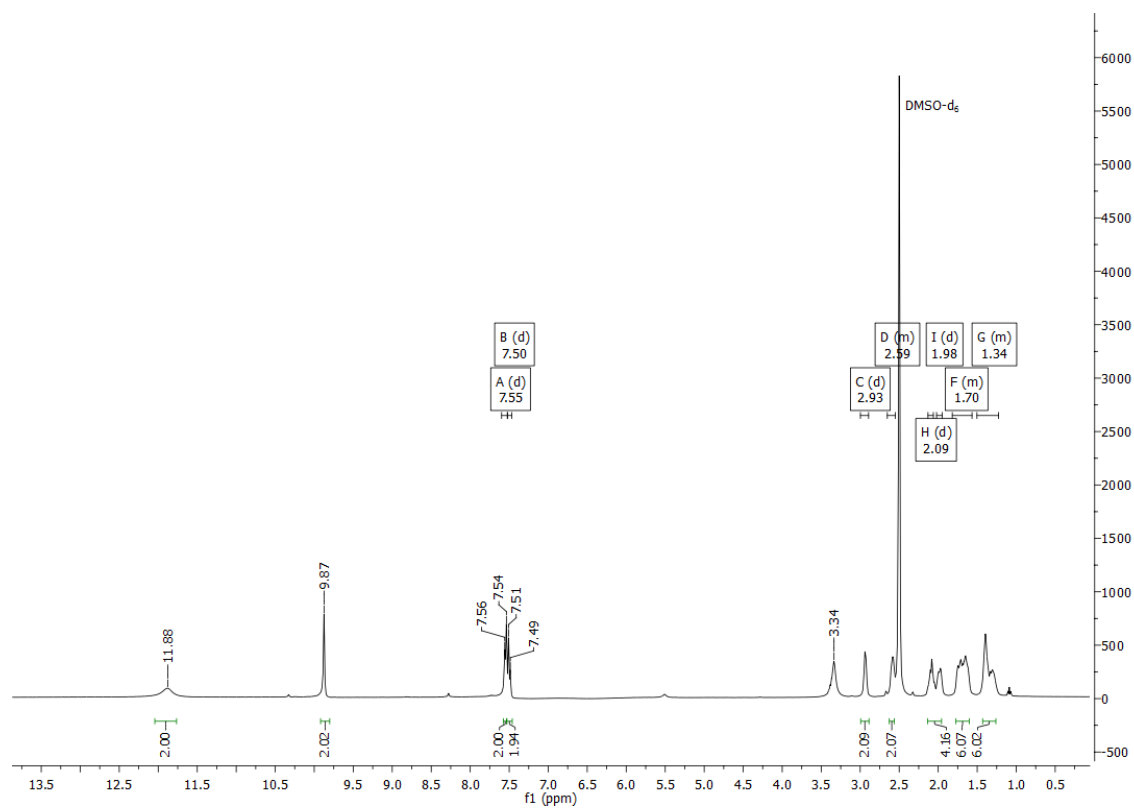
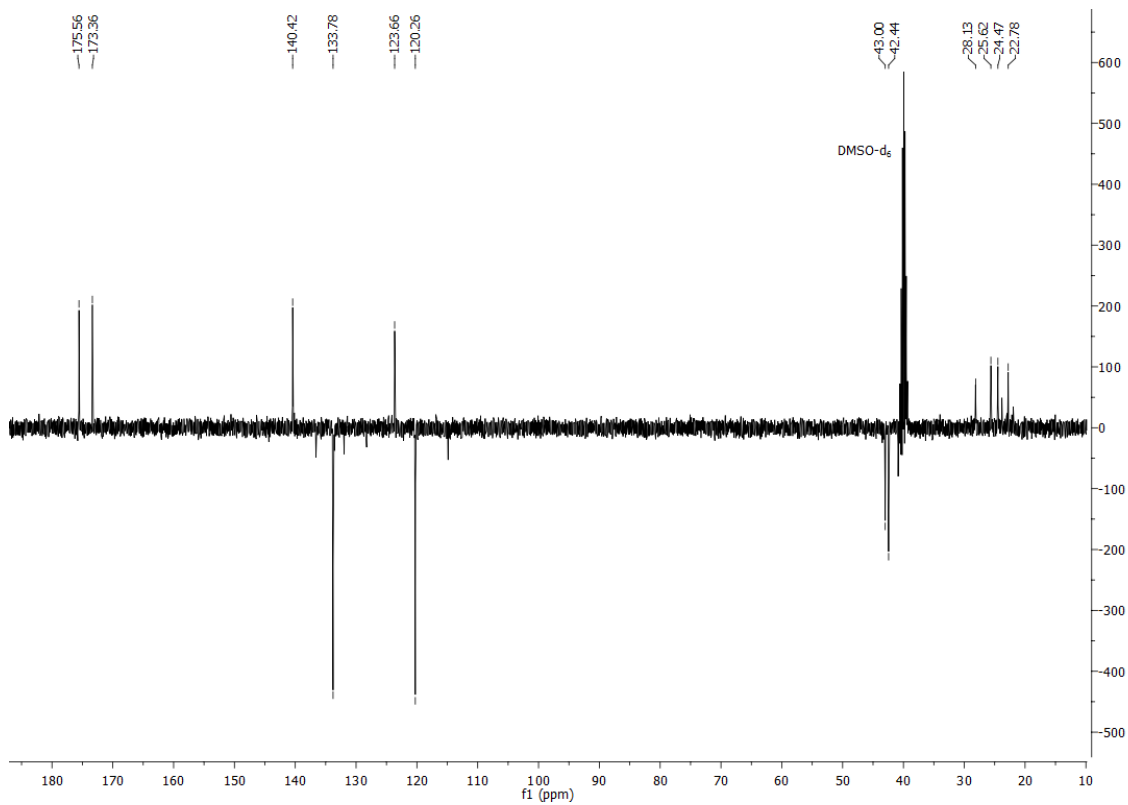
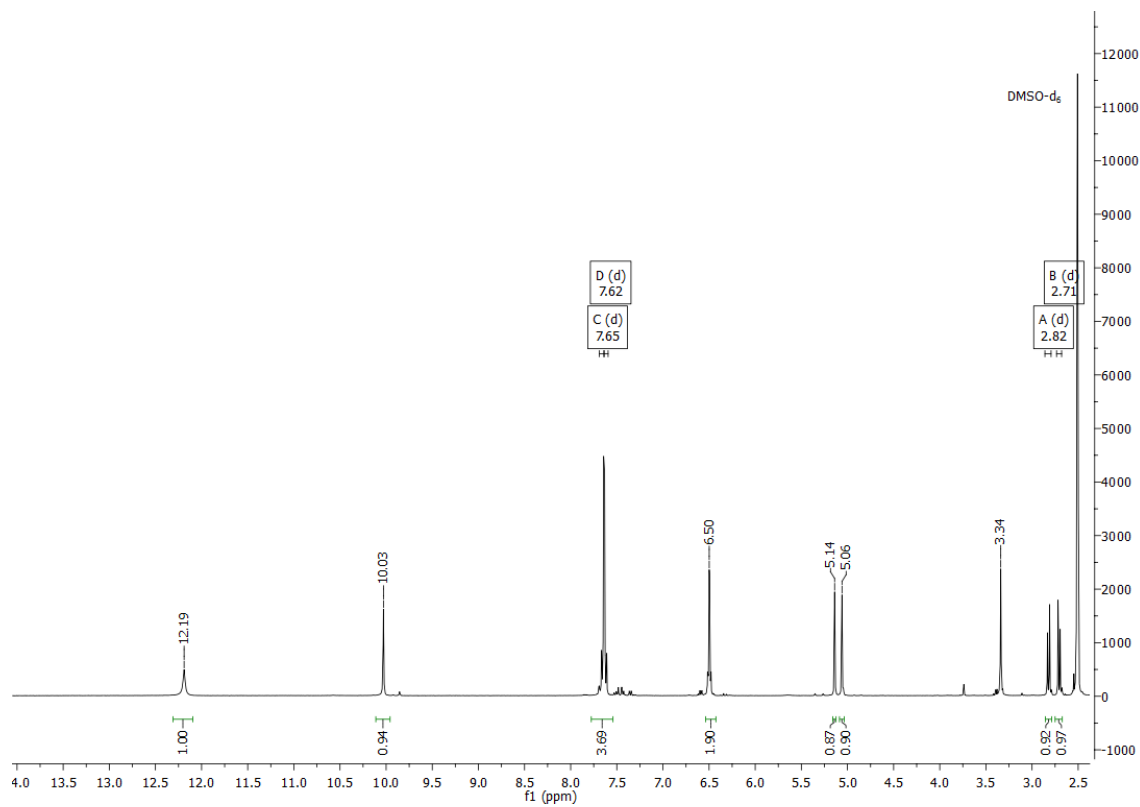


Figure 10S. <sup>1</sup>H NMR of 7a.

Figure 11S. <sup>13</sup>C APT NMR of 7a.Figure 12S. <sup>1</sup>H NMR of 8a.

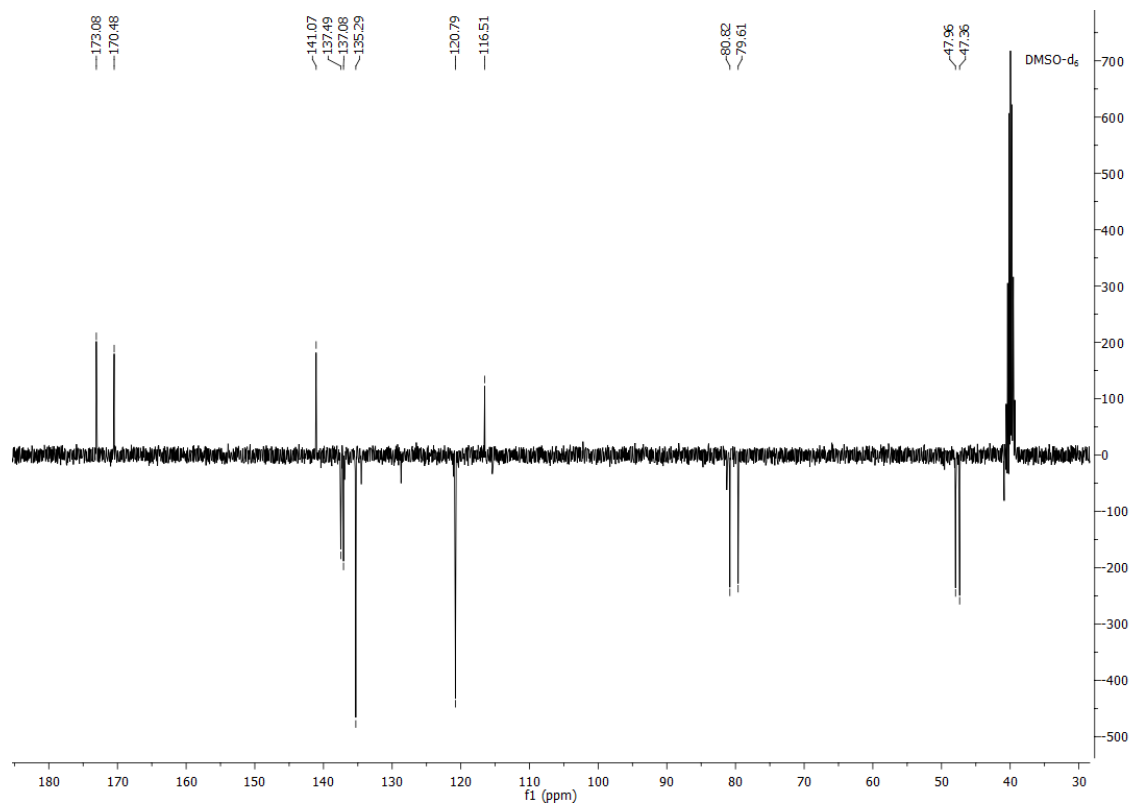


Figure 13S.  $^{13}\text{C}$  APT NMR of 8a.

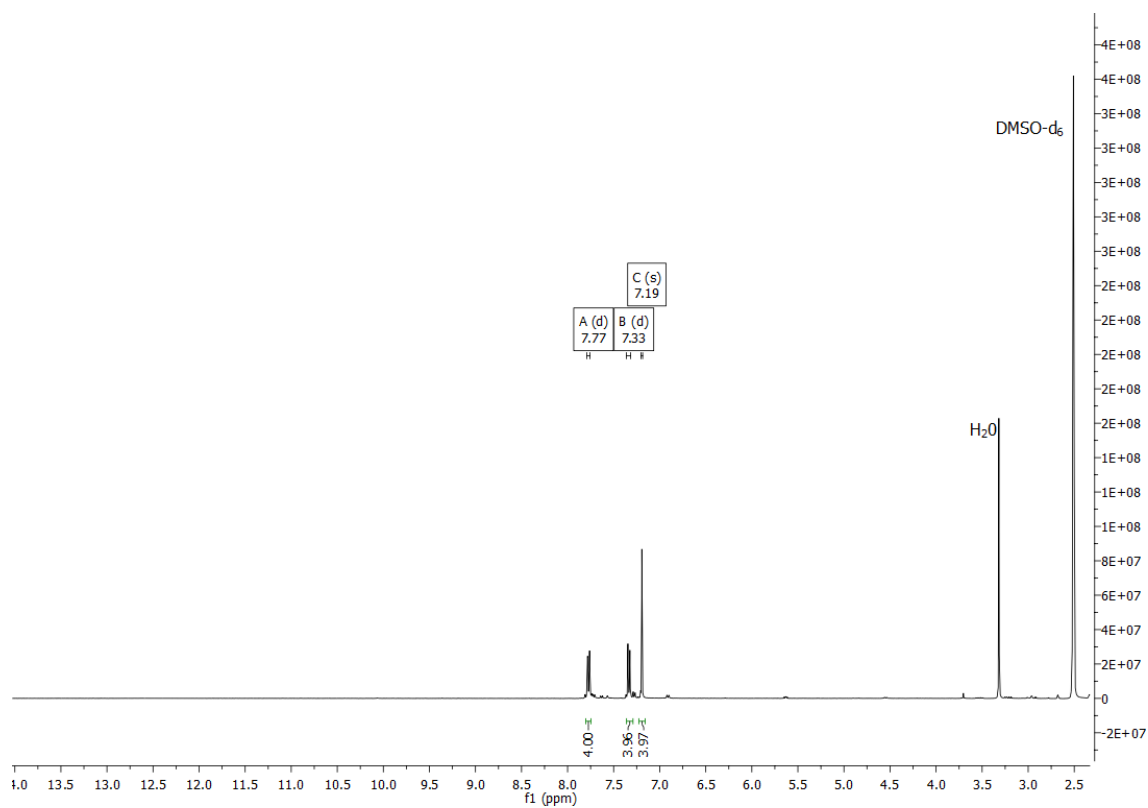
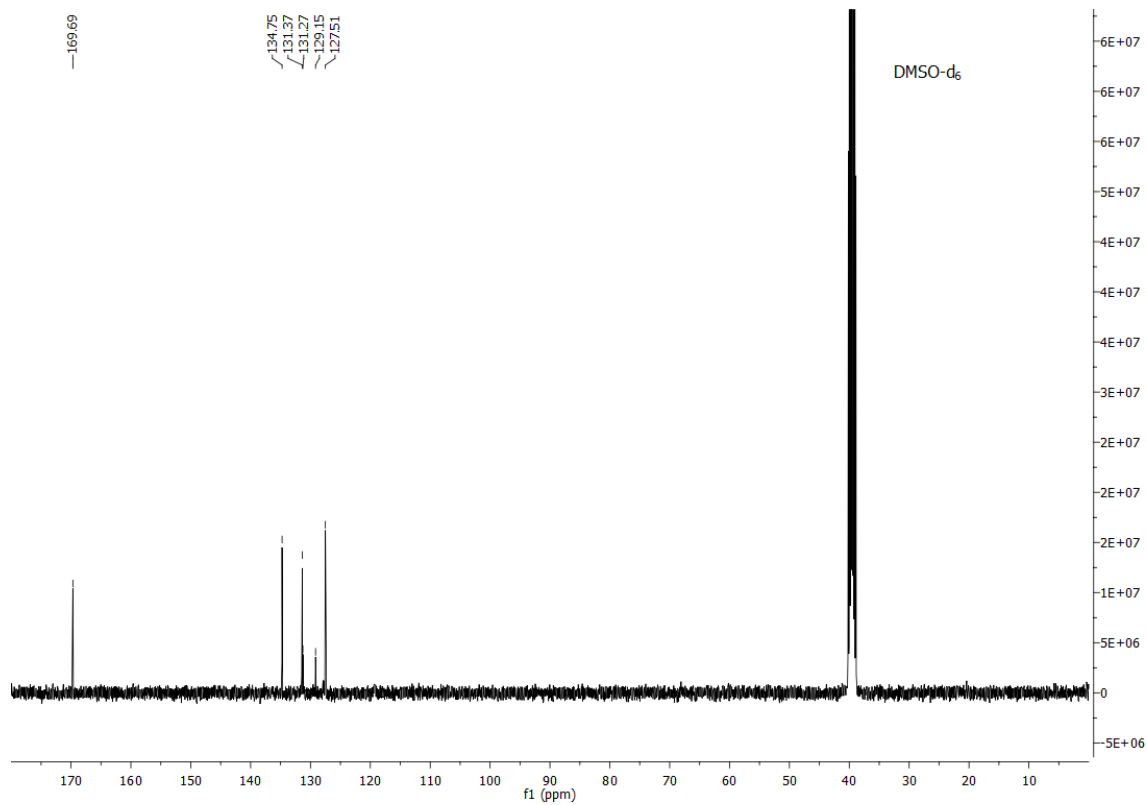
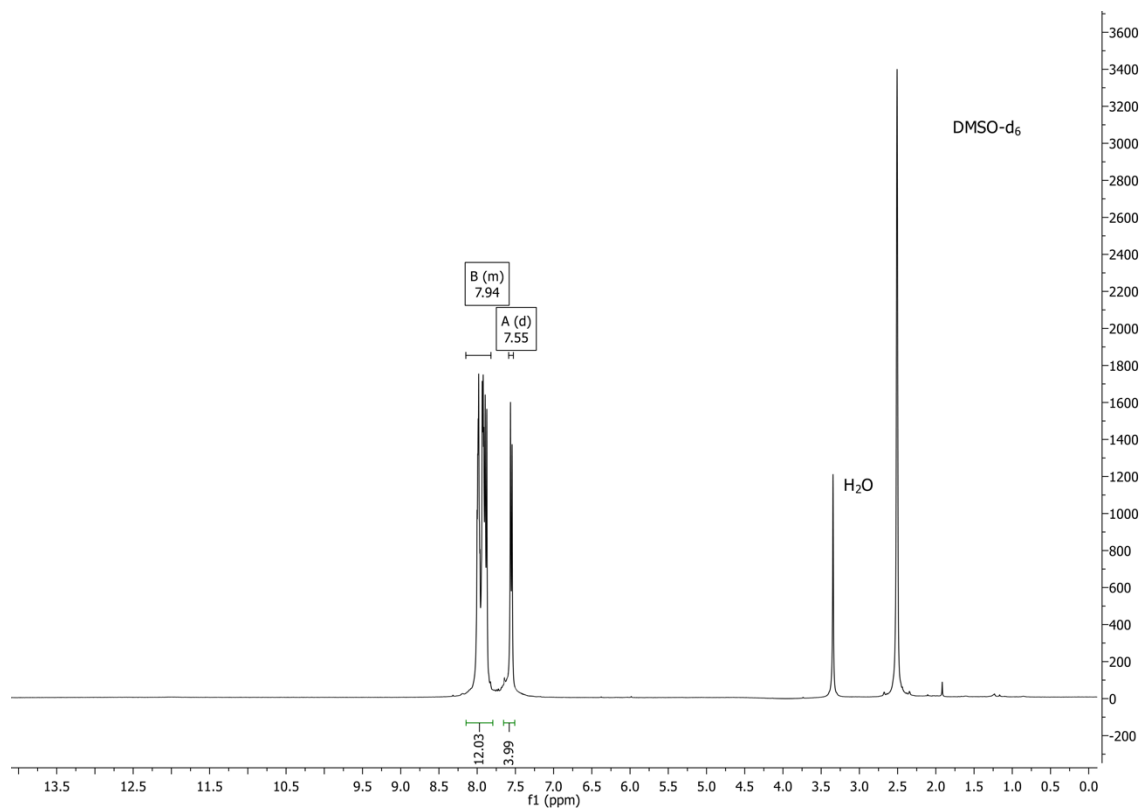


Figure 14S.  $^1\text{H}$  NMR of 9a.

Figure 15S.  $^{13}\text{C}$  NMR of 9a.Figure 16S.  $^1\text{H}$  NMR of 10a.

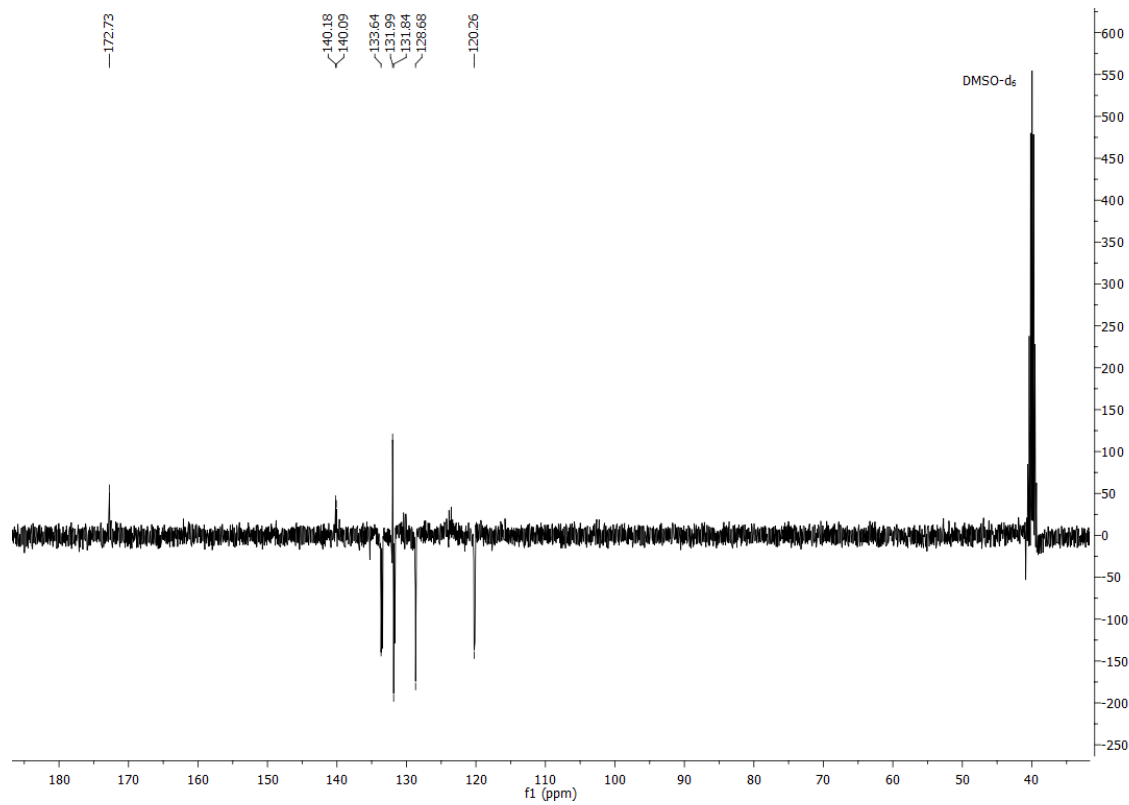


Figure 17S. <sup>13</sup>C APT NMR of 10a.

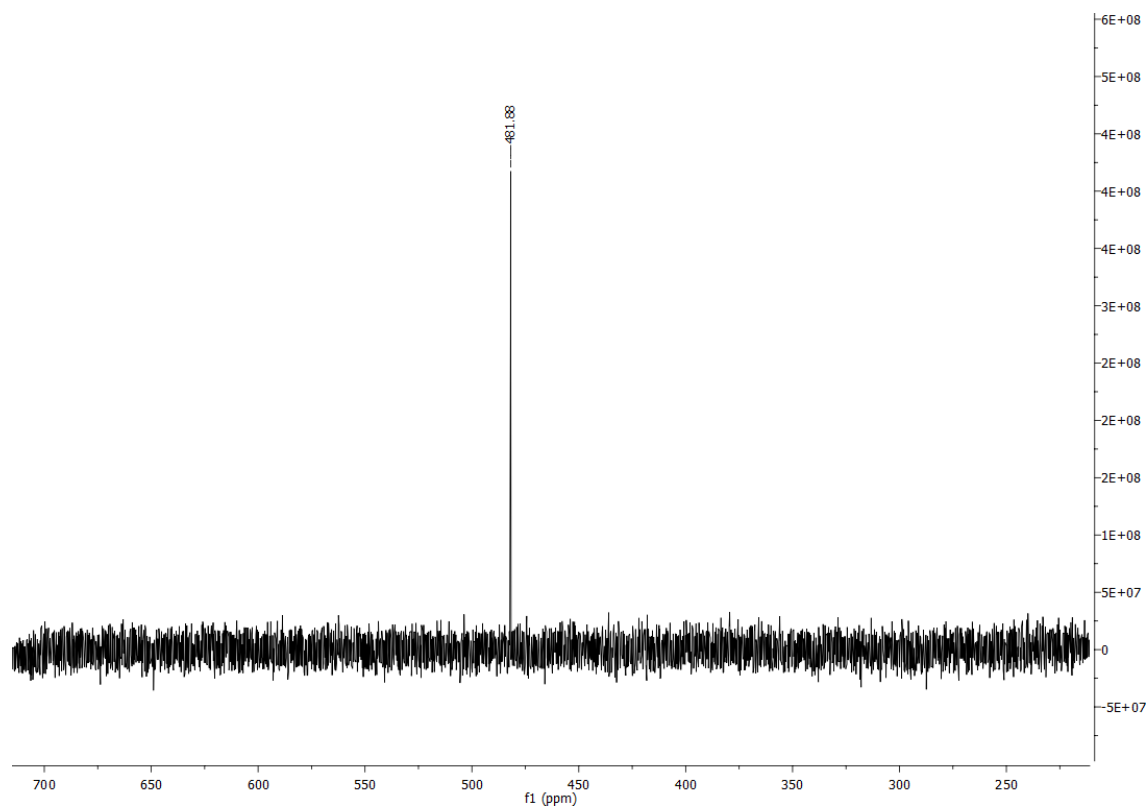
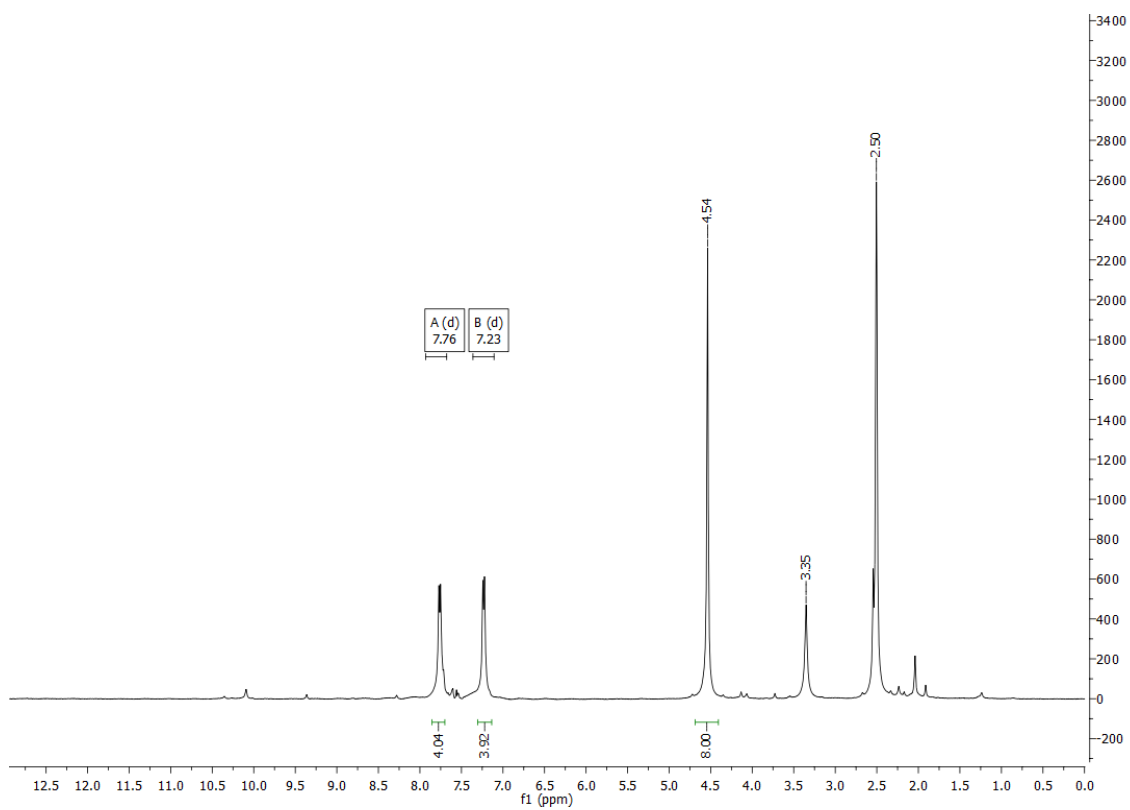
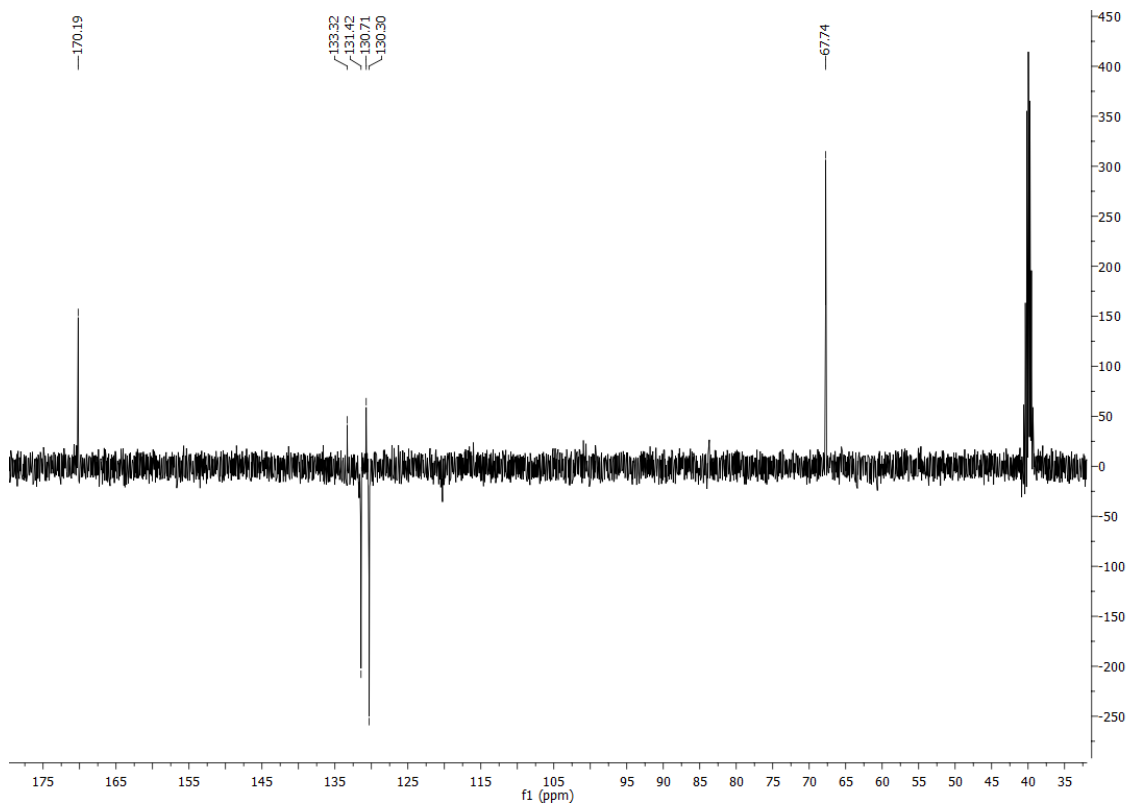


Figure 18S. <sup>77</sup>Se NMR of 10a.

Figure 19S.  $^1\text{H}$  NMR of 11a.Figure 20S.  $^{13}\text{C}$  APT NMR of 11a.



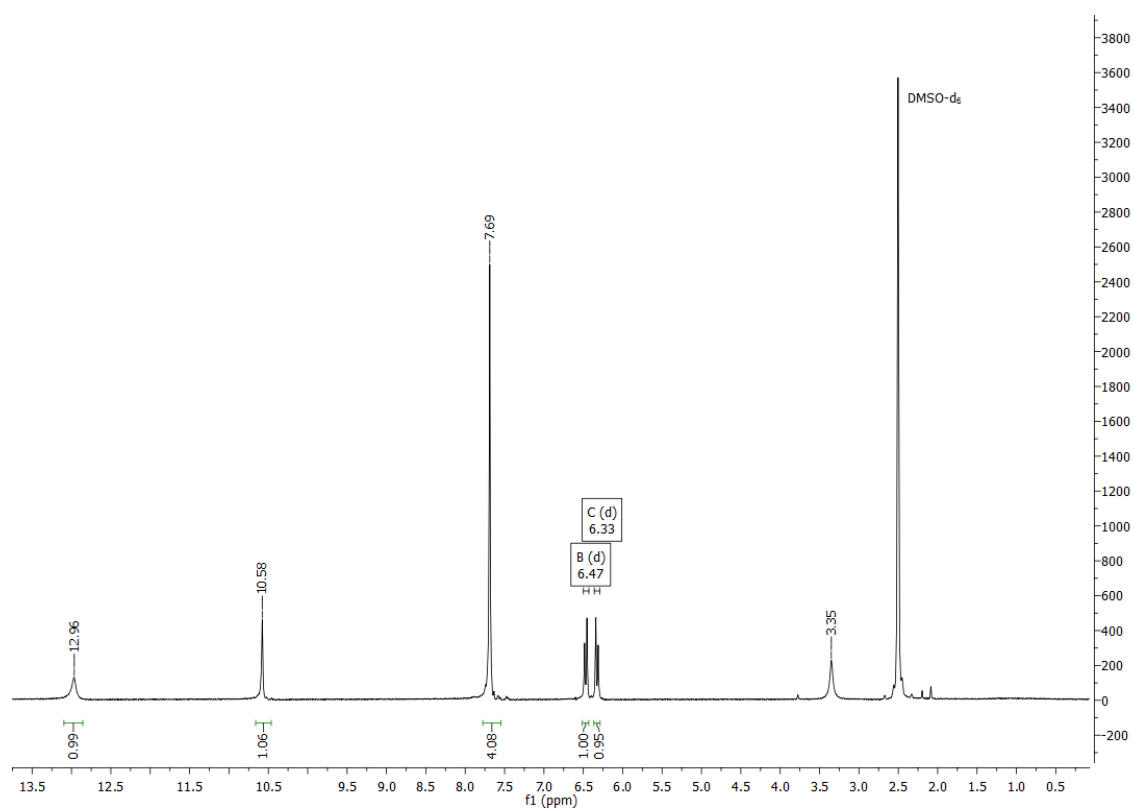


Figure 21S.  $^1\text{H}$  NMR of 1b.

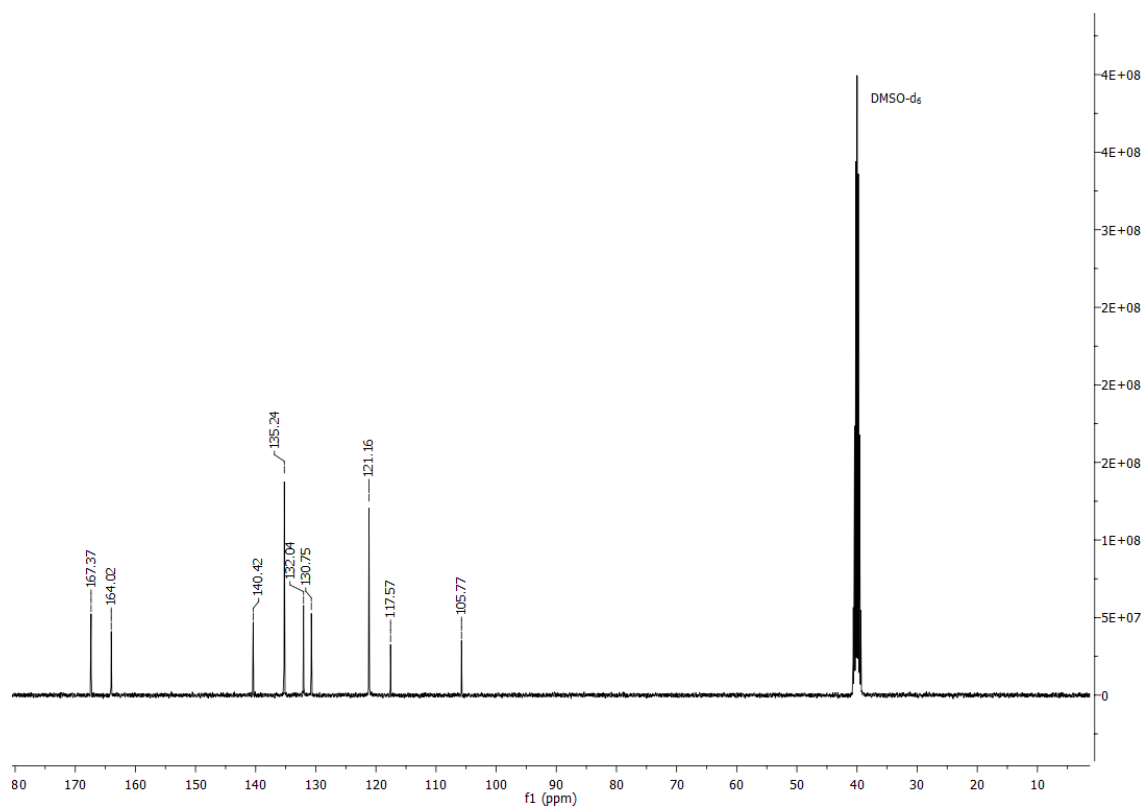
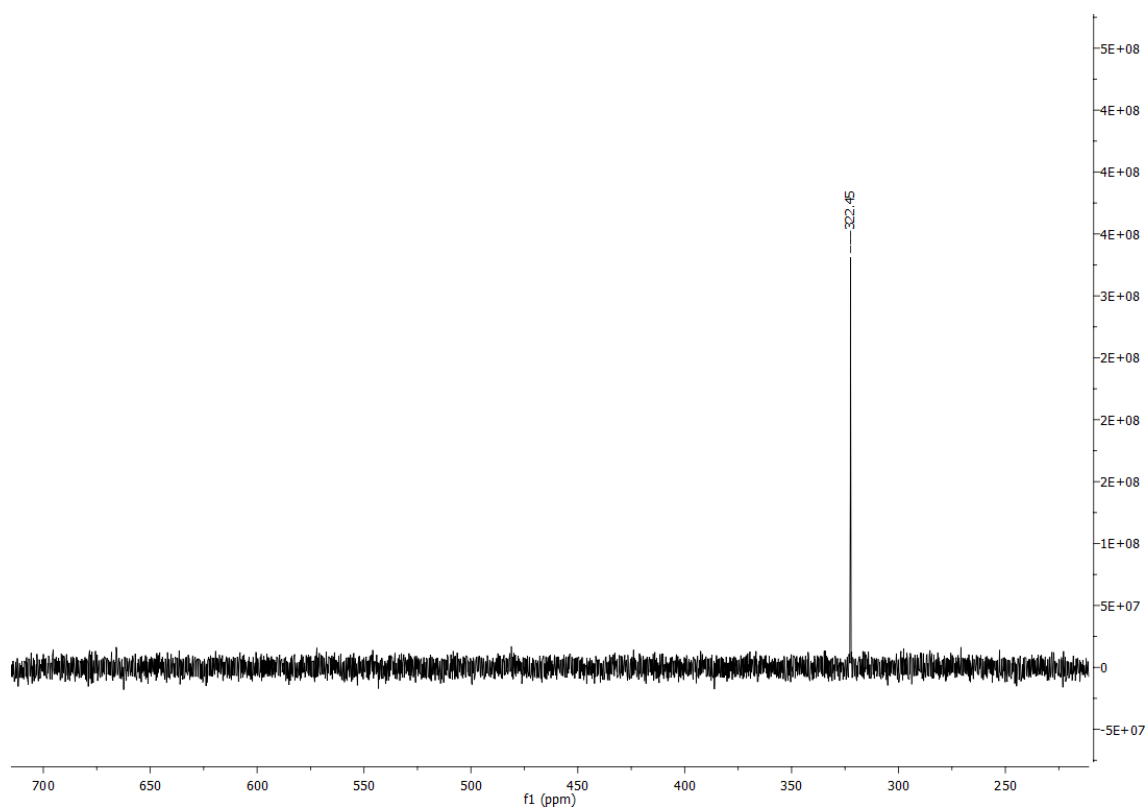
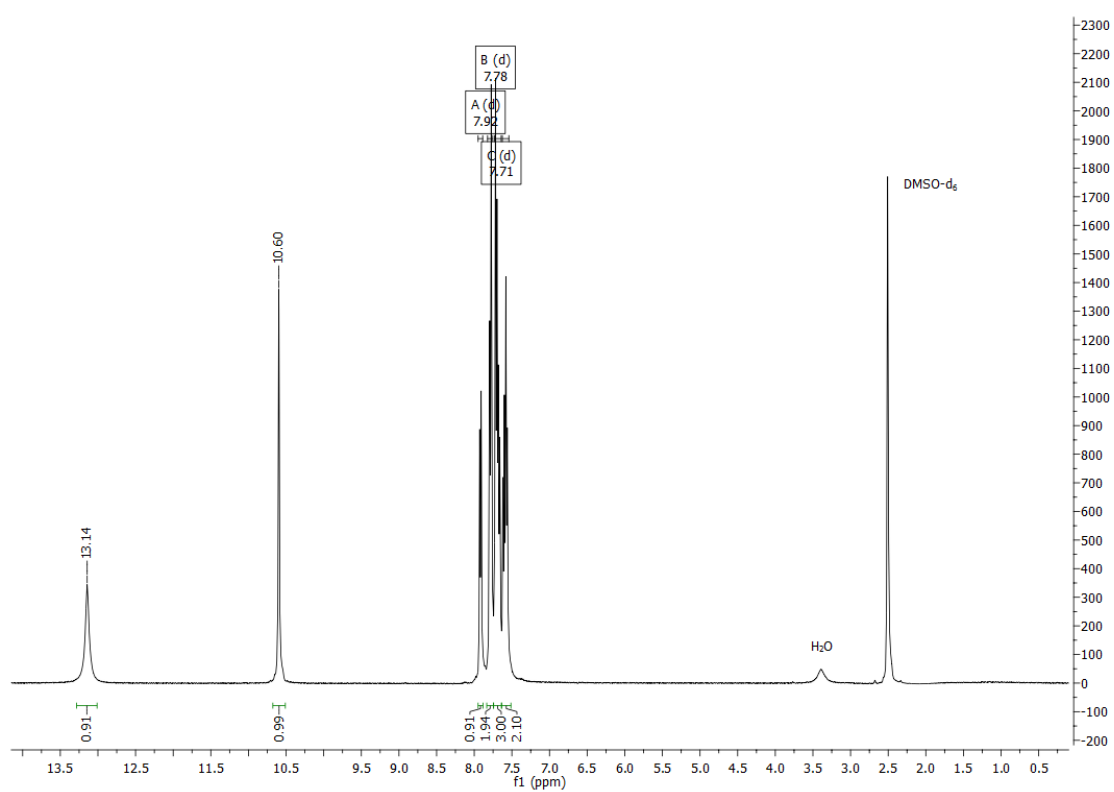


Figure 22S.  $^{13}\text{C}$  NMR of 1b.

Figure 23S.  $^{77}\text{Se}$  NMR of 1b.Figure 24S.  $^1\text{H}$  NMR of 2b.

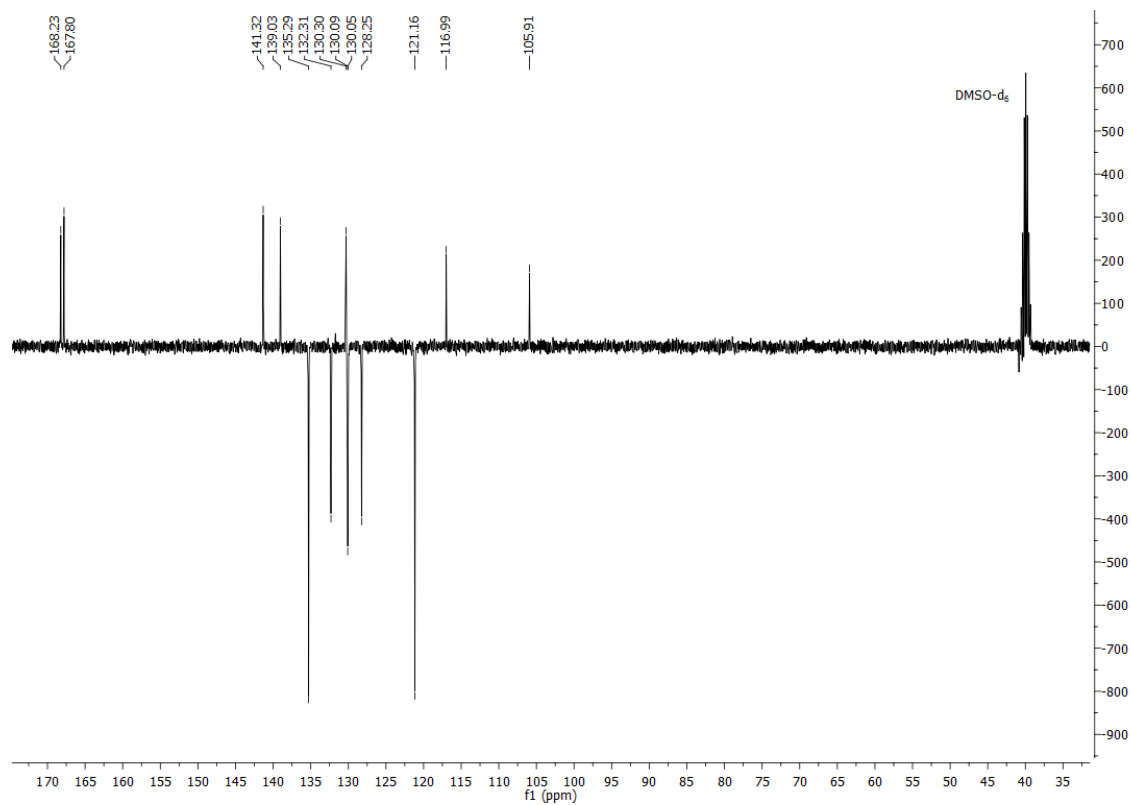


Figure 25S. <sup>13</sup>C APT NMR of **2b**.

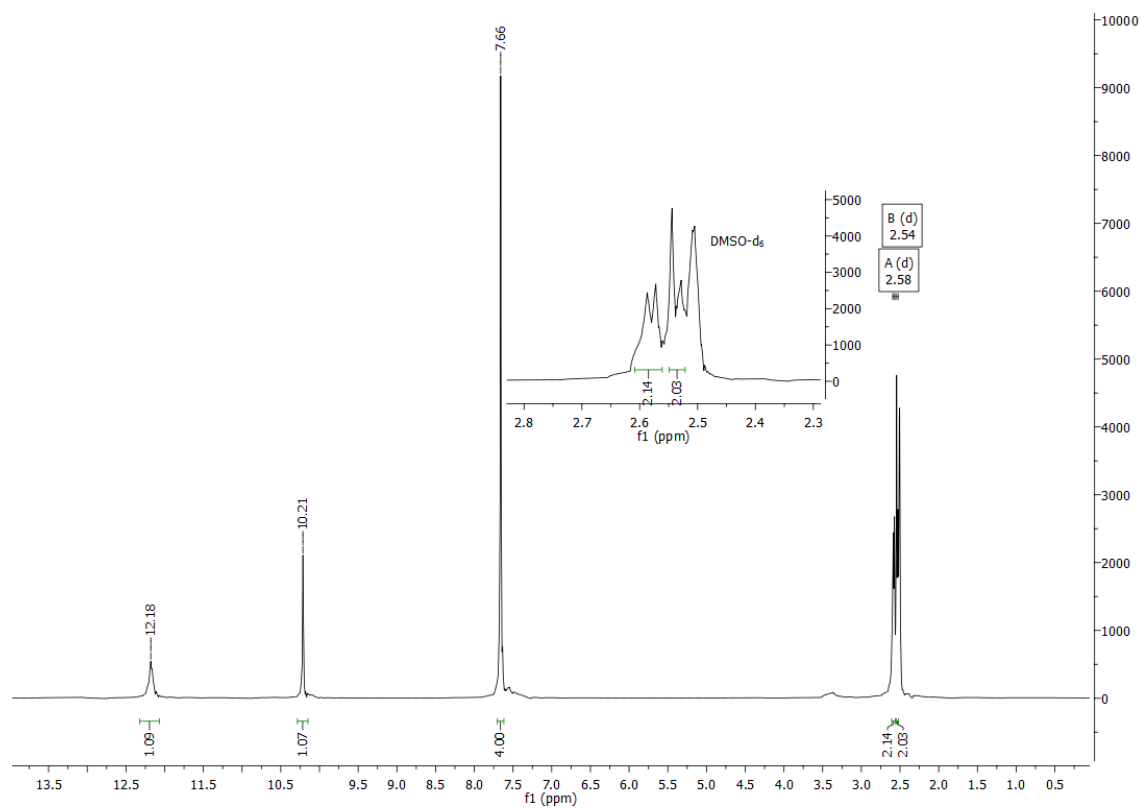
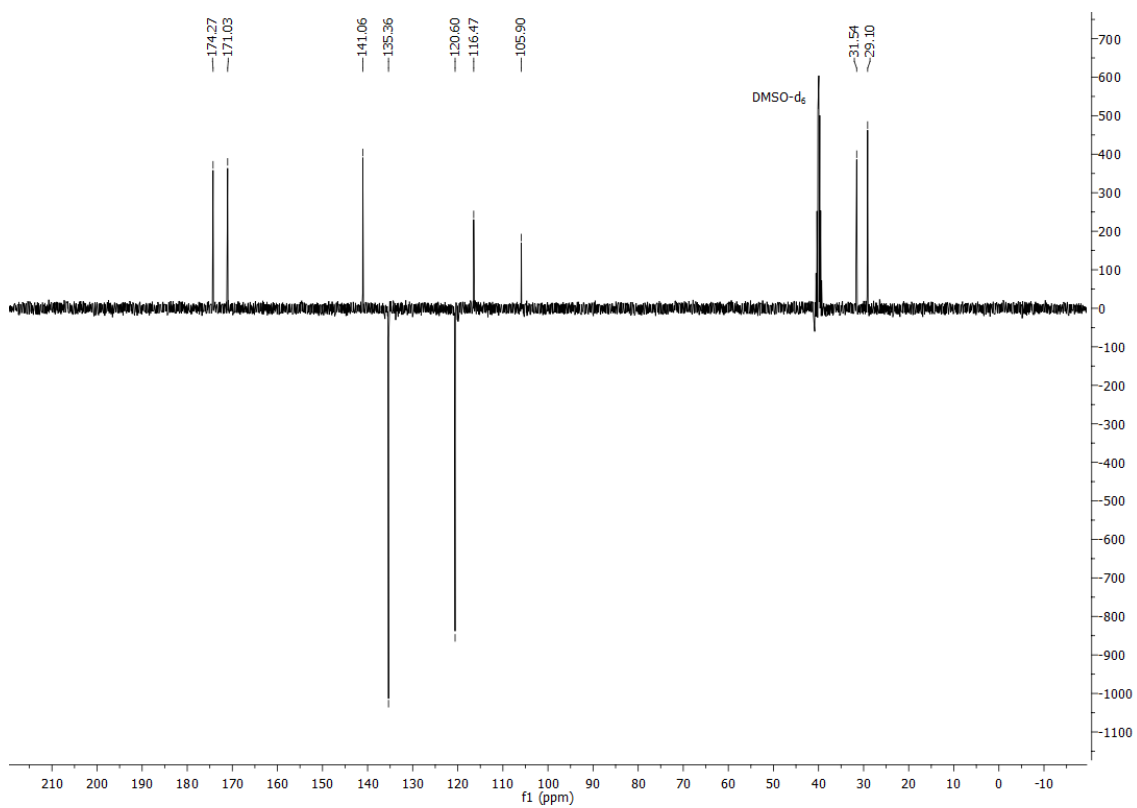
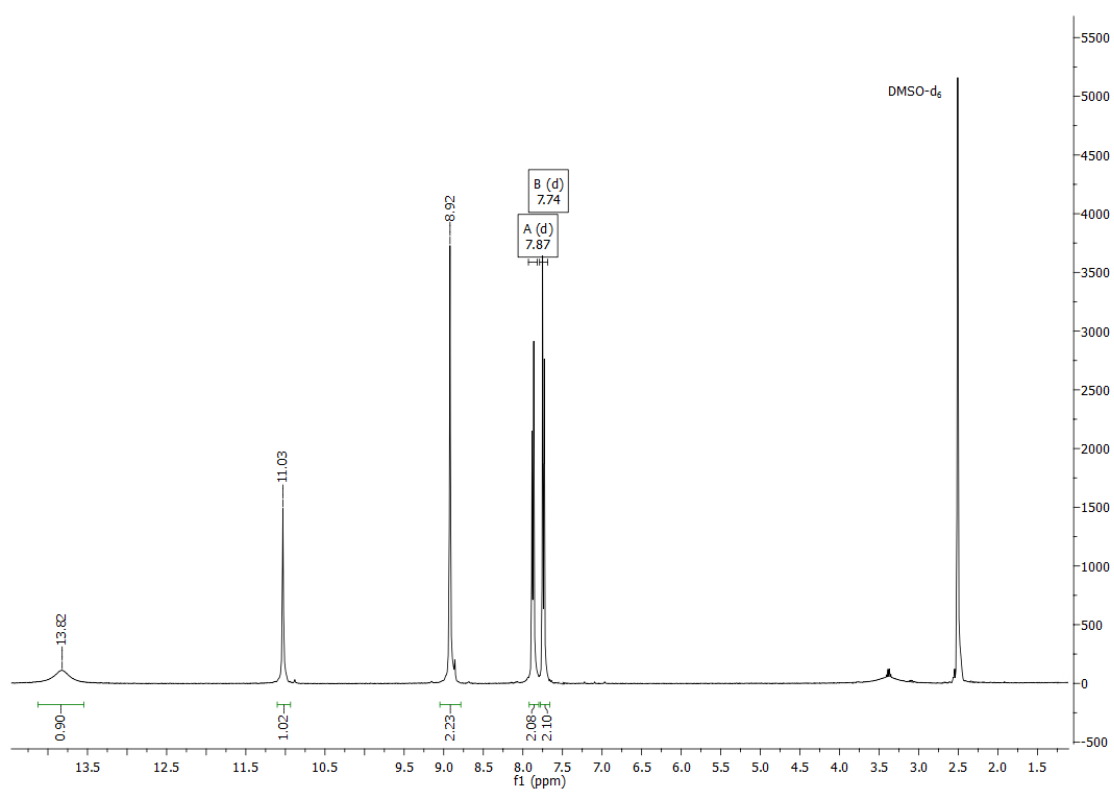


Figure 26S. <sup>1</sup>H NMR of **3b**.

Figure 27S.  $^{13}\text{C}$  APT NMR of **3b**.Figure 28S.  $^1\text{H}$  NMR of **4b**.

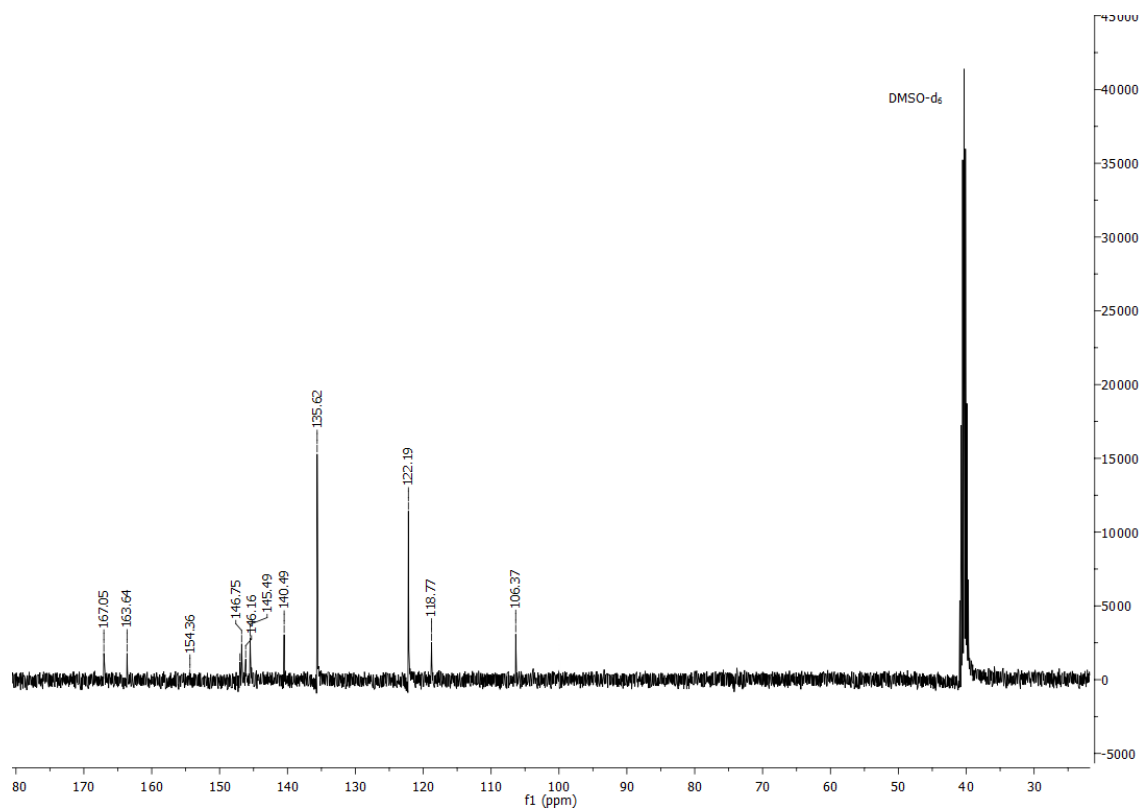


Figure 29S. <sup>13</sup>C NMR of 4b.

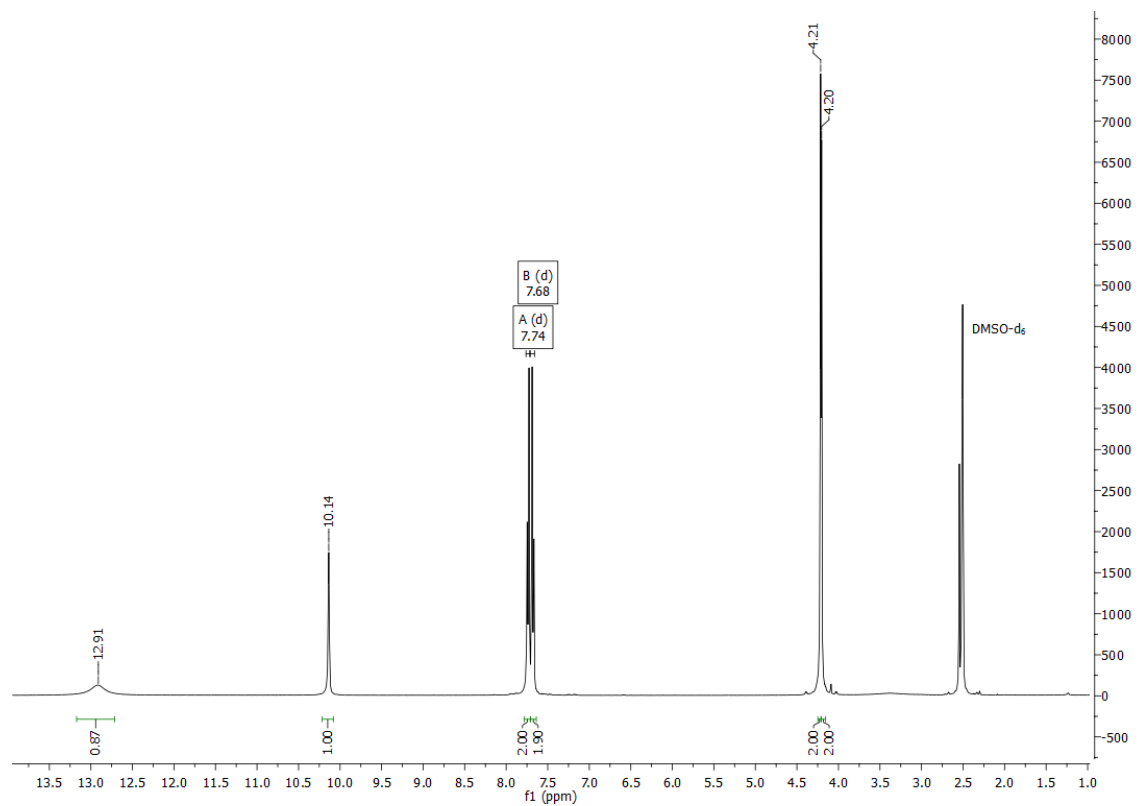
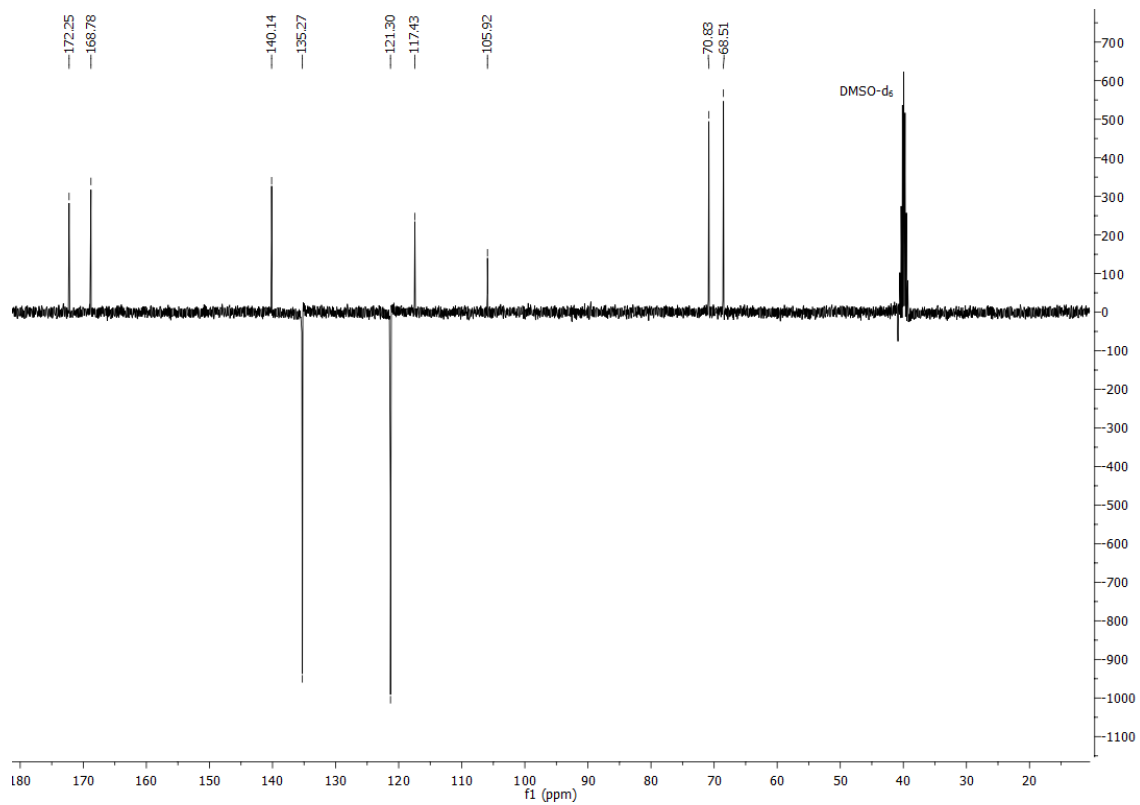
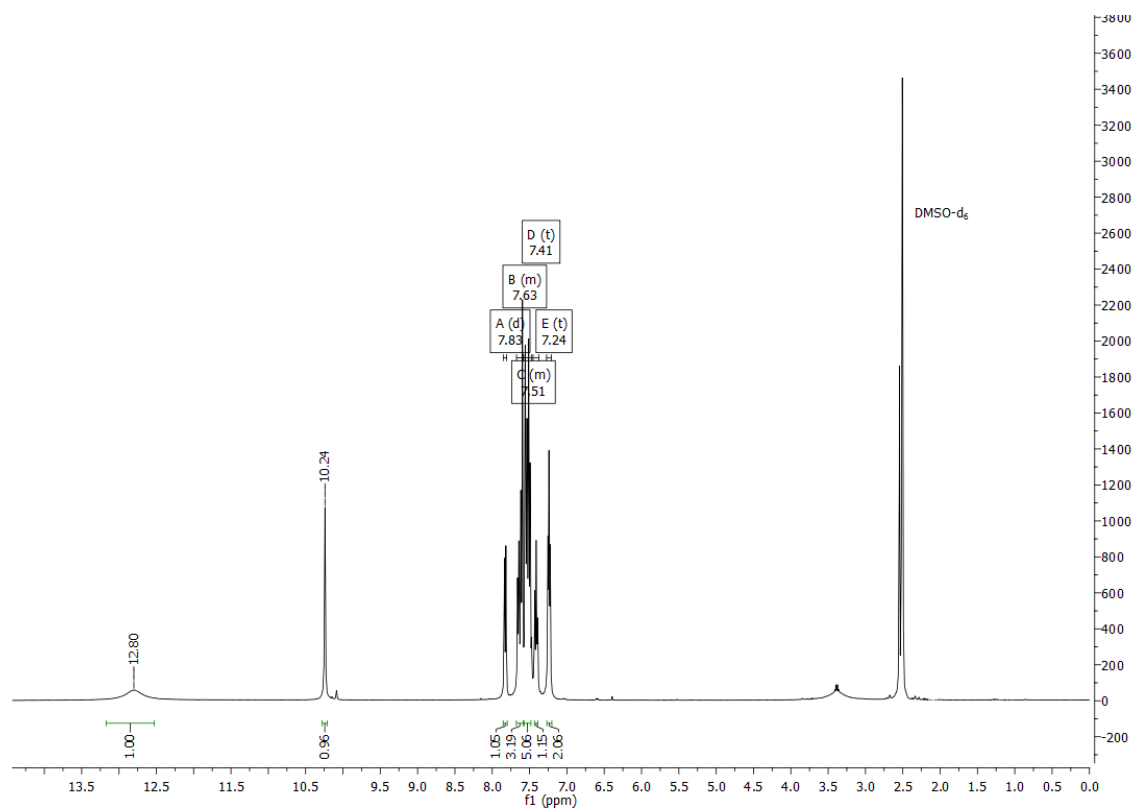


Figure 30S. <sup>1</sup>H NMR of 5b.

Figure 31S.  $^{13}\text{C}$  APT NMR of **5b**.Figure 32S.  $^1\text{H}$  NMR of **6b**.

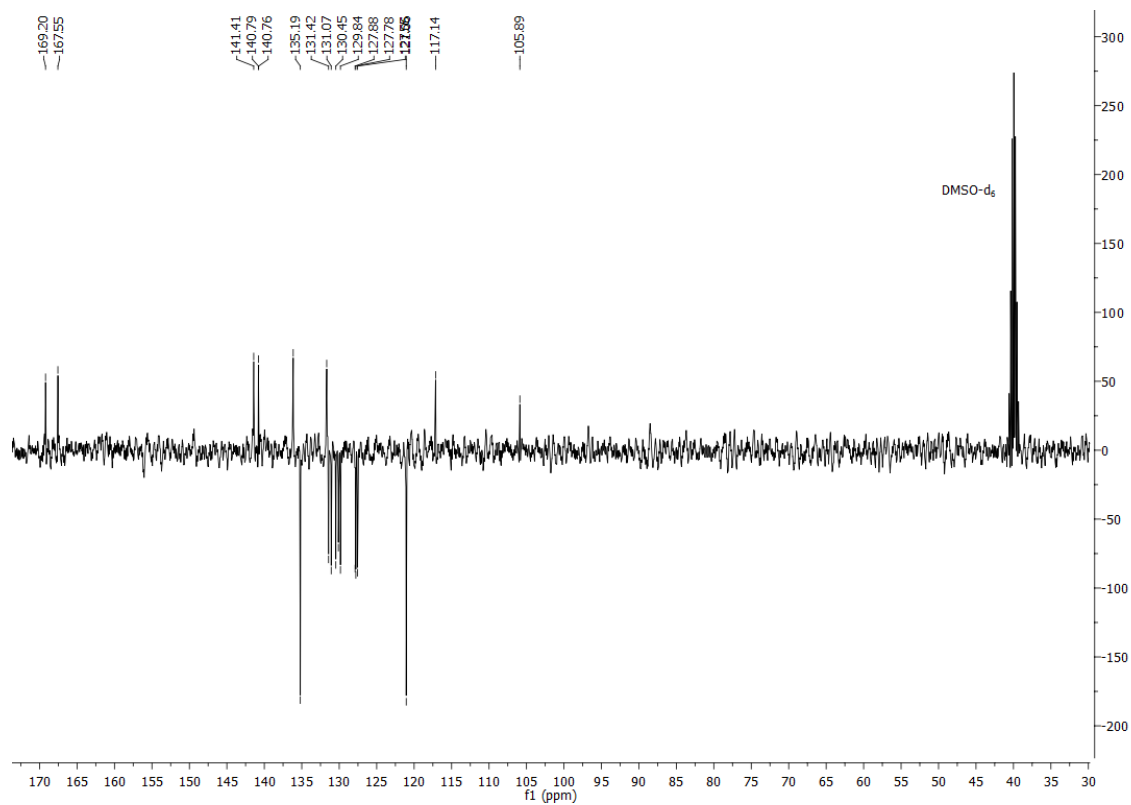


Figure 33S. <sup>13</sup>C APT NMR of 6b.

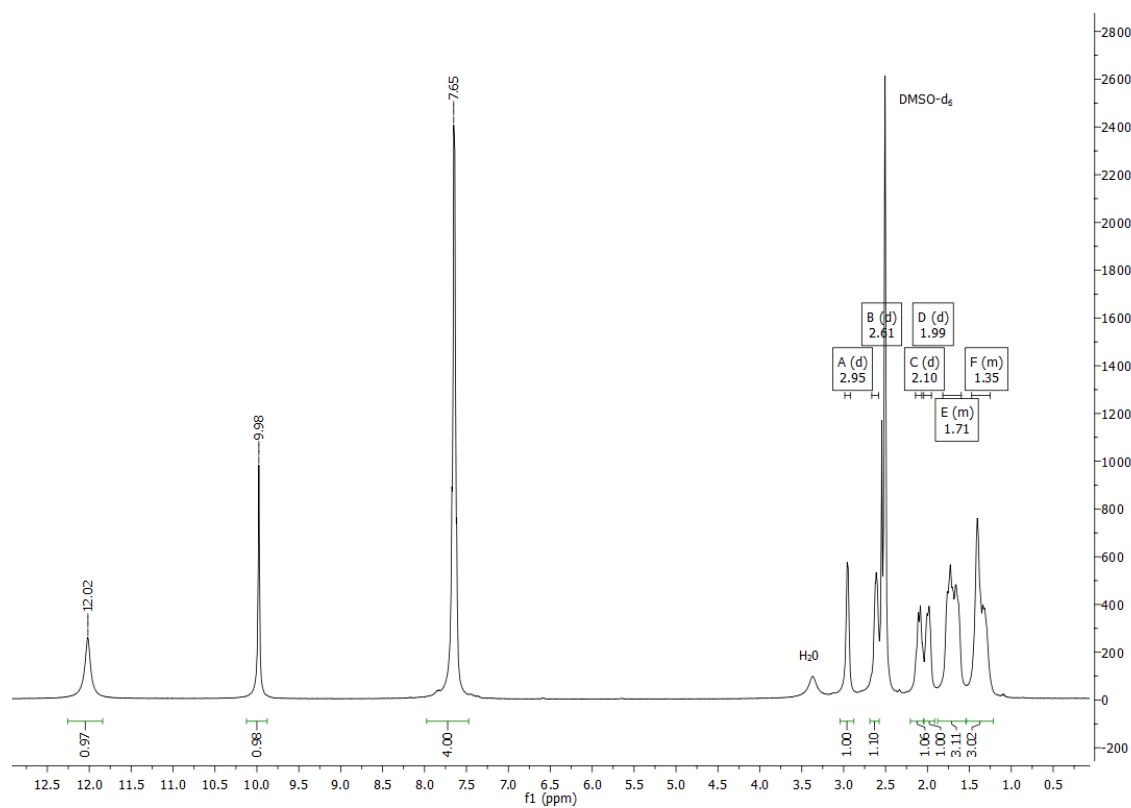
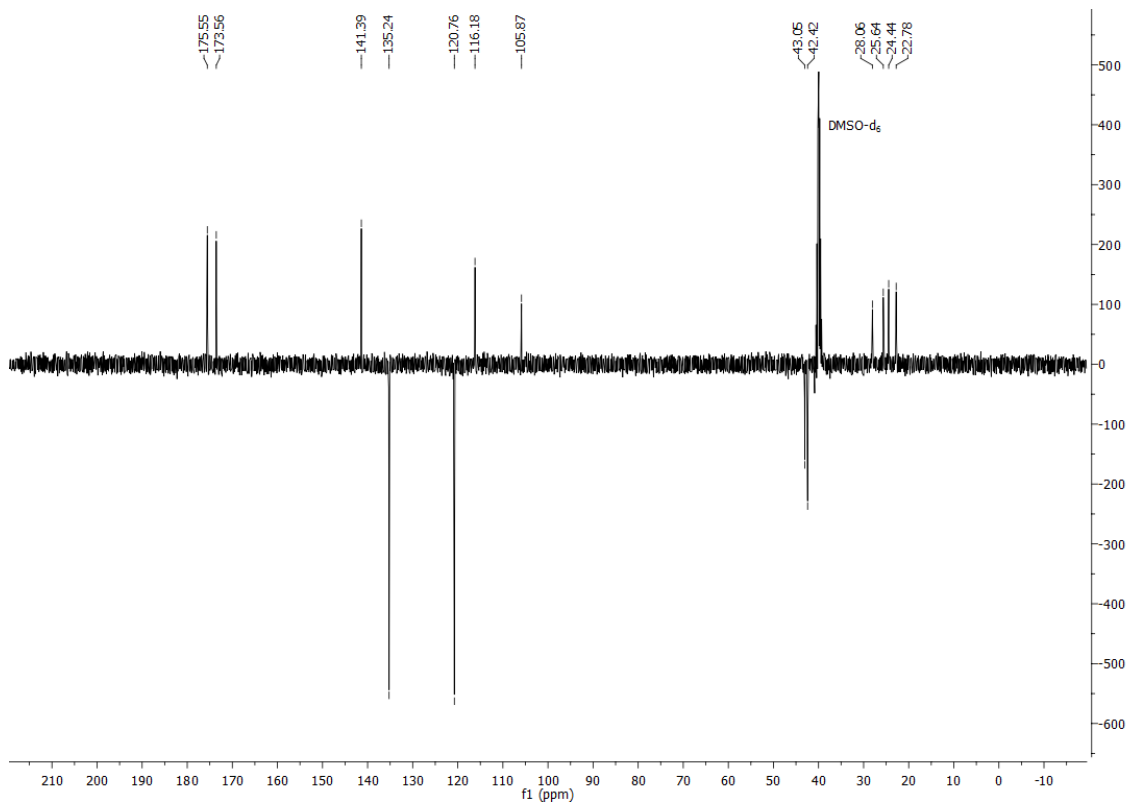
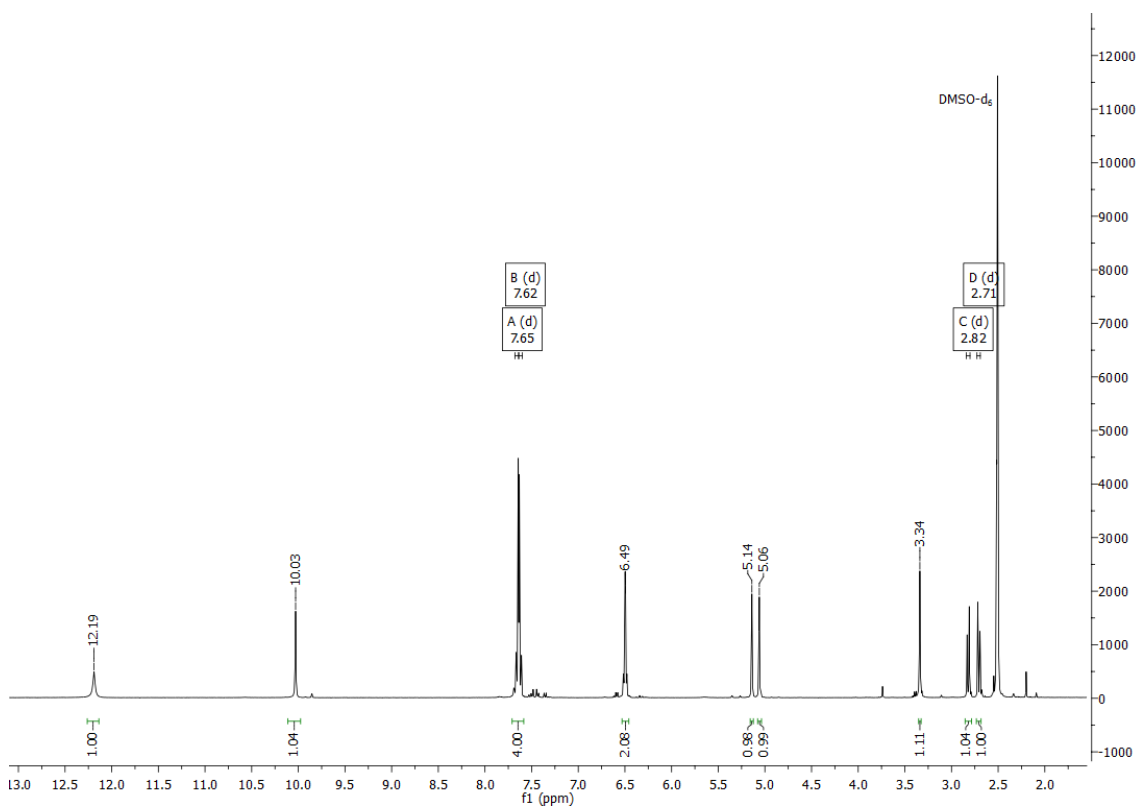


Figure 34S. <sup>1</sup>H NMR of 7b.

Figure 35S. <sup>13</sup>C APT NMR of 7b.Figure 36S. <sup>1</sup>H NMR of 8b.



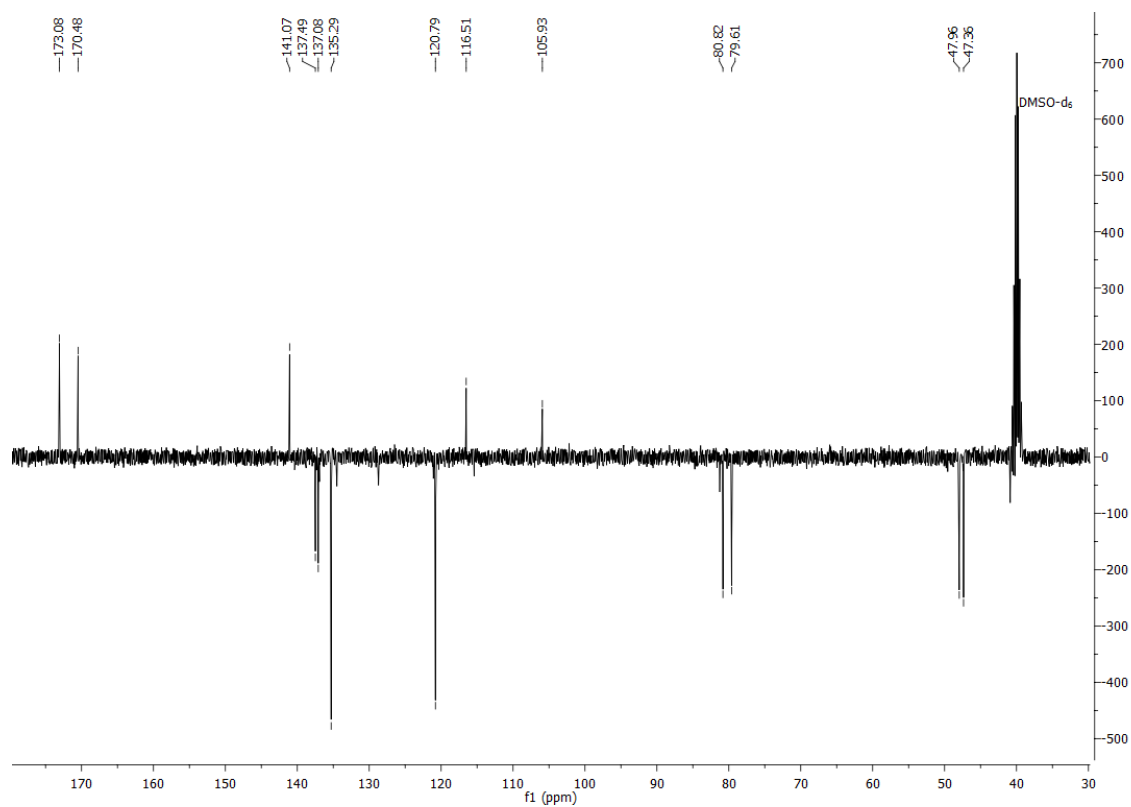


Figure 37S. <sup>13</sup>C APT NMR of 8b.

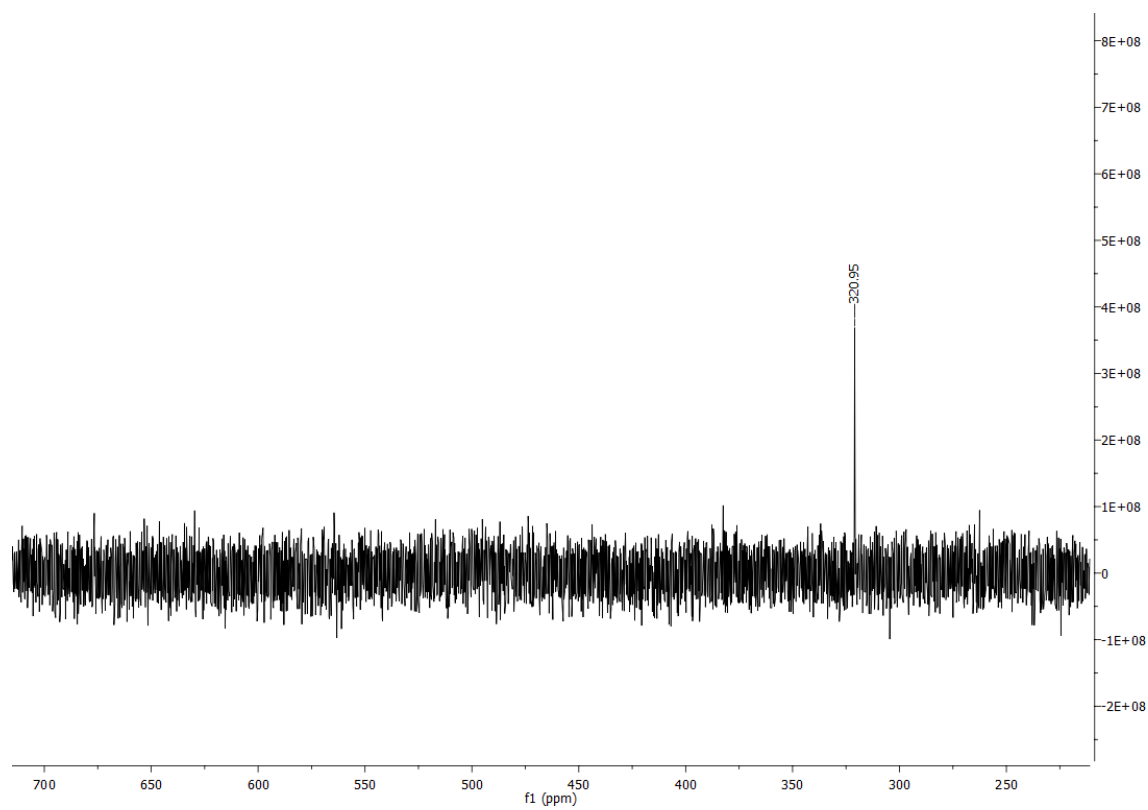


Figure 38S. <sup>77</sup>Se NMR of 8b.

.

### 3. Biological evaluation

#### 3.1. Cell cultures

Cell lines were purchased from the American Type Culture Collection (ATCC). MCF7, CRRF-CEM, HT-29, HTB-54, K-562 and PC-3 cell lines were grown in RPMI 1640 medium (Gibco) supplemented with 10% fetal bovine serum (FBS; Gibco), 100 units/mL penicillin and 100 mg/mL streptomycin (Gibco). BEAS-2B cell line (normal epithelial lung) was cultured in DMEM (Gibco), 10% FBS, 100 units/mL penicillin and 100 µg/mL streptomycin. 184B5 cells were grown in DMEM/F12 medium supplemented with 5% FBS, 1 ITS (Lonza), 100 nM hydrocortisone (Aldrich), 2 mM sodium pyruvate (Lonza), 20 ng/mL EGF (Sigma-Aldrich), 0.3 nM *trans*-retinoic acid (Sigma-Aldrich), 100 units/mL penicillin and 100 mg/mL streptomycin. Cells were maintained at 37°C and 5% CO<sub>2</sub>.

#### 3.2. Cytotoxic and antiproliferative activities

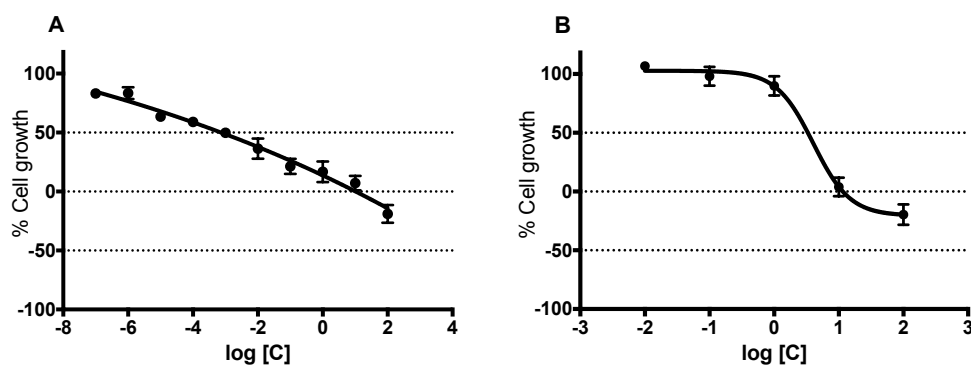
Cell viability was determined using the MTT 3-(4,5-dimethylthiazol-2-yl)-2,5-diphenyl-tetrazolium bromide) method at 10 and 100 µM to perform the screening. In order to build full dose-response curves five different doses ranging from 0.01 to 100 µM, for some compounds lower doses were needed in order to reach 50% cell growth. Depending on cell size, 8,000 to 40,000 cells were seeded per well in 96-well plates and incubated overnight. Then treated with the compounds for 48 h, cells were then incubated with 50 µL of MTT (2 mg/mL stock) for 4 h, medium was removed by aspiration and formazan crystals dissolved in 150 µL of DMSO. The absorbance was measured at 550 nm in a microplate reader (Sunrise reader, Tecan). At least three independent experiments performed in quadruplicate were analysed. Results are expressed as GI<sub>50</sub>, the concentration that reduces by 50% the growth of treated cells with respect to untreated controls, TGI, the concentration that completely inhibits cell growth, and LC<sub>50</sub>, the concentration that kills 50% of the cells.

Table S1. Average values of GI<sub>50</sub>, TGI and LD<sub>50</sub> (μM) and calculated SI

Code	PC-3			HTB-54			HT-29			MOLT-4			K562			CCRF-CEM			MCF-7		
	GI <sub>50</sub>	TGI	LD <sub>50</sub>	GI <sub>50</sub>	TGI	LD <sub>50</sub>	GI <sub>50</sub>	TGI	LD <sub>50</sub>	GI <sub>50</sub>	TGI	LD <sub>50</sub>	GI <sub>50</sub>	TGI	LD <sub>50</sub>	GI <sub>50</sub>	TGI	LD <sub>50</sub>	GI <sub>50</sub>	TGI	LD <sub>50</sub>
1b	30.44	61.35	92.89	46.95	72.42	93.75	>100	>100	>100	>100	>100	>100	58.58	98.17	>100	6.77	38.33	91.19	1.93	14.83	73.09
2b	19.38	>100	>100	>100	>100	>100	>100	>100	>100	>100	>100	>100	42.82	61.91	88.70	30.16	64.24	95.49	7.71	59.13	>100
4b	68.52	>100	>100	100	>100	>100	>100	>100	>100	>100	>100	>100	>100	>100	>100	46.52	>100	>100	6.47	>100	>100
8a	4.51	17.03	50.55	27.51	55.94	85.49	5.74	33.38	>100	73.77	84.71	94.62	25.32	59.67	94.62	59.13	75.84	>100	7.50	9.18	11.56
8b	21.05	43.22	70.44	47.83	72.42	>100	11.89	42.82	93.75	59.67	69.80	80.15	67.89	80.15	92.04	68.52	>100	>100	3.33	11.56	>100
9a	13.52	36.61	67.89	8.30	14.29	24.18	14.16	20.67	31.01	7.50	15.67	33.69	48.72	69.80	87.08	20.29	47.39	78.69	6.01	11.89	16.57
10a	8.30	33.08	>100	4.91	51.97	>100	11.67	>100	>100	91.19	>100	>100	80.89	>100	>100	>100	>100	>100	0.0007	10.20	>100
0b	1.02	1.54	2.30	0.87	1.00	1.13	0.27	1.11	5.28	3.33	3.39	3.42	1.03	1.29	1.58	1.71	2.74	4.43	1.00	1.48	2.20
0a	0.80	1.62	2.98	0.21	0.80	2.16	<0.01	1.78	8.37	3.84	5.95	8.06	0.95	1.19	1.48	5.28	16.87	42.82	0.75	0.96	1.16
Cisplatin	5.01	50.1	>100	n.d.	n.d.	n.d.	7.94	>100	>100	1.58	63.10	>100	5.01	>100	>100	1.00	79.43	>100	3.16	>100	>100

Code	184B5			SI	BFAS-2B			SI
	GI <sub>50</sub>	TGI	GI <sub>50</sub>		GI <sub>50</sub>	TGI	LD <sub>50</sub>	
1b	>100	>100	>100	>51.73	10.45	42.82	80.15	0.22
2b	>100	>100	>100	>12.98	4.43	24.63	>100	<0.39
4b	>100	>100	>100	15.46	52.93	>100	>100	<0.16
8a	8.93	11.25	15.67	1.19	1.05	4.43	15.53	0.04
8b	77.25	91.19	>100	23.19	15.82	51.02	77.25	0.33
9a	40.51	63.07	86.29	6.74	1.97	43.62	73.77	0.24
10a	60.78	>100	>100	82969.59	0.75	20.86	61.91	0.15
0a	6.29	14.03	30.44	8.39	0.73	0.88	1.09	3.44
0b	0.88	1.06	1.27	0.88	7.92	14.69	27.51	9.06



**Figure 39S.** Dose response curves MCF-7 cell line for compounds **10a** (37SA) and **8b** (37SB). For compound **10a** further dilutions were needed apart from the five standard concentrations to reach a 50% growth.

### 3.3. Evaluation of cell cycle progression and cell death

A fixed population of MCF7 cells per flask were seeded in 25 cm<sup>2</sup> flasks then incubated overnight. Cultures were treated with the corresponding amount of compounds **10a**, **8b**, DMSO (control) or 6  $\mu$ M camptothecin (positive control). Seeded population was dependent on studied time point:  $3 \times 10^6$  cells/flask for 24 h or shorter treatment,  $2 \times 10^6$  cells/flasks for 48 h treatment and finally  $1 \times 10^6$  cells/flask for 72 h experiments. Apo-Direct kit (BD Pharmigen) was used to determine cell cycle distribution and cell death percentage. Cells were fixed in a 1% paraformaldehyde solution in PBS for 30-40 min at 0°C, washed with PBS twice and incubated for 30 min with 70% ethanol on ice. Staining was performed following manufacturer's protocol and samples were analysed by flow cytometry using a Counter Epics XL cytometer (Beckman Counter).

Inhibition assays cells were pre-treated with 50  $\mu$ M of the pan-caspase inhibitor Z-VAD-FMK (BD Pharmigen) or 100 nM of the autophagy inhibitor wortmannin (Santa Cruz) for 1 h or 10  $\mu$ M of chloroquine (Sigma Aldrich). The cells were treated with 80  $\mu$ M of **8b** or **10a**, DMSO was added to the control cells. Samples were processed following the same methodology stated above. At least three independent experiments were performed in duplicate.

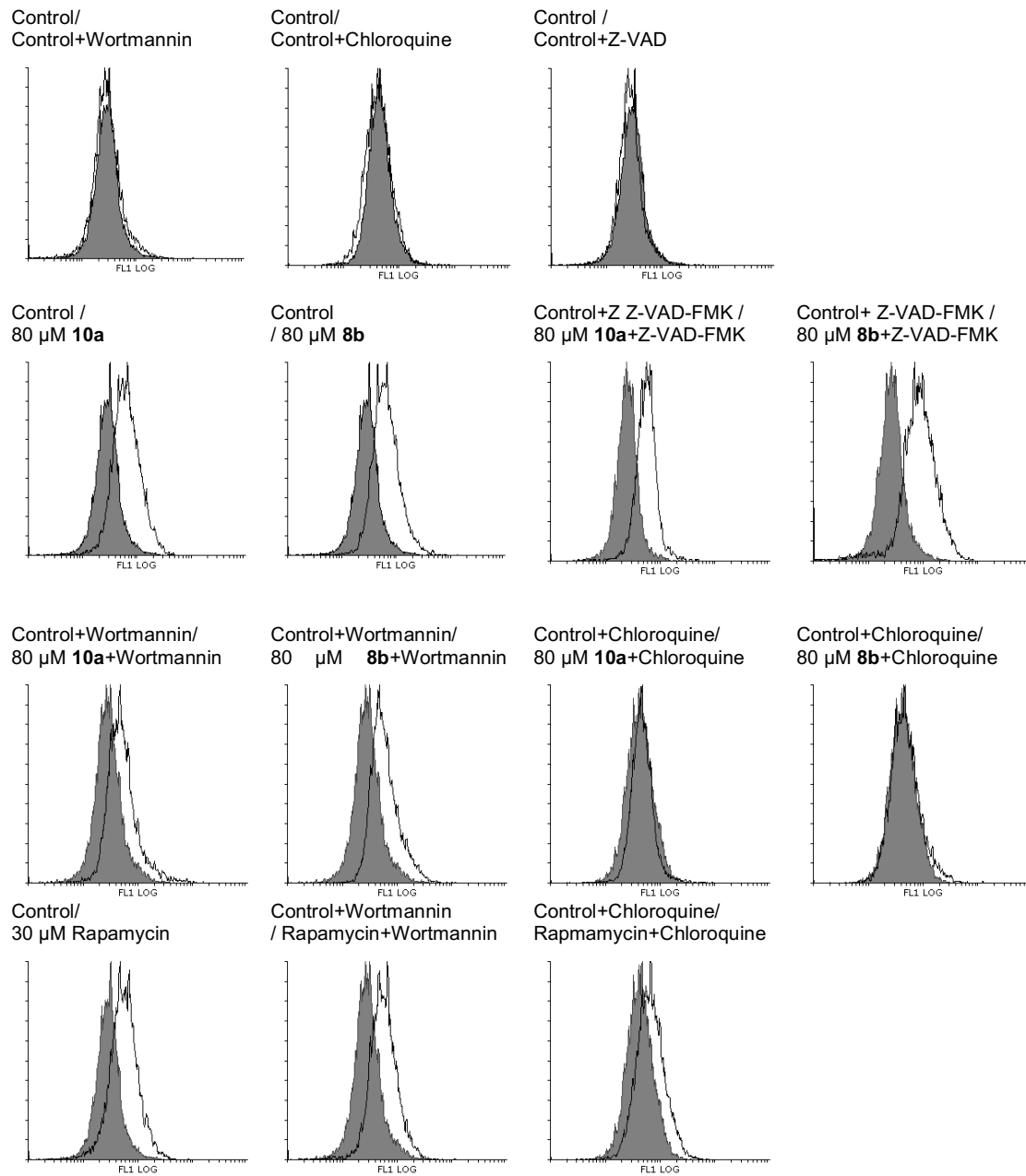


**Figure 40S.** Cell death induced by compounds **10a** and **8b** at 80  $\mu$ M concentration is blocked by wortmannin and chloroquine but not by caspase inhibitor Z- VAD-FMK. Figure shows representative experiments stacked with the control graphs for each experiment including experiments for the reference drug Rapamycin at 30  $\mu$ M. Control histograms are color-coded in grey while the corresponding treatment histogram is plotted as a transparent histogram.

#### 3.4. Statistical analysis

Statistical data represent the mean  $\pm$  SEM of at least three independent experiments performed in duplicate. Mann-Whitney U-test was used to establish statistical significance of differences between control and treatment groups. Graphad Prism version 7 was used, significant differences were considered \* $p < 0.05$ , \*\* $p < 0.01$  and \*\*\* $p < 0.001$ .











Pre-clinical evidences of the potential antileishmanial effects of diselenides and selenocyanates.

Pablo Garnica <sup>a,1</sup>, Mikel Etxebeste-Mitxeltoena <sup>a,b,1</sup>, Daniel Plano <sup>a</sup>, Esther Moreno <sup>b</sup>, Socorro Espuelas <sup>b</sup>, Juan Antonio Palop <sup>a</sup>, Antonio Jiménez-Ruiz <sup>c</sup>, Carmen Sanmartín <sup>a,b,\*</sup>

<sup>a</sup> Department of Organic and Pharmaceutical Chemistry, University of Navarra, Irúnlarrea, 1, E-31008 Pamplona, Spain

<sup>b</sup> Institute of Tropical Health, University of Navarra, Pamplona, Spain; Pharmacy and Pharmaceutical Technology Department, University of Navarra, Pamplona, Spain

<sup>c</sup> Department of Biochemistry and Molecular Biology, Universidad de Alcalá, Carretera Madrid-Barcelona km 33,600, E-28871 Alcalá de Henares, Madrid, Spain

<sup>1</sup> Authors have contributed equally to this article

This paper is under preparation to be submitted to *Bioorganic and Medicinal Chemistry Letters*.

The selenocyanate and diselenide moieties have been included in the past by our research group to yield promising leishmanicidal agents. In this present paper thirty-one selenocyanate and diselenide derivatives were tested against *Leishmania infantum* amastigotes. Selectivity was assessed by screening the structures against a human monocyte cell line (THP-1). Compounds were ranked according to potency and selectivity using edelfosine and miltefosine as reference drugs. Six leader compounds were selected to further determine their mechanism of action by testing infection rate defense potency and TryR inhibition capacity.





## Pre-clinical evidences of the potential antileishmanial effects of diselenides and selenocyanates.

Pablo Garnica <sup>a,1</sup>, Mikel Etxebeste-Mitxeltoarena <sup>a,b,1</sup>, Daniel Plano <sup>a</sup>, Esther Moreno <sup>b</sup>, Socorro Espuelas <sup>b</sup>, Juan Antonio Palop <sup>a</sup>, Antonio Jiménez-Ruiz <sup>c</sup>, Carmen Sanmartín <sup>a,b,\*</sup>

<sup>a</sup> Department of Organic and Pharmaceutical Chemistry, University of Navarra, Iruñlarrea, 1, E-31008 Pamplona, Spain

<sup>b</sup> Institute of Tropical Health, University of Navarra, Pamplona, Spain; Pharmacy and Pharmaceutical Technology Department, University of Navarra, Pamplona, Spain

<sup>c</sup> Department of Biochemistry and Molecular Biology, Universidad de Alcalá, Carretera Madrid-Barcelona km 33,600, E-28871 Alcalá de Henares, Madrid, Spain

<sup>1</sup> Authors have contributed equally to this article

### ARTICLE INFO

#### Article history:

Received

Revised

Accepted

Available online

#### Keywords:

Leishmanicidal agents

Selenocompounds

Diselenides

Selenocyanates

### ABSTRACT

A series of thirty-one selenocompounds covering a wide chemical space was assessed for *in vitro* leishmanicidal activities against *Leishmania infantum* amastigotes. The cytotoxicity of those compounds was also evaluated on human THP-1 cells. Interestingly most tested derivatives were active in the low micromolar range and seven of them stood out for selectivity indexes higher than the ones exhibited by miltefosine and edelfosine. These leader compounds were evaluated against infected macrophages and their trypanothione reductase (TryR) inhibition potency was measured to further approach the mechanism by which they caused their action. Among them diselenide tested structures were pointed out for their ability to reduce infection rates. Three of the leader compounds inhibited TryR effectively, therefore this enzyme may be implicated in the mechanism of action by which these compounds cause their leishmanicidal effect.

2009 Elsevier Ltd. All rights reserved.

Leishmaniasis is one tropical fatal disease caused by different species of protozoa belonging to the genus *Leishmania*. It is transmitted to humans by the bite of female phlebotomine and it is endemic in 98 countries. In spite of the existence of around 53 species of *Leishmania*, only 20 are capable of infecting humans<sup>1</sup>.

Leishmaniasis can present three main clinical forms: cutaneous, which is the most common and causes skin sores; visceral or kala-azar, which is the most serious form and affects several internal organs (spleen, liver and bone marrow) and mucocutaneous, which destroys the mucous membranes of nose, mouth and throat<sup>2-4</sup>. Drugs including pentavalent antimonial derivatives such as Pentostam® and Glucantime® or more recently amphotericin B, miltefosine, paramomycin, sitamaquine and edelfosine have several complications such as toxicity, side effects, low efficacy, drug resistances and high costs, among others<sup>5-9</sup>. These reasons reinforce the urgent need of new treatments and new targets that must be explored for treating this illness<sup>10-11</sup>.

In the search of new drugs growing evidence suggests a connection between selenium (Se) and parasites, particularly

trypanosomatids. In fact, some parasites have been proven to express selenoproteins and metabolize Se<sup>12-13</sup>. This indicates the potential importance of Se as a privileged core to design new leishmanicidal agents. In this context, in the past years, our research group has reported a set of organoselenium compounds with this activity<sup>14-19</sup>. Different chemical frameworks have been explored such as selenocyanate, diselenide and methylseleno moieties. Among these series new antikinetoplastid derivatives bis(4-aminophenyl)diselenide and 4-aminophenylselenocyanate exhibited interesting properties as antiparasitic agents. With these observations in mind, we decided to modulate bis(4-aminophenyl)diselenide and 4-aminophenylselenocyanate with different derivatizations (**Fig.1**) with the aim to improve polarity, solubility, activity and selectivity obtaining maximal 3D structural enrichment as well as providing us with information on the effects of electronic modulation. Among these functionalizations we have selected selenoureas due to their recent description in structures as reactive oxygen species (ROS) scavengers<sup>20</sup>. One of the main limitations of the selenium derivatives in the drug development

\* Corresponding author. Tel.: +34 948 425 600; fax: +34 948 425 649; e-mail: sanmartin@unav.es

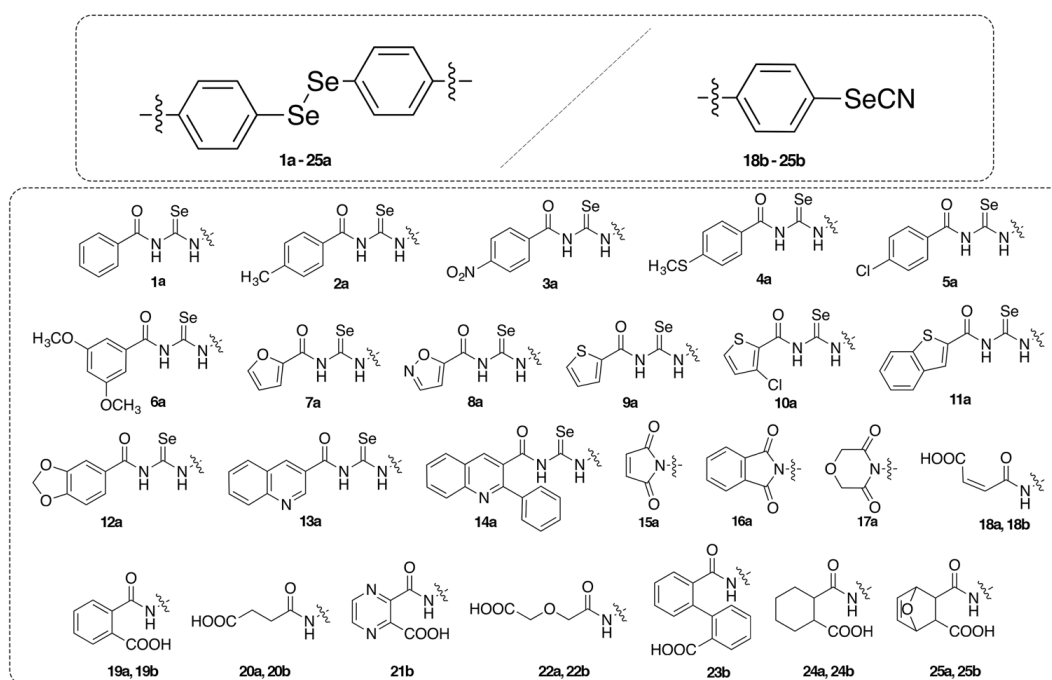


Fig. 1. Structures for the Se-containing derivatives tested in this work.

process is their poor water solubility which is detrimental for their bioavailability. Therefore, we proposed a series of compounds including carboxylic acids as logical approach to increase water solubility, also enabling us to explore their cyclic imide homologs.

Among the potential targets for the treatment of leishmaniasis and due to the intracellular nature of the parasite, we focused on the redox regulatory systems. Parasites are highly sensitive to (ROS), which are produced under conditions of oxidative stress. In this sense, all *Trypanosomatids*, including *Leishmania*, present diverse regulatory pathways for protecting them to the oxidative damage. Trypanothione Reductase (TryR) is one of the most relevant and studied enzymes that plays an important role in the survival of the parasite, due to its implication in the redox system. This enzyme catalyzes the reduction of trypanothione disulfide to trypanothione. Additionally, on the basis the chemical analogy of sulfur and selenium, we decided to explore diselenide and selenocyanate derivatives to generate new TryR inhibitors. In addition, this flavoenzyme is exclusive of *Trypanosomatids*. Due to its absence in the human host, TryR is considered a promising target for the development of new drugs that improve the efficacy, potency and safety of the reference drugs mentioned above<sup>14, 16, 21</sup>.

In this work, we assess the antileishmanial effect of a library of thirty-one organoseleno compounds (Fig. 1) against *Leishmania infantum* axenic amastigotes as well as the cytotoxicity against THP-1 cells in order to evaluate their selectivity. Furthermore, the most active compounds were evaluated in *L. infantum*-infected macrophages and have been tested to study the potential role played by trypanothione reductase as putative target.

The synthesis of this second-generation derivatives followed two different synthetic pathways. Briefly, the formation of acylselenoureas (1a-14a) involved acylisosenocyanates as intermediates that were then reacted with bis(4-aminophenyl)diselenide following a synthetic pathway previously described by our research group<sup>22</sup>. On the other hand, derivatives containing amide acids (18a-25a and 18b-25b) or imides (15a-

17a) were formed by the reaction of symmetric anhydrides with either bis(4-aminophenyl)diselenide for compounds 15a-25a or 4-aminophenylselenocyanate for derivatives 18b-25b<sup>23</sup>. These compounds met the required purity to be tested for their biological activity confirmed by microanalysis, <sup>1</sup>H and <sup>13</sup>C NMR spectroscopy, infrared spectroscopy and mass spectrometry.

The leishmanicidal activity of thirty-one synthesized Se-containing compounds was analyzed against *Leishmania Infantum* axenic amastigotes at 24 h treatment time. This form of the parasite was selected due to the fact that promastigotes are more susceptible form of the parasite and therefore drug-induced effects can be magnified. Moreover, amastigotes are responsible for clinical manifestations in humans. Miltefosine and edelfosine were used as reference drugs. Three independent experiments were performed according to a previously described procedure<sup>14</sup> and results are expressed as IC<sub>50</sub> values in Table 1. Selectivity is a compulsory property for any antileishmanial drug as toxicity in human cells is a non-desired effect in drug development. In order to assess this factor, cytotoxicity obtained after 24 h of exposure to the compounds in THP-1 cells was tested according to previously described procedure<sup>14</sup>. Selectivity index (SI) was calculated as the ratio of IC<sub>50</sub> value obtained for THP-1 cells and IC<sub>50</sub> values obtained for *L. infantum* amastigotes.

Table 1. IC<sub>50</sub> values for compounds 1a-25a and 18b-25b on amastigotes and cytotoxic activity on THP-1 cell line

Code	IC <sub>50</sub> (mean ± SEM), μM		SI
	Amastigotes	THP-1	
1a	>25	>25	n.d.
2a	15.03 ± 0.78	>25	>1.66
3a	2.27 ± 0.91	>25	>11.01

4a	13.48 ± 2.21	>25	>1.85
5a	>25	>25	n.d
6a	9.22 ± 0.95	>25	>2.77
7a	0.67 ± 0.15	7.44 ± 1.47	11.19
8a	0.35 ± 0.06	1.07 ± 0.07	3.10
9a	4.55 ± 0.71	22.16	4.87
10a	5.57 ± 0.80	>25	>4.48
11a	14.6 ± 0.90	>25	>1.71
12a	9.98 ± 0.75	13.45 ± 1.26	1.35
13a	3.08 ± 0.43	12.77 ± 1.50	4.15
14a	6.18 ± 0.19	8.50 ± 0.40	1.34
15a	1.54 ± 0.25	15.23 ± 2.3	9.91
16a	2.07 ± 0.21	22.97 ± 1.2	11.08
17a	10.40 ± 0.21	8.53 ± 1.4	0.82
18a	>25	>25	n.d.
19a	4.57 ± 0.99	>25	>5.47
20a	7.9 ± 0.23	>25	>3.16
22a	12.10 ± 1.72	>25	>2.06
24a	2.03 ± 0.36	>25	>12.31
25a	1.31 ± 0.16	>25	>19.13
18b	>25	>25	n.d.
19b	>25	>25	n.d.
20b	11.33 ± 0.84	>25	>2.20
21b	>25	>25	n.d.
22b	>25	>25	n.d.
23b	10.66 ± 0.51	>25	>2.34
24b	10.61 ± 1.0	>25	>2.35
25b	3.22 ± 0.46	21.53 ± 0.6	7.76
miltefosine	2.84 ± 0.10	18.5 ± 0.6	6.51
edelfosine	0.82 ± 0.13	4.96 ± 0.16	6.01

Data obtained revealed high bioactivity for seven of the analyzed compounds (**3a**, **7a**, **8a**, **15a**, **16a**, **24a** and **25a**) which met the threshold stated by the reference drug miltefosine ( $IC_{50} = 2.84 \mu\text{M}$ ) in terms of potency. Derivatives **7a** and **8a** even exceeded the edelfosine standard for this assay ( $IC_{50} = 0.82 \mu\text{M}$ ). Interestingly, only diselenide derivatives matched or surpassed the potency obtained for the reference drugs. The results found for compounds **7a** and **8a** were comparable to or higher than those obtained for bis(4-aminophenyl)diselenide, common fragment for diselenide derivatives ( $IC_{50} = 0.65 \mu\text{M}$ ). If we make the corresponding comparison of selenocyanate derivatives with their parent drug 4-aminophenylselenocyanate ( $IC_{50} = 9.29 \mu\text{M}$ ), compound **25b** stood out for the significant antileishmanial activity.

Low cytotoxicity is required for a good antileishmanial drug, consequently  $IC_{50}$  values obtained for THP-1 and SI have to carefully be observed in order to satisfy this condition. Compounds **3a**, **7a**, **15a**, **16a**, **24a**, **25a** and **25b** outperformed

miltefosine and edelfosine (SI = 6.51 and 6.01 respectively) in terms of selectivity (Table 1).

Taking into consideration both potency and selectivity, six derivatives (**7a**, **15a**, **16a**, **24a**, **25a** and **25b**) were assayed in amastigote-infected THP-1 cells. Compound **3a** was not further tested due to the reproducibility issues showed by this derivative pertaining to its lack of solubility under the assay conditions. All tested compounds reduced infection significantly at  $3 \mu\text{M}$  concentration as shown in Fig. 2. Compounds **7a**, **16a** and **25a** reduced infection rates after  $3 \mu\text{M}$  48 h treatment to values under the ones obtained for the treatment of  $3 \mu\text{M}$  of the reference drug edelfosine. Five of the tested compounds correspond to diselenide derivatives, all of them exhibited infection reduction potential in the range of the one found for edelfosine. On the other hand, selenocyanate derivative **25b** did not meet this standard, again this fact pointed to diselenide moiety over selenocyanate in general terms of potential as leishmanicidal structures.

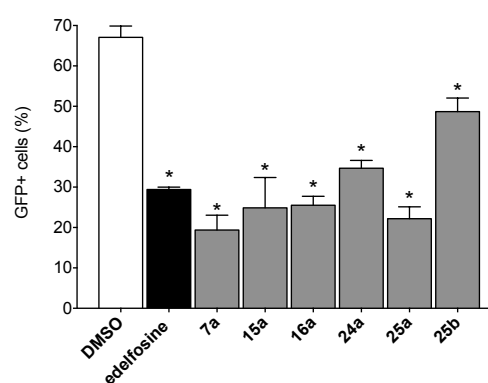


Fig. 2. Infection rates of THP-1 cells by amastigotes after  $3 \mu\text{M}$  48 h treatment, autofluorescence correction applied.

To further determine the mechanism of action of the six leader compounds we assessed their ability to inhibit TryR. Six different concentrations ranging from 75 to  $0.1 \mu\text{M}$  were screened. Mepacrine was used as a positive control due to its proven TryR inhibition properties. Three out of the six tested compounds (**7a**, **15a** and **25b**) exceeded inhibition potency of mepacrine<sup>24</sup>, compounds **15a** and **25b** were 30-fold more active than the positive control. On the other hand, compounds **16a**, **24a** and **25a** did not show significant inhibitory activity suggesting that other mechanisms may be implicated in the potent leishmanicidal activity.

Table 2.  $IC_{50}$  for the selected compounds against TryR inhibition

Code	$IC_{50}$ (mean ± SEM), $\mu\text{M}$
7a	9.22 ± 1.50
15a	0.23 ± 0.01
16a	21.81 ± 2.55
24a	18.51 ± 0.16
25a	25.00 ± 0.69
25b	0.54 ± 0.13
mepacrine	16.99 ± 1.18

**Table 3.** Theoretical ADME properties for lead compounds

Code	Molinspiration calculations <sup>a</sup>							preADMET <sup>b</sup>	
	MW	LogP	TPSA	nON	nOHNH	NV	Vol	HIA (%)	Caco-2 (nm/s)
<b>7a</b>	742.3	5.9	108.5	8	4	2	474.8	97.8	36.9
<b>15a</b>	502.3	3.2	78.2	6	0	1	337.1	97.7	22.9
<b>16a</b>	602.4	6.7	78.2	6	0	2	425.1	98.2	31.4
<b>24a</b>	650.5	6.1	132.8	8	4	2	499.3	99.5	11.1
<b>25a</b>	674.4	3.7	151.3	10	4	1	483.3	98.4	16.2
<b>edelfosine</b>	523.7	0.75	77.1	7	0	1	550.9	98.6	21.7

<sup>a</sup>MW, molecular weight; LogP, octanol-water partition coefficient; TPSA, topological polar surface area; nON, hydrogen bond acceptors; nOHNH, hydrogen bond donors; NV, number of violations; Vol, volume. <sup>b</sup>HIA, Human Intestinal Absorption; Caco-2, permeability.

As a preliminary approach and employing a series of freeware tools, physicochemical properties related to their absorption and bioavailability were calculated. Lipinski's rule of five analysis helps us predict and explain small molecules' biological behavior (Table 3). Edelfosine was also subjected to this estimation using Molinspiration software and the resulting analysis revealed the violation of one of Lipinski's rules. Compounds **15a** and **25a** matched this same result (Table 3). It is well-known that some drug candidates have failed in clinical tests because of ADMET (absorption, distribution, metabolism, excretion and toxicity) problems. In order to estimate these properties, we used the web-based application PreADMET. Human intestinal absorption (HIA) and Caco-2 permeability are good indicators of drug absorbance. All tested compounds showed excellent intestinal absorption while permeability values for Caco-2 cells were moderate though in the same order of magnitude than edelfosine (Table 3).

In conclusion, the present study reports the evaluation of the *in vitro* leishmanicidal activity against *L. infantum* amastigotes along with cytotoxicity in THP-1 cells of thirty-one diselenide and selenocyanate derivatives. In general terms diselenide derivatives were found to be more potent and selective than selenocyanate-containing structures. Seven diselenides matched the potency of miltefosine against *L. infantum* amastigotes. In terms, activity against amastigotes, derivatives **7a** and **8a** improved the potency obtained for edelfosine in this same assay. When compared with their parent drugs, the previously mentioned diselenide derivatives, matched or improved activity against amastigotes. Moreover, seven derivatives (**3a**, **7a**, **15a**, **16a**, **24a**, **25a** and **25b**) exhibited selectivity indexes higher than both reference drugs. These promising results encouraged further studies in infected macrophages with the derivatives that fulfilled this last criterion. Compounds **7a**, **16a** and **25a** were more potent against intracellular amastigotes than the profile exhibited by the reference drug mepacrine. In order to get further information on the molecular mechanism implicated, the inhibition of TryR was determined. All tested compounds inhibited TryR, **15a** and **25b** potency was 30-fold higher than the one recorded for mepacrine. No clear correlation was found between leishmanicidal potential and enzyme inhibition which suggest the existence of different targets in this family of compounds. In terms of structure-activity relationship only one selenocyanate derivative passed the screening phase of the study while the rest of the leader structures corresponded to diselenide derivatives. The predicted values for HIA are excellent for all six diselenide derivatives tested (**3a**, **7a**, **15a**, **16a**, **24a** and **25a**). Derivatives **7a** and **25a** can be selected as the leader compounds of this series of compounds due to their high potency both in amastigote and intracellular amastigotes and great selectivity. They have also showed moderate inhibitory activity against TryR though no clear correlation with their leishmanicidal

potency can be inferred. Thus, more detailed mechanism of action studies are being conducted.

### Acknowledgments

The research leading to these results has received funding from "la Caixa" Banking Foundation. P. Garnica wishes to express his gratitude to the Asociación de Amigos de la Universidad de Navarra for the pre-doctoral fellowship. Furthermore, the authors wish to express their gratitude to the Plan de Investigación de la Universidad de Navarra, PIUNA (Ref 2014–26) as well as Caixa Foundation-UNED for financial support for the project.

### References

- de Mello, M. V. P.; Abraham-Vieira, B. A.; Domingos, T. F. S.; de Jesus, J. B.; de Sousa, A. C. C.; Rodrigues, C. R.; Souza, A. M. T., A comprehensive review of chalcone derivatives as antileishmanial agents. *Eur J Med Chem* **2018**, *150*, 920-929.
- CDC Leishmaniasis. <https://www.cdc.gov/parasites/leishmaniasis/index.html> (accessed 14/12/2017).
- WHO Leishmaniasis fact sheet. <http://www.who.int/mediacentre/factsheets/fs375/en/> (accessed 14/12/2017).
- WHO Leishmaniasis. <http://www.who.int/leishmaniasis/en/> (accessed 14/12/2017).
- Solomon, M.; Pavlotzky, F.; Barzilay, A.; Schwartz, E., Liposomal amphotericin b in comparison to sodium stibogluconate for *leishmania braziliensis* cutaneous leishmaniasis in travelers. *J Am Acad Dermatol* **2013**, *68* (2), 284-289.
- Seifert, K.; Munday, J.; Syeda, T.; Croft, S. L., *In vitro* interactions between sitamaquine and amphotericin b, sodium stibogluconate, miltefosine, paromomycin and pentamidine against *leishmania donovani*. *J Antimicrob Chemother* **2011**, *66* (4), 850-854.
- Loiseau, P. M.; Cojean, S.; Schrevel, J., Sitamaquine as a putative antileishmanial drug candidate: From the mechanism of action to the risk of drug resistance. *Parasite* **2011**, *18* (2), 115-119.
- Varela, M. R.; Villa-Pulgarin, J. A.; Yepes, E.; Muller, I.; Modolell, M.; Munoz, D. L.; Robledo, S. M.; Muskus, C. E.; Lopez-Aban, J.; Muro, A.; Velez, I. D.; Mollinedo, F., *In vitro* and *in vivo* efficacy of ether lipid edelfosine against *leishmania spp.* And sbv-resistant parasites. *PLoS Negl Trop Dis* **2012**, *6* (4), e1612.
- Ponte-Sucre, A.; Gamarro, F.; Dujardin, J. C.; Barrett, M. P.; Lopez-Velez, R.; Garcia-Hernandez, R.; Pountain, A. W.; Mwenechanya, R.; Papadopoulou, B., Drug resistance and treatment failure in leishmaniasis: A 21st century challenge. *PLoS Negl Trop Dis* **2017**, *11* (12), e0006052.
- Sundar, S.; Singh, B., Emerging therapeutic targets for treatment of leishmaniasis. *Expert Opin Ther Targets* **2018**, (1744-7631), 1-20.

11. Vijayakumar, S.; Das, P., Recent progress in drug targets and inhibitors towards combating leishmaniasis. *Acta Trop* **2018**, *181* (1873-6254), 95-104.
12. da Silva, M. T.; Silva-Jardim, I.; Thiemann, O. H., Biological implications of selenium and its role in trypanosomiasis treatment. *Curr Med Chem* **2014**, *21* (15), 1772-80.
13. Bonilla, M.; Krull, E.; Irigoien, F.; Salinas, G.; Comini, M. A., Selenoproteins of african trypanosomes are dispensable for parasite survival in a mammalian host. *Mol Biochem Parasitol* **2016**, *206* (1-2), 13-9.
14. Baquedano, Y.; Alcolea, V.; Toro, M. A.; Gutierrez, K. J.; Nguewa, P.; Font, M.; Moreno, E.; Espuelas, S.; Jimenez-Ruiz, A.; Palop, J. A.; Plano, D.; Sanmartin, C., Novel heteroaryl selenocyanates and diselenides as potent antileishmanial agents. *Antimicrob Agents Chemother* **2016**, *60* (6), 3802-3812.
15. Font, M.; Baquedano, Y.; Plano, D.; Moreno, E.; Espuelas, S.; Sanmartin, C.; Palop, J. A., Molecular descriptors calculation as a tool in the analysis of the antileishmanial activity achieved by two series of diselenide derivatives. An insight into its potential action mechanism. *J Mol Graph Model* **2015**, *60*, 63-78.
16. Baquedano, Y.; Moreno, E.; Espuelas, S.; Nguewa, P.; Font, M.; Gutierrez, K. J.; Jimenez-Ruiz, A.; Palop, J. A.; Sanmartin, C., Novel hybrid selenosulfonamides as potent antileishmanial agents. *Eur J Med Chem* **2014**, *74*, 116-123.
17. Moreno, D.; Plano, D.; Baquedano, Y.; Jimenez-Ruiz, A.; Palop, J. A.; Sanmartin, C., Antileishmanial activity of imidothiocarbamates and imidoselenocarbamates. *Parasitol Res* **2011**, *108* (1), 233-239.
18. Plano, D.; Baquedano, Y.; Moreno-Mateos, D.; Font, M.; Jimenez-Ruiz, A.; Palop, J. A.; Sanmartin, C., Selenocyanates and diselenides: A new class of potent antileishmanial agents. *Eur J Med Chem* **2011**, *46* (8), 3315-3323.
19. Fernandez-Rubio, C.; Campbell, D.; Vacas, A.; Ibanez, E.; Moreno, E.; Espuelas, S.; Calvo, A.; Palop, J. A.; Plano, D.; Sanmartin, C.; Nguewa, P. A., Leishmanicidal activities of novel methylseleno-imidocarbamates. *Antimicrob Agents Chemother* **2015**, *59* (9), 5705-5713.
20. Romero-Hernandez, L. L.; Merino-Montiel, P.; Montiel-Smith, S.; Meza-Reyes, S.; Vega-Baez, J. L.; Abasolo, I.; Schwartz, S., Jr.; Lopez, O.; Fernandez-Bolanos, J. G., Diosgenin-based thio(seleno)ureas and triazolyl glycoconjugates as hybrid drugs. Antioxidant and antiproliferative profile. *Eur J Med Chem* **2015**, *99*, 67-81.
21. Martín-Montes, A.; Plano, D.; Martín-Escolano, R.; Alcolea, V.; Diaz, M.; Perez-Silanes, S.; Espuelas, S.; Moreno, E.; Marin, C.; Gutierrez-Sanchez, R.; Sanmartin, C.; Sanchez-Moreno, M., Library of seleno-compounds as novel agents against *leishmania* species. *Antimicrob Agents Chemother* **2017**, *61* (6), e02546-16.
22. Garnica, P.; Encio, I.; Plano, D.; Palop, J. A.; Sanmartin, C., Combined acylselenourea-diselenide structures: New potent and selective antitumoral agents as autophagy activators. *ACS Med. Chem. Lett.* **2018**, *9* (4), 306-311.
23. Garnica, P.; Encio, I.; Plano, D.; Palop, J. A.; Sanmartin, C., Organoseleno cytostatic derivatives: Autophagic cell death inducers that activate the pi3k/akt pathway. Submitted to ACS Med Chem Lett, 2018.
24. Eberle, C.; Burkhard, J. A.; Stump, B.; Kaiser, M.; Brun, R.; Krauth-Siegel, R. L.; Diederich, F., Synthesis, inhibition potency, binding mode, and antiprotozoal activities of fluorescent inhibitors of trypanothione reductase based on mepacrine-conjugated diaryl sulfide scaffolds. *ChemMedChem* **2009**, *4* (12), 2034-44.

#### Supplementary Material

Supplementary data associated with this article includes full description of the methodologies used in order to evaluate the leishmanicidal activity of the compounds presented in this work.



## Supplementary Material

### Pre-clinical evidences of the potential antileishmanial effects of diselenides and selenocyanates.

Pablo Garnica <sup>a,1</sup>, Mikel Etxebeste-Mitxeltoarena <sup>a,b,1</sup>, Daniel Plano <sup>a</sup>, Esther Moreno <sup>b</sup>, Socorro Espuelas <sup>b</sup>, Juan Antonio Palop <sup>a</sup>, Antonio Jiménez-Ruiz <sup>c</sup>, Carmen Sanmartin <sup>a,b,\*</sup>

<sup>a</sup> Department of Organic and Pharmaceutical Chemistry, University of Navarra, Irunlarrea, 1, E-31008 Pamplona, Spain

<sup>b</sup> Institute of Tropical Health, University of Navarra, Pamplona, Spain; Pharmacy and Pharmaceutical Technology Department, University of Navarra, Pamplona, Spain

<sup>c</sup> Department of Biochemistry and Molecular Biology, Universidad de Alcalá, Carretera Madrid-Barcelona km 33,600, E-28871 Alcalá de Henares, Madrid, Spain

<sup>1</sup> Authors have contributed equally to this article

#### 1.1. Chemistry

The synthesis, purification and characterization methodologies for the presented compounds has been described by our group in recent publications<sup>1-2</sup>.

#### 1.2. Cells and culture conditions

*L. infantum* promastigotes (MCAN/ES/89/IPZ229/1/89) were grown in RPMI 1640 medium (Sigma-Aldrich, St. Louis, MO) supplemented with 10% heat-inactivated fetal calf serum (FCS), antibiotics, and 25 mM HEPES (pH 7.2) at 26°C.

*L. infantum* axenic amastigotes were obtained by incubation of  $4.5 \times 10^6$  late-logarithmic-phase promastigotes in 5 ml of M199 medium (Invitrogen, Leiden, The Netherlands) supplemented with 10% heat-inactivated FCS, 1 g liter<sup>-1</sup> of  $\beta$ -alanine, 100 mg liter<sup>-1</sup> of l-asparagine, 200 mg liter<sup>-1</sup> of sucrose, 50 mg liter<sup>-1</sup> of sodium pyruvate, 320 mg liter<sup>-1</sup> of malic acid, 40 mg liter<sup>-1</sup> of fumaric acid, 70 mg liter<sup>-1</sup> of succinic acid, 200 mg liter<sup>-1</sup> of  $\alpha$ -ketoglutaric acid, 300 mg liter<sup>-1</sup> of citric acid, 1.1 g liter<sup>-1</sup> of sodium bicarbonate, 5 g liter<sup>-1</sup> of morpholineethanesulfonic acid (MES), 0.4 mg liter<sup>-1</sup> of hemin, and 10 mg liter<sup>-1</sup> of gentamicin, pH 5.4, at 37°C. After 48 h of incubation, all parasites had a rounded morphology without a flagellum and divided during several weeks under the described conditions.

THP-1 cells were grown in RPMI 1640 medium (Gibco, Leiden, The Netherlands) supplemented with 10% heat-inactivated FCS, 5% penicillin/streptomycin, 1 mM HEPES, 2 mM glutamine, and 1 mM sodium pyruvate, pH 7.2, at 37°C and 5% CO<sub>2</sub>.

#### 1.3. Leishmanicidal activity and cytotoxicity assays

Drug treatment of amastigotes was performed during the logarithmic growth phase at a concentration of  $1 \times 10^6$  parasites/ml at 37°C for 24 h. Drug treatment of THP-1 cells was performed during the logarithmic growth phase at a concentration of  $4 \times 10^5$  cells/ml at 37°C and 5% CO<sub>2</sub> for 24 h. The percentage of living cells was evaluated by flow cytometry by the propidium iodide (PI) exclusion method.<sup>3</sup> Drug concentrations ranged from 0.04  $\mu$ M to 25  $\mu$ M.

#### 1.4. Leishmania infection assay

Human THP-1 monocytic cells were seeded at  $1.2 \times 10^5$  cells/ml in 24-multidish plates (Nunc, Roskilde, Denmark) and differentiated to macrophages for 24 h in 1 ml of RPMI 1640 medium containing 10 ng/ml of phorbol 12-myristate 13-acetate (PMA) (Sigma-Aldrich, St. Louis, MO). Medium culture was removed, and  $1.2 \times 10^6$  *Leishmania* amastigotes in 1 ml of THP-1 medium were added to each well. Four hours later, all medium with noninfective amastigotes was removed, washed 3 times with 1 $\times$  phosphate-buffered saline (PBS), and

---

\* Corresponding author. Tel.: +34 948 425 600; fax: +34 948 425 649; e-mail: sanmartin@unav.es

replaced with new THP-1 medium and corresponding treatment (3 $\mu$ M) experiment was performed in triplicate. After 48 h of treatment, medium was removed; THP-1 cells were washed 3 times with 1 $\times$  PBS and detached with TrypLE Express (Invitrogen, Leiden, The Netherlands) according to the manufacturer's indications. Infection quantification was measured by flow cytometry.

#### 1.5. Trypanothione reductase assay

Oxidoreductase activity was determined according to the method described by Toro et al.<sup>4</sup> Briefly, reactions were carried out at room temperature in 250  $\mu$ l of 40 mM HEPES buffer (pH 8.0) containing 1 mM EDTA, 150  $\mu$ M NADPH, 30  $\mu$ M NADP<sup>+</sup>, 25  $\mu$ M DTNB [5,5'-dithiobis-(2-nitrobenzoic acid) or Ellman's reagent], 1  $\mu$ M T[S]2, 0.02% glycerol, 1.5% dimethyl sulfoxide (DMSO), and 7 nM recombinant Li-TryR. Enzyme activity was monitored by the increase in absorbance at 412 nm for 1 h at 26°C in a VERSAmax microplate reader (Molecular Devices, CA). All the assays were conducted in triplicate in at least three independent experiments. Data were analyzed using a nonlinear regression model with Grafit6 software (Erithacus, Horley, Surrey, United Kingdom).

#### 1.6. 4.2.6. Physico-chemical and absorption properties calculations

The physico-chemical properties of the most active compounds were calculated using the Molinspiration (<http://www.molinspiration.com/cgi-bin/properties>). The absorption properties were calculated using PreADMET program (<https://preadmet.bmdrc.kr/adme/>).

## References

1. Garnica, P.; Encio, I.; Plano, D.; Palop, J. A.; Sanmartin, C., Combined acylselenourea-diselenide structures: New potent and selective antitumoral agents as autophagy activators. *ACS Med Chem Lett* **2018**, *9* (4), 306-311.
2. Garnica, P.; Encio, I.; Plano, D.; Palop, J. A.; Sanmartin, C., Organoseleno cytostatic derivatives: Autophagic cell death inducers that activate the pi3k/akt pathway. Submitted to *ACS Med Chem Lett*, 2018.
3. Alzate, J. F.; Arias, A. A.; Moreno-Mateos, D.; Alvarez-Barrientos, A.; Jimenez-Ruiz, A., Mitochondrial superoxide mediates heat-induced apoptotic-like death in leishmania infantum. *Mol Biochem Parasitol* **2007**, *152* (2), 192-202.
4. Toro, M. A.; Sanchez-Murcia, P. A.; Moreno, D.; Ruiz-Santaquiteria, M.; Alzate, J. F.; Negri, A.; Camarasa, M. J.; Gago, F.; Velazquez, S.; Jimenez-Ruiz, A., Probing the dimerization interface of leishmania infantum trypanothione reductase with site-directed mutagenesis and short peptides. *Chembiochem* **2013**, *14* (10), 1212-1217.









Article

# Antitumoural Sulphur and Selenium Heteroaryl Compounds: Thermal Characterization and Stability Evaluation

Verónica Alcolea <sup>1,†</sup>, Pablo Garnica <sup>1,†</sup>, Juan A. Palop <sup>1</sup>, Carmen Sanmartín <sup>1,\*</sup>,  
Elena González-Peñas <sup>1</sup>, Adrián Durán <sup>2</sup> and Elena Lizarraga <sup>1</sup>

<sup>1</sup> Department of Organic and Pharmaceutical Chemistry, Faculty of Pharmacy and Nutrition, University of Navarra, Irunlarrea 1, 31008 Pamplona, Spain; valcolea@alumni.unav.es (V.A.); pgarnica@alumni.unav.es (P.G.); jpalop@unav.es (J.A.P.); mgpenas@unav.es (E.G.-P.); elizarraga@unav.es (E.L.)

<sup>2</sup> Department of Chemistry, Faculty of Sciences, University of Navarra, Irunlarrea 1, 31008 Pamplona, Spain; adrianduran@unav.es

\* Correspondence: sanmartin@unav.es; Tel.: +34-948-425600

† Authors have contributed equally to this article.

Stability is a crucial factor in the drug design process and therefore must be evaluated to prevent degradation or other non-desirable processes. This work has the goal of establishing stability thermal stability and assess structure stability under oxidative, acid and alkaline conditions. This methodology was developed and validated on a selection of leader compounds previously synthesized by our research group. Polymorphic behaviors were also studied in order to predict possible solid-state transitions in the formulation process that might affect the final outcome of the drug. This work also includes the synthesis and antitumor evaluation of a series of compounds. The analysis of thermal stability and polymorphic behavior of a library of compounds was performed in order identify patterns in stability and structure relationship.



Article

# Antitumoural Sulphur and Selenium Heteroaryl Compounds: Thermal Characterization and Stability Evaluation

Verónica Alcolea <sup>1,†</sup>, Pablo Garnica <sup>1,†</sup>, Juan A. Palop <sup>1</sup>, Carmen Sanmartín <sup>1,\*</sup>,  
Elena González-Peñas <sup>1</sup>, Adrián Durán <sup>2</sup> and Elena Lizarraga <sup>1</sup>

<sup>1</sup> Department of Organic and Pharmaceutical Chemistry, Faculty of Pharmacy and Nutrition, University of Navarra, Irunlarrea 1, 31008 Pamplona, Spain; valcolea@alumni.unav.es (V.A.); pgarnica@alumni.unav.es (P.G.); jpalop@unav.es (J.A.P.); mgpenas@unav.es (E.G.-P.); elizarraga@unav.es (E.L.)

<sup>2</sup> Department of Chemistry, Faculty of Sciences, University of Navarra, Irunlarrea 1, 31008 Pamplona, Spain; adrianduran@unav.es

\* Correspondence: sanmartin@unav.es; Tel.: +34-948-425600

† Authors have contributed equally to this article.

Received: 29 June 2017; Accepted: 4 August 2017; Published: 8 August 2017

**Abstract:** The physicochemical properties of a compound play a crucial role in the cancer development process. In this context, polymorphism can become an important obstacle for the pharmaceutical industry because it frequently leads to the loss of therapeutic effectiveness of some drugs. Stability under manufacturing conditions is also critical to ensure no undesired degradations or transformations occur. In this study, the thermal behaviour of 40 derivatives of a series of sulphur and selenium heteroaryl compounds with potential antitumoural activity were studied. In addition, the most promising cytotoxic derivatives were analysed by a combination of differential scanning calorimetry, X-ray diffraction and thermogravimetric techniques in order to investigate their polymorphism and thermal stability. Moreover, stability under acid, alkaline and oxidative media was tested. Degradation under stress conditions as well as the presence of polymorphism was found for the compounds VA6E and VA7J, which might present a hurdle to carrying on with formulation. On the contrary, these obstacles were not found for derivative VA4J.

**Keywords:** thermal analysis; activity; stability; polymorphism; differential scanning calorimetry; thermogravimetry; X-ray diffraction; HPLC

## 1. Introduction

Cancer is a leading cause of death worldwide; the World Health Organization estimates the growth rate of new cases to peak at 70% in the next twenty years [1]. If we draw the focus to US territory, an estimated 1650 deaths per day will be due to cancer [2]. Many treatment patterns include some kind of chemotherapy or molecularly-targeted therapy drugs. Cancer research is nowadays encountering two major obstacles, side-effects and tumour resistance, both intrinsic and acquired [3,4]. Therefore, the synthesis of new, safer and more effective drugs is urgent in order to be able to overcome those previously mentioned difficulties developed by some of the present treatments.

Among the arsenal of new anti-cancer agents, selenium (Se)-containing compounds stand out for their anti-tumour potency and safety [5]. These properties strongly depend on the chemical form and dose used [6]. For the past decade, our group has focused on the synthesis of sulphur (S) and Se-containing molecules as antitumour agents with encouraging results [7,8]. In the present study, the homology between those two atoms will be explored in order to widen the variety of chemical entities. The introduction of this structural duality will enable us to contrast Se and S influence in terms of anti-cancer activity, stability and thermal characterization.



It has been found that pharmaceutical compounds such as cephalexin, chloramphenicol, digoxin, spironolactone, sulfathiazole, carbamazepine and retroviral agents [9–12] undergo transitions during drying processes, spraying, grinding, compression, excipient addition and the preparation of tableting. Polymorphism in pharmaceutical solids can be a critical manufacturing variable and therefore has to be investigated [13].

Physicochemical properties such as bioavailability and stability are directly related to the crystal structure and possible polymorphism [14,15]. Therefore, the prediction of polymorphism in the early stages of drug development provides valuable information to selectively synthesize or isolate the crystalline structure with the best characteristics. In addition, polymorphic transformations can occur during some steps of the synthesis including purification, crystallization, drying and storage [16,17]. Furthermore, this property influences several parameters such as solubility, shelf life, and formulation processes [18].

Investigating the relative thermal stability of polymorphs is also essential because the instant appearance or disappearance of a crystalline structure can lead to serious consequences if the polymorphic transformation occurs in the dosage form [19]. Da Silva et al. [20] have found that the solubility and dissolution properties of finasteride, which is widely used for prostate cancer treatment, were significantly affected by polymorphism. This disparity in bioavailability is related to the diverse dissolution rate of the different polymorphic forms. In some cases, the metastable form of some active ingredients may be twice as active as the stable form [21]. In addition, Yoshida et al. [22] have observed that the degradation products after drug stress conditions are related to some events that appeared in the calorimetric curves.

The study of the physical stability of drugs should be properly conducted in order to determine the characteristics of the proposed formulation and predict possible changes in the solid state of the drug. Certain pharmaceutical processes (granulation, drying, and compression) can lead to polymorphic transformations and thus the critical steps in this process must be identified and controlled to ensure stability until the end of the drug's shelf life [23].

If we narrow the view to Se and S derivatives, those properties have proved to be critical. Some Se-containing structures i.e., ebselen, produce two different polymorphs when crystallized from different solvents that differ in the antioxidant activity related to the ability of Se–N bond cleavage as well as the potential for Se–O interactions [24]. Moreover, S derivative compounds such as dalcetrapib [25], probenecid [26] or tauroursodeoxycholic acid [27] showed the ability to crystallize in different structures, an ability that dramatically affects their biological activity profile.

Those heteroaryl derivatives that exhibited promising cytotoxic activity (VA7J, VA6O and VA5P) in previous publications from the group [28,29] have the potential to continue the drug discovery process. With the objective of predicting the non-desired transitions or degradation processes that may occur along with the already mentioned pharmaceutical manufacturing processing, we proceeded to the thermal characterization and preliminary stability studies of the leader compounds. In addition, the biological and thermal characterization of the novel compounds recently developed by our group have also been included in this work. Inactive analogues were also studied following the same methodology in order to be able to establish a comparison.

## 2. Results and Discussion

### 2.1. Synthesis and Selection Criteria

The selected compounds for this study were synthesized in the Organic and Pharmaceutical Synthesis Unit of the University of Navarra. A total of 40 compounds were included in this work. They were divided into 12 series (series B to P, Figure 1) according to their central skeleton. They are hybrid derivatives containing diverse substituents with S or Se and several active heterocyclic scaffolds. Six novel derivatives (VA6G, VA6H, VA6I, VA2J, VA4J and VA6J) were incorporated to complete the series. The compounds VA6G, VA6H, VA6I and VA6J were synthesized according to a previously published procedure by reaction of the corresponding alkyl halides with potassium thiocyanate in acetone under reflux conditions [30]. To obtain compound VA2J, 2,3-

dichloroquinoxaline was treated with thiourea in a 1:2.2 (reagent/thiourea) molar ratio at reflux, using absolute ethanol as solvent. VA4J was synthesized by the treatment of derivative VA2J with a potassium hydroxide solution in DMSO and stirring at room temperature (r.t.), with a posterior methylation with methyl iodide. The final compound was purified taking advantage of its solubility properties. The synthesis of the remaining 34 derivatives has been previously published by our group [28,29].

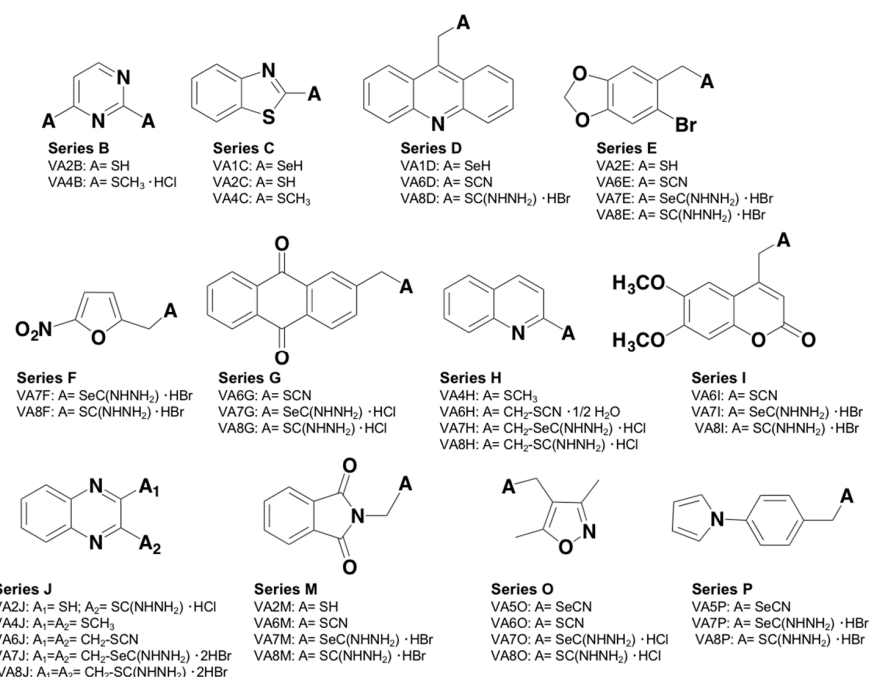


**Figure 1.** Structures of S and Se heteroaryl compounds studied in this work. The compounds VA6G, VA6H, VA6I, VA2J, VA4J and VA6J are novel molecules. The structures of series 7 and 8 have been previously described [29] and the remaining ones have been extracted from a previous work from our group [28].

In order to perform the thermal characterization and preliminary stability studies of those compounds with the best drug-likeness profile, the cytotoxic potency was evaluated by the MTT (3-(4,5-dimethylthiazol-2-yl)-2,5-diphenyltetrazolium bromide) assay.

The novel synthetic compounds VA2J, VA4J, VA6G, VA6H, VA6I and VA6J were tested in breast adenocarcinoma (MCF-7) and non-malignant mammary-gland-derived (184B5) cell lines to be able to establish their potency and selectivity. The reference drug used was methylseleninic acid (MSA) as a Se-containing structure with promising in vitro and in vivo results against different tumour types [31,32]. Results are expressed as the concentration that inhibits 50% cell growth (GI<sub>50</sub>), the concentration that inhibits completely cell growth (TGI) and the concentration that kills 50% of cells (LD<sub>50</sub>). The selectivity index (SI) is calculated as GI<sub>50</sub>(184B5)/GI<sub>50</sub>(MCF-7).

As shown in Table 1, five out of the six tested compounds (VA2J, VA4J, VA6G, VA6H and VA6I) exhibited GI<sub>50</sub> values under 10 μM. If we move to selectivity values, the compound VA4J emerges as the most selective derivative with an SI over 50 times higher than MSA.

For the remaining compounds of series 1, 2, 3, 4, 5 and 6, cytotoxic activity had already been evaluated following the same methodology [28]. Cell viability assays for compounds of series 7 and 8 had already been screened in a panel of six human cancer cell lines: 1205Lu (melanoma), A549 (lung), DU145 (prostate), HCT116 (colon), PANC-1 (pancreas) and BxPC3 (pancreas) [29].

**Table 1.** Average values of GI<sub>50</sub>, TGI and LD<sub>50</sub> (μM) and calculated SI.

Compound	Cell Lines						SI
	MCF-7			184B5			
	GI <sub>50</sub>	TGI	LD <sub>50</sub>	GI <sub>50</sub>	TGI	LD <sub>50</sub>	
VA2J	2.20	13.90	44.02	12.45	15.97	20.48	5.66
VA4J	1.02	>100	>100	52.45	>100	>100	51.25
VA6G	3.59	23.95	67.27	14.29	34.32	64.84	3.99
VA6H	8.53	14.83	24.18	27.76	75.84	>100	3.25
VA6I	4.51	>100	>100	2.26	>100	>100	0.50
VA6J	18.50	50.55	83.93	39.77	69.80	94.62	2.15
MSA	1.28	3.43	>100	1.79	3.84	>100	1.40

Based on all the synthetic data and antitumour preliminary activity evaluation, the following criteria were established to select the most promising structures to proceed to their thermal characterization and preliminary stability studies:

- Synthetic yield has to be higher than 40% as lower yields might present limitations to a future production scale-up.
- High activity against cancer cells must be exhibited.

Taking into account these criteria, the structure VA4J was chosen as the most promising one of the newly studied structures with a yield of 53%, GI<sub>50</sub> value against MCF-7 cells under 10 μM and an SI of 51.25.

Derivative VA7J was selected from series 7 and 8 with 82% yield and the most potent activity profile. Even though the MTT assay conditions were slightly different in this work, a clear leader can be established. Compound VA7J was selected from this group of structures as it shows IC<sub>50</sub> values under 10 μM in all six cell lines even at short time points.

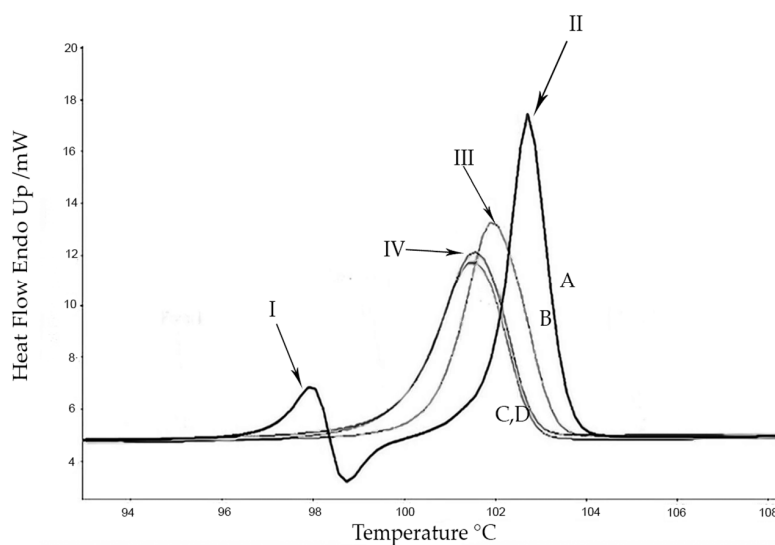
Focusing on the compounds remaining of series 1, 2, 3, 4, 5 and 6, compounds VA6O and VA5P were selected in the referenced work as the most potent ones. Nevertheless, VA6O and VA5P had to be dismissed for this study as VA6O has an oily physical appearance and VA5P showed fusion with decomposition in a preliminary test. Therefore, we followed the criteria of SI, potency and potential safety, to select the representative compound for these structures. According to these criteria, derivatives VA2E and VA6E were chosen. Compound VA2E did not meet the yield condition with a 5% yield, so it was ruled out. Finally, the compound VA6E was selected as it has a reasonable yield, high potency and it is fourteen times more selective than MSA [28].

## 2.2. Compound Thermal Characterization

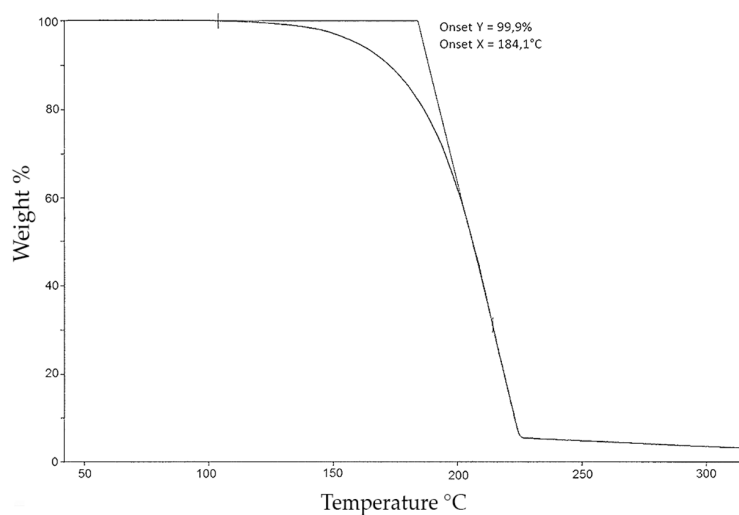
The combination of several techniques is necessary in order to properly confirm polymorphism presence and thermal stability. The methodology employed to perform the complete thermal characterization of a compound include IR spectroscopy, powder X-ray diffractometry (PXRD) and thermal methods, especially differential scanning calorimetry (DSC) and thermogravimetry (TG).

### 2.2.1. Compound VA6E

The DSC results of compound VA6E are shown in Figure 2a and Table 2. During the first thermal scan (curve A), three processes were observed. The first corresponds with a typical endothermic process of the original product (Form I), followed by a recrystallization process to another form (Form II), which then melts. After cooling, in the sample—through a polymorphic phase transition—Form II changes into another form which shows fusion processes (Form III, curve B). In the third scan a new endothermic process happened at a lower temperature (curve C), with the appearance of a new polymorph (Form IV). The complete thermogram (Figure 2b) shows that other processes at another temperature (higher or lower) can be excluded.



(a)



(b)

**Figure 2.** DSC and TG of compound VA6E (a,b) respectively. (a) Curve A: first scan (fusion Form I and Form II); curve B: second scan (fusion of Form III) and curves C and D: third and fourth scan (fusion of Form IV); (b) TG of compound VA6E at 10 °C/min.

**Table 2.** Fusion–recrystallization of compound VA6E.

Scan	Form I		Recrystallization		New Polymorphs	
	$T_{onset}$ (°C)	$\Delta H$ (J g <sup>-1</sup> )	$T_{onset}$ (°C)	$\Delta H$ (J g <sup>-1</sup> )	$T_{onset}$ (°C)	$\Delta H$ (J g <sup>-1</sup> )
1st	97.2	7.9	98.5	-8.8	101.9	75.6
	(Form I)				(Form II)	
2nd	-	-	-	-	100.7	80.3
					(Form III)	
3rd	-	-	-	-	100.1	76.7
					(Form IV)	
4th	-	-	-	-	99.9	76.0
					(Form IV)	

Marked differences were found in the positions of the peaks between the diffractograms of the different forms. In Figure 3, the diffractogram in black corresponds to the sample after melting and the subsequent recrystallization. Some of the peaks matched with those from the original sample (diffractogram in red). However, other peaks only appeared after melting and recrystallization ( $2\theta = 6.7^\circ, 13.4^\circ, 20.3^\circ, 22.8^\circ, 29.2^\circ, 33.9^\circ$  and  $34.1^\circ$ ). In this case, we think Form I has partially transformed into another polymorphic form (Form II), while preserving part of the original form.

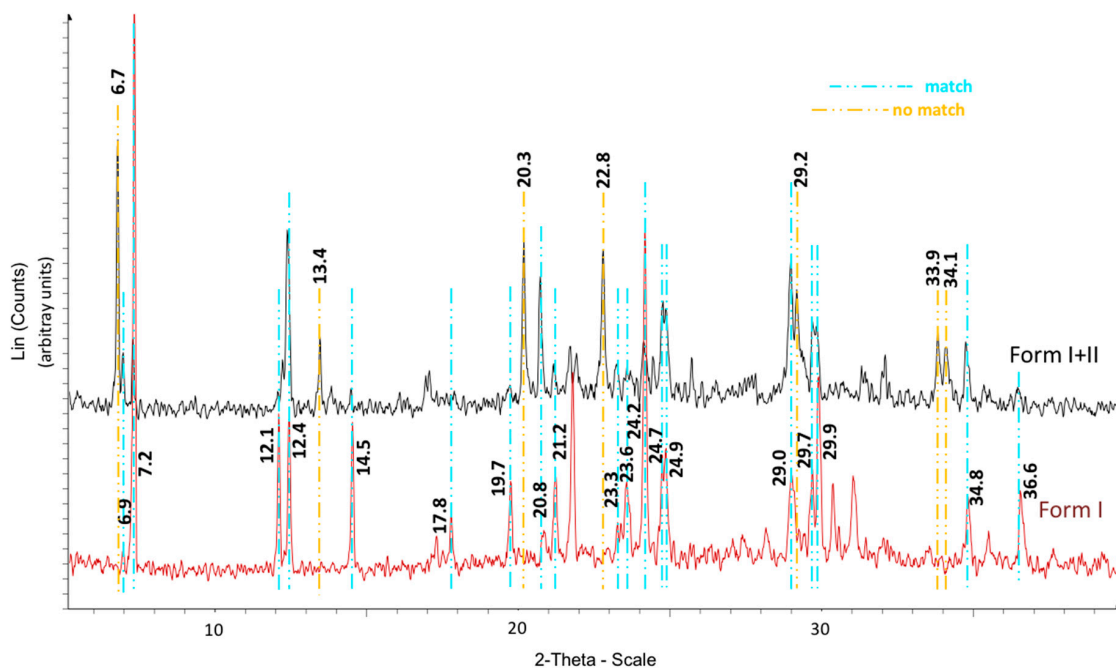


**Figure 3.** X-ray diffractograms for compound VA6E. Form I shows the diffractogram of the original polymorph and Form I + II, the one obtained after one cycle of melting-recrystallization.

Figure 4 shows the X-ray diffractograms after different and consecutive melting-recrystallization cycles. As discussed before, after one cycle, a mixture of Forms I and II can be observed. The following cycle provoked the appearance of a new polymorphic form (Form III), but the original Forms I and II are also present (diffractogram in red) as the match of the position of the peaks  $2\theta = 20.3^\circ, 20.8^\circ, 23.3^\circ,$  and  $24.9^\circ$  shows. Form III (diffractogram in blue) showed a peak at  $2\theta = 20.4^\circ$  that was not detected in Forms I and II, as well as the absence of other signals present in Forms I and II (peaks at  $2\theta = 7.2^\circ$  and  $34.8^\circ$ ). Finally, Form IV was observed after another cycle (diffractogram in green). The differences between the resulting form from this last cycle and the previous ones are highlighted in yellow dotted lines. Peaks at  $2\theta = 20.4^\circ, 29.8^\circ$  and  $30.8^\circ$  are present in Form III but not in the last polymorphic form. Peaks at  $7.2^\circ$  and  $34.8^\circ$ , present in Form I + II, do not appear in Form IV. After successive heating-cooling processes the same Form IV was isolated. Taken together, the results of the X-ray diffraction indicate that all four forms observed by DSC were indeed distinct.

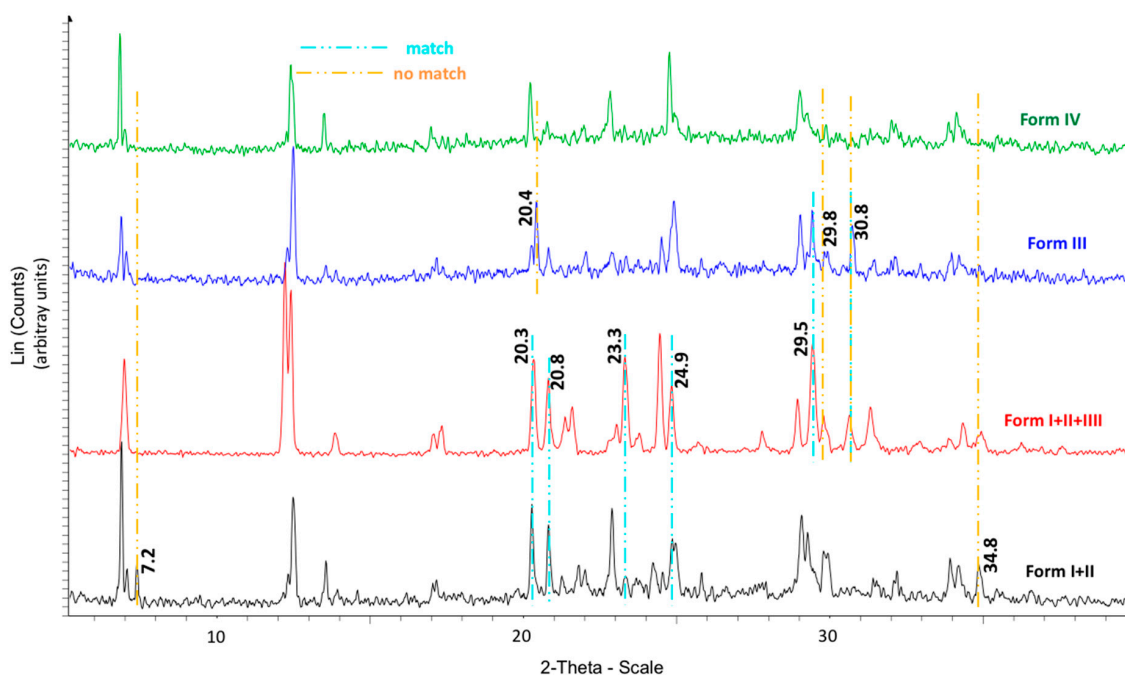
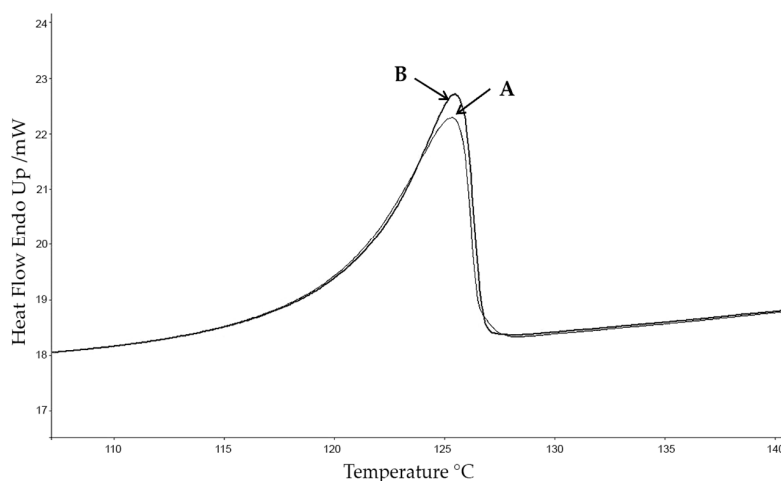


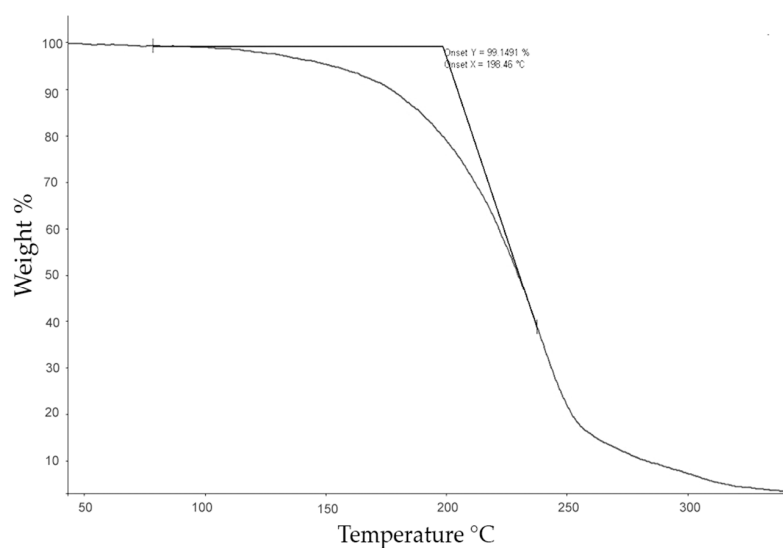
**Figure 4.** X-ray diffractograms of the forms of VA6E obtained after successive cycles of melting–recrystallization.

#### 2.2.2. Compound VA4J

DSC results (Figure 5a and Table 3) show that the compound VA4J does not alter its thermal behaviour after an initial fusion–recrystallization cycle. Under these conditions there is no evidence of polymorphism. During the first thermal curve of compound VA4J (curve A in Figure 5a), a classic endothermic process of Form I was discerned (Table 3), typical of a melting process. After cooling the sample, the melted form recrystallized in the same form, as indicated by the same endothermic process in curve B.



(a)



(b)

**Figure 5.** DSC (a) and TG (b) of compound VA4J. (a) Curve A: first scan (fusion of Form I) and curve B: second scan (fusion of recrystallized form); (b) TG of compound VA4J at 10 °C/min.

**Table 3.** Fusion–recrystallization of compound VA4J.

	$T_{onset}$ (°C)	$\Delta H$ (J g <sup>-1</sup> )	
1st scan	119.84	93.58	Form I
2nd scan	119.59	93.91	Form I

To further confirm the absence of polymorphism, both samples were analysed by using PXRD. An excellent match of the position of the peaks in both diffractograms was observed (see peaks at  $2\theta$  at 11.5°, 11.9°, 20.9°, 24.1°, 26.2°, 27.6°, 29.3° and 33.0° in Figure 6). The differences in the relative intensities of some of the peaks were probably due to some preferred orientation in the samples derived from the absence of random orientation of crystal grains in space.

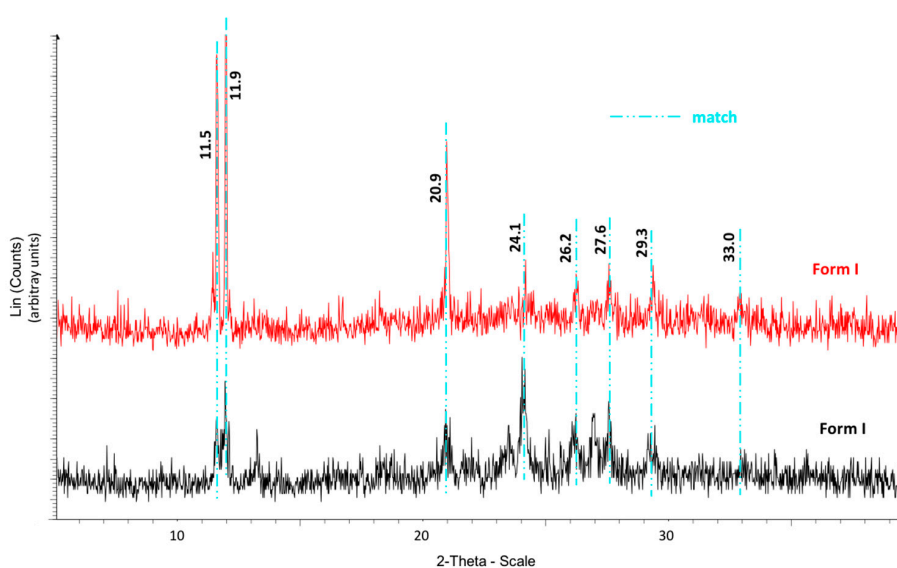
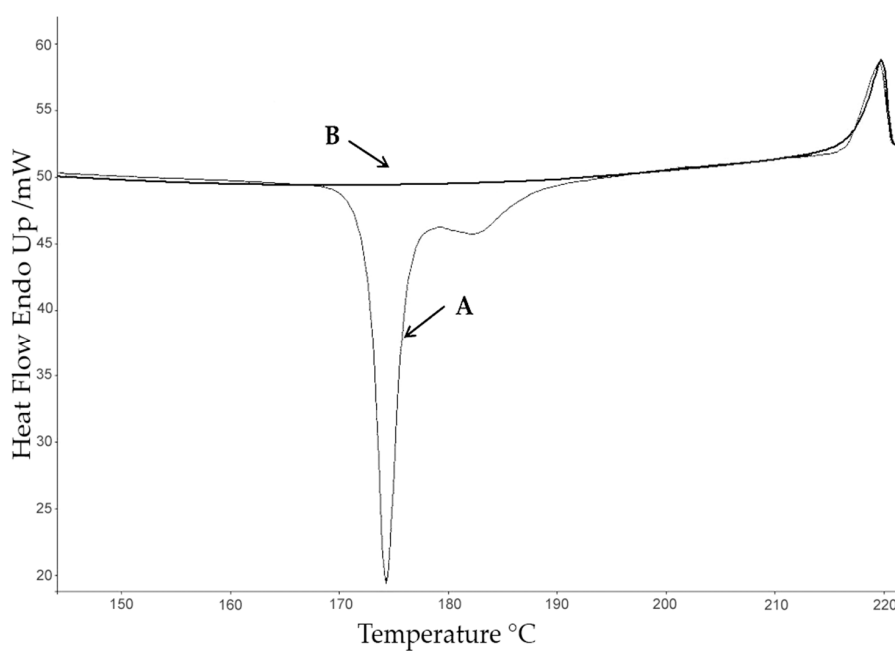


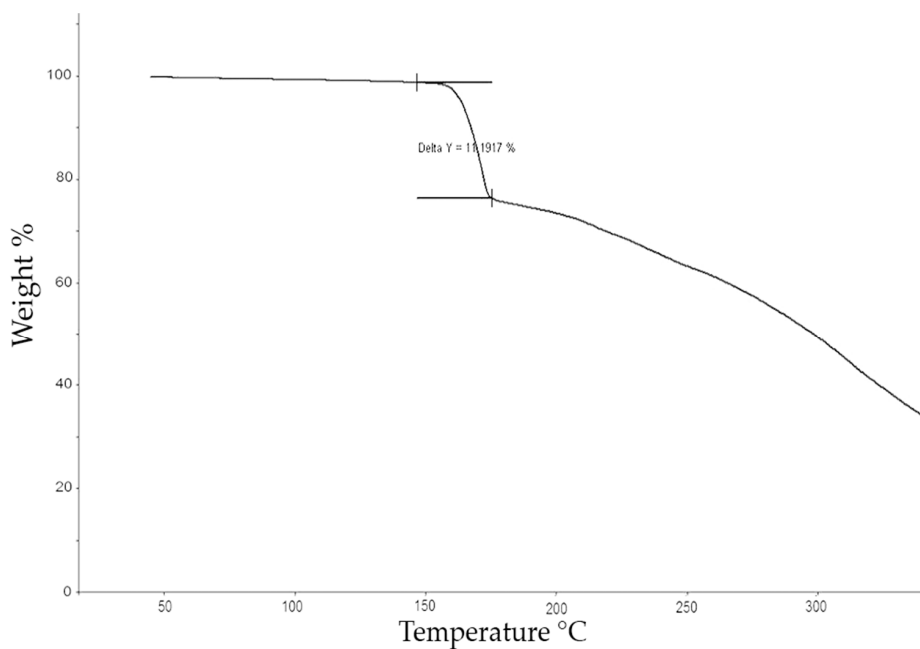
**Figure 6.** X-ray diffractograms of the original form of VA4J (in black) and those obtained after successive cycles of melting–recrystallization (in red).

### 2.2.3. Compound VA7J

In the first heating scan, the original form of compound VA7J melts with desolvation. A new endothermic fusion of the anhydrous product generated confirms the polymorphism (pseudopolymorphism or phase transition of the hydrated form to the corresponding anhydride) of this compound (curve A, Figure 7a). After cooling the sample, it can be observed (curve B) that the subsequent endothermic process occurs at the same temperature (curve B, Figure 7a, Table 4).



(a)



(b)

**Figure 7.** DSC (a) and TG (b) of compound VA7J. (a) Curve A: first scan (desolvation) and curve B: second scan; (b) TG of compound VA7J at 10 °C/min.



**Table 4.** Fusion–recrystallization of compound VA7J.

Behaviour III	$T_{onset}$ (°C)	$\Delta H$ (J g <sup>-1</sup> )	
1st scan	173.8	−88.4	Form I
	218.2	18.7	Form II
2nd scan	219.7	17.4	Form II

Two different compounds were detected in the sample VA7J by using PXRD (Figure 8). Several differences were found between the peak positions in the raw sample (diffractogram in black) and the sample after one desolvation/phase transition process (diffractogram in red). Peaks at  $2\theta = 19.3^\circ$ ,  $21.2^\circ$ ,  $22.1^\circ$ ,  $23.8^\circ$ ,  $24.7^\circ$ ,  $26.6^\circ$ ,  $28.4^\circ$  and  $32.7^\circ$  were present in the original compound (Form I) but disappeared in Form II of anhydrous compound. This confirms the appearance of a new polymorphic form.

The diffractogram collected after a melting scan and a subsequent recrystallization process of Form II of the compound (diffractogram in green) is very similar to the one obtained from the first cycle (in red). Therefore, a new polymorphic form is not present. In Figure 8, the majority of the diffraction peaks match in the  $2\theta$  position (see peaks at  $2\theta = 21.9^\circ$ ,  $23.4^\circ$ ,  $26.1^\circ$ ,  $26.4^\circ$ ,  $27.9^\circ$  and  $31.2^\circ$ ) and the observed differences between both diffractograms are in terms of the relative intensities.

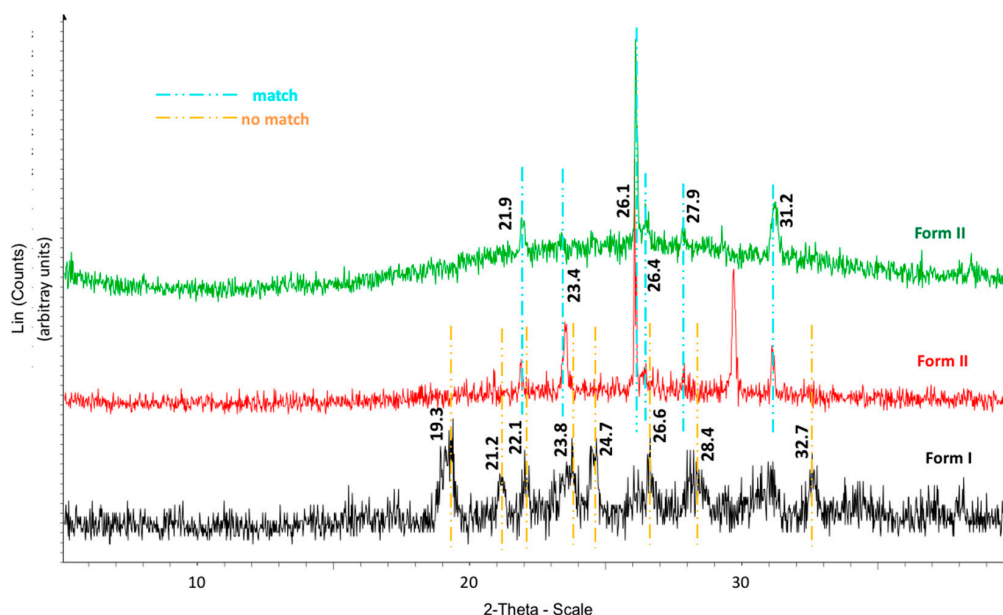


**Figure 8.** X-ray diffractograms of the forms of VA7J obtained after successive cycles of melting–recrystallization.

### 2.3. Compound Stability Tests

#### 2.3.1. Thermal Stability

Thermogravimetric analyses were performed to evaluate the thermal stability of the compounds (Figures 2b, 5b and 7b, Table 5). The TG analysis of the compounds VA4J and VA6E show that the decomposition or desolvation processes in the temperature range studied (100–135 °C and 94–108 °C, respectively) can be excluded. On the other hand, the thermogravimetric curve of the compound VA7J shows a debromhidration process at 173 °C, and when further heated, decomposition of desolvated compound from 228 °C.

Table 5. Thermal data obtained by DSC and TG.

Ref.	R	DSC			Behaviour	TG	
		Scan	T <sub>o</sub> /°C	ΔH <sub>f</sub> /J g <sup>-1</sup>		T <sub>o</sub> /°C	
<b>Series B</b>							
VA2B	SH	1st	-	-	V	263.3	
VA4B	SCH <sub>3</sub>	1st	-	-	V	103.5	
<b>Series C</b>							
VA1C	SeH	1st	175.5	91.3	I	218.4	
		2nd	-	-			
VA2C	SH	1st	178.8	85.9	III	224.7	
		2nd	178.6	86.6			
VA4C	SCH <sub>3</sub>	1st	-	-	V	131.8	
<b>Series D</b>							
VA1D	SeH	1st	-	-	V	244.7	
VA6D	SCN	1st	-	-	V	205.0	
VA8D	SC(NHNH <sub>2</sub> )	1st	196.7	-90.3	*	193.1	
<b>Series E</b>							
VA2E	SH	1st	148.8	34.0	I	266.2	
		2nd	-	-			
VA6E	SCN	2nd	97.2	7.8	IV	184.1	
			1st	98.4			-8.8
			101.9	75.6			
			2nd	100.7			80.3
			3th	100.1			76.7
VA7E	SeC(NHNH <sub>2</sub> )	2nd	4th	99.9	76.0	II	205.2
			1st	183.8	21.5		
			2nd	177.2	28.1		
VA8E	SC(NHNH <sub>2</sub> )	2nd	3th	-	-	I	215.1
			1st	196.1	33.8		
			208.5	-37.4			
<b>Series F</b>							
VA7F	SeC(NHNH <sub>2</sub> )	1st	214.4	-63.6	*	214.7	
VA8F	SC(NHNH <sub>2</sub> )	1st	198.3	-64.6	*	190.8	
<b>Series G</b>							
VA6G	SCN	1st	-	-	V	238.3	
VA7G	SeC(NHNH <sub>2</sub> )	1st	-	-	V	198.2	
VA8G	SC(NHNH <sub>2</sub> )	1st	-	-	V	243.7	
<b>Series H</b>							
VA4H	SCH <sub>3</sub>	1st	54.9	75.7	I	105.6	
		2nd	-	-			
VA6H	SCN	1st	78.9	116.6	I	139.1	
		2nd	-	-			
VA7H	SeC(NHNH <sub>2</sub> )	1st	113.7	42.0	I	145.8	
		2nd	-	-			
VA8H	SC(NHNH <sub>2</sub> )	1st	176.2	49.3	I	190.2	
		2nd	-	-			
<b>Series I</b>							
VA6I	SCN	1st	234.9	110.8	I	246.9	
		2nd	-	-			
VA7I	SeC(NHNH <sub>2</sub> )	1st	230.1	30.1	*	226.4	
			234.4	-14.4			
VA8I	SC(NHNH <sub>2</sub> )	1st	263.2	39.6	*	272.4	
			265.4	-36.7			
<b>Series J</b>							
VA2J	SH/SC(NHNH <sub>2</sub> )	1st	206.5	-63.9	*	199.2	

VA4J	SCH <sub>3</sub>	1st	119.84	93.58	I	197.42
		2nd	119.59	93.91		
VA6J	SCN	2nd	167.6	-227.0	*	165.0
		1st	173.8	-88.4		
VA7J	SeC(NHNH <sub>2</sub> )	1st	218.2	18.5	IV	From 228
		2nd	219.7	17.4		
		3th	219.6	17.4		
VA8J	SC(NHNH <sub>2</sub> )	1st	222.9	31.3	I	251.05
		2nd	224.1	-95.3		
<b>Series M</b>						
VA2M	SH	1st	113.6	68.1	III	166.0
		2nd	110.2	70.7		
VA6M	SCN	1st	143.3	50.8	I	164.8
		2nd	-	-		
VA7M	SeC(NHNH <sub>2</sub> )	1st	211.6	34.4	IV	255.8
			216.0	-68.7		
		2nd	220.0	4.4		
VA8M	SC(NHNH <sub>2</sub> )	2nd	219.7	10.3	I	233.1
		3th	219.8	14.8		
		1st	228.7	116.7		
<b>Series O</b>						
VA5O	SeCN	1st	67.7	76.0	III	141.7
		2nd	65.6	66.2		
VA7O	SeC(NHNH <sub>2</sub> )	1st	-	-	V	185.9
VA8O	SC(NHNH <sub>2</sub> )	1st	194.7	21.1	II	201.8
		2nd	199.8	45.8		
		3rd	-	-		
<b>Series P</b>						
VA5P	SeCN	1st	161.3	79.6	*	149.4
VA7P	SeC(NHNH <sub>2</sub> )	1st	180.2	-84.7	*	175.8
VA8P	SC(NHNH <sub>2</sub> )	1st	200.6	1.7	*	199.8
		2nd	210.1	-60.4		

\* fusion with decomposition.

### 2.3.2. Stability after Stress Conditions

The stability of compounds VA4J (without polymorphic behaviour) and VA6E and VA7J (with polymorphic behaviour) was investigated after the application of diverse stress conditions: acid hydrolysis (HCl 1 M), basic hydrolysis (NaOH 0.1 M) and oxidation (H<sub>2</sub>O<sub>2</sub> 3%). Chromatographic studies using HPLC/UV-DAD were performed with this purpose.

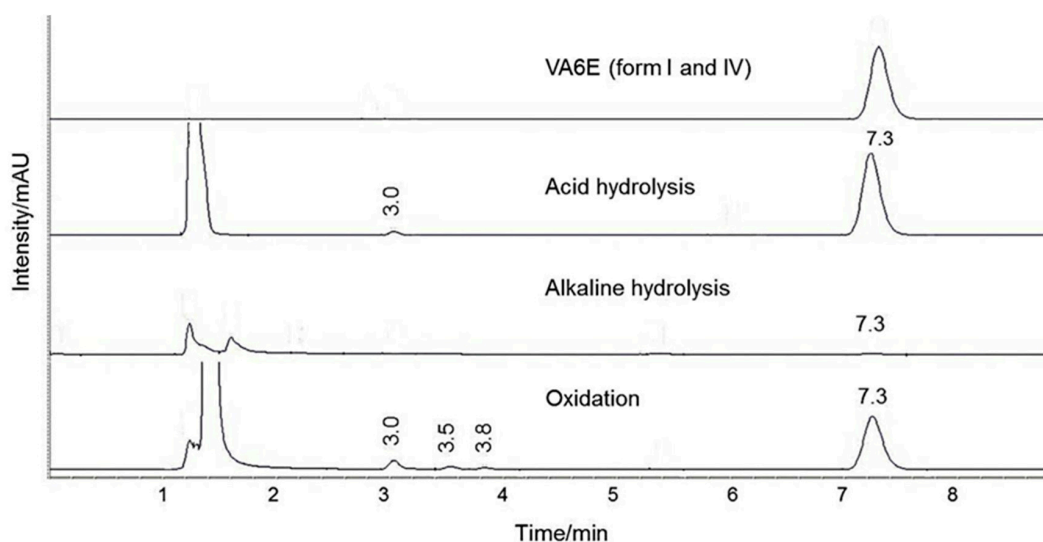
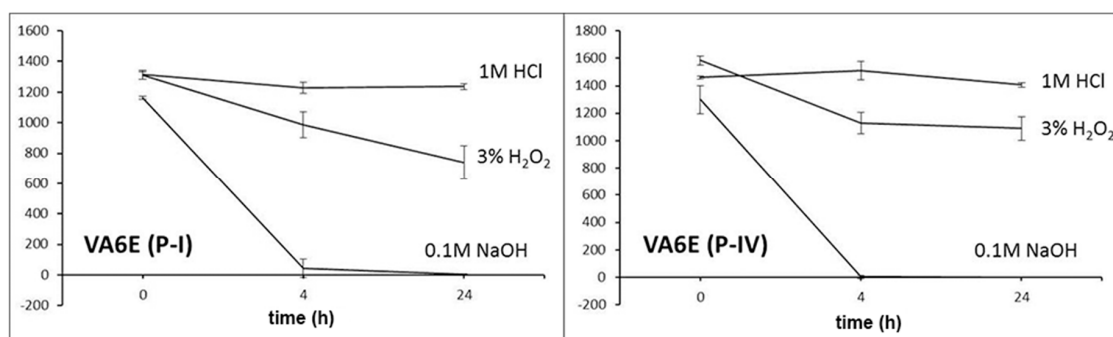
During calibration sample analysis, compound VA4J had a retention time of 4.9 min, compound VA6E of 7.3 min (for both Form I and IV), and compound VA7J of 1.1 min (for both form I and II).

The linearity showed an adequate relationship between the instrumental response (peak areas) and the respective sample concentration ( $x$ ). Intra-day precision (Relative Standard Deviation (RSD) < 7%) was satisfactorily obtained in the ranges evaluated for the three compounds (Table 6). When new peaks appeared after stress conditions, they were adequately separated from the parent peak.

Compound VA6E (Form I and IV)—similar stability for the two polymorphs was found after application of different stress conditions (Figures 9 and 10). The highest degradation occurred in the alkaline medium, as both forms degraded almost completely after 4 h of exposure to NaOH. Although the stability was higher, degradation product peaks were also detected after acid hydrolysis ( $t_R$  3.0 min) and oxidation ( $t_R$  3.0, 3.5 and 3.8 min).

**Table 6.** Limit of Quantification (LOQ), linearity data and within-day precision.

	$t_R$ (min)	LOQ ( $\mu\text{g/mL}$ )	Range ( $\mu\text{g/mL}$ )	Curve Equation	$r^2$	Slope Interval ( $p = 95\%$ )	Within-Day Precision	
							[ $\mu\text{g/mL}$ ]	%RSD ( $n = 3$ )
VA4J	4.9	0.8	0.8–59.5	$y = 97.7x - 51.1$	0.999	96.0–99.9	0.8	5.6
							1.0	5.5
							6.0	4.6
							23.8	2.6
							59.5	0.5
VA6E	7.3	3.0	3.0–119.0	$y = 26.2x - 59.2$	0.996	25.3–27.1	3.0	0.8
							6.0	2.4
							11.9	3.9
							47.6	1.5
							119.0	0.7
VA7J	1.1	0.8	0.8–59.5	$y = 97.5x + 37.1$	0.999	94.9–100.0	0.8	6.5
							1.0	3.9
							6.0	10.5
							23.8	1.7
							59.5	0.9

**Figure 9.** VA6E (form I and IV) chromatogram before and after 24 h application of diverse stress conditions: acid and alkaline hydrolysis and oxidation.**Figure 10.** Stability of compound VA6E (polymorph I and IV) after 0, 4 and 24 h of exposition to HCl, NaOH and  $\text{H}_2\text{O}_2$ .

Compound VA4J—The compound was stable after all the stress conditions studied. The VA4J chromatogram before and after 24 h application of acid and alkaline hydrolysis and oxidation showed

no change in the peak area at 4.9 min  $t_R$  and no new peaks were detected at other retention times (data not shown).

Compound VA7J—The compound was stable to acid hydrolysis and only a minor degradation due to alkaline conditions was detected. However, it totally degraded in the presence of  $H_2O_2$ , as no peak was detected at its retention time at zero time of exposure to oxidation (Figure 11). A new chromatographic peak was detected at  $t_R$  of 1.4 min, corresponding to an oxidized form of VA7J, probably an *N*-oxide derivative.

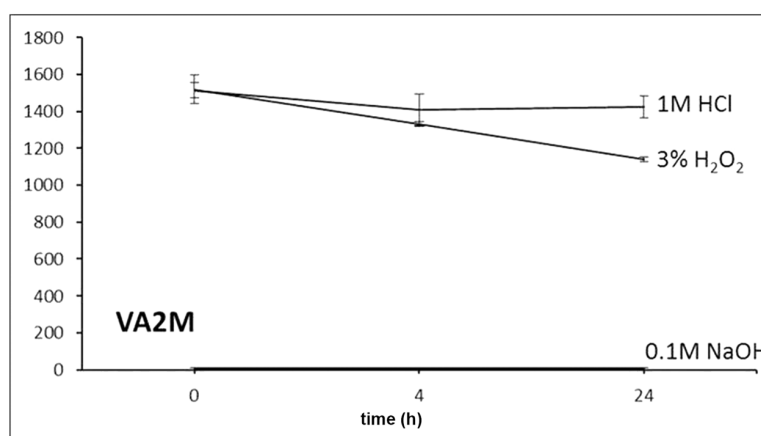


**Figure 11.** Stability of compound VA7J (polymorph I and II) after application of stress conditions.

#### 2.4. Polymorphic Behaviours

To establish general polymorphic behaviours, samples of all the compounds synthesized (Figure 1) were exposed to successive cycles of melting–recrystallization using DSC. Calorimetric analyses were performed before the beginning of the degradation process (Table 6). The analysis of the thermal data revealed interesting calorimetric performance for some of these compounds. The results showed that there are five types of calorimetric behaviours:

- Behaviour I—Compounds that show a polymorphic phase transition into an amorphous or mainly amorphous solid form after a first melting–cooling scan. This behaviour was shown by several compounds: VA1C, VA2E, VA8E, series H, VA6I, VA8J, VA6M and VA8M. DSC and PXRD results of compound VA7H are shown as supplementary material (Figures S1 and S2 and Table S1).
- Behaviour II—Compounds that change into a new polymorphic form with a different  $T_{onset}$  of fusion than the one observed at the first melting–recrystallization scan after cooling. These compounds are VA7E and VA8O. DSC and PXRD results of compound VA7E are shown as supplementary material (Figures S3 and S4, Table S2).
- Behaviour III—These compounds show a fusion process without modifications in the thermal behaviour after an initial fusion–recrystallization cycle. Consequently, there is no evidence of polymorphic behaviour. The compounds VA2C, VA2M, VA4J and VA5O belong to this group. DSC and PXRD results of compound VA2M are shown as supplementary material (Figures S5 and S6, Table S3).
- Behaviour IV—Compounds that show recrystallization or other types of phase transition of the original form into another crystalline one in the first heat scan. In the successive cycles of melting–recrystallization, the new form may not alter its crystalline form or transit to another polymorphic form. Compounds VA6E, VA7J and VA7M show this behaviour.
- Behaviour V—Compounds without fusion processes at the range of temperatures studied. The original compound shows an amorphous form that does not recrystallize into any crystalline form in the successive melting–recrystallization cycles. The compounds that showed this thermal behaviour are VA2B, VA4B, VA4C, VA1D, VA6D, series G, and VA7O.

no change in the peak area at 4.9 min  $t_R$  and no new peaks were detected at other retention times (data not shown).

Compound VA7J—The compound was stable to acid hydrolysis and only a minor degradation due to alkaline conditions was detected. However, it totally degraded in the presence of  $H_2O_2$ , as no peak was detected at its retention time at zero time of exposure to oxidation (Figure 11). A new chromatographic peak was detected at  $t_R$  of 1.4 min, corresponding to an oxidized form of VA7J, probably an *N*-oxide derivative.

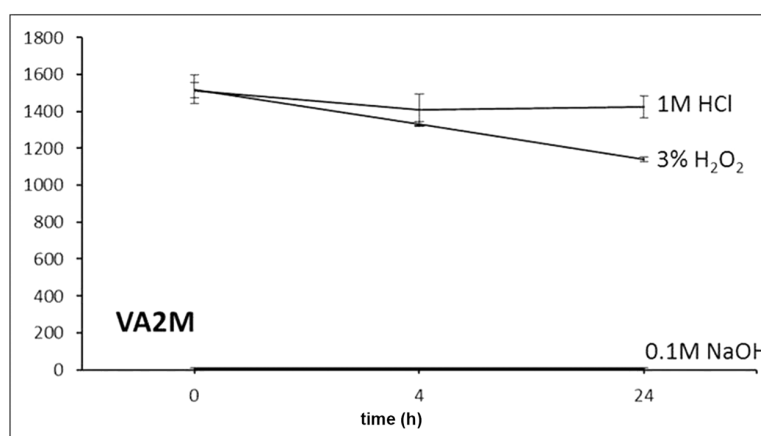


**Figure 11.** Stability of compound VA7J (polymorph I and II) after application of stress conditions.

#### 2.4. Polymorphic Behaviours

To establish general polymorphic behaviours, samples of all the compounds synthesized (Figure 1) were exposed to successive cycles of melting–recrystallization using DSC. Calorimetric analyses were performed before the beginning of the degradation process (Table 6). The analysis of the thermal data revealed interesting calorimetric performance for some of these compounds. The results showed that there are five types of calorimetric behaviours:

- Behaviour I—Compounds that show a polymorphic phase transition into an amorphous or mainly amorphous solid form after a first melting–cooling scan. This behaviour was shown by several compounds: VA1C, VA2E, VA8E, series H, VA6I, VA8J, VA6M and VA8M. DSC and PXRD results of compound VA7H are shown as supplementary material (Figures S1 and S2 and Table S1).
- Behaviour II—Compounds that change into a new polymorphic form with a different  $T_{onset}$  of fusion than the one observed at the first melting–recrystallization scan after cooling. These compounds are VA7E and VA8O. DSC and PXRD results of compound VA7E are shown as supplementary material (Figures S3 and S4, Table S2).
- Behaviour III—These compounds show a fusion process without modifications in the thermal behaviour after an initial fusion–recrystallization cycle. Consequently, there is no evidence of polymorphic behaviour. The compounds VA2C, VA2M, VA4J and VA5O belong to this group. DSC and PXRD results of compound VA2M are shown as supplementary material (Figures S5 and S6, Table S3).
- Behaviour IV—Compounds that show recrystallization or other types of phase transition of the original form into another crystalline one in the first heat scan. In the successive cycles of melting–recrystallization, the new form may not alter its crystalline form or transit to another polymorphic form. Compounds VA6E, VA7J and VA7M show this behaviour.
- Behaviour V—Compounds without fusion processes at the range of temperatures studied. The original compound shows an amorphous form that does not recrystallize into any crystalline form in the successive melting–recrystallization cycles. The compounds that showed this thermal behaviour are VA2B, VA4B, VA4C, VA1D, VA6D, series G, and VA7O.

Polymorphic behaviour is affected by reaction conditions and purification processes, as they include temperature modifications that can lead to modifications in the final solid state structure. General patterns are therefore difficult to extract as these factors vary among the 12 series. The main skeleton of the structure differs in each of these series and it has a crucial effect on the internal organization.

Some general patterns within each series of compounds can be found. All the derivatives from series B, D and G share the same behaviour (V), those compounds do not suffer transformations due to heating as they only exhibit one polymorphic form (except for compound VA8D that melts with decomposition). In the same line, compounds of series H exhibit behaviour I, which leads us to think that the conditions for the original crystalline structure to transform to the polymorph were probably not met during the synthetic process. Therefore, the structural nucleus is the main factor that determines internal organization in this series.

Interestingly, the polymorphic behaviour of some of the series changes depending on the substituent. For example, series E shows three different polymorphic behaviours depending on the attached substituent in position 5. Therefore, the substituents play an important role in the calorimetric performance of the resulting derivatives. However, no general patterns could be established in terms of the effect of substituents on internal organization, probably because of the strong effect that main nucleus modifications have among them. Thus, each series should be evaluated independently.

### 2.5. Comparative Thermal Stability

The values of thermal degradation temperatures obtained for the S and Se heteroaryl compounds are also shown in Table 6. Thermal stability is affected by intramolecular interactions and electron delocalization inside the core of the structure, as well as by interactions that might exist between the core and the substituents.

A comparison between compounds substituted with the same chemical group is hard to establish since only compounds **6**, **7** and **8** are present in most of the mentioned series. Moreover, the variability of the chemical nature of the heterocycles used enables us to observe only general trends in the analysis. For example, quinolone-based structures (series H) are less stable with  $T_{onset}$  values of 139.1 °C, 145.8 °C and 190.2 °C for the corresponding derivatives **6**, **7** and **8**, respectively. On the other hand, the structures of series I are among the most stable with  $T_{onset}$  over 220 °C in all three cases and ranking among the two most stable compounds in derivatives **6**, **7** and **8**.

Patterns relating to the substituent nature and thermal stability of the compounds can be spotted when focusing on those compounds with a common core structure (Series B, C, D, E, F, G, H, I, J, M, O and P).

Stability is enhanced in structures with the ability to establish hydrogen intermolecular interactions. Overall, SH (compound **2**) or SeH (compound **1**) groups improve stability dramatically. If we look at other substituents that can establish hydrogen interactions such as  $-\text{Se}-\text{C}(\text{NH}_2)=\text{NH}$  or  $-\text{S}-\text{C}(\text{NH}_2)=\text{NH}$ , we can also observe an increase in the thermal stability. Although compounds of series **7** and **8** are homologs except for the presence of Se or S atoms, S derivatives are more stable than Se-substituted compounds in general.

Considering the other substituents, compounds with a nitrile (CN; compounds **5** and **6**) or methyl (CH<sub>3</sub>; compounds **4**) group showed lower  $T_{onset}$  values of degradation, with this effect being more pronounced for the methyl group. Methyl-substituted structures might be less stable because they do not have the ability to establish either hydrogen interaction.

## 3. Materials and Methods

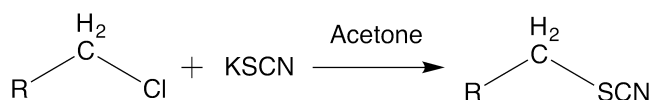
### 3.1. Chemistry

Proton (<sup>1</sup>H) and carbon (<sup>13</sup>C) NMR spectra were recorded on a Brüker 400 Ultra-shield™ spectrometer (Brüker, Rheinstetten, Germany) using DMSO-*d*<sub>6</sub> or CDCl<sub>3</sub> as solvent. IR spectra were recorded on a Thermo Nicolet FT-IR Nexus spectrophotometer (Thermo Nicolet, Madison, WI, USA) using KBr pellets for solid samples or NaCl plates for oil compounds. Elemental analysis was

performed on a LECO CHN-900 Elemental Analyzer (LECO, Saint Joseph, MI, USA). The purity of all final compounds was 99% or higher. Chemicals were purchased from E. Merck (Darmstadt, Germany), Panreac Química S.A. (Barcelona, Spain), Sigma-Aldrich Química, S.A. (Madrid, Spain) and Acros Organics (Janssen Pharmaceuticaaan, Geel, Belgium). The synthesis of 34 out of the 40 compounds analysed in this work has been previously described [28,29].

### 3.1.1. General Procedure for the Synthesis of Compounds VA6G, VA6H, VA6I and VA6J

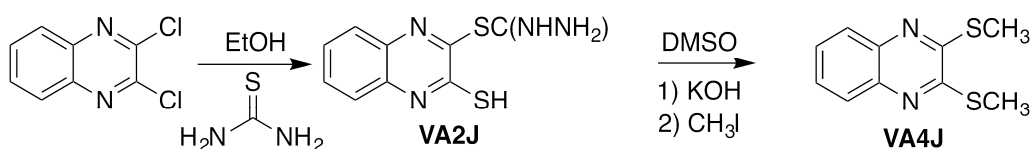
The synthesis (Scheme 1) was carried out from the corresponding alkyl-halide reagent and potassium-thiocyanate in acetone at reflux, as previously described. The corresponding halide reagent (1 mmol) was added to a mixture of 1.2 mmol of potassium thiocyanate in dry acetone (20 mL). The mixture was stirred at reflux for 3.5–4 h and the product was isolated by filtration after the addition of 50 mL of water and purified by washing or recrystallization.



**Scheme 1.** Reaction scheme to yield compounds VA6G, VA6H, VA6I and VA6J.

### 3.1.2. 3-Mercaptoquinoxalin-2-yl Carbamimidothioate Hydrochloride (VA2J)

To obtain compound VA2J, 2,3-dichloroquinoxaline was treated with thiourea in a 1:2.2 (reagent/thiourea) molar ratio (Scheme 2) at reflux for 4 h using absolute ethanol as solvent (20 mL). The product was purified by recrystallization from methanol. An orange powder was obtained. Yield: 42%; melting point (m.p.): 197–198 °C (direct combustion). <sup>1</sup>H-NMR (400 MHz, DMSO-*d*<sub>6</sub>): δ 7.54 (t, 1H, *J* = 7.3 Hz, H6), 7.66–7.72 (m, 2H, H5 + H7), 7.90 (d, 1H, *J* = 8.1 Hz, H8), 9.76 + 9.95 (bs + bs, 4H, NH + NH<sub>2</sub> + HCl), 15.13 ppm (bs, 1H, SH). <sup>13</sup>C-NMR (100 MHz, DMSO-*d*<sub>6</sub>): δ 117.4 (C6), 127.4 (C7), 128.7 (C5), 131.9 (C8), 132.0 (C4a), 135.6 (C8a), 160.7 (C3), 165.4 (C2), 171.4 ppm (S–C–(NH)(NH<sub>2</sub>)). IR (KBr):  $\tilde{\nu}$  3380–3200 (s; N–H, N–H<sub>2</sub>), 1625 cm<sup>−1</sup> (s; C=N). MS [*m/z* (% abundance)]: 194 (100), 161 (16), 150 (43), 134 (25). Elemental analysis calculated (%) for C<sub>9</sub>H<sub>8</sub>N<sub>4</sub>S<sub>2</sub>·HCl: C: 39.63, H: 3.33, N: 20.54; found: C: 39.92, H: 3.61, N: 20.19.



**Scheme 2.** Synthesis schematics for compounds VA2J and VA4J.

### 3.1.3. 2,3-Bis(methylsulfanyl)quinoxaline (VA4J)

VA4J was synthesized by adding 1 mmol of VA2J to a suspension of 3.6 mmol of potassium hydroxide in DMSO (5 mL) and stirring for 1 h at room temperature (r.t.). Then, 4 mmol of methyl iodide were added and stirred for additional 4 h at r.t. (Scheme 2). The reaction medium was then poured into ice and the resultant precipitate was filtered and solved in dichloromethane (40 mL). The insoluble fraction was discarded and the solvent was removed under vacuum by rotatory evaporation. A yellow powder was obtained. Yield: 53%; mp: 118–119 °C. <sup>1</sup>H-NMR (400 MHz, CDCl<sub>3</sub>): δ 2.75 (s, 6H, (CH<sub>3</sub>) × 2), 7.58–7.61 (m, 2H, H6 + H7), 7.91–7.96 ppm (m, 2H, H5 + H8). <sup>13</sup>C-NMR (100 MHz, DMSO-*d*<sub>6</sub>): δ 13.7 ((CH<sub>3</sub>) × 2), 128.1 (C5 + C8), 129.4 (C6 + C7), 139.9 (C4a + C8a), 155.3 ppm (C2 + C3). IR (KBr):  $\tilde{\nu}$  2919 (m; C–H<sub>aliph</sub>), 1615 cm<sup>−1</sup> (s; C=N). MS [*m/z* (% abundance)]: 222 (52; M<sup>+</sup>), 207 (100), 192 (31), 175 (8), 160 (20), 102 (17). Elemental analysis calculated (%) for C<sub>10</sub>H<sub>10</sub>N<sub>2</sub>S<sub>2</sub>·1/2H<sub>2</sub>O: C: 51.87, H: 4.76, N: 12.10; found: C: 51.63, H: 4.56, N: 12.46.



### 3.1.4. (9,10-Dioxo-9,10-dihydroanthracen-2-yl)methyl Thiocyanate (VA6G)

From 2-(chloromethyl)-9,10-dioxo-9,10-dihydroanthracen. Conditions: 3.5 h at reflux; recrystallized from ethanol. A yellow powder was obtained. Yield: 46%; m.p.: 174–175 °C. <sup>1</sup>H-NMR (400 MHz, DMSO-*d*<sub>6</sub>): δ 4.58 (s, 2H, –CH<sub>2</sub>–), 7.93–7.96 (m, 3H, H1 + H3 + H4), 8.20–8.29 ppm (m, 4H, H5 + H6 + H7 + H8). <sup>13</sup>C-NMR (100 MHz, DMSO-*d*<sub>6</sub>): δ 37.1 (–CH<sub>2</sub>–), 113.7 (–SCN), 127.6 (C5 + C8), 128.0 (C1), 128.3 (C4), 133.4 (C3), 133.8 (C4a), 134.1 (C6 + C7), 135.4 (C8a + C10a), 135.7 (C9a), 144.1 (C2), 183.0 ppm (C9 + C10). IR (KBr):  $\tilde{\nu}$  2149 (m, C≡N), 1671 cm<sup>−1</sup> (s, C=O). MS [*m/z* (% abundance)]: 279 (5; M<sup>+</sup>), 221 (100), 193 (51), 165 (27). Elemental analysis calculated (%) for C<sub>16</sub>H<sub>9</sub>NO<sub>2</sub>S: C: 68.80, H: 3.25, N: 5.01; found: C: 68.59, H: 3.31, N: 4.82.

### 3.1.5. Quinolin-2-ylmethyl Thiocyanate (VA6H)

The commercially available 2-(chloromethyl)quinoline hydrochloride was treated with basic water (50 mL) in order to obtain the free base, which was used for the synthesis of VA6H. Conditions: 4 h at reflux. The precipitate was washed with ethyl ether (20 mL). A brown powder was obtained. Yield: 41%; m.p.: 80–81 °C. <sup>1</sup>H-NMR (400 MHz, DMSO-*d*<sub>6</sub>): δ 4.74 (s, 2H, –CH<sub>2</sub>–), 7.63–7.66 (m, 2H, H3 + H6), 7.80 (t, 1H, *J* = 7.8 Hz, H7), 8.01 (d, 2H, *J* = 8.6 Hz, H5 + H8), 8.44 ppm (d, 1H, *J* = 8.5 Hz, H4). <sup>13</sup>C NMR (100 MHz, DMSO-*d*<sub>6</sub>): δ 40.0 (–CH<sub>2</sub>–), 113.9 (–SCN), 121.8 (C3), 127.8 (C6), 127.9 (C4a), 128.8 (C5), 129.3 (C8), 131.0 (C7), 138.2 (C4), 147.8 (C8a), 156.4 ppm (C2). IR (KBr):  $\tilde{\nu}$  3058 (m; C–H<sub>arom</sub>), 2946 (m; C–H<sub>aliph</sub>), 2147 (s; C≡N), 1655 cm<sup>−1</sup> (m; C=N). MS [*m/z* (% abundance)]: 200 (100; M<sup>+</sup>), 174 (6), 142 (100), 128 (9), 115 (47). Elemental analysis calculated (%) for C<sub>11</sub>H<sub>8</sub>N<sub>2</sub>S·1/2H<sub>2</sub>O: C: 63.08, H: 4.30, N: 13.99; found: C: 62.96, H: 4.42, N: 13.15.

### 3.1.6. (6,7-Dimethoxy-2-oxo-2H-chromen-4-yl)methyl Thiocyanate (VA6I)

From 4-(bromomethyl)-6,7-dimethoxy-2-oxo-2H-chromene. Conditions: 4 h at reflux. The product was washed with ethyl ether and dichloromethane (20 mL of each). A white powder was obtained. Yield: 70%; m.p.: 204–205 °C. <sup>1</sup>H-NMR (400 MHz, DMSO-*d*<sub>6</sub>): δ 3.83 + 3.88 (s, 6H, (–OCH<sub>3</sub>) × 2), 4.56 (s, 2H, –CH<sub>2</sub>–), 6.41 (s, 1H, H3), 7.13 (s, 1H, H5), 7.38 ppm (s, 1H, H8). <sup>13</sup>C-NMR (100 MHz, DMSO-*d*<sub>6</sub>): δ 33.6 (–CH<sub>2</sub>–), 57.1 + 57.3 ((–OCH<sub>3</sub>) × 2), 101.5 (C8), 107.2 (C5), 110.0 (–SCN), 113.3 (C3), 114.0 (C4a), 146.9 (C6), 150.4 (C8a), 150.7 (C7), 153.8 (C4), 160.8 ppm (C2). IR (KBr):  $\tilde{\nu}$  3065 (w; C–H<sub>arom</sub>), 2999–2849 (m; C–H<sub>aliph</sub>), 2154 (s; C≡N), 1711 cm<sup>−1</sup> (C=O). MS [*m/z* (% abundance)]: 277 (100; M<sup>+</sup>), 234 (6), 219 (27), 191 (69), 147 (18). Elemental analysis calculated (%) for C<sub>13</sub>H<sub>11</sub>NO<sub>4</sub>S: C: 56.31, H: 4.00, N: 5.05; found: C: 56.40, H: 3.98, N: 4.88.

### 3.1.7. Quinoxalin-2,3-diyl dimethanediyl Bisthiocyanate (VA6J)

From 2,3-bis(bromomethyl)quinoxaline. Conditions: 4 h. at reflux. The product was washed with ethyl ether (20 mL). A brown powder was obtained. Yield: 88%; m.p.: 158–159 °C (direct combustion). <sup>1</sup>H-NMR (400 MHz, DMSO-*d*<sub>6</sub>): δ 4.98 (s, 4H, (–CH<sub>2</sub>–) × 2), 7.91–7.93 (m, 2H, H6 + H7), 8.11–8.14 ppm (m, 2H, H5 + H8). <sup>13</sup>C-NMR (100 MHz, DMSO-*d*<sub>6</sub>): δ 37.7 ((–CH<sub>2</sub>–) × 2), 112.0 ((–SCN) × 2), 128.4 (C5 + C8), 128.4 (C6 + C7), 143.7 (C4a + C8a), 160.3 ppm (C2 + C3). IR (KBr):  $\tilde{\nu}$  2926 (m; C–H<sub>aliph</sub>), 2155 (s; C≡N), 1563–1485 cm<sup>−1</sup> (m; C–C<sub>arom</sub>). MS [*m/z* (% abundance)]: 272 (36; M<sup>+</sup>), 245 (14), 214 (100), 187 (15), 170 (13), 155 (30), 129(13). Elemental analysis calculated (%) for C<sub>12</sub>H<sub>8</sub>N<sub>4</sub>S<sub>2</sub>: C: 52.92, H: 2.96, N: 20.57; found: C: 52.7, H: 3.07, N: 20.77.

## 3.2. Biological Evaluation

The antitumoural evaluation of 34 out of the 40 compounds analysed in this work has been previously described [28,29].

### 3.2.1. Cell Culture

Cell lines were purchased from the American Type Culture Collection (ATCC, Barcelona, Spain). MCF7 cell lines were grown in Roswell Park Memorial Institute (RPMI) medium (Gibco, Madrid,

Spain) supplemented with 10% fetal bovine serum (FBS; Gibco), 100 units/mL penicillin and 100 mg/mL streptomycin (Gibco, Madrid, Spain). 184B5 cells were grown in DMEM/F12 medium supplemented with 5% FBS, 1x ITS (Lonza, Barcelona, Spain), 100 nM hydrocortisone (Sigma Aldrich, Madrid, Spain), 2 mM sodium pyruvate (Lonza), 20 ng/mL EGF (Sigma Aldrich, Madrid, Spain), 0.3 nM trans-retinoic acid (Sigma-Aldrich) 100 units/mL penicillin and 100 mg/mL streptomycin. Cells were maintained at 37 °C and 5% CO<sub>2</sub>.

### 3.2.2. Cell Viability

Compounds were dissolved in DMSO at a concentration of 0.01 M. Serial dilutions were prepared with non-supplemented medium. The cytotoxic effect of each compound was tested at eight different concentrations ranging between 0.01 and 100 µM.

A total of 10<sup>4</sup> cells/well in 96 well-plates were treated with either DMSO or increasing concentrations of the corresponding compound for 72 h and cell viability was determined using the MTT (3-(4,5-dimethylthiazol-2-yl)-2,5-diphenyltetrazolium bromide) (Sigma Aldrich, Madrid, Spain) assay [33]. Briefly, cells were incubated with 50 µL of MTT (2 mg/mL stock) for 4 h. The medium was then removed by aspiration and the formazan crystals were dissolved in 150 µL of DMSO. The absorbance was measured at 550 nm in a microplate reader (Sunrise, Tecan, Männedorf, Switzerland). Results are expressed as GI<sub>50</sub>, the concentration that reduces by 50% the growth of treated cells with respect to untreated controls, TGI, the concentration that completely inhibits cell growth, and LC<sub>50</sub>, the concentration that kills 50% of the cells. Data were obtained from at least three independent experiments performed in quadruplicate.

### 3.3. Thermal Analysis

The thermogravimetric (TG) studies were carried out with a Perkin–Elmer TGA-7 (Perkin Elmer, Inc. Watham, MA, USA) which was calibrated with alumel and nickel at 10 °C·min<sup>-1</sup>. The calibration of the oven temperatures was carried out automatically and mass calibrated with a certified sample of 10 mg (ASTM E617, provided by Perkin Elmer, Inc. Watham, MA, USA). TG analyses were performed under a nitrogen atmosphere with a gas flow of 40 mL·min<sup>-1</sup>, from 50 to 350 °C, at a heating rate of 10 °C·min<sup>-1</sup>, using a sample of approximately 3 mg, in order to obtain the values of the  $T_{onset}$  and  $T_{max}$  of the degradation process as well as any associated mass loss.

For calorimetric studies a Perkin–Elmer DSC diamond calibrated with indium and zinc (provided by Perkin–Elmer (Perkin Elmer, Inc. Watham, MA, USA) and fabricated according to guideline ISO35) at 10 °C·min<sup>-1</sup> and nitrogen flow of 20 mL·min<sup>-1</sup> was employed. The gas connected to the equipment was nitrogen with a purity of 99.999%. Calorimetric analyses were carried out in aluminium capsules for volatilities of 10 µL, at a heating rate of 10 °C·min<sup>-1</sup>, using a sample of approximately 3 mg, in order to establish the  $T_{onset}$ ,  $T_{max}$  and the enthalpy of fusion  $\Delta H_f$ .

The calorimetric analyses started with the study of the thermal behaviour of the compounds before the process of degradation in order to evidence the possible existence of polymorphism. For this preliminary study, samples of all the compounds were exposed to successive cycles of heating–cooling. All samples were heated from 50 °C to temperatures 15–20 °C below  $T_{onset}$  of the degradation process, in order to ensure that compounds were not degraded (Table 6). After melting the samples, they were left at room temperature for enough time to allow the compounds to recrystallize before the successive thermal process. Additional cycles of heating–cooling were performed if polymorphism was detected.

### 3.4. Powder X-ray Diffraction

The X-ray diffraction experiments were performed by using a Bruker D8 Advance diffractometer, under the conditions of a step size of 0.02° and 1 s time/step, from 5° < 2θ < 40°. The equipment consisted of an X-ray generator with a Cu anode (radiation Cu Kα = 1.54 Å, 40 kV, 30 mA) and a scintillator detector. Experiments were performed in reflectance mode. Measurements were carried out on samples laid on a glass slide without additional manipulation. The preferential grain

orientations that are likely to exist in these compounds could not be avoided due to the absence of grinding of the samples and also to the impossibility of using spinning capillary in our equipment.

### 3.5. Chromatography

Chromatographic studies were performed using an HPLC/UV-DAD (HP 1200, Agilent Technologies, Santa Clara, CA, USA) with a C18 column (Gemini-NX 150 × 4.6 mm, 5 μm) from Phenomenex (Phenomenex, Torrance, CA, USA). The mobile phase was a mixture of acetonitrile/water (80:20; *v/v*) for compound VA4J, (50:50; *v/v*) for VA6E and (80:20, 0.1% formic acid; *v/v*) for compound VA7J. The injection volume was 50 μL and the flow rate was 1 mL/min. Chromatography was performed at 35 °C. UV-DAD detection was established at  $\lambda = 254$  nm.

In the assessment of linearity, calibration curves were plotted in the range of 3–119 μg/mL for VA6E and 0.8–59.5 μg/mL for VA4J and VA7J. Calibration curves were evaluated by the analysis of the distribution properties of the residuals, correlation coefficient  $r^2 > 0.990$ , slope of the linear calibration curve statistically different from 0 ( $p = 95\%$ ) and the intercept not statistically different from 0 ( $p = 95\%$ ). Precision (as RSD%) of the method was evaluated by analysing three replicate calibration samples at five concentration values (including lower, medium and higher value) of the calibration curve.

Stock standard solutions containing 1 mg/mL of compound VA4J, VA6E and VA7J were prepared by diluting each compound in a mixture of acetonitrile/water (50:50; *v/v*). Calibration samples in the mobile phase were prepared by the dilution of the stock standard solutions.

For stability evaluation in stress conditions, working solutions of 47.6 μg/mL were prepared by diluting 20 μL of each standard solution in 200 μL of acetonitrile and 200 μL of (a) 1 M HCl, (b) 0.1 M NaOH and (c) 3% H<sub>2</sub>O<sub>2</sub>. Data were recorded at zero time and after 4 and 24 h of exposure.

## 4. Conclusions

The thermal characterization of compounds with antitumour potency is crucial to further continue the drug discovery process. In order to predict the non-desired transformations that might occur in the pharmaceutical manufacturing process, the polymorphism of the most promising compounds has been studied.

Regarding the results of differential scanning calorimetry, powder X-ray diffraction and the stability studies under stress conditions:

- Compound VA6E: temperature conditions have to be carefully selected as solid state behaviour includes four different polymorphs. In terms of stability, alkaline, acid and oxidation media are not suggested as they cause degradation.
- Compound VA7J: oxidation conditions and desolvation have to be taken into account as they lead to immediate degradation and crystal structure modification, respectively.
- Compound VA4J: there is no evidence of polymorphism and stress conditions do not affect the solid-state structure.

Taken together we can conclude that compounds VA6E and VA7J present some obstacles to further development as drugs as both temperature and stress conditions affect the original structure. On the other hand, compound VA4J proved to be safe to work with under the conditions studied. Therefore, this compound is of special interest for further development as it shows promising activity, selectivity and stability.

In addition, it has been found that the polymorphic behaviour as well as the thermal stability of these compounds can be modified by the introduction of different functional groups in the heterocycle under consideration. According to our data, the incorporation of a selenol or thiol group improves the thermal stability.

**Supplementary Materials:** supplementary material are available online.

**Acknowledgments:** The authors wish to express their gratitude to the Plan de Investigación de la Universidad de Navarra, PIUNA (Ref 2014-26), for financial support for the project. V. Alcolea and P. Garnica wish to express

their gratitude to the Asociación de Amigos de la Universidad de Navarra for the pre-doctoral fellowship. The research leading to these results has received funding from “la Caixa” Banking Foundation.

**Author Contributions:** Carmen Sanmartín, Elena Lizarraga and Juan Antonio Palop conceived and designed the experiments; Verónica Alcolea performed the synthesis of the compounds; Pablo Garnica performed the biological evaluation, Elena Lizarraga the experiments in thermal analysis; Adrián Durán the experiments in X-ray diffraction and Elena González Peñas designed and performed the experiments in HPLC. Elena Lizarraga, Elena González Peñas, Adrián Durán, Pablo Garnica, Verónica Alcolea and Carmen Sanmartín analyzed the data; all the authors wrote the paper.

**Conflicts of Interest:** The authors declare no conflict of interest.

## References

1. World Health Organization. *Cancer Fact Sheet February 2017*; World Health Organization: Geneva, Switzerland, 2017.
2. Siegel, R.L.; Miller, K.D.; Jemal, A. Cancer statistics, 2017. *CA Cancer J. Clin.* **2017**, *67*, 7–30.
3. Holohan, C.; Van Schaeybroeck, S.; Longley, D.B.; Johnston, P.G. Cancer drug resistance: An evolving paradigm. *Nat. Rev. Cancer* **2013**, *13*, 714–726.
4. Miller, K.D.; Siegel, R.L.; Lin, C.C.; Mariotto, A.B.; Kramer, J.L.; Rowland, J.H.; Stein, K.D.; Alteri, R.; Jemal, A. Cancer treatment and survivorship statistics, 2016. *CA Cancer J. Clin.* **2016**, *66*, 271–289.
5. Wallenberg, M.; Misra, S.; Bjornstedt, M. Selenium cytotoxicity in cancer. *Basic Clin. Pharmacol. Toxicol.* **2014**, *114*, 377–386.
6. Fernandez-Herrera, M.A.; Sandoval-Ramirez, J.; Sanchez-Sanchez, L.; Lopez-Muñoz, H.; Escobar-Sanchez, M.L. Probing the selective antitumour activity of 22-oxo-26-selenocycloheptane derivatives. *Eur. J. Med. Chem.* **2014**, *74*, 451–460.
7. Romano, B.; Plano, D.; Encio, I.; Palop, J.A.; Sanmartin, C. In vitro radical scavenging and cytotoxic activities of novel hybrid selenocarbamates. *Bioorg. Med. Chem.* **2015**, *23*, 1716–1727.
8. Plano, D.; Sanmartín, C.; Moreno, E.; Prior, C.; Calvo, A.; Palop, J.A. Novel potent organoselenium compounds as cytotoxic agents in prostate cancer cells. *Bioorg. Med. Chem. Lett.* **2007**, *17*, 6853–6859.
9. Otsuka, M.; Kaneniwa, N. Dehydration of cephalixin hydrates. *Chem. Pharm. Bull.* **1983**, *31*, 1021–1029.
10. Borka, L.; Halebian, J.K. Crystal polymorphism of pharmaceuticals. *Acta Pharm. Jugosl.* **1990**, *40*, 71–94.
11. Takahashi, Y.; Nakashima, K.; Ishihara, T.; Nakagawa, H.; Sugimoto, I. Polymorphism of fostedil: Characterization and polymorphic change by mechanical treatments. *Drug Dev. Ind. Pharm.* **2008**, *11*, 1543–1563.
12. Correa, J.C.R.; Perissinato, A.G.; Serra, C.H.D.; Trevisan, M.G.; Salgado, H.R.N. Polymorphic stability of darunavir and its formulation. *J. Therm. Anal. Calorim.* **2016**, *123*, 2185–2190.
13. Bonfílio, R.; Pires, S.A.; Ferreira, L.M.; de Almeida, A.E.; Doriguetto, A.C.; de Araujo, M.B.; Salgado, H.R. A discriminating dissolution method for glimepiride polymorphs. *J. Pharm. Sci.* **2012**, *101*, 794–804.
14. Giron, D. Thermal-analysis and calorimetric methods in the characterization of polymorphs and solvates. *Thermochim. Acta* **1995**, *248*, 1–59.
15. Du, Y.; Xue, J. Investigation of polymorphism and cocrystallization of active pharmaceutical ingredients using vibrational spectroscopic techniques. *Curr. Pharm. Des.* **2016**, *22*, 4917–4928.
16. Barnes, A.F.; Hardy, M.J.; Lever, T.J. A review of the applications of thermal methods within the pharmaceutical-industry. *J. Therm. Anal.* **1993**, *40*, 499–509.
17. Wang, L.Y.; Zhu, L.; Sha, Z.L.; Li, X.C.; Wang, Y.F.; Yang, L.B.; Zhao, X.Y. Characterization, thermal stability, and solid-state phase transition behaviors of gestodene polymorphs and amorphous phase. *J. Therm. Anal. Calorim.* **2017**, *127*, 1533–1542.
18. Waszkielewicz, A.M.; Cegła, M.; Zesławska, E.; Nitek, W.; Słoczyńska, K.; Marona, H. N-[(2,6-dimethylphenoxy)alkyl]aminoalkanols-their physicochemical and anticonvulsant properties. *Bioorg. Med. Chem.* **2015**, *23*, 4197–4217.
19. Jiang, S.F.; Jansens, P.J.; ter Horst, J.H. Mechanism and kinetics of the polymorphic transformation of o-aminobenzoic acid. *Cryst. Growth Des.* **2010**, *10*, 2123–2128.
20. Da Silva, L.M.; Montanari, C.M.; Santos, O.M.; Cazedey, E.C.; Angelo, M.L.; de Araujo, M.B. Quality evaluation of the finasteride polymorphic forms i and ii in capsules. *J. Pharm. Biomed. Anal.* **2015**, *105*, 24–31.
21. Carrer, H.; Cortez, J.; Frare, L.M.; Costa, M.B.; Bittencourt, P.R.S. Thermal characterization of the bromopride recrystallized from different solvents and at different temperature conditions. *J. Therm. Anal. Calorim.* **2016**, *123*, 927–931.

22. Yoshida, M.I.; Gomes, E.C.; Soares, C.D.; Cunha, A.F.; Oliveira, M.A. Thermal analysis applied to verapamil hydrochloride characterization in pharmaceutical formulations. *Molecules* **2010**, *15*, 2439–2452.
23. Huang, L.F.; Tong, W.Q. Impact of solid state properties on developability assessment of drug candidates. *Adv. Drug. Deliv. Rev.* **2004**, *56*, 321–334.
24. Thomas, S.P.; Satheeshkumar, K.; Muges, G.; Guru Row, T.N. Unusually short chalcogen bonds involving organoselenium: Insights into the Se-N bond cleavage mechanism of the antioxidant ebselen and analogues. *Chem. Eur. J.* **2015**, *21*, 6793–6800.
25. Neumann, M.A.; Van de Streek, J.; Fabbiani, F.P.; Hidber, P.; Grassmann, O. Combined crystal structure prediction and high-pressure crystallization in rational pharmaceutical polymorph screening. *Nat. Commun.* **2015**, *6*, 7793.
26. Nauha, E.; Bernstein, J. “Predicting” polymorphs of pharmaceuticals using hydrogen bond propensities: Probenecid and its two single-crystal-to-single-crystal phase transitions. *J. Pharm. Sci.* **2015**, *104*, 2056–2061.
27. Xu, K.; Zheng, S.; Zhai, Y.; Guo, L.; Tang, P.; Yan, J.; Wu, D.; Li, H. Two solid forms of tauroursodeoxycholic acid and the effects of milling and storage temperature on solid-state transformations. *Int. J. Pharm.* **2015**, *486*, 185–194.
28. Alcolea, V.; Plano, D.; Encio, I.; Palop, J.A.; Sharma, A.K.; Sanmartin, C. Chalcogen containing heterocyclic scaffolds: New hybrids with antitumoural activity. *Eur. J. Med. Chem.* **2016**, *123*, 407–418.
29. Alcolea, V.; Plano, D.; Karelia, D.N.; Palop, J.A.; Amin, S.; Sanmartin, C.; Sharma, A.K. Novel seleno- and thio-urea derivatives with potent in vitro activities against several cancer cell lines. *Eur. J. Med. Chem.* **2016**, *113*, 134–144.
30. Plano, D.; Baquedano, Y.; Moreno-Mateos, D.; Font, M.; Jiménez-Ruiz, A.; Palop, J.A.; Sanmartín, C. Selenocyanates and diselenides: A new class of potent antileishmanial agents. *Eur. J. Med. Chem.* **2011**, *46*, 3315–3323.
31. Wang, L.; Guo, X.; Wang, J.; Jiang, C.; Bosland, M.C.; Lu, J.; Deng, Y. Methylseleninic acid superactivates p53-senescence cancer progression barrier in prostate lesions of pten-knockout mouse. *Cancer Prev. Res.* **2016**, *9*, 35–42.
32. Fernandes, A.P.; Gandin, V. Selenium compounds as therapeutic agents in cancer. *Biochim. Biophys. Acta* **2015**, *1850*, 1642–1660.
33. Lamberto, I.; Plano, D.; Moreno, E.; Font, M.; Palop, J.A.; Sanmartin, C.; Encio, I. Bisacylimidoselenocarbamates cause g<sup>2</sup>/m arrest associated with the modulation of cdk1 and chk2 in human breast cancer mcf-7 cells. *Curr. Med. Chem.* **2013**, *20*, 1609–1619.

**Sample Availability:** Samples of the compounds reported in this paper are available from the authors.



© 2017 by the authors. Licensee MDPI, Basel, Switzerland. This article is an open access article distributed under the terms and conditions of the Creative Commons Attribution (CC BY) license (<http://creativecommons.org/licenses/by/4.0/>).

**Appendix A: supplementary data**
*Compound VA7H (behaviour I)*

*Differential scanning calorimetry.* As an example, the DSC results of compound VA7H are shown in Figure S1 and Table S1. During the first thermal scan (curve A), two processes were observed. The first one is typical of a glass transition ( $T_g$ ) and then, an endothermic melting process happened, demonstrating that amorphous and crystalline forms coexist in the original compound. After cooling the sample, through a polymorphic phase transition, the initial form (Form I) changed into an amorphous one which did not show more fusion processes (Form II, curve B). The complete thermogram shows that other processes at another temperature (higher or lower) can be excluded.

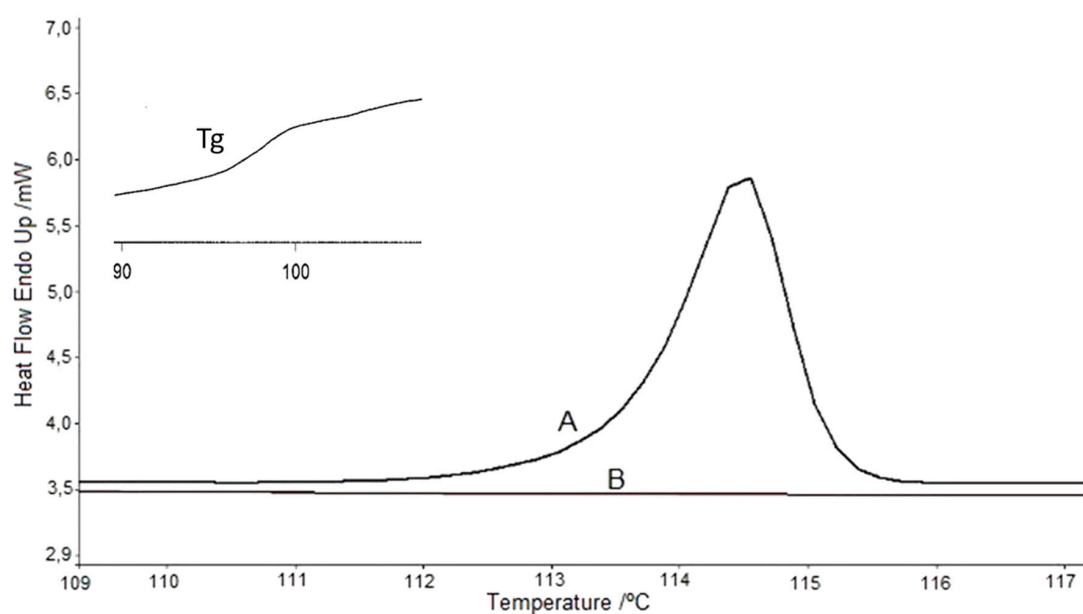


**Figure S1.** DSC of compound VA7H (curve A: first scan; curve B: second scan)

**Table S1.** Fusion-recrystallization of compound VA7H

Behaviour I	$T_{onset}$ (°C)	$\Delta H$ (Jg <sup>-1</sup> )	
1 <sup>st</sup> scan	113.7	42.1	Form I
2 <sup>nd</sup> scan	-	-	Form II

Regarding *XRD results*, two different polymorphic forms were detected: Form I with a low degree of crystallinity and Form II, mostly amorphous form. Peaks at  $2\theta=5.9, 21.3, 22.4, 23.5, 26.9, 27.9, 29.7$  and  $30.0$  in diffractograms differed from one another as shown in Figure S2.

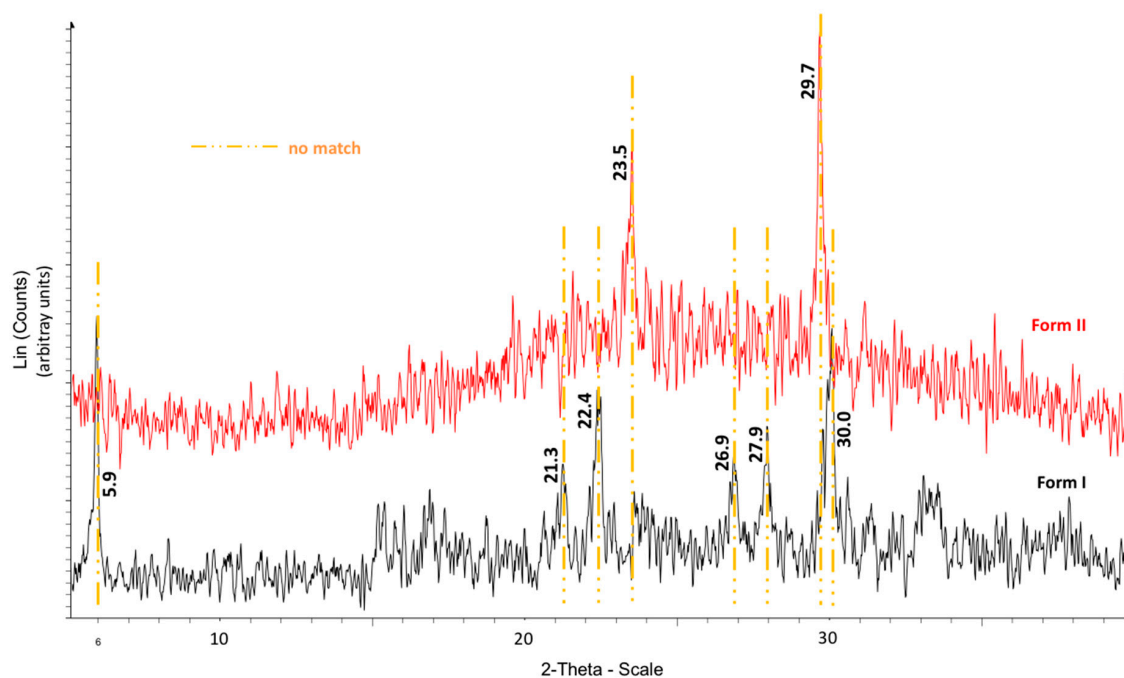


Figure S2. X-ray diffractogram for VA7H (Form I: original polymorph and form II: mostly amorphous form)

#### Compound VA7E (behaviour II)

After a first thermal curve of compound VA7E (curve A in Figure S3) with a typical endothermic process of Form I (Table S2), in a second scan, a new endothermic process happened at a lower temperature (curve B), with the appearance of a new polymorph (Form II) that turned into an amorphous form after cooling. No eutectic peak at lower temperatures was detected.

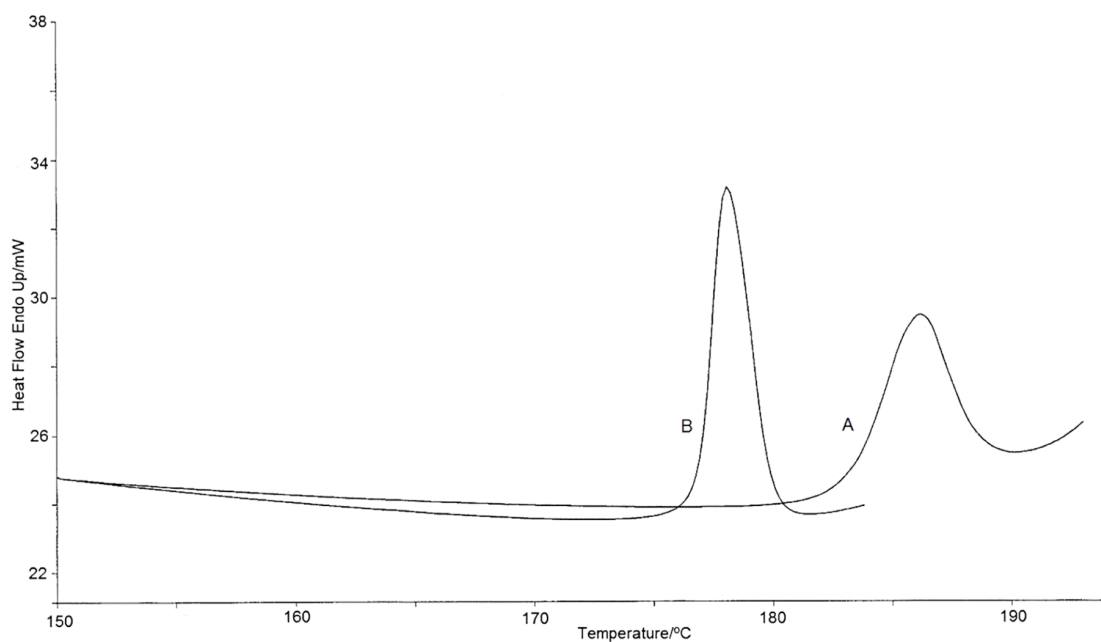
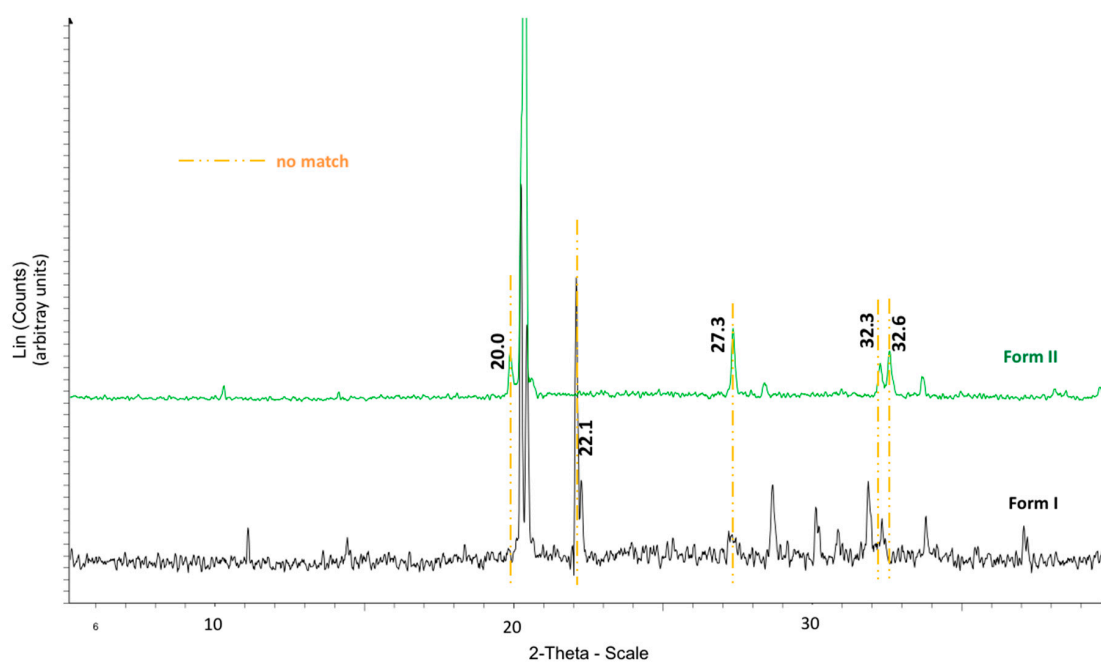


Figure S3. DSC of compound VA7E (curve A: first scan; curve B: second scan)

**Table S2.** Fusion-recrystallization of compound VA7E

Behaviour II	$T_{onset}$ (°C)	$\Delta H$ (Jg <sup>-1</sup> )	
1 <sup>st</sup> scan	183.8	21.5	Form I
2 <sup>nd</sup> scan	177.2	28.1	Form II
3 <sup>rd</sup> scan	-	-	Amorphous form

Two polymorphic forms were detected in the *X-ray diffraction studies* (Figure S4). Peaks at  $2\theta=20.0$ , 27.3, 32.3 and 32.6 only appeared in Form II whereas signal at  $2\theta=22.1$  was exclusive of Form I.



**Figure S4.** X-ray diffractogram for compound VA7E. Form I shows the diffractogram of the original polymorph and II the one obtained after heat treatment

*Compound VA2M (behaviour III):*

This compound shows a fusion process without modifications in the thermal behaviour after successive fusion-recrystallization cycles (Figure S5 and Table S3). Consequently, there is no evidence of polymorphic behaviour.



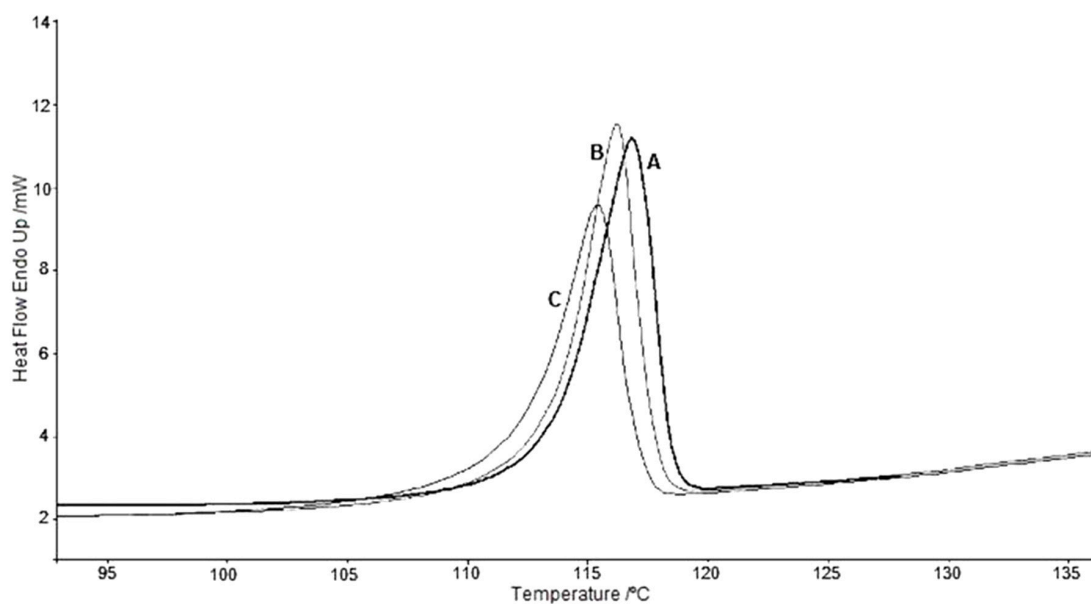
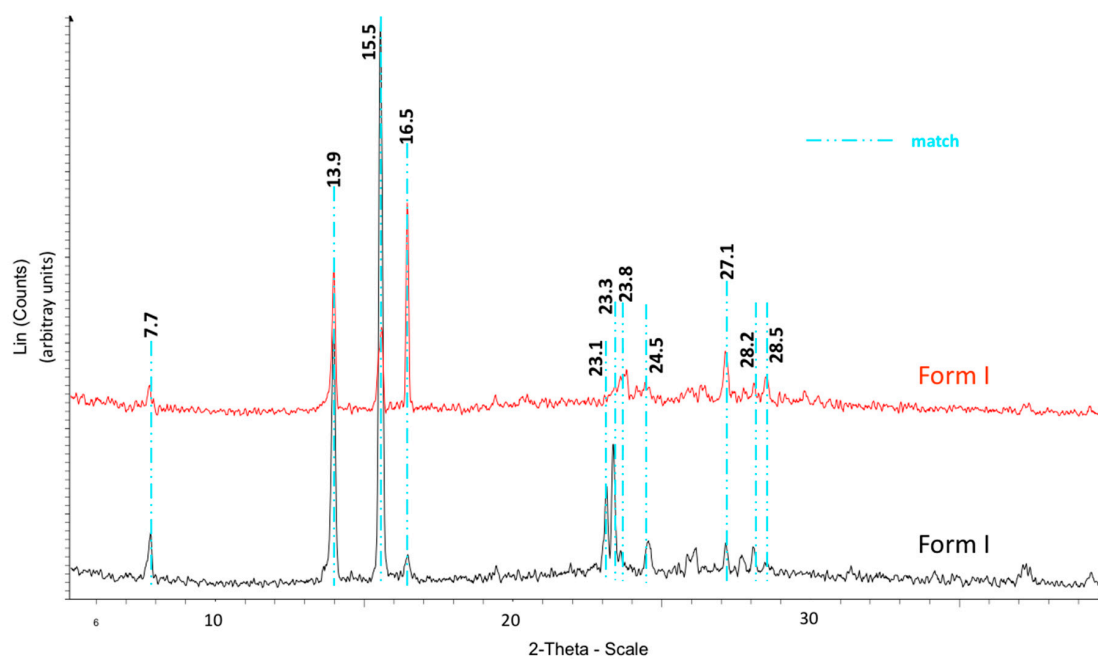


Figure S5. DSC of compound VA2M. Curve A: first scan; curve B: second scan; curve C: third scan

Table S3. Fusion-recrystallization of compound VA2M

Behaviour III	$T_{onset}$ (°C)	$\Delta H$ (Jg <sup>-1</sup> )	
1 <sup>st</sup> scan	113.7	68.1	Form I
2 <sup>nd</sup> scan	110.2	70.7	Form I

*X-ray powder diffractometry:* to further confirm the absence of polymorphism, both samples were analysed by X-ray powder diffractometry. As it can be observed in Figure S6, no differences were found in the positions of the peaks between the original sample (after the synthesis and purification) and the one obtained after melting and a subsequent recrystallization process. The differences in the intensities of some of the peaks were probably due to some preferred orientation in the samples derived from the absence of random orientation of crystal grains in space. Anyway, we could observe a very good match between peak positions in both diffractograms.



**Figure S6.** X-ray diffractogram for compound VA2M diffractogram of the original compound before (black XRD) and after heat treatment (red XRD)



**PAPER 5**

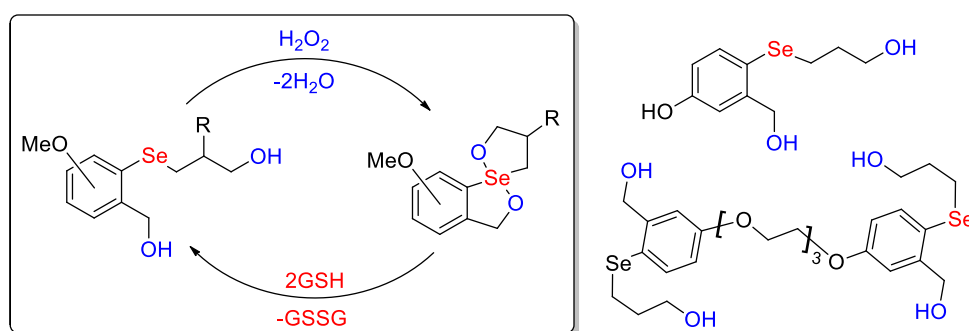
---



## Enhanced Glutathione Peroxidase Activity of Water-Soluble and Polyethylene Glycol-Supported Selenides, Related Spirodioxyselenuranes, and Pincer Selenuranes

Nicole M. R. McNeil, David J. Press, Don M. Mayder, Pablo Garnica, Lisa M. Doyle, and Thomas G. Back\*

Department of Chemistry, University of Calgary, 2500 University Drive N.W., Calgary, Alberta T2N 1N4, Canada



Organoseleno compounds have widely been described, as described in the background section for their antioxidant activity and ability to maintain ROS homeostasis. In this work, a cluster of twenty-four selenuranes were tested to determine their potency as GPx mimetics. Two different methodologies were compared in this paper, and HPLC-based and an NMR-based methodology. For leader compounds further studies were performed to establish the catabolic mechanism and the kinetics involved. Some preliminary radical inhibitor tests were also conducted.

McNeil N, Press DJ, Mayder DM, Garnica P, Doyle LM, Back TG. Enhanced Glutathione Peroxidase Activity of Water-Soluble and Polyethylene Glycol-Supported Selenides, Related Spirodioxyselenuranes, and Pincer Selenuranes. [J. Org. Chem.](#), 2016, 81(17), 7884-7897. DOI: 10.1021/acs.joc.6b01593





## **DISCUSSION**

---



Cancer is a worldwide health issue and represents one of the main causes of death in high-income countries as well as low-middle-income countries. Technology and research advance together rapidly in the last decade, still chemotherapies cause undesirable secondary effects and resistances. Secondary effects are due to the difficulties that treatments face to distinguish between normal and tumor cells. For this reason, the development of safer, more effective and more selective drugs is necessary.

On the other hand, leishmaniasis is a neglected tropical disease that affects 1.3 million people annually. Geographically this disease is spread worldwide with 87 endemic countries. Treatments require patient compliance which is difficult especially in poor areas where leishmaniasis is more common. The appearance of resistances among other reasons encourages drug research in this area with the goal of safer, cheaper, more effective drugs of easy administration.

This work aims to fulfil those two challenges at once with the development of Se compounds that present antitumoural and leishmanicidal activities. The synthesis methodologies should not be too complex as this fact will have an impact on the final price of the drug, especially if we take into account the situation that many leishmaniasis patients suffer socioeconomically. The duality of this action may be achieved as both diseases share common pathways and Se has been proven implicated in many of them.

Many factors contribute to the variety of biological response promoted by Se treatment, particularly the chemical form and the concentration in which it is administered. Metabolism plays a crucial role in the final effects of seleno-containing structures. Therefore, we performed an extensive bibliography review that combined with the research group experience yielded the design of two series of compounds containing selenocyanate, diselenide and selenourea chemical entities. All synthesized compounds were evaluated in order to establish their potential as antitumor and leishmanicidal structures. The start-up point for the design of the structures were bis(4-aminophenyl)diselenide and 4-aminophenylselenocyanate, structures of our group chemical library of compounds that have antitumor and leishmanicidal activity. Our goal therefore was to establish whether the proposed structural modifications could enhance the biological activity of the final derivatives.

The synthetic methodologies are highly efficient in terms of time, most of the reactions are one-pot. The reactions consist of one or two steps maximum of around 24 h each. In cost terms reactions do not depend on expensive catalysts and purification techniques are easy as most of them are based on washing with different solvents and extractions. As previously stated this last condition is crucial for the development of leishmanicidal drugs.

In series I (**Figure 28**) a clear fragment-based drug design strategy was followed as the introduction of active fragments in one same structure. Considering that symmetry is a common feature of a broad range of structures with antitumoural properties. (137) The main core of the structure was selected for its activity and reactive versatility (bis(4-aminophenyl)diselenide). On this core, selenourea group was added with the properties already described in the background section. Moreover, carbocyclic and heterocyclic endings modulated volume and electronic factors, a dual goal was foreseen as some of them had already antitumor properties. Sixteen

compounds with those characteristics were synthesized, eight with carbocyclic endings and eight with heterocyclic endings. In terms of reactivity benzoyl substituted chlorides were more reactive and in heterocyclic carbonyl chlorides reactivity decreased presumably due to steric impairments.

In series II a comparison between diselenide and selenocyanate homologs was proposed, moreover the formation of cyclic imides enabled us to study the effect of carboxy groups and NH protons on activity. Again the main core for diselenide derivatives was bis(4-aminopheny)diselenide and for selenocyanates 4-aminophenydiselenocyanate was selected. The modifications on that nucleus covered a wide chemical space. Besides, the introduction of carboxylic acid chemical entity enhanced solubility properties, one issue some of our previous compounds found in the drug development process (133,138). Some diselenide derivative homologs could not be synthesized due the lack of reactivity balance between lone pair electrons of the amine nitrogen in the main core of the structure and the electrophilic center in the reagent anhydride. Subseries have been categorized: **a** for diselenide derivatives, **b** for selenocyanates (**Figure 28**).

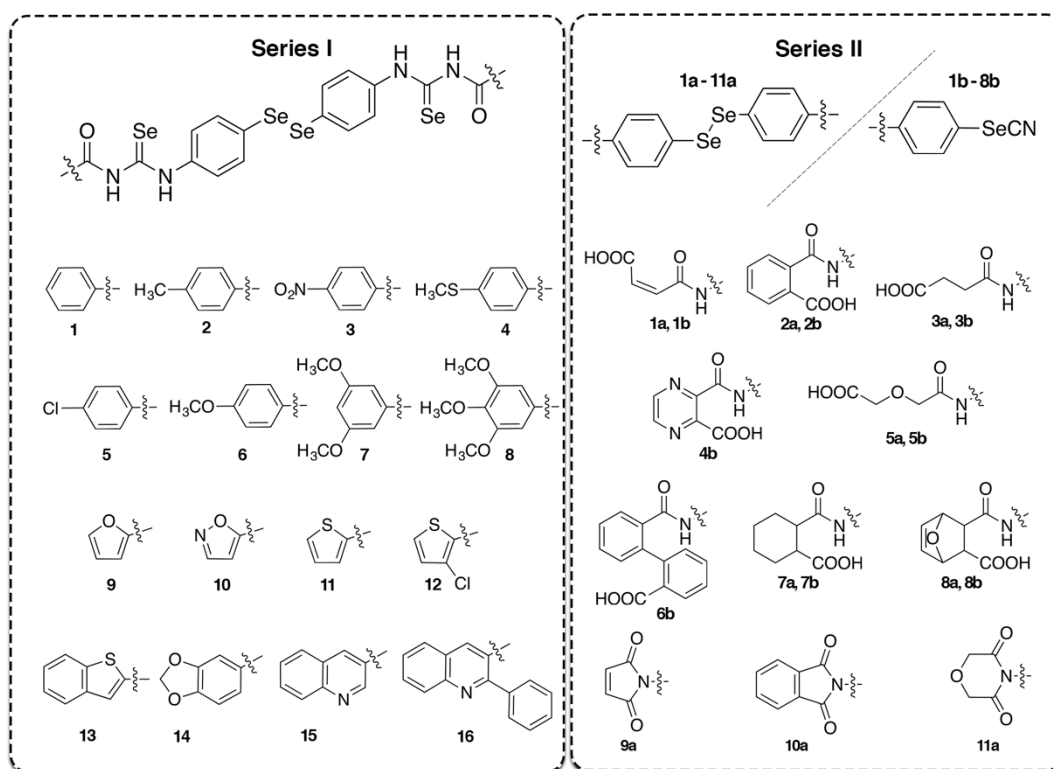


**Figure 28.** Structures synthesized in this work

Compounds have been structurally characterized by  $^1\text{H}$  NMR,  $^{13}\text{C}$  NMR, IR spectroscopy and mass spectrometry. Biological test standards purity was guaranteed by microanalysis of percentages of carbon, nitrogen and hydrogen.

Synthesized compounds were screened for their cytotoxic and antiproliferative activities against a panel of seven human tumor cell lines: CCRF-CEM (acute lymphoblastic leukemia), K-562 (lymphocytic leukemia), MCF-7 (breast adenocarcinoma), PC-3 (prostatic adenocarcinoma), HTB-54 (lung carcinoma), and HT-29 (colon carcinoma). Furthermore, an extra acute lymphoblastic leukemia cell line (MOLT-4) was added for the testing of series II compounds. Breast adenocarcinoma stood out as the most sensitive cell line to the treatment with these compounds, sixteen of the screened compounds exhibited GI<sub>50</sub> values under 10 μM in this cell line. In series I in terms of general potency carbocyclicly-ended derivatives were more active than their heterocyclic homologs. If we draw our attention to series II no general trends could be observed in terms of potency. In this last study core fragments bis(4-aminophenyl)diselenide and 4-aminophenylselenocyanate were included in the test, showing a potent cytotoxic profile. If we study dose response curves we can conclude that series I compounds have a cytotoxic profile with the ability to kill cells while the active compounds of series II have a more cytostatic profile related to inhibitory growth effects.

One of the main issues with chemotherapeutics is selectivity, the ability to set apart tumoral cells from normal cells. With the aim to study this parameter, compound cytotoxicity was also evaluated on two non-malign derived cell lines, 184B5 (mammary derived) and BEAS-2B (derived from bronchial epithelium). In general results showed no general selectivity for lung cancer cells. Very different perspectives were found when breast adenocarcinoma SI were studied. Eleven of the tested compounds were at least ten times more selective for MCF-7 cell line than for 184B5. Main core fragments revealed themselves to be non-selective cytotoxic agents. In this property, very high-end values were found for compounds **1**, **2**, **4**, **5**, **7** and **10a** which gave us an idea of the staggering selectivity of those compounds for breast adenocarcinoma cells. One of our goals was achieved as we had enhanced the selectivity indexes for those compounds enormously.

With the aim of further study the mechanism of action of the active compounds we selected two leader compounds from each series in terms of potency and selectivity. The effect of those four compounds (**2**, **7**, **8b** and **10a**) on cell cycle and cell death was determined by flow cytometry technique in MCF-7 cell line. Studies show concordance with cytotoxicity assays in terms of cell death rates. For tested compounds of series I high rates of cell death were observed even at short time exposures (6 h) at 10 μM concentration. For assayed derivatives of series II higher time treatment and doses were needed to cause this same effect, confirming the cytostatic profiling observed in the MTT assays. All four compounds caused cell cycle arrest, derivatives **2** and **7** in G<sub>2</sub>/M phase and derivatives **10a** and **8b** in S phase. When inhibitor pre-incubating was performed in this same assay, autophagy was pointed out as a possible mechanism of action as wortmannin blocked cell death induced by treatment. This mechanism was confirmed by protein studies by Western Blot analysis for compounds **2** and **7**.

Thirty-one of the synthesized compounds were also screened for their leishmanicidal activity in *L. infantum* amastigotes. Cytotoxicity on THP-1 cells was also evaluated in order to establish their SI. Seven of the tested compounds exhibited IC<sub>50</sub> and SI values in the range of reference drug miltefosine. In general terms, series II derivatives showed a much more promising antileishmanial profile than series I

structures. Only one selenocyanate was selected to further study the mechanism of action when they were ranked by SI values and reference drug values were established as threshold. Therefore, in general diselenide derivatives of series II are more potent and selective than their selenocyanate homologs. To further understand their mechanism of action, their ability to protect against *Leishmania* infection and their TryR inhibition potencies were studied. Five of the tested compounds reduced infection rates to reference drug levels (Edelfosine) and three of them showed IC<sub>50</sub> values for the TryR assay lower than the ones obtained for mepacrine.

Structures that were marked as leader compounds of series II for antineoplastic activity also exhibited leishmanicidal properties (**8b** and **10a**). This same correlation was not found for leader compounds of series I.

The next steps for drug development process require stability to be tested as this process may include heating and treatments with various conditions. With the aim of predicting non-desired degradations in this process, a protocol was standardized for the testing of stability under heating, oxidizing, alkaline and acid conditions.

To gain a better understanding of the mechanisms of action implicated in the biological action of selenocompounds, an internship was planned during this work to develop and verify methodologies to evaluate their potential as GPx mimetics. These techniques included <sup>1</sup>H NMR quantification and HPLC analysis and will give us the capability to establish this evaluation as normalized tests in our research group.

In summary, this study validates our initial hypothesis and validates our structural modifications on the core structures as a valid strategy to develop potent and selective anti-tumoral and leishmanicidal drugs. We have established an effective protocol to narrow down a large number of potentially active compounds based on their potency and SI in the screening tests.

## BIBLIOGRAPHY

133. Baquedano Y, Alcolea V, Toro MA, Gutierrez KJ, Nguewa P, Font M, et al. Novel heteroaryl selenocyanates and diselenides as potent antileishmanial agents. *Antimicrob Agents Chemother.* **2016**;60(6):3802-3812.
137. Sanmartin C, Font M, Palop JA. Molecular symmetry: A structural property frequently present in new cytotoxic and proapoptotic drugs. *Mini Rev Med Chem.* **2006**;6(6):639-650.
138. Diaz-Argelich N, Encio I, Plano D, Fernandes AP, Palop JA, Sanmartin C. Novel methylselenoesters as antiproliferative agents. *Molecules.* **2017**;22(8): 1228.

## **CONCLUSIONS**

---





This work presents the design, synthesis and characterization of thirty-three selenocyanate- and diselenide-containing derivatives as well as the evaluation of their antitumor activity. Moreover, a study of their leishmanicidal potential was also carried out. This research work has led to the following conclusions:

1. The synthesized derivatives containing diselenide and selenocyanate moieties have shown promising results in cancer and leishmaniasis in *in vitro* studies.
2. Twenty-five compounds show GI<sub>50</sub> values lower than 10 μM in at least one of the tested cancer cell lines confirming our hypothesis. Two different dose-response profiles can be observed, a cytotoxic profile for acylselenourea-diselenide structures and a cytostatic profile for diselenide/selenocyanate homologs containing carboxylic or imide groups.
3. Among the cancer cell lines tested, MCF-7 was the most susceptible one with GI<sub>50</sub> values in the nanomolar range for diselenide derivatives **1**, **2**, **3**, **4**, **5**, **7** and **10a**. Moreover, compounds were selective for breast adenocarcinoma with SI higher than 1000 calculated for **1**, **2**, **4**, **5**, **7** and **10a**. Compounds **7** and **10a** stood out for their staggering SI for breast adenocarcinoma cells (69,673 and over the 82,269 respectively).
4. When results are compared to their parent compound's activities in terms of cytotoxic potency and selectivity, those properties have been enhanced. Therefore, verifying that our structural modulation has a positive effect on anticancer activity and thus confirming our initial hypothesis.
5. Among the selenourea containing derivatives structure endings have a crucial effect on selectivity for breast adenocarcinoma cells as carbocyclic endings result in more selective derivatives than heterocyclic endings.
6. When screened to evaluate their anticancer activity selenocyanate derivatives containing carboxylic moiety were overall more potent than their diselenide carboxylic homologs. The presence of the imide group proved to have a crucial role in potency against cancer cells.
7. Compounds **2** and **7** induce cell cycle arrest in G<sub>2</sub>/M phase and autophagy pathway is implicated in the mechanism by which they cause cell death in MCF-7 cell line.
8. Compounds **8b** and **10a** induced cell cycle arrest in S phase and this arrest causes their cytostatic chemotherapeutic profile at concentrations up to 40 μM for 48 h treatment. At higher doses or treatment times they cause cell death by autophagy pathways in MCF-7 cell line.
9. Seven out of thirty-one tested compounds against *Leishmania infantum* matched potency of miltefosine against amastigotes and exceeded the SI exhibited by the reference drug.
10. In general, diselenide derivatives are more active and selective as leishmanicidal agents than their selenocyanate analogs. All diselenide selected compounds matched the activity of edelfosine against infected macrophages.
11. If we compare leishmanicidal potency of the synthesized compounds with the one obtained for core fragments, diselenide derivatives matched the previous

results in the assay performed on infected macropages. In some cases even exceeded the activity shown by bis(4-aminophenyl)diselenide partially confirming the initial hypothesis.

12. TryR might be implicated in the mechanism of action of tested compounds as five out of the six tested compounds exceeded the potency shown by mepacrine. Specially, compounds **9a** and **8b** were 100-fold more active than the positive control.
13. The analysis of stability of promising active compounds under production-like conditions to prevent non-desirable degradations or solid-state transitions that affect the final outcome of the drug is possible and necessary.
14. The evaluation of GPx mimetic properties of organoseleno compounds is possible by two new methodologies HPLC and NMR based and have been validated with a cluster of twenty-four compounds.
15. Derivatives **8b** and **10a** proved to be potent and selective both against cancer cells and leishmania amastigotes therefore confirming the potential treatment duality of these organoseleno compounds.

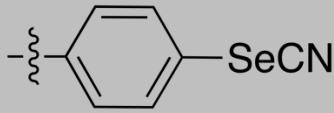
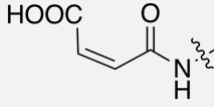
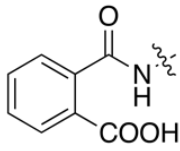
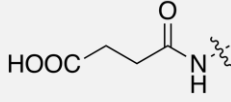
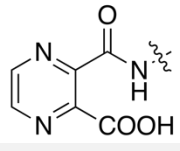
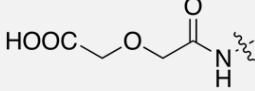
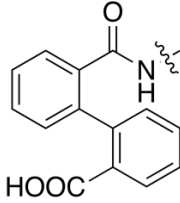
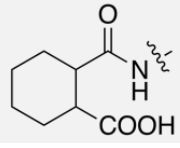
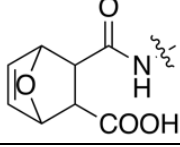
## **APENDIX 1: SYNTHESIZED COMPOUNDS**

---



Series I				
Ref.	Name	R	Paper 3 Ref.	
1	<i>N,N'</i> -[(diselanediybis(benzene-4,1-diyl)selenecarbamoyl)] dibenzamide		1a	
2	<i>N,N'</i> -[(diselanediybis(benzene-4,1-diyl)selenecarbamoyl)] di-4-methylbenzamide		2a	
3	<i>N,N'</i> -[(diselanediybis(benzene-4,1-diyl)selenecarbamoyl)] di-4-nitrobenzamide		3a	
4	<i>N,N'</i> -[(diselanediybis(benzene-4,1-diyl)selenecarbamoyl)] di-4-methylthiobenzamide		4a	
5	<i>N,N'</i> -[(diselanediybis(benzene-4,1-diyl)selenecarbamoyl)] di-4-chlorobenzamide		5a	
6	<i>N,N'</i> -[(diselanediybis(benzene-4,1-diyl)selenecarbamoyl)] di-4-methoxybenzamide			
7	<i>N,N'</i> -[(diselanediybis(benzene-4,1-diyl)selenecarbamoyl)] di-3,5-dimethoxybenzamide		6a	
8	<i>N,N'</i> -[(diselanediybis(benzene-4,1-diyl)selenecarbamoyl)] di-3,4,5-trimethoxybenzamide			
9	<i>N,N'</i> -[(diselanediybis(benzene-4,1-diyl)selenecarbamoyl)] di-2-furanamide		7a	
10	<i>N,N'</i> -[(diselanediybis(benzene-4,1-diyl)selenecarbamoyl)] diisoxazole-5-amide		8a	
11	<i>N,N'</i> -[(diselanediybis(benzene-4,1-diyl)selenecarbamoyl)] di-2-thiophenamide		9a	
12	<i>N,N'</i> -[(diselanediybis(benzene-4,1-diyl)selenecarbamoyl)] di-3-chlorothiophen-2-amide		10a	
13	<i>N,N'</i> -[(diselanediybis(benzene-4,1-diyl)selenecarbamoyl)] di-benzo[b]thiophene-2-amide		11a	
14	<i>N,N'</i> -[(diselanediybis(benzene-4,1-diyl)selenecarbamoyl)] di-1,3-benzodioxole-5-amide		12	
15	<i>N,N'</i> -[(diselanediybis(benzene-4,1-diyl)selenecarbamoyl)] di-3-quinolineamide		13a	
16	<i>N,N'</i> -[(diselanediybis(benzene-4,1-diyl)selenecarbamoyl)] di-2-phenyl-4-quinolineamide		14a	

Series II			
Ref.	Name	R	Paper 3 Ref
1a	(2Z,2'Z)-4,4'-oxo-4,4'-[(diselenodiyldibenzene-4,1-diyl)diaminol]bis(but-2-enoic acid)		18a
2a	2,2'-[(diselenodiyldibenzene-4,1-diyl)dicarbamoyl]bis(benzoic acid)		19a
3a	4,4'-oxo-4,4'-[(diselenodiyldibenzene-4,1-diyl)diaminol]bis(butanoic acid)		20a
5a	2,2'-[(diselenodiyldibenzene-4,1-diyl)dicarbamoylmethoxy]bisacetic acid		22a
7a	2,2'-[(diselenodiyldibenzene-4,1-diyl)dicarbamoyl]bis(cyclohexanoic acid)		24a
8a	3,3'-[(diselenodiyldibenzene-4,1-diyl)dicarbamoyl]bis(7-oxabicyclo[2.2.1]hept-5-ene-2-carboxylic acid)		25a
9a	1,1'-(diselenodiyldibenzene-4,1-diyl)bis(1H-pyrrole-2,5-dione)		15a
10a	1,1'-(diselenodiyldibenzene-4,1-diyl)bis(1H-isoindole-1,3(2H)-dione)		16a
11a	1,1'-(diselenodiyldibenzene-4,1-diyl)bis(morpholine-3,5-dione)		17a

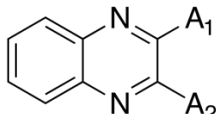
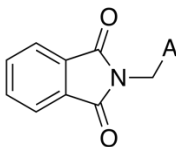
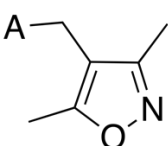
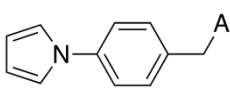
			
Ref.	Name	R	Paper 3 Ref.
1b	(2Z)-4-oxo-4-[(4-selenocyanatophenyl)amino]but-2-enoic acid		18b
2b	2-[(4-selenocyanatophenyl)carbamoyl]benzoic acid		19b
3b	4-oxo-4-[(4-selenocyanatophenyl)amino]butanoic acid		20b
4b	3-[(4-selenocyanatophenyl)carbamoyl]pyrazine-2-carboxylic acid		21b
5b	2-[(4-selenocyanatophenyl)carbamoylmethoxy] acetic acid		22b
6b	2'-[(4-selenocyanatophenyl)carbamoyl]-[1,1'-biphenyl]-2-carboxylic acid		23b
7b	2-[(4-selenocyanatophenyl)carbamoyl]cyclohexanoic acid		24b
8b	3-[(4-selenocyanatophenyl)carbamoyl]-7-oxabicyclo[2.2.1]hept-5-ene-2-carboxylic acid		25b

Appendix 1: synthesized structures

Compounds included in paper 4 were synthesized by Dra Veronica Alcolea and presented in her PhD.(Alcolea, V. Diseño, síntesis y evaluación biológica de nuevos derivados selenados con actividad antitumoral y leishmanicida. University of Navarre, School of Pharmacy; 2016). The structures are described in the following tables.

Ref.	Name	Structure	A
VA2B	Pyrimidine-2,4-dithiol		-SH
VA4B	2,4-Bis(methylsulfanyl)pyrimidine hydrochloride		-S-CH <sub>3</sub>
VA1C	Benzo[d]thiazole-2-selenol		-SeH
VA2C	Benzo[d]thiazole-2- thiol		-SH
VA4C	2-(Methylsulfanyl)benzo[d]thiazole		-S-CH <sub>3</sub>
VA1D	Acridin-9-ylmethaneselenol		-SeH
VA6D	Acridin-9-ylmethyl thiocyanate		-SCN
VA8D	Acridin-9-ylmethyl carbamimidothioate hydrobromide		-S-C(NH <sub>2</sub> )=NH
VA2E	(6-Bromobenzo[d][1,3]dioxol-5-yl)methanethiol		-SH
VA6E	(6-Bromobenzo[d][1,3]dioxol-5-yl)methyl thiocyanate		-SCN
VA7E	(6-Bromobenzo[d][1,3]dioxol-5-yl)methyl carbamimidoselenoate hydrobromide		-Se-C(NH <sub>2</sub> )=NH
VA8E	(6-Bromobenzo[d][1,3]dioxol-5-yl)methyl carbamimidothioate hydrobromide		-S-C(NH <sub>2</sub> )=NH
VA7F	(5-Nitrofuran-2-yl)methyl carbamimidoselenoate hydrobromide		-Se-C(NH <sub>2</sub> )=NH
VA8F	(5-Nitrofuran-2-yl)methyl carbamimidothioate hydrobromide		-S-C(NH <sub>2</sub> )=NH
VA6G	(9,10-Dioxo-9,10-dihydroantracen-2-yl)methyl thiocyanate		-SCN
VA7G	(9,10-Dioxo-9,10-dihydroantracen-2-yl)methyl carbamimidoselenoate hydrochloride		-Se-C(NH <sub>2</sub> )=NH
VA8G	(9,10-Dioxo-9,10-dihydroantracen-2-yl)methyl carbamimidothioate hydrochloride		-S-C(NH <sub>2</sub> )=NH
VA4H	2-(Methylsulfanyl)quinoline		-S-CH <sub>3</sub>
VA6H	(Quinolin-2-yl)methyl thiocyanate		-CH <sub>2</sub> -SCN
VA7H	(Quinolin-2-yl)methyl carbamimidoselenoate hydrochloride		-CH <sub>2</sub> -Se-C(NH <sub>2</sub> )=NH
VA8H	(Quinolin-2-yl)methyl carbamimidothioate hydrochloride		-CH <sub>2</sub> -S-C(NH <sub>2</sub> )=NH
VA6I	(6,7-Dimethoxy-2-oxo-2H-cromen-4-yl)methyl thiocyanate		-SCN
VA7I	(6,7-Dimethoxy-2-oxo-2H-cromen-4-yl)methyl carbamimidoselenoate hydrobromide		-Se-C(NH <sub>2</sub> )=NH
VA8I	(6,7-Dimethoxy-2-oxo-2H-cromen-4-yl)methyl carbamimidothioate hydrobromide		-S-C(NH <sub>2</sub> )=NH



<b>VA2J</b>	3-Mercaptoquinoxalin-2-yl carbamimidothioate hydrochloride		A <sub>1</sub> = -S-C(NH <sub>2</sub> )=NH A <sub>2</sub> = -SH
<b>VA4J</b>	2,3-Bis(methylsulfanyl)quinoxaline		A <sub>1</sub> =A <sub>2</sub> =-SCH <sub>3</sub>
<b>VA6J</b>	Quinoxalin-2,3-diildimethanediyl bithiocyanate		A <sub>1</sub> =A <sub>2</sub> =-CH <sub>2</sub> -SCN
<b>VA7J</b>	Quinoxalin-2,3-diylbis(methylene) dicarbamidoseleenoate dihydrobromide		A <sub>1</sub> =A <sub>2</sub> =-CH <sub>2</sub> -Se-C(NH <sub>2</sub> )=NH
<b>VA8J</b>	Quinoxalin-2,3-diylbis(methylene)dicarbamidothioate dihydrobromide		A <sub>1</sub> =A <sub>2</sub> =-CH <sub>2</sub> -S-C(NH <sub>2</sub> )=NH
<b>VA2M</b>	2-(Sulfanylmethyl)-1 <i>H</i> -isoindole-1,3(2 <i>H</i> )-dione		-SH
<b>VA6M</b>	(1,3-Dioxo-1,3-dihydro-2 <i>H</i> -isoindol-2-yl)methyl thiocyanate		-SCN
<b>VA7M</b>	(1,3-Dioxoisindolin-2-yl)methyl carbamidoseleenoate hydrobromide		-Se-C(NH <sub>2</sub> )=NH
<b>VA8M</b>	(1,3-Dioxoisindolin-2-yl)methyl carbamidothioate hydrobromide		-S-C(NH <sub>2</sub> )=NH
<b>VA50</b>	(3,5-Dimethylisoxazol-4-yl)methyl selenocyanate		-SeCN
<b>VA60</b>	(3,5-Dimethylisoxazol-4-yl)methyl thiocyanate		-SCN
<b>VA70</b>	(3,5-Dimethylisoxazol-4-yl)methyl carbamidoseleenoate hydrochloride		-Se-C(NH <sub>2</sub> )=NH
<b>VA80</b>	(3,5-Dimetilisoxazol-4-il)metil carbamidothioate hydrochloride		-S-C(NH <sub>2</sub> )=NH
<b>VA5P</b>	4-(1 <i>H</i> -Pyrrol-1-il)benzyl selenocyanate		-SeCN
<b>VA7P</b>	4-(1 <i>H</i> -Pyrrol-1-il)benzyl carbamidoseleenoate hydrobromide		-Se-C(NH <sub>2</sub> )=NH
<b>VA8P</b>	4-(1 <i>H</i> -Pyrrol-1-il)benzyl carbamidothioate hydrobromide		-S-C(NH <sub>2</sub> )=NH



